Identification and characterization of a new potato immune receptor against *Phytophthora infestans*

Yerisf Torres Ascurra

Propositions

1. Some pattern recognition receptors exhibit greater evolutionary dynamics than certain nucleotide-binding leucine-rich repeat receptors.
   (this thesis)

2. Genotype selection for map-based gene cloning strategy is crucial.
   (this thesis)

3. Mastery of computational skills will become imperative for scientists in a very near future.

4. Dog breed is a poor indicator of behavior and personality.

5. Consumerism threatens to banish humanity from Earth like fleas with a mere shake.

6. Cultured meat will alleviate the suffering endured by animals in intensive farming practices.

Propositions belonging to the thesis, entitled:

"Identification and characterization of a new potato immune receptor against *Phytophthora infestans*"

Yerisf C. Torres Ascurra
Wageningen, 30 November 2023

Identification and characterization of a new potato immune receptor against *Phytophthora infestans*

Yerisf C. Torres Ascurra

Thesis committee

Promotor
Prof. Dr Richard G.F. Visser
Professor of Plant Breeding
Wageningen University & Research

Co-promotor
Dr Vivianne G.A.A. Vleeshouwers
Assistant professor, Plant Breeding
Wageningen University & Research

Other members
Prof. Dr Geert Smant, Wageningen University & Research
Prof. Dr Laura Grenville-Briggs, Swedish University of Agricultural Sciences, Uppsala, Sweden
Dr Mathieu Joosten, Wageningen University & Research
Dr Manos Domazakis, Enza Zaden, Enkhuizen, the Netherlands

This research was conducted under the auspices of the Graduate School Experimental Plant Sciences

Identification and characterization of a new potato immune receptor against *Phytophthora infestans*

Yerisf C. Torres Ascurra

Thesis

submitted in fulfilment of the requirements for the degree of doctor
at Wageningen University
by the authority of the Rector Magnificus,
Prof. Dr A.P.J. Mol,
in the presence of the
Thesis Committee appointed by the Academic Board
to be defended in public
on Thursday 30 November 2023
at 11 a.m. in the Omnia Auditorium

Yerisf C. Torres Ascurra
Identification and characterization of a new potato immune receptor against *Phytophthora infestans*, 172 pages.

PhD thesis, Wageningen University, Wageningen, the Netherlands (2023)
With references, with summary in English

ISBN: 978-94-6447-942-3
DOI: 10.18174/640479

Table of contents

Chapter 1

General introduction

This chapter was partly based on insights from:

Saraiva, M., Ściślak, M. E., Torres Ascurra, Y., Marti Ferrando, T., Zic, N., Henard, C., van West P., Trusch, F. & Vleeshouwers, V. G. The molecular dialog between oomycete effectors and their plant and animal hosts. Fungal Biology Reviews, 2023. 43: p. 100289.

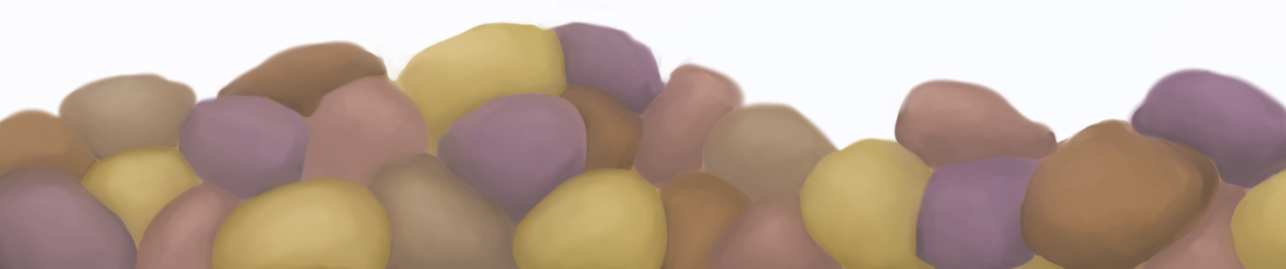

Potato

Potato (*Solanum tuberosum* L.) is the most important non-cereal food crop, exhibiting a consistent increase in production over the past three decades, with a yield of more than 359 million tons in 2020 [1]. Potato is an important staple for 1.3 billion people [2], and is considered a key crop for food security because of its efficiency (requires less land to produce the same amount of calories), versatility (can be grown in different climates), precocity (they produce tubers in only 60 days) and nutritional profile (a valuable source of vitamins, minerals and phytonutrients) [3].

The origin of cultivated potato has not been elucidated completely. Some studies indicate that potato domestication took place between 8,000-10,000 years ago, from wild species in the Andes of southern Peru [4, 5]. Phylogenetic analyses supported a monophyletic origin of cultivated potatoes from the northern component of the *S. brevicaule* complex in southern Peru [4]. By the time the Spanish invaders arrived to South America, potato was already an ancient domesticated plant, archeologically and historically evidenced by amazing ceramic pots depicting a potato tuber from the Moche culture in Peru (Fig. 1), and drawings of potato harvests from Felipe Huaman Poma de Ayala, respectively [6]. The first record of the modern cultivated potato outside of South America was reported in the Canari Islands (Spain), in 1567; then potato become rapidly cultivated in Europa and afterwards worldwide [7].

The modern cultivars, native cultivated potatoes (landraces) and wild potato species are grouped in the genus *Solanum* L. section *Petota*, the tuber-bearing *Solanum* species. The taxonomy of section *Petota* has been subject of intensive and continuous research, since it is complicated because of its introgression, interspecific hybridization, sexual compatibility, the mixture of sexual and asexual reproduction [7]. In 1990, Hawkes described 228 wild species and 7 cultivated, while in 2006, a total of 188 wild and 1 cultivated species were estimated for this section, along with 3 species in section *Etuberosa* [7]. The most recent taxonomic revision recognizes 107 wild and 4 cultivated species [8]. The tuber-bearing *Solanum* species were classified by Hawkes in 19 series. However, the boundaries between some series are unclear, and not supported by molecular data [9]. Instead, now they are divided into four clades (1-4) based on plastid restriction site data or three clades based on nuclear DNA sequencing data [10].

The potato landraces, which are highly diverse (around 4000 varieties), are found in the Andean mountains and southern Chile, and are still grown and preserved by native farmers [11]. In contrast, wild *Solanum* species have a broader distribution, occurring from the southwestern United States to the south of Argentina, and Peru stands out for the high number of wild potato species as well as for the high number of rare wild potato species [12]. Given their widespread geographic distribution, wild potato species have adapted to a wide range of biotic and abiotic stresses, making them an invaluable resource for potato breeding. Modern genomic tools have

confirmed the crucial role of wild species in the spreading and evolution of the cultivated potato by transmitting alleles for tolerance or sequence variants that enabled *S. tuberosum* cultivation in Europe and the USA [5].

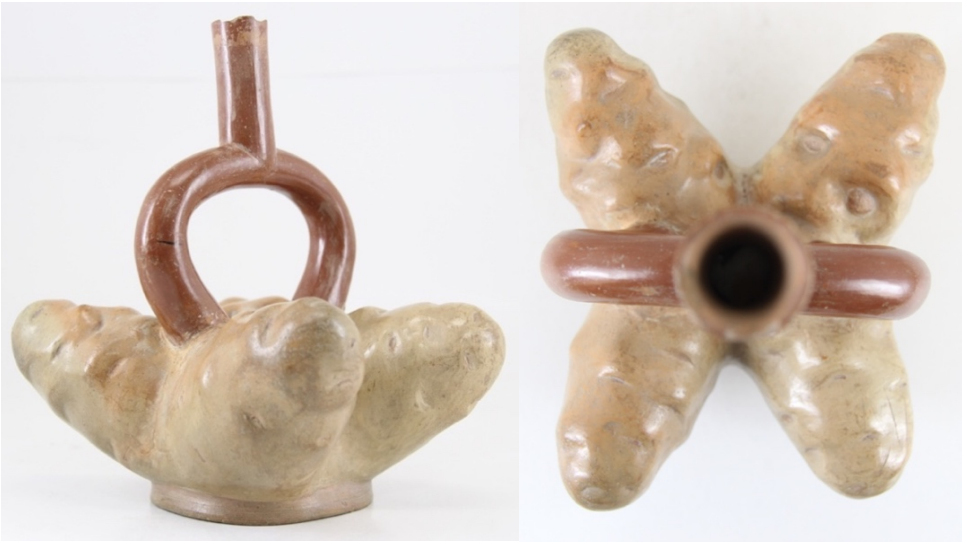

Figure 1. Sculptural ceramic of four potato tubers from the Moche culture (Museo Larco, Lima - Perú. ML013572). The Moche culture considered this Andean tuber as a symbol of the inner world, representing the world below, as it is the tuberous root of the plant that its edible. Images reproduced by kind permission of Museo Larco, Lima.

Potato cultivation is constantly threatened by many pathogens and pests, that significantly impact its production yield and quality. Among these threats, *Phytophthora infestans* causes the most devastating disease: late blight. Traditionally, resistance genes against *P. infestans* (*Rpi* genes) have been explored and exploited for breeding resistance. To date, almost 50 *Rpi* genes have been cloned from different *Solanum* species like *S. demissum*, *S. bulbocastanum*, *S. edinense*, *S. schenckii*, *S. hjertingii*, *S. stoloniferum*, *S. americanum*, *S. nigrescens*, *S. chacoense*, *S. mochiquense*, *S. venturii*, *S. phureja, S. tarijense* and others [13]. All these genes encode intracellular NLRs. However, the vast majority of the cloned *Rpi* genes can be overcome by the, adequately denominated, plant and *Rpi* gene destroyer [14-17]. Consequently, other sources of durable resistance are needed.

Phytophthora infestans

Phytophthora species belong to the oomycetes, a diverse group of the Stramenopiles clade [18], that includes both saprophytes and pathogens of plants, animals and microorganisms. The genus *Phytophthora,* which was named after the Greek word for 'plant destroyer' encompasses more than 150 species and cause immense economic losses to important crops like potato, tomato, soybean, tobacco, cacao and others [19, 20]. A study of the more important plant-pathogenic oomycetes in plant pathology, ranked six *Phytophthora* species in the top 10 (*P. infestans*, *P. ramorum*, *P. sojae*, *P.capsici*, *P. cinammomi* and *P. parasitica*) [21], highlighting the economic and academic significance of the genus.

Phytophthora infestans (Mont.) de Bary*,* infamous for attacking the European potato crop in the mid-1840s and causing the Irish famine, is the causal agent of late blight, which is considered the most important disease affecting potato worldwide. It is estimated that the total losses (cost of control and damage) are close to € 9.4 billion per year [22, 23]. Scientifically, *P. infestans* has also been important, it was the first microorganism proven to be responsible for disease, contributing to changing concepts about plant diseases [24]. Overall, the adversarial role of this pathogen in society, both in the past and present, is evident.

The infection cycle of *P. infestans* starts with a sporangium, which germinates directly or releases swimming biflagellated zoospores on the plant surface, that encyst and germinate to form a knife-like structure at the end of the germ tube, which apply force under an oblique angle breaking the surface and mediating host entry. This mechanism was recently discovered and was denominated 'naifu invasion' after the Japanese knives [25]. Upon penetration, an infection vesicle is formed inside the first invaded cell, from which the hyphae grow intercellularly and extend digit-like haustoria into host cells and the successful infection progresses. Later, *P. infestans* switches to necrotrophic growth, in which the cells die and are digested, showing visible lesions in the plant [26, 27]. The asexual cycle of *P. infestans* can be completed rapidly, producing huge amounts of sporangia that lead to devastating epidemics (Fig. 2) [14]. Besides, this pathogen can also reproduce sexually, contributing to genetic diversity, survival, population structure and disease epidemics [28].

Genomic studies have contributed to understand why *P. infestans* is such a successful pathogen. For instance, its genome is much larger (240 Mb) than other related *Phytophthora* species; has an extremely high repeat content; and a distinctive organization, with expanded, repeat-rich and gene-sparse regions that contain effector genes, and repeat-poor and gene-dense regions that contain housekeeping genes [29]. Rafaelle et al. reported a two-speed *P. infestans* genome, with different regions evolving at markedly different rates. They found that the gene-sparse, repeat-rich regions, enriched in genes induced in plants, have higher rates of structural polymorphism and positive selection, pointing to host adaptation as a driving force behind. *P. infestans* genome evolution [30].

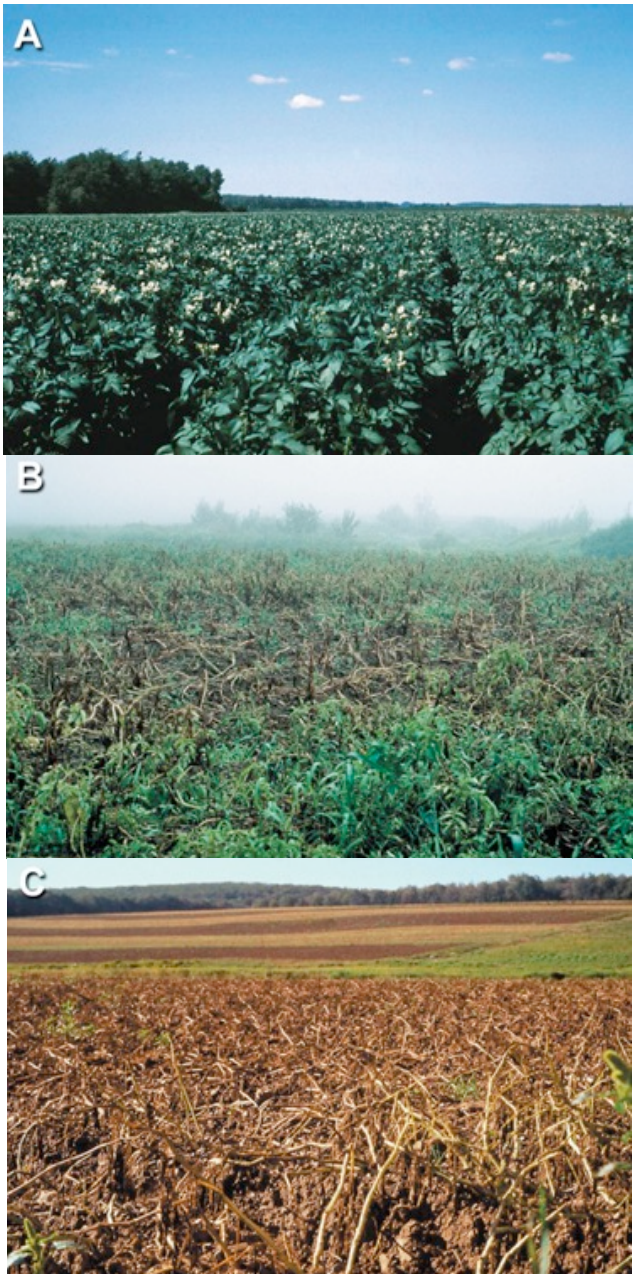

Figure 2. Destruction of a potato field by *Phytophthora infestans* A. Week 1, an apparently healthy potato field is observed, B. Week 2, the field shows severely diseased plants, C. Week 3, the field is destroyed by the oomycete. Figure taken from Fry. 2008 [14].

Plant immunity

Plants defend themselves from pathogens using a two-layered immune system, which has been conceptualized by the zig-zag model [31]. The frontline defense employs pattern recognition receptors (PRRs) that recognize microbe- or pathogen-associated molecular patterns (MAMPs or PAMPs) at the cell surface and activate pattern-triggered immunity (PTI); however, many pathogens deploy effectors that can suppress PTI, resulting in effector-triggered susceptibility (ETS) [31]. The second line of defense uses intracellular nucleotide-binding domain leucine-rich repeat containing receptors (NLRs) that recognize those effectors, and activate effector triggered immunity (ETI). PTI gives a basal defense generally effective against non-adapted pathogens, whereas ETI responses occur faster, and are more prolonged/robust against adapted pathogens [31, 32]. However, this distinction between PTI and ETI is not clear, instead, the discovery of ligands and receptors with intermediate characteristics indicate that there is a continuum between PTI and ETI [33].

PTI and ETI involve different activation mechanisms and early signaling cascades, however, recent studies have shown that these two layers are co-dependent and mutually potentiate to confer resistance against pathogens [34, 35]. On one hand, it has been observed that the activation of effector-triggered immunity (ETI) response requires the presence of PRRs and co-receptors. This was demonstrated using a mutant strain of *Pseudomonas syringae*, lacking effector genes (except *AvrRpt2*, which activates RPS2) and coronatine biosynthesis, in which ETI was not activated in lines deficient in PRRs and co-receptors [35]. Similar findings were reported using PstDC3000 engineered to express *AvrRps4* [34]. On the other hand, experiments with *A. thaliana* lines carrying inducible bacterial effectors revealed interesting observations. The expression of *AvrRps4* alone did not activate reactive oxygen species (ROS), but it enhanced the production of ROS induced by PAMPs [34]. Likewise, the expression of *AvrRpt2* alone triggered a weak and slower ROS burst, but in presence of flg22 it induced a stronger and sustained ROS burst [35]. Besides, it was reported that ETI upregulated both transcript and protein level of PTI pathway components. These two studies indicate that ETI requires PTI, and ETI potentiates PTI to enhance resistance against *P. syringae* in *Arabidopsis*, unifying the two layers of immunity and redefining our current view of plant immunity (Figure 3).

Besides the functional link of PRRs and NLRs, an evolutionary correlation between the number of these receptors across plants species was found, which likely implies that PRRs and NLRs are interdependent and they operate synergistically to mount strong immune responses against pathogens [36].

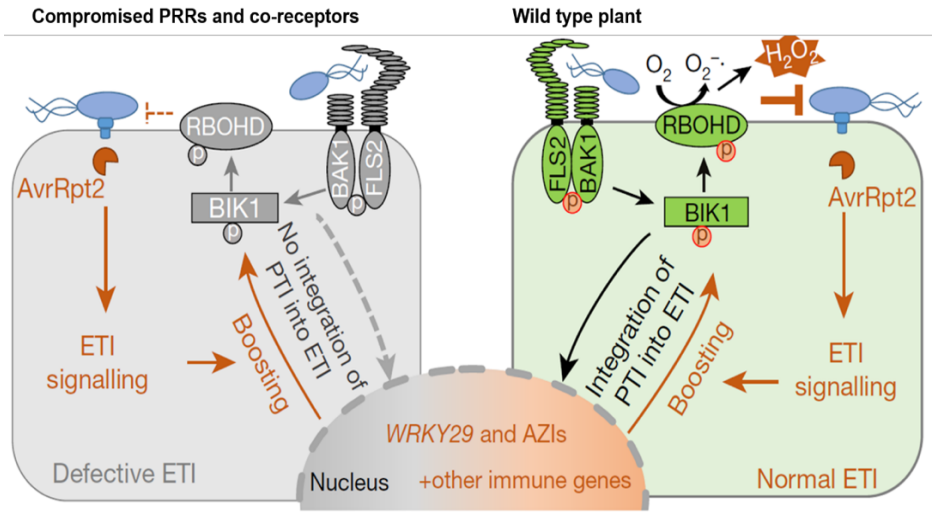

Figure 3. PRR and co-receptors are required for ETI. The recognition of the effector AvrRpt2 by the NLR RPS2 triggers the accumulation of multiple PRR signalling components which boost the PTI response. However, in absence of PRRs and co-receptors (grey), although NLR activation still induces PTI components, many of these components, such as BIK1 and RBOHD, are inactive, leading to lack of ROS production and defective ETI. Figure taken from Yuan et al. 2021 [35] and reproduced with permission from Springer Nature.

The frontline: PRRs and PAMPs

PAMPs are conserved epitopes within molecules that are indispensable for the microbial survival and fitness. These epitopes are widely distributed within a class of microbes and are absent in the host [37-39]. These patterns are sensed by a broad range of potential hosts through PRRs, that so far include receptor-like kinases (RLKs) and receptor-like proteins (RLPs) that reside at the plant cell surface. RLKs contain a ligand-binding ectodomain, a single-pass transmembrane domain, and an intracellular kinase domain, while RLPs lack an intracellular signaling domain [39]. The PRRs that are best studied to date have leucine-rich repeats (LRR) as their ligand-binding ectodomain which preferentially bind proteins or peptides, such a flg22 (bacterial flagellin) or elf18 (bacterial elongation factor EF-Tu). Flg22 and its corresponding RLK identified in *Arabidopsis thaliana*, FLAGELLIN-SENSING 2 (FLS2), represent canonical PAMP-PRR pair [40, 41].

PRRs form complexes with other kinases to start the immune signaling. For example, after flg22 binding, FLS2 and the BRASSINOSTEROID INSENSITIVE 1-ASSOCIATED KINASE1 (BAK1) form a complex *in vivo* (in a specific ligand-dependent manner), that results in their trans-phosphorylation almost instantaneously [42, 43]. The rapid heterodimerization with BAK1 and phosphorylation induced by ligand perception

also occurs with other LRR-RLKs, like EF-TU RECEPTOR (EFR) and PEP1 RECEPTOR (PEPR1), receptors of elf18 and endogenous AtPep1, respectively [43]. The crystal structure of the complex FLS2/BAK1/flg22 has revealed that BAK1 acts as a co-receptor by recognizing the C-terminal segment of FLS2-bound flg22 [44]. Nowadays, it is well-documented that BAK1 forms complexes with many LRR-containing receptors involved in immunity, growth and development; and acts as a co-receptor not only for LRR-RLK, but also for LRR-RLPs [39].

Unlike the RLKs, the RLPs lack a signaling kinase domain, so they must interact with additional components for intracellular activation of immune signaling. It was found that the tomato orthologues of the *A. thaliana* SUPPRESSOR OF BIR-1 (SOBIR1) and SOBIR1-like interact with the RLPs Cf-4 and Ve1 and are required for the immune responses mediated by these receptors [45]. Further research has shown that RLP23, Cf-4, Cf-9 and ELICITIN RESPONSE protein (ELR) constitutively associates with SOBIR1, and that BAK1 is recruited to this bipartite receptor complex upon ligand binding [46-48]. So, it has been postulated that SOBIR1 and LRR-RLPs constitutively interact to form a bipartite RLKs, which can recruit BAK1 upon ligand perception [49].

The BOTRYTIS-INDUCED KINASE (BIK1) is a central signaling component, that links the PAMP receptor complex to downstream intracellular signaling [50, 51]. After flg22 perception, BAK1 phosphorylates BIK1, then BIK1 trans-phosphorylates BAK1 and dissociates from the PRR complex to propagate the signaling downstream [52]. BIK1 also interacts with EFR, CHITIN ELICITOR RECEPTOR KINASE 1(CERK1) and PEPR1 [53, 54]. Interestingly, it was found that BIK1, which positively regulates flg22-induced ROS, acts as a negative regulator of receptor-like proteins such as RLP23 [55].

Upon recognition of a PAMP by its specific PRR, defense responses are initiated, for instance, influx of calcium, ROS, activation of mitogen cascade, transcriptional reprogramming and ultimately immunity [39, 56]. The calcium channels CYCLID NUCLEOTIDE-GATED CHANNEL (CNGNs) and OSCA1.3 are activated by BIK1, which leads to the rapid calcium influx, that in turn activates CALCIUM-DEPENDENT PROTEIN KINASES (CDPKs) [57, 58]. This is followed by ROS production, via the RESPIRATORY BURST NADPH OXIDASE HOMOLOG D (RBOHD), which is directly phosphorylated by BIK1 upon PAMP perception [59]. The rapid activation of mitogen-activated protein kinases (MAPKs) is also part of the PTI responses, it was found that there are two different cascades that lead to the activation of four MAPKs in *Arabidopsis* upon PAMP treatment [51, 60, 61]. Not only MAPKs, but CDPKs and RLCKs phosphorylate and activate multiple defense-related transcription factors that leads to a transcriptional reprogramming [62]. Other important players are the defense-related hormones, such as ethylene (ET), salicylic acid (SA) and jasmonic acid (JA), the three hormones are required for local PAMP induced resistance to pathogens [63] and may induce secondary transcriptional waves [51]. One of the latest typical responses is the callose deposition [56], to reinforce the cell wall at sites of infection and undermine pathogen growth. All these responses together lead to the establishment of PTI.

NLRs and effectors

Effectors are pathogen-secreted molecules with dual activity, they manipulate host cell structure and function to facilitate infection, and/or trigger defense responses [64]. So far, it is known that effectors activities are sensed by NLRs by three mechanisms: direct recognition; indirect recognition, by monitoring effector targets or decoy proteins; and combination of direct and indirect recognition, through the incorporation in the NLRs of integrated domains (IDs) that mimic pathogen targets [65]. The NLRs consist of a non-conserved N-terminal domain, a central NB-ARC domain (nucleotide-binding adaptor shared by Apaf-1, resistance proteins (R) and CED-4) and a C-terminal LRR domain [66]. Based on their N-terminal domain they can be divided in three classes: coiled-coil (CC) NLRs (CNLs), Toll/interleukin-1 receptor/Resistance protein (TIR) NLRs (TNLs) and RESISTANCE TO POWDERY MILDEW 9-like coiled-coil NLRs (RNLs) [66].

Functionally, two types of NLRs can be distinguished: sensor NLRs that are involved in the recognition of effectors, and helper NLRs that are required by other NLRs to initiate immune signaling [67]. Although most of sensor NLRs appear to engage other molecules to function, working as pairs or complex networks, some CNLs mediate immune responses alone, as a unit, and are called singleton NLRs [68]. HOPZ-ACTIVATED RESISTANCE 1 (ZAR1) is a well-studied singleton CNL that indirectly recognizes the bacterial effectors AvrAC by its association with the RESISTANCE-RELATED KINASE 1 (RKS1), and recruits the uridylylated decoy PBS1-like protein (PBL2) to trigger ZAR1 activation [69]. Cryo-electron microscopy of ZAR1 has revealed that the uridylylated PBL2 is exclusively recognized by RKS1, which interacts with the LRR domain of ZAR1, this association allosterically promotes the release of ADP from the inactive ZAR1 which leads to an intermediate state [69]. However, when ATP is present, the ZAR1-RKS1-PBL2 complex oligomerizes and forms the ZAR1 resistosome, a wheel-like pentameric structure, where the very N-terminal α-helix of ZAR1 becomes solvent-exposed and forms a funnel-shaped structure that is required for plasma membrane association, cell death and disease resistance [70]. A recent study has shown that the ZAR1 resistosome acts as a calcium-permeable cation channel to trigger immunity and cell death [71].

Helper NLRs participate in signaling networks downstream of sensor NLRs, these can be RNLs or NLR-required for cell death (NRC). So far, there are two types of RNLs: the ACTIVATED DISEASE RESISTANCE 1 (ADR1) family, required for complete function of some TNLs and CNLs; and the N-REQUIREMENT GENE 1 (NRG1) family required for others TNLs [72]. On the other hand, the NRCs are required by many Solanaceae CNLs, NRCs and the NRC-dependent NLRs form complex genetic network to confer resistance against oomycetes, bacteria, viruses, nematodes and insects [73]. Additionally, all TNL proteins require the lipase-like protein ENHANCED DISEASE SUSCEPTIBILITY 1 (EDS1), which forms stable heterodimers with SENESCENCE-ASSOCIATED GENE 101 (SAG101) or PHYTOALEXIN DEFICIENT 4 (PAD4) [74]. CNLs do

not appear to directly require EDS1, but they are dependent on the integrin-like NON-RACE-SPECIFIC DISEASE RESISTANCE 1 (NDR1) protein [75]. Recently, it was found that EDS1, PAD4 and ADR1 have a prominent role for the immune responses mediated by LRR-RLPs, such as RLP23 [76], evidencing again the connection of PTI and ETI.

Oomycete PAMPs/apoplastic effectors and their PRRs

During infection oomycetes release PAMPs and apoplastic effectors that can be recognized by plant PRRs. Up to now, only few pairs of PAMP/apoplastic effector-PRR have been elucidated (Fig. 4). For instance, elicitins, which are a family of structurally related 10 kDa proteins; secreted by oomycetes, particularly *Phytophthora* and *Pythium* species; do not show sequence similarity to plant proteins. In this way they can be recognized as non-self-molecules and bind sterols and other lipids that are important for oomycetes growth and sporulation [77], contributing to genetic variation which potentially increases the virulence of certain strains due to higher selective pressure resistance [78]. INF1 is a major elicitin secreted by *P. infestans* [79]. Its receptor, the LRR-RLP ELR, was identified in the wild potato *Solanum microdontum*. ELR associates constitutively with SOBIR1, and upon INF1 treatment, the complex recruits BAK1 to specifically recognizes elicitins of *Phytophthora* spp. [47, 80]. ELR expression into cultivated potato resulted in enhanced resistance to *P. infestans* [80]. A novel receptor for elicitins called LRR-RLP REL (Responsive to Elicitins) has been recently identified in *Nicotiana benthamiana* [81].

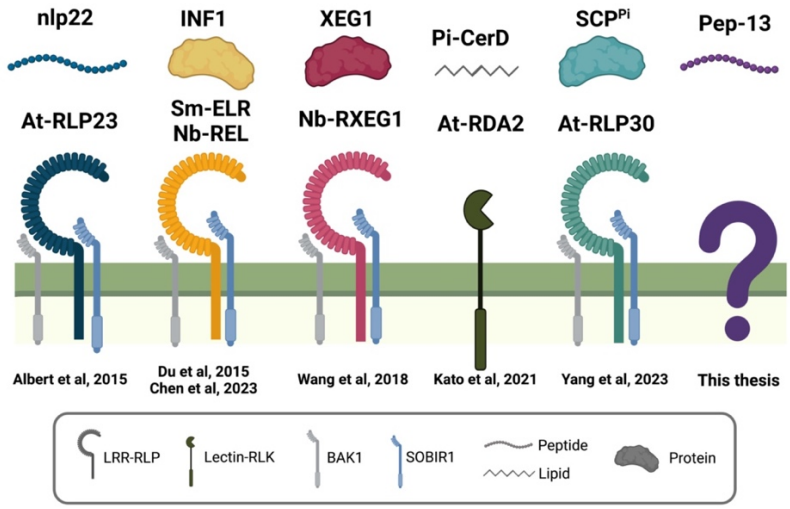

Figure 4. Characterized PRRs and their corresponding oomycetes elicitors. Abbreviations for plant species: *A. thaliana*, At; *S. microdontum*, Sm; *N. benthamiana*, Nb. This figure was created with Biorender.

Unlike the elicitins, the NEP1 (for necrosis and ethylene-inducing peptide 1) LIKE PROTEINS (NLPs) show a wide taxonomic distribution, they occur in oomycetes, fungi and bacteria [82]. NLPs are 24 kDa conserved proteins that activate defense-associated responses, such as leaf necrosis, ethylene synthesis, expression of defense-related genes, and cell death; and contribute to the virulence of necrotrophic fungi and bacteria [82]. It was found that a peptide fragment, the nlp20 motif, behaves like a immunogenic pattern, similar to flg22 [83]. The PRR responsible for the recognition of nlp20, LRR-RLP RLP23, was identified in *Arabidopsis*. In a similar way to ELR, RLP23 forms a complex with SOBIR1, that recruits BAK1 after the nlp20 binding; and its transfer to *Solanum tuberosum* confers nlp20 recognition and enhanced resistance to *P. infestans* [46].

The glycoside hydrolase family 12 (GH12) protein XEG1 is produced by the soybean pathogen *Phytophthora sojae* and exhibits xyloglucanase and β-glucanase activity. It was found that PsXEG1 can trigger cell death in *N. benthamiana*, tomato, pepper and soybean; a response that requires the secretion of PsXEG1 and the presence of BAK1, which indicates that XEG1 is recognized in the extracellular space as a PAMP or apoplastic effector. Using a high-throughput approach, the LRR receptor-like protein RESPONSE TO XEG1 (RXEG1) was identified in *N. benthamiana* as the responsible one for the recognition of PsXEG1. RXEG1 associates with PsXEG1 via the LRR domain and forms a complex with BAK and SOBIR1 [84]. Overexpression of RXEG1 in *N. benthamiana* significantly reduces disease severity caused by *P. parasitica*, contributing to plant immunity [84]. A remarkable arms race has been documented for XEG1. When it is secreted at early stages of infection, it acts as an important virulence factor [85]. However, PsXEG1 is degraded by the host aspartic protease GmAP5, which is reduced after N-glycosylation of PsXEG1. To further increase XEG1 activity in the apoplast, a PsXEG1 paralogue (PsXLP1) which is protected against GmAP5 proteolysis by a C-terminal deletion is secreted to reduce total GmAP5 activity [86] (Fig. 5). This continuous arms race for physiological dominance is driving the (co-) evolution of host defence and virulence genes in the apoplast.

Recently, the ceramide D (Pi-CerD) was reported as an elicitor from *P. infestans*, and it has been shown that Pi-CerD induces immune responses in potato and *Arabidopsis* [87]. This study also reported that Pi-CerD is cleaved in the apoplast by the ceramidase NCER, and the resulting 9-methyl-branched sphingoid base is recognized as a PAMP by the lectin RLK RDA2 [87]. Besides, RDA2 and NCER contribute to the Arabidopsis immune against the pathogen *Hyaloperonospora arabidopsidis* [87].

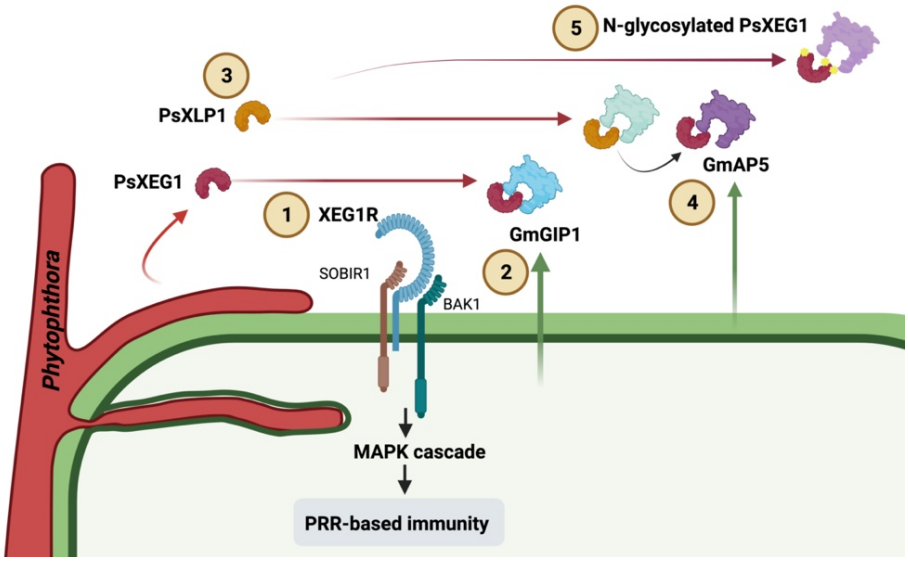

Figure 5. Schematic representation of and integrated counterdefense by *P. sojae* against GmGIP1 and GmAP5 attacks on PsXEG1 (adapted from Saraiva et al. 2023). (1) *Phytophthora sojae* secretes apoplastic hydrolases like the glycoside hydrolase PsXEG1, which upon recognition by RXEG1 initiates the PRR-based immunity. (2) PsXEG1 can be inhibited by GmGIP1, however, (3) *P. sojae* secretes the decoy PsXLP1 to protect PsXEG1. (4) In response a second inhibitor GmAP5 degrades PsXEG1, and (5) as a counteract the N-glycosylation protects PsXEG1 from degradation.

The Arabidopsis receptor-like protein (RLP30) detects the SMALL CYSTEINE-RICH PROTEIN (SCP^{SS}) secreted by *Sclerotinia sclerotiorum* [88]. SCP^{SS} is closely related to the PAMP VmE02 from *Valsa mali* (recognized by *N. benthamiana* RLP RE02) [89], and can be recognized by RE02 in *N. benthamiana*. RLP30 can also recognize SCPs from fungi and oomycetes. For instance, the *P. infestans* homolog, SCP^{Pi}, can be sensed by RLP30 in Arabidopsis [88].

One of the first, and well characterized PAMP of *Phytophthora* is Pep-13. Its story brings us back to 1991, when a 42 kDa glycoprotein was purified and identified from *Phytophthora sojae* culture filtrate, as a potent elicitor of phytoalexin accumulation in cultured parsley cells and protoplasts [90] (Fig. 6A). Using endo- and exopeptidases, it was found that an oligopeptide of 13 amino acids, Pep-13 (H_2N-VWNQPVRGFKVYE-COOH), within this glycoprotein was necessary and sufficient to trigger a complex defense response in parsley cells [91] (Fig. 6B), comprising H^+/Ca^{2+} influxes, K^+/Cl^- effluxes, oxidative burst, activation of Ca^{2+} permeable ion channel, posttranslational and transcriptional activation of MAP kinases, expression of defense-related genes, phytoalexin formation and ethylene biosynthesis [91-93]. Pep-25, a slightly longer

version of Pep-13, exhibited the same elicitor activity as Pep-13 [91]. Alanine substitution scanning allowed the identification of two single amino acids residues (Tryptophane-231 and Proline-234) as important for elicitor activity in parsley cells [91]. Further studies showed that this 42 kDa glycoprotein (GP42) is a calcium-dependent cell wall-associated transglutaminase (TGase), and that Pep-13 is a surface-exposed motif present and conserved among different species of *Phytophthora* Tgases [94] (Fig. 6C). Besides, the previously reported amino acids to be important to elicit defense response, were found to be important also for the TGase activity [94] (Fig. 6D).

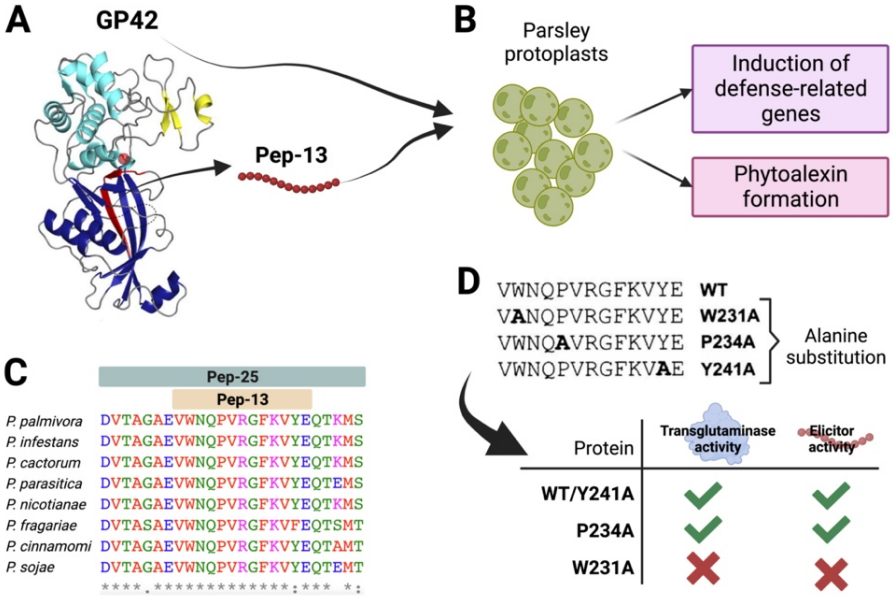

Figure 6. The *Phytophthora* PAMP Pep-13. A. *P. sojae* GP42 glycoprotein structure and the fragment Pep-13 highlighted in red [95]. B. Pep-13 produce the same defense responses as GP42 in parsley. C. Transglutaminse GP42 homologs are conserved among the genus *Phytophthora*. Pep-13 was highly conserved among all species analyzed. D. Schematic representation of the mutations introduced, and their effects on enzyme and elicitor activity. This figure was created with Biorender.

Transglutaminase enzymes (EC 2.3.2.13) catalyze calcium-dependent acyltransferase reactions between a γ-carboxyamide group of glutamine and the ε-amino group of lysine or other primary amines, resulting in irreversible protein cross-linking [94, 96, 97]. These enzymes are widely distributed in archaea, bacteria, and eukaryotes, although GP42-related proteins are only present in plant pathogenic

oomycetes from the Peronosporales order and in marine *Vibrio* bacteria [95]. It was previously found by immunolocalization assays that GP42 is associated with hyphal cell walls of *P. sojae* [98]. *P. infestans* TGases (M81 family) were reported to share characteristics consistent with being secreted or components of the cell wall [97]. For instance, presence of signal peptides, acidic pIs (3.9 to 5.5), sites for O-glycosylation, extensive proline- and threonine-rich domain and serine- and alanine-rich tracts [97]. M81C and M81D expression was detected during zoosporogenesis, while M81E expression was restricted to hyphae [97]. Additionally, high expression of PITG_22117 (that encodes another *P. infestans* TGase) was reported in zoospores, appressoria and mainly germinating cysts [99]. Recently, chemical treatment and RNAi silencing assays showed that the transglutaminases are crucial for grow, germination and subsequent pathogenicity of *P. infestans* [100]. These findings together suggest that the role of the GP42-related proteins is to strengthen cell walls or enhance adhesion during interaction of *P. infestans* with its host.

Interestingly, it has been shown that Pep-13 triggers also defense responses in potato cultured cells and plants, such as expression of defense-related genes, ROS production, and hypersensitive response-like cell death in leaves [94, 101]. When potato plants unable to accumulate SA are treated with Pep-13, responses like cell death, ROS burst and JA accumulation are impaired, which indicates that SA is important for the defense responses triggered by Pep-13; however the expression of defense-related genes is not impaired, indicating that Pep-13 might activate SA-dependent and -independent responses in potato [101]. Furthermore, it was reported that early responses like ROS production and MAP kinases activation are highly reduced in SERK3A/B-iRNA potato plants treated with Pep-13 [102], which might indicate that a LRR-containing PRR is involved in Pep-13 recognition. Despite all the accumulated knowledge about Pep-13, the identity of its corresponsive PRR has remained elusive until now.

Outline of the thesis

Almost 180 years after the infamous Irish Potato Famine, late blight caused by *P. infestans* remains the most devastating disease of global potato production [103]. *Rpi* genes have been traditionally studied and utilized to confer resistance against *P. infestans*. *Rpi genes* encode for NLRs that provide a strong immune response in plants, called ETI. However, individual *Rpi* genes have been rendered ineffective against this pathogen. In the context of potato- *P. infestans* interaction, PTI has been understudied and unexploited, compared to ETI. So far, only one *Solanum* PRR (ELR) has been identified, many PRRs remain to be found, characterized and deployed against *P. infestans*. Only the complete understanding of the pathosystem will allow the generation of effective solutions to late blight disease.

In **Chapter 2**, we describe and provide a detailed protocol for a combined approach to identify new PRRs. Firstly, applying a Bulked segregant RNA-Seq (BSR-Seq) to accelerate and leave out the traditional genetic mapping that involves the development of a high number of molecular markers. Secondly, using a high-throughput recombinant screening of *in vitro* plants, that optimizes the fine-mapping process in terms of time, space and labor.

In **Chapter 3**, we apply the previously described protocol, to fine-map the potato receptor of Pep13/25. The wild *Solanum microdontum* genotype GIG362-6, identified as a Pep-25 responding plant, was used to generate a segregating population. BSR-Seq of responsive and non-responsive bulks allowed the mapping of the Pep-25 receptor to the top of chromosome 3. The further fine-mapping, BAC library screening and BACs sequencing led to the construction of the GIG362-6 physical map, and determination of a narrowed mapping interval (not completely covered by the BAC sequences), that contains candidate genes. We also explore the degree of conservation of Pep-13 among *Phytophthora,* oomycetes and other filamentous pathogens.

The absence of a high-quality genome sequence of GIG362-6 hampered the identification of the Pep-25 receptor. So, in **Chapter 4,** we decide to exploit the reference potato genome genotype DM1-3 516 R44, which is also Pep-13/25 responsive, and has a high-quality genome sequence [104]. A new mapping population was generated, and the receptor was fine-mapped to a small mapping interval with new candidate genes in this different genetic background. The complementation assays revealed us the identity of the gene responsible for the recognition of Pep-13 and was named *PERU* (**Pe**p-13 **R**eceptor **U**nit). We employ a multidisciplinary approach to characterize this new PRR and demonstrate its specific interaction with Pep-13 and co-receptors. Disease assays using transgenic lines overexpressing *PERU* or knock-out plants for *PERU* show the role of PERU for immunity against *P. infestans*.

In **Chapter 4**, we also explore the presence and distribution of Pep-13/25 recognition in the *Solanum* section *Petota*. By screening 476 *Solanum* genotypes, including both wild and cultivated species, we aim to explore the ligand specificity across the section *Petota*. Additionally, valuable insights into the origin of the PERU receptor are obtained through studying the geographic origins of the examined *Solanum* genotypes and conducting phylogenomic analyses.

In **Chapter 5**, we attempt to deploy the RLK PERU by stacking it with the RLP RLP23, since both have shown to enhance resistance against *Phytophthora infestans*. We first aimed to determine the sensitivity of potato cultivar Atlantic to Pep-13 and nlp20, and we explored if the presence of these two PRRs had an additive effect on the potato immune responses like ROS production and ethylene accumulation, and ultimately on the resistance against *P. infestans*.

Finally, **Chapter 6** summarizes and discusses the results of this thesis, taking into consideration the new plant immunity findings.

References

1. FAO. *FAOSTAT Statistical Database*. 2022 17-03-2022]; Available from: https://www.fao.org/faostat/en/#data/QCL.
2. Stokstad, E., *The new potato.* Science, 2019. **363**(6427): p. 574-577.
3. Navarre, D.A., A. Goyer, and R. Shakya, *Chapter 14 - Nutritional Value of Potatoes: Vitamin, Phytonutrient, and Mineral Content*, in *Advances in Potato Chemistry and Technology*, J. Singh and L. Kaur, Editors. 2009, Academic Press: San Diego. p. 395-424.
4. Spooner, D.M., et al., *A single domestication for potato based on multilocus amplified fragment length polymorphism genotyping.* Proceedings of the National Academy of Sciences of the United States of America, 2005. **102**(41): p. 14694-14699.
5. Hardigan, M.A., et al., *Genome diversity of tuber-bearing Solanum uncovers complex evolutionary history and targets of domestication in the cultivated potato.* Proceedings of the National Academy of Sciences, 2017. **114**(46): p. E9999-E10008.
6. Hawkes, J.G., *History of the potato*, in *The Potato Crop: The scientific basis for improvement*, P.M. Harris, Editor. 1992, Springer Netherlands: Dordrecht. p. 1-12.
7. Spooner, D. and A. Salas, in *Handbook of potato production, improvement and post-harvest management.*, J.a.K. Gopal, S. M, Editor. 2006, Binghampton: NY. p. 1-39.
8. Spooner, D.M., et al., *Systematics, Diversity, Genetics, and Evolution of Wild and Cultivated Potatoes.* The Botanical Review, 2014. **80**(4): p. 283-383.
9. Jacobs, M.M.J., et al., *AFLP analysis reveals a lack of phylogenetic structure within Solanum section Petota.* BMC Evolutionary Biology, 2008. **8**(1): p. 145.
10. Spooner, D.M., et al., *Systematics, Diversity, Genetics, and Evolution of Wild and Cultivated Potatoes.* Botanical Review, 2014. **80**(4): p. 283-383.
11. Spooner, D.M. and W.L.A. Hetterscheid, *13. Origins, Evolution, and Group Classifi cation of Cultivated Potatoes*, in *Darwin's Harvest: New Approaches to the Origins, Evolution, and Conservation of Crops*, M. Timothy, Editor. 2006, Columbia University Press. p. 285-307.
12. Hijmans, R.J. and D.M. Spooner, *Geographic distribution of wild potato species.* American Journal of Botany, 2001. **88**(11): p. 2101-2112.
13. Paluchowska, P., J. Śliwka, and Z. Yin, *Late blight resistance genes in potato breeding.* Planta, 2022. **255**(6): p. 127.
14. Fry, W., *Phytophthora infestans: the plant (and R gene) destroyer.* Molecular Plant Pathology, 2008. **9**(3): p. 385-402.
15. Vleeshouwers, V.G.A.A., et al., *Understanding and Exploiting Late Blight Resistance in the Age of Effectors.* Annual Review of Phytopathology, 2011. **49**(1): p. 507-531.
16. Du, J. and V.G.A.A. Vleeshouwers, *New Strategies Towards Durable Late Blight Resistance in Potato*, in *The Potato Genome*, S. Kumar Chakrabarti, C. Xie, and J. Kumar Tiwari, Editors. 2017, Springer International Publishing: Cham. p. 161-169.
17. Witek, K., et al., *A complex resistance locus in Solanum americanum recognizes a conserved Phytophthora effector.* Nature Plants, 2021. **7**(2): p. 198-208.
18. Keeling, P.J., et al., *The tree of eukaryotes.* Trends in Ecology & Evolution, 2005. **20**(12): p. 670-676.
19. Thines, M., *Taxonomy and phylogeny of Phytophthora and related oomycetes.* Phytophthora: A Global Perspective. CABI, UK, 2013: p. 11-8.
20. Yang, X., B.M. Tyler, and C. Hong, *An expanded phylogeny for the genus Phytophthora.* IMA Fungus, 2017. **8**(2): p. 355-384.
21. Kamoun, S., et al., *The Top 10 oomycete pathogens in molecular plant pathology.* Molecular Plant Pathology, 2015. **16**(4): p. 413-434.
22. Haverkort, A.J., et al., *Societal Costs of Late Blight in Potato and Prospects of Durable Resistance Through Cisgenic Modification.* Potato Research, 2008. **51**(1): p. 47-57.

23. Haverkort, A.J., et al., *Durable Late Blight Resistance in Potato Through Dynamic Varieties Obtained by Cisgenesis: Scientific and Societal Advances in the DuRPh Project.* Potato Research, 2016. **59**(1): p. 35-66.
24. Judelson, H.S. and F.A. Blanco, *The spores of Phytophthora: weapons of the plant destroyer.* Nature Reviews Microbiology, 2005. **3**(1): p. 47-58.
25. Bronkhorst, J., et al., *A slicing mechanism facilitates host entry by plant-pathogenic Phytophthora.* Nature Microbiology, 2021. **6**(8): p. 1000-1006.
26. Whisson, S.C., et al., *The cell biology of late blight disease.* Current Opinion in Microbiology, 2016. **34**: p. 127-135.
27. Boevink, P.C., et al., *Devastating intimacy: the cell biology of plant–Phytophthora interactions.* New Phytologist, 2020. **228**(2): p. 445-458.
28. Fry, W.E., et al., *Population Genetics and Population Diversity of Phytophthora infestans*, in *Oomycete Genetics and Genomics*. 2009. p. 139-164.
29. Haas, B.J., et al., *Genome sequence and analysis of the Irish potato famine pathogen Phytophthora infestans.* Nature, 2009. **461**(7262): p. 393-398.
30. Raffaele, S., et al., *Genome Evolution Following Host Jumps in the Irish Potato Famine Pathogen Lineage.* Science, 2010. **330**(6010): p. 1540-1543.
31. Jones, J.D.G. and J.L. Dangl, *The plant immune system.* Nature, 2006. **444**(7117): p. 323-329.
32. Dodds, P.N. and J.P. Rathjen, *Plant immunity: towards an integrated view of plant–pathogen interactions.* Nature Reviews Genetics, 2010. **11**(8): p. 539-548.
33. Thomma, B.P.H.J., T. Nürnberger, and M.H.A.J. Joosten, *Of PAMPs and Effectors: The Blurred PTI-ETI Dichotomy.* The Plant Cell, 2011. **23**(1): p. 4-15.
34. Ngou, B.P.M., et al., *Mutual potentiation of plant immunity by cell-surface and intracellular receptors.* Nature, 2021. **592**(7852): p. 110-115.
35. Yuan, M., et al., *Pattern-recognition receptors are required for NLR-mediated plant immunity.* Nature, 2021. **592**(7852): p. 105-109.
36. Ngou, B.P.M., et al., *Concerted expansion and contraction of immune receptor gene repertoires in plant genomes.* Nature Plants, 2022. **8**(10): p. 1146-1152.
37. Nürnberger, T., et al., *Innate immunity in plants and animals: striking similarities and obvious differences.* Immunological Reviews, 2004. **198**(1): p. 249-266.
38. Schwessinger, B. and C. Zipfel, *News from the frontline: recent insights into PAMP-triggered immunity in plants.* Current Opinion in Plant Biology, 2008. **11**(4): p. 389-395.
39. Boutrot, F. and C. Zipfel, *Function, Discovery, and Exploitation of Plant Pattern Recognition Receptors for Broad-Spectrum Disease Resistance.* Annual Review of Phytopathology, 2017. **55**(1): p. 257-286.
40. Chinchilla, D., et al., *The Arabidopsis Receptor Kinase FLS2 Binds flg22 and Determines the Specificity of Flagellin Perception.* The Plant Cell, 2005. **18**(2): p. 465-476.
41. Gómez-Gómez, L. and T. Boller, *FLS2: An LRR Receptor–like Kinase Involved in the Perception of the Bacterial Elicitor Flagellin in Arabidopsis.* Molecular Cell, 2000. **5**(6): p. 1003-1011.
42. Chinchilla, D., et al., *A flagellin-induced complex of the receptor FLS2 and BAK1 initiates plant defence.* Nature, 2007. **448**(7152): p. 497-500.
43. Schulze, B., et al., *Rapid Heteromerization and Phosphorylation of Ligand-activated Plant Transmembrane Receptors and Their Associated Kinase BAK1.* Journal of Biological Chemistry, 2010. **285**(13): p. 9444-9451.
44. Sun, Y., et al., *Structural Basis for flg22-Induced Activation of the* Arabidopsis *FLS2-BAK1 Immune Complex.* Science, 2013. **342**(6158): p. 624-628.
45. Liebrand, T.W.H., et al., *Receptor-like kinase SOBIR1/EVR interacts with receptor-like proteins in plant immunity against fungal infection.* Proceedings of the National Academy of Sciences, 2013. **110**(24): p. 10010-10015.

46. Albert, I., et al., *An RLP23–SOBIR1–BAK1 complex mediates NLP-triggered immunity.* Nature Plants, 2015. **1**(10): p. 15140.
47. Domazakis, E., et al., *The ELR-SOBIR1 Complex Functions as a Two-Component Receptor-Like Kinase to Mount Defense Against Phytophthora infestans.* Molecular Plant-Microbe Interactions®, 2018. **31**(8): p. 795-802.
48. Postma, J., et al., *Avr4 promotes Cf-4 receptor-like protein association with the BAK1/SERK3 receptor-like kinase to initiate receptor endocytosis and plant immunity.* New Phytologist, 2016. **210**(2): p. 627-642.
49. Liebrand, T.W.H., H.A. van den Burg, and M.H.A.J. Joosten, *Two for all: receptor-associated kinases SOBIR1 and BAK1.* Trends in Plant Science, 2014. **19**(2): p. 123-132.
50. Ngou, B.P.M., J.D.G. Jones, and P. Ding, *Plant immune networks.* Trends in Plant Science, 2022. **27**(3): p. 255-273.
51. Couto, D. and C. Zipfel, *Regulation of pattern recognition receptor signalling in plants.* Nature Reviews Immunology, 2016. **16**(9): p. 537-552.
52. Lu, D., et al., *A receptor-like cytoplasmic kinase, BIK1, associates with a flagellin receptor complex to initiate plant innate immunity.* Proceedings of the National Academy of Sciences, 2010. **107**(1): p. 496-501.
53. Zhang, J., et al., *Receptor-like Cytoplasmic Kinases Integrate Signaling from Multiple Plant Immune Receptors and Are Targeted by a Pseudomonas syringae Effector.* Cell Host & Microbe, 2010. **7**(4): p. 290-301.
54. Liu, Z., et al., *BIK1 interacts with PEPRs to mediate ethylene-induced immunity.* Proceedings of the National Academy of Sciences, 2013. **110**(15): p. 6205-6210.
55. Wan, W.-L., et al., *Comparing Arabidopsis receptor kinase and receptor protein-mediated immune signaling reveals BIK1-dependent differences.* New Phytologist, 2019. **221**(4): p. 2080-2095.
56. Boller, T. and G. Felix, *A Renaissance of Elicitors: Perception of Microbe-Associated Molecular Patterns and Danger Signals by Pattern-Recognition Receptors.* Annual Review of Plant Biology, 2009. **60**(1): p. 379-406.
57. Thor, K., et al., *The calcium-permeable channel OSCA1.3 regulates plant stomatal immunity.* Nature, 2020. **585**(7826): p. 569-573.
58. Tian, W., et al., *A calmodulin-gated calcium channel links pathogen patterns to plant immunity.* Nature, 2019. **572**(7767): p. 131-135.
59. Kadota, Y., et al., *Direct Regulation of the NADPH Oxidase RBOHD by the PRR-Associated Kinase BIK1 during Plant Immunity.* Molecular Cell, 2014. **54**(1): p. 43-55.
60. Asai, T., et al., *MAP kinase signalling cascade in Arabidopsis innate immunity.* Nature, 2002. **415**(6875): p. 977-983.
61. Suarez-Rodriguez, M.C., et al. *MEKK 1 Is Required for flg 22-Induced MPK 4 Activation in Arabidopsis Plants 1 [C] [W]*. 2007.
62. Ngou, B.P.M., P. Ding, and J.D.G. Jones, *Thirty years of resistance: Zig-zag through the plant immune system.* The Plant Cell, 2022.
63. Zipfel, C., *Combined roles of ethylene and endogenous peptides in regulating plant immunity and growth.* Proceedings of the National Academy of Sciences, 2013. **110**(15): p. 5748-5749.
64. Kamoun, S., *A Catalogue of the Effector Secretome of Plant Pathogenic Oomycetes.* Annual Review of Phytopathology, 2006. **44**(1): p. 41-60.
65. Saur, I.M.L., R. Panstruga, and P. Schulze-Lefert, *NOD-like receptor-mediated plant immunity: from structure to cell death.* Nature Reviews Immunology, 2021. **21**(5): p. 305-318.
66. Tamborski, J. and K.V. Krasileva, *Evolution of Plant NLRs: From Natural History to Precise Modifications.* Annual Review of Plant Biology, 2020. **71**(1): p. 355-378.

67. Adachi, H., L. Derevnina, and S. Kamoun, *NLR singletons, pairs, and networks: evolution, assembly, and regulation of the intracellular immunoreceptor circuitry of plants.* Current Opinion in Plant Biology, 2019. **50**: p. 121-131.
68. Wu, C.-H., L. Derevnina, and S. Kamoun, *Receptor networks underpin plant immunity.* Science, 2018. **360**(6395): p. 1300-1301.
69. Wang, J., et al., *Ligand-triggered allosteric ADP release primes a plant NLR complex.* Science, 2019. **364**(6435): p. eaav5868.
70. Wang, J., et al., *Reconstitution and structure of a plant NLR resistosome conferring immunity.* Science, 2019. **364**(6435): p. eaav5870.
71. Bi, G., et al., *The ZAR1 resistosome is a calcium-permeable channel triggering plant immune signaling.* Cell, 2021. **184**(13): p. 3528-3541.e12.
72. Feehan, J.M., et al., *Plant NLRs get by with a little help from their friends.* Current Opinion in Plant Biology, 2020. **56**: p. 99-108.
73. Wu, C.-H., et al., *NLR network mediates immunity to diverse plant pathogens.* Proceedings of the National Academy of Sciences, 2017. **114**(30): p. 8113-8118.
74. Lapin, D., D.D. Bhandari, and J.E. Parker, *Origins and Immunity Networking Functions of EDS1 Family Proteins.* Annual Review of Phytopathology, 2020. **58**(1): p. 253-276.
75. Monteiro, F. and M.T. Nishimura, *Structural, Functional, and Genomic Diversity of Plant NLR Proteins: An Evolved Resource for Rational Engineering of Plant Immunity.* Annual Review of Phytopathology, 2018. **56**(1): p. 243-267.
76. Pruitt, R.N., et al., *The EDS1–PAD4–ADR1 node mediates Arabidopsis pattern-triggered immunity.* Nature, 2021. **598**(7881): p. 495-499.
77. Kamoun, S., H. Lindqvist, and F. Govers, *A Novel Class of Elicitin-like Genes from Phytophthora infestans.* Molecular Plant-Microbe Interactions®, 1997. **10**(8): p. 1028-1030.
78. Chepsergon, J., et al., *Organize, Don't Agonize: Strategic Success of Phytophthora Species.* Microorganisms, 2020. **8**(6): p. 917.
79. Kamoun, S., et al., *A Gene Encoding a Protein Elicitor of Phytophthora infestans Is Down-Regulated During Infection of Potato.* Molecular Plant-Microbe Interactions®, 1997. **10**(1): p. 13-20.
80. Du, J., et al., *Elicitin recognition confers enhanced resistance to Phytophthora infestans in potato.* Nature Plants, 2015. **1**(4): p. 15034.
81. Chen, Z., et al., *Convergent evolution of immune receptors underpins distinct elicitin recognition in closely related Solanaceous plants.* The Plant Cell, 2023. **35**(4): p. 1186-1201.
82. Qutob, D., et al., *Phytotoxicity and Innate Immune Responses Induced by Nep1-Like Proteins.* The Plant Cell, 2006. **18**(12): p. 3721-3744.
83. Böhm, H., et al., *A Conserved Peptide Pattern from a Widespread Microbial Virulence Factor Triggers Pattern-Induced Immunity in Arabidopsis.* PLOS Pathogens, 2014. **10**(11): p. e1004491.
84. Wang, Y., et al., *Leucine-rich repeat receptor-like gene screen reveals that Nicotiana RXEG1 regulates glycoside hydrolase 12 MAMP detection.* Nature Communications, 2018. **9**(1): p. 594.
85. Ma, Z., et al., *A Phytophthora sojae Glycoside Hydrolase 12 Protein Is a Major Virulence Factor during Soybean Infection and Is Recognized as a PAMP.* The Plant Cell, 2015. **27**(7): p. 2057-2072.
86. Xia, Y., et al., *N-glycosylation shields Phytophthora sojae apoplastic effector PsXEG1 from a specific host aspartic protease.* Proceedings of the National Academy of Sciences, 2020. **117**(44): p. 27685-27693.
87. Kato, H., et al., *Pathogen-derived 9-methyl sphingoid base is perceived by a lectin receptor kinase in Arabidopsis.* bioRxiv, 2021: p. 2021.10.18.464766.

88. Yang, Y., et al., *Convergent evolution of plant pattern recognition receptors sensing cysteine-rich patterns from three microbial kingdoms.* Nature Communications, 2023. **14**(1): p. 3621.
89. Nie, J., et al., *A receptor-like protein from Nicotiana benthamiana mediates VmE02 PAMP-triggered immunity.* New Phytologist, 2021. **229**(4): p. 2260-2272.
90. Jane E. Parker, W.S., Klaus Hahlbrock, and Dierk Scheel, *An Extracellular Glycoprotein from Phytophthora megasperma f. sp. glycinea Elicits Phytoalexin Synthesis in Cultured Parsley Cells and Protoplasts.* Molecular Plant-Microbe Interactions®, 1991. **4**(1): p. 19-27.
91. Nürnberger, T., et al., *High affinity binding of a fungal oligopeptide elicitor to parsley plasma membranes triggers multiple defense responses.* Cell, 1994. **78**(3): p. 449-460.
92. Ligterink, W., et al., *Receptor-Mediated Activation of a MAP Kinase in Pathogen Defense of Plants.* Science, 1997. **276**(5321): p. 2054-2057.
93. Zimmermann, S., et al., *Receptor-mediated activation of a plant Ca^{2+}-permeable ion channel involved in pathogen defense.* Proceedings of the National Academy of Sciences, 1997. **94**(6): p. 2751-2755.
94. Brunner, F., et al., *Pep-13, a plant defense-inducing pathogen-associated pattern from Phytophthora transglutaminases.* The EMBO Journal, 2002. **21**(24): p. 6681-6688.
95. Reiss, K., et al., *Structural and Phylogenetic Analyses of the GP42 Transglutaminase from Phytophthora sojae Reveal an Evolutionary Relationship between Oomycetes and Marine Vibrio Bacteria*.* Journal of Biological Chemistry, 2011. **286**(49): p. 42585-42593.
96. Folk, J.E., *Transglutaminases.* Annual Review of Biochemistry, 1980. **49**(1): p. 517-531.
97. Fabritius, A.-L. and H.S. Judelson, *A Mating-Induced Protein of Phytophthora infestans Is a Member of a Family of Elicitors with Divergent Structures and Stage-Specific Patterns of Expression.* Molecular Plant-Microbe Interactions®, 2003. **16**(10): p. 926-935.
98. Hahlbrock, K., et al., *Oligopeptide elicitor-mediated defense gene activation in cultured parsley cells.* Proceedings of the National Academy of Sciences, 1995. **92**(10): p. 4150-4157.
99. Grenville-Briggs, L.J., et al., *Identification of appressorial and mycelial cell wall proteins and a survey of the membrane proteome of Phytophthora infestans.* Fungal Biology, 2010. **114**(9): p. 702-723.
100. Brus-Szkalej, M., et al., *A family of cell wall transglutaminases is essential for appressorium development and pathogenicity in Phytophthora infestans.* bioRxiv, 2021: p. 2021.11.23.469665.
101. Halim, V.A., et al., *The oligopeptide elicitor Pep-13 induces salicylic acid-dependent and -independent defense reactions in potato.* Physiological and Molecular Plant Pathology, 2004. **64**(6): p. 311-318.
102. Nietzschmann, L., et al., *Early Pep-13-induced immune responses are SERK3A/B-dependent in potato.* Scientific Reports, 2019. **9**(1): p. 18380.
103. Dong, S.-m. and S.-q. Zhou, *Potato late blight caused by Phytophthora infestans: From molecular interactions to integrated management strategies.* Journal of Integrative Agriculture, 2022. **21**(12): p. 3456-3466.
104. Pham, G.M., et al., *Construction of a chromosome-scale long-read reference genome assembly for potato.* GigaScience, 2020. **9**(9).

Chapter 2

Identification of *Solanum* immune receptors by Bulked Segregant RNA-Seq and high-throughput recombinant screening

Yerisf C. Torres Ascurra, Xiao Lin X, Pieter J. Wolters and Vivianne G.A.A. Vleeshouwers

This chapter was published as:

Torres Ascurra Y, Lin X, Wolters PJ, Vleeshouwers VGAA. Identification of *Solanum* Immune Receptors by Bulked Segregant RNA-Seq and High-Throughput Recombinant Screening. Methods Mol Biol. 2021;2354:315-330. doi: 10.1007/978-1-0716-1609-3_15.

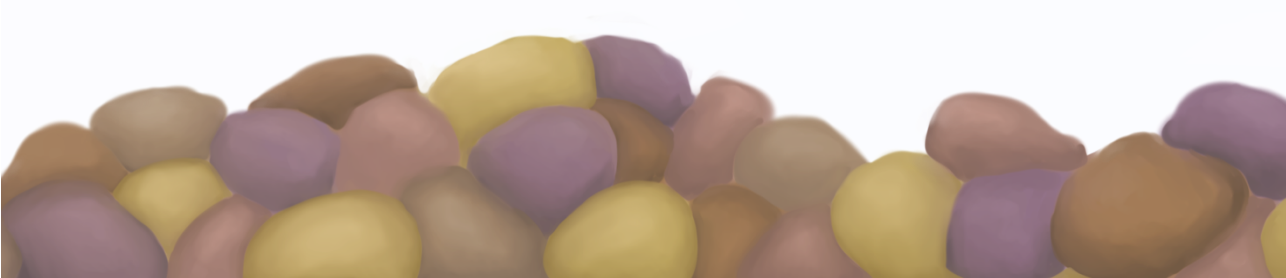

Abstract

The identification, understanding and deployment of immune receptors is crucial to achieve high level and durable resistance for crops against pathogens. In potato, many *R* genes have been identified using map-based cloning strategies. However, this is a challenging and laborious task, that involves the development of a high number of molecular markers for the initial mapping, and the screening of thousands of plants for fine-mapping. Bulked Segregant RNA-Seq (BSR-Seq) has proven to be an efficient technique for the mapping of resistance genes. The RNA from two bulks of plants with contrasting phenotypes is sequenced and analysed to identify single nucleotide polymorphism (SNPs) markers linked to the target gene. Subsequently, the SNP markers that are identified can be used to delimit the mapping interval. Additionally, we designed an *in vitro* recombinant screening strategy that is advantageous for analysing a large number of plants, in terms of time, space and cost. Tips and detailed protocols, including BSR-Seq, bioinformatic analysis and recombinant screening, are provided in this chapter.

Key words: Pattern recognition receptors (PRR), Receptor-like proteins (RLP), Receptor-like kinases (RLK), Nucleotide-binding site leucine-rich repeat (NLR), Resistance genes (R genes), Effectors, Genetic mapping, Bulked segregant analysis (BSA), Mapping, Effectoromics.

1. Introduction

Potato (*Solanum tuberosum* L.) is a staple food for 1.3 billion people [1], and its global production is close to 400 MT yearly [2]. Unfortunately, potato is host to many pathogens that can affect all organs of the plant and diminish its production [3]. There are 35 economically important bacterial, fungal and oomycete diseases of potato worldwide [4]. Among these, late blight, caused by the oomycete *Phytophthora infestans*, is the most pernicious, especially in developing countries [5]. It is estimated that the total costs due to losses and to control this disease is close to € 9.4 billion per year [6, 7]. Therefore, the development of new cultivars that are resistant to economically important diseases is essential.

Plants have evolved a recognition-based immune system to defend themselves against pathogens [8-10]. Pattern recognition receptors (PRRs) that are located on the cell surface recognize microbial associated molecular patterns (MAMPs) or apoplastic effectors and activate defense responses. Intracellular nucleotide-binding site leucine-rich repeat (NLR) proteins that are encoded by resistance (*R*) genes recognize cytoplasmic effectors, also called AVR proteins [8]. In case of late blight, potato breeders and researchers have relied mainly on the use of *R* genes. More than 20 *R* genes have been cloned [11], and many of them have been introgressed into cultivars with initial success [12]. The first and only characterized PRR in potato is the receptor-like protein (RLP) ELR (elicitin response) that recognizes INF1 elicitin from *P. infestans*. *ELR* overexpression resulted in enhanced resistance to the pathogen, although the resistance level is not as strong as most *R* genes [13]. The suitable deployment of immune receptors in crop plants, particularly by stacking multiple receptors seems to be the key to obtain a durable resistance against pathogens [14-17].

Traditionally, wild and cultivated relatives of potato have starred as plentiful sources of resistance in potato breeding programs [18]. For many years, techniques as field, greenhouse and laboratory assays have been used to screen *Solanum* species for disease resistance [3]. In the last years, the effectoromics strategy has come onto the scene to accelerate identifying resistance and understanding plant immunity [11]. Effectoromics is a high-throughput functional genomic approach that uses mainly two *Agrobacterium*-based functional assays, agroinfiltration and PVX agroinfection, to transiently express effectors in plant cells and monitor for the occurrence of macroscopic cell death responses [19, 20]. Additionally, for apoplastic effectors or microbe-associated molecular patterns (MAMPs), it has been shown that infiltration of effector proteins or peptides also represents an efficient way to screen responses [21].

The map-based cloning strategy has commonly been used to identify *R* genes in potato [12, 22-24], and in combination with the effectoromics approach, it has allowed the rapid cloning of various *R* genes and a surface immune receptor against late blight, like *Rpi-sto1*, *Rpi-pta1* and *ELR,* respectively [13, 25]. The central procedure of map-based cloning is the genetic mapping of the target gene, which is performed in a segregating population, using molecular markers distributed along each chromosome to identify markers delimiting the genetic region that contains the target gene [26]. Then, new markers are developed within the region and used to identify recombinants from a much larger population. These recombinants are then phenotyped/tested for response/resistance to narrow the genetic interval down in a process called fine-mapping [26]. The final goal of fine-mapping is to determine a sufficiently small interval that allows the prediction of candidate genes. For potato, the whole process used to take several years, but fortunately with the emergence of next generation sequencing (NGS) technologies [27, 28] and the availability of the potato genome sequence [29-31], new strategies can be used to shorten this process [32].

Bulked Segregant Analysis (BSA) is an efficient method to identify markers linked to any specific gene or genomic region. In BSA, two bulks of plants with contrasting phenotypes for a specific trait are generated and analyzed to identify markers that discriminate the bulks [33]. BSA is a flexible approach that can be assisted by NGS technologies for the development of molecular markers [34]. Bulked segregant RNA-Seq (BSR-Seq) was developed as a new genetic mapping strategy by combining BSA and RNA-Seq [35] and has recently been used to accelerate the mapping of genes of interest [36-38]. RNA-Seq is commonly used for gene expression profiling but also for identification of single nucleotide polymorphism (SNPs) that can be used as molecular markers [39, 40]. Compared to whole genome sequencing, RNA-Seq requires a lower sequencing depth and additionally provides useful gene expression data from the candidate genes [34]. When required, this strategy is followed by fine-mapping. To gather the necessary number of recombinants, a large number of individuals from the population (usually a few thousand) have to be genotyped with flanking markers. This is typically time-consuming and requires a large amount of space and labor in a greenhouse facility. By screening for recombinants *in vitro* before transferring plants to the greenhouse, the efficiency of this process can be much improved. In this chapter, we describe a detailed protocol for BSR-Seq and the subsequent high-throughput recombinant screening under *in vitro* conditions to facilitate and accelerate the fine-mapping of immune receptors in potato.

2. Materials

2.1. Sowing of potato seeds under *in vitro* conditions and micropropagation of plants

1. 70% Ethanol.
2. 1.5% Sodium hypochlorite.
3. Sterilized tap water.
4. MS20 medium: 4.4 g of Murashigue and Skoog basal salt mixture (including vitamins) and 20 g of sucrose dissolved in 900 mL of double distilled water (ddH_2O). Adjust pH to 5.6 using KOH or NaOH, and complete the volume to 1 L. Add 8 g of micro agar and autoclave.
5. 100.000 ppm gibberellic acid (GA_3) stock solution: 1 g of GA_3 dissolved in 10 ml of ddH_2O. Filter-sterilize.

2.2. RNA isolation

1. RNeasy Plus Mini Kit, Qiagen.
2. Spectrophotometer for DNA/RNA quantity/purity evaluation.

2.3. DNA isolation

1. CTAB buffer: 100 mL 1 M Tris-HCl (pH 7.5), 140 mL of 5M NaCl, 20 mL of 0.5 M EDTA (pH 8.0), 740 mL of MilliQ water and 20 g of CTAB (Cetyl trimethylammonium bromide) in 1 L of ddH_2O.
2. RNase 20 mg/mL (add 1 µL/mL of CTAB buffer just prior to use).
3. β-mercaptoethanol (add 2 µL/mL of CTAB buffer just prior to use).
4. Chloroform:isoamyl alcohol (24:1 [v/v]).
5. Isopropanol.
6. 70% Ethanol.MilliQ water.
7. TissueLyser II and steel beads (3.2 mm).
8. Polypropylene cluster tubes: 1.2 mL 8-tubes strips and strip caps, assembled in 96-tube racks.

2.4. Genetic mapping

1. LightScanner System (BioFire) or any other suitable device for high resolution melting analysis.
2. LC Green Plus (BioFire).
3. Phire Hot Start II DNA Polymerase (Thermo Fisher Scientific).
4. White-96 well plates (4titude).
5. Restriction enzymes (see Note 1).

6. QIAquick PCR purification kit (Qiagen).
7. Genomic resources:
   CAPS Designer (Sol Genomic Network,
   https://solgenomics.net/tools/caps_designer/caps_input.pl),
   Potato reference genomes of DM1-3 516 R44
   (http://solanaceae.plantbiology.msu.edu/pgsc_download.shtml) and
   Solyntus (https://www.plantbreeding.wur.nl/Solyntus/).

3. Methods

3.1. Bulked segregant RNA-Seq

1. Identify diploid *Solanum* genotypes that respond to a specific effector or that are resistant to a certain pathogen (R), as well as genotypes that do not respond or that are susceptible (NR).
2. Generate a mapping population by crossing the R and NR genotypes (*see* **Note 2**).
3. Select 30 R and 30 NR individuals (*see* **Note 3**).
4. Sample leaves from the R parent, NR parent, 30 R plants and 30 NR plants. Freeze the leaves in liquid nitrogen and store at -80°C until use.
5. Isolate RNA using the RNeasy Plus Mini Kit from Qiagen following the manufacturer's instructions, and remove genomic DNA using the gDNA eliminator columns (part of RNA isolation kit) or by on-colum DNase digestion using RNAse-free DNase Set (Qiagen). Evaluate the quantity and purity of the RNA using a spectrophotometer, and use 1 µl of sample for gel electrophoresis to evaluate RNA integrity (*see* **Note 4**).
6. Prepare 4 samples: 1) R parent, 2) R bulk (mix equal amounts of RNA from the 30 R plants), 3) NR parent and 4) NR bulk (mix equal amounts of RNA from the 30 NR plants) (*see* **Note 5**).
7. Send the RNA samples for sequencing (*see* **Note 6**).
   An overview of the BSR-seq strategy is shown in Fig. 1.

3.2. Bioinformatic analysis

1. Process the fastq files to remove adapter sequences, bad reads and low quality bases using software such as fastp [41].
2. Map RNAseq reads to the reference of choice using a splice-aware aligner like STAR [42].
3. Use the alignment files for variant calling and the identification of SNPs (VarScan)[42].
4. Filter for putative SNPs linked to response or resistance (heterozygous in the responding/resistant parent and progeny pool, while absent or homozygous in the non-responding/susceptible parent and progeny pool).

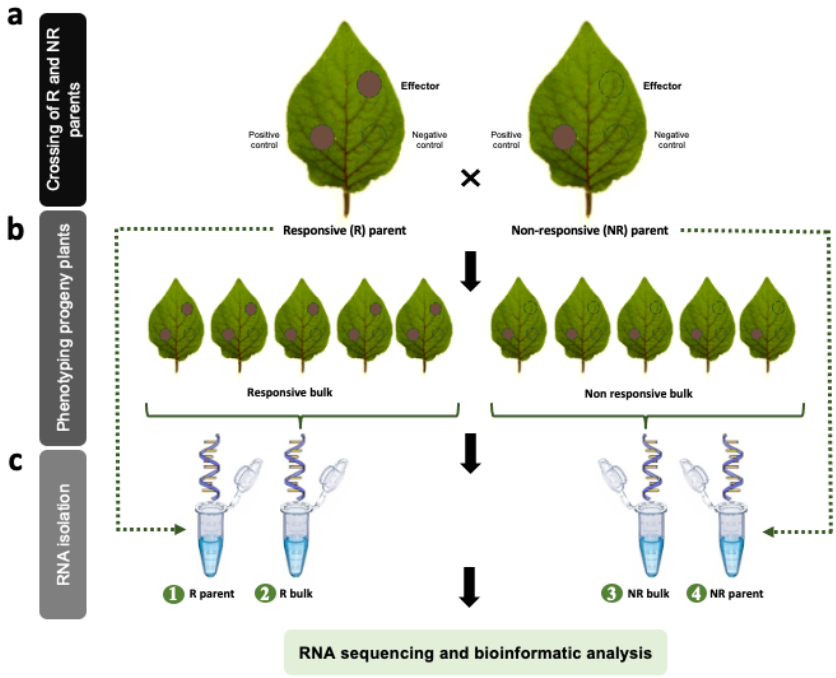

Figure 1. Bulk segregant RNA-Seq strategy to map *Solanum* immune receptors. (a) Selected responsive (R) and non-responsive (NR) genotypes are crossed to generate a segregating population. (b) Progeny plants with clear and confirmed phenotypes are selected to form the R and NR bulks. (c) Leaves are collected to form four samples, i.e. R parent, R bulk, NR parent and NR bulk; the RNA is isolated and sent for sequencing.

3.3. Genetic mapping and marker development

From identified SNPs (see Section 3.2), develop molecular markers covering the complete mapping interval (*see* **Note 7**):

1. Design primers to target the previously identified SNPs, and test them in the parents and a small set of R and NR plants using one of the methods described below (*see* **Note 8**).
2. Analyse the population with the selected markers to identify the flanking markers.

3.3.1. High Resolution Melting (HRM) markers

1. Design a PCR primer set producing ideally an 80-120 bp (base pair) fragment (*see* **Note 9**).
2. Prepare a 10 µL PCR reaction: 5.0 µL MilliQ water, 2 µL Phire Reaction Buffer, 0.4 µL 5 mM dNTPs, 0.25 µL of each 10 µM primer , 1 µL LC-Green® Plus, 0.1 µL Phire Hot Start II DNA Polymerase, and 1 µL of genomic DNA (10-20 ng).

3. Dispense the solution in white-wells PCR plates, and add 20 µL of mineral oil.
4. Use the following PCR conditions: 98°C for 30 seconds followed by 40 cycles of PCR amplification (98°C for 5 seconds, Ta (annealing temperature) for 10 seconds, and 72°C for 15 seconds) and terminated by an incubation at 72°C for 60 seconds and 25°C for 30 seconds.
5. Run the samples in the LightScanner and perform the HRM analysis to genotype the samples.

3.3.2. Cleaved amplified polymorphic sequence markers (CAPS)

1. Design a PCR primer set producing ideally a 500-1000 bp fragment. Target informative SNPs or another region inside the mapping interval.
2. Prepare a 15 µL reaction: 11.3 µL MilliQ water, 1.5 µL Reaction Buffer, 0.6 µL 5 mM dNTPs, 0.3 µL of each 10 µM primer, 0.06 µL DreamTaq DNA Polymerase, and 1 µL of genomic DNA (10-20 ng). Dispense the solution in standard PCR plates.
3. Use the following PCR conditions: 95°C for 3 minutes, followed by 35 cycles of PCR amplification (95°C for 30 seconds, Ta for 30 seconds, and 72°C for 1 minute), and and terminated by an incubation at 72°C for 10 minutes.
4. Run 3 µL of PCR product on a 1% agarose gel, and verify the presence of single bands for the parents. Purify and sequence the PCR products of both parents using the QIAquick PCR purification kit or any other.
5. Find the most suitable restriction enzymes using the CAPS Designer tool (*see* **Note 10**).
6. Digest all the PCR products using the selected restriction enzyme, and run 5 µL of the digested sample on a 1% agarose gel
7. Determine the marker polymorphisms and genotype the plant samples. For each marker, analyse the band pattern of the parents and score the population accordingly.

3.4. High-throughput recombinant screening

To narrow down the mapping interval, the screening of a few thousand of plants from the population is required. The plants are genotyped using the previously identified flanking markers to find the plants with recombination events (recombinants). This results in new flanking markers and therefore a smaller mapping interval (Fig 2).

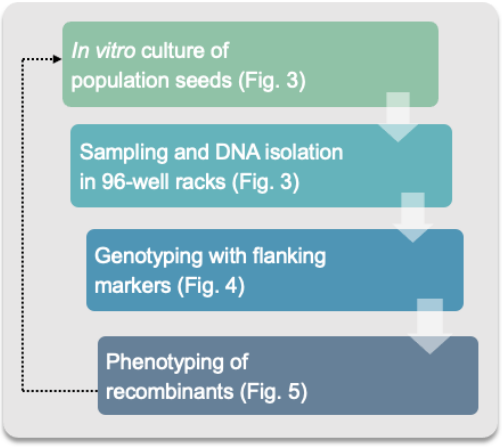

Figure 2. Workflow for the high-throughput recombinants screening

3.4.1. *In vitro* sowing of seeds

1. Rinse seeds three times with tap water.
2. Soak seeds in 200 mL of 70% ethanol for 1 minute.
3. Inside a flow cabinet, remove ethanol and soak the seeds in 1.5% sodium hypochlorite for 15 minutes (*see* **Note 11**).
4. Rinse seeds three times with sterile tap water to remove the sodium hypochlorite.
5. Sow the seeds on Murashige and Skoog [43] medium supplemented with 20 g/l sucrose (MS20) and 100 ppm GA_3 and incubate them in a climate room in the dark for two weeks (*see* **Note 1**2).
6. Transfer the first emerging seedlings to a new pot with fresh MS20 medium. Place 24 plants in each pot and assign a unique number to each plant (Fig. 3).
7. Incubate the plants in a climate room for two weeks.

3.4.2. DNA isolation in 96 tubes - racks

1. Fill a rack with 2 steel beads per well.
2. Inside a flow cabinet, take one leaf from the first plant of the first pot and place in position A1 of the rack, maintain the rack on ice during sampling. Fill each position in the rack with the samples from four pots (Fig. 3) (*see* **Note 13**).
3. Grind the samples using a TissueLyser at 25 Hz for 90 seconds.
4. To add buffers, use a repeating pipette, and to transfer the aqueous phase to new tubes use an 8-channel pipette.

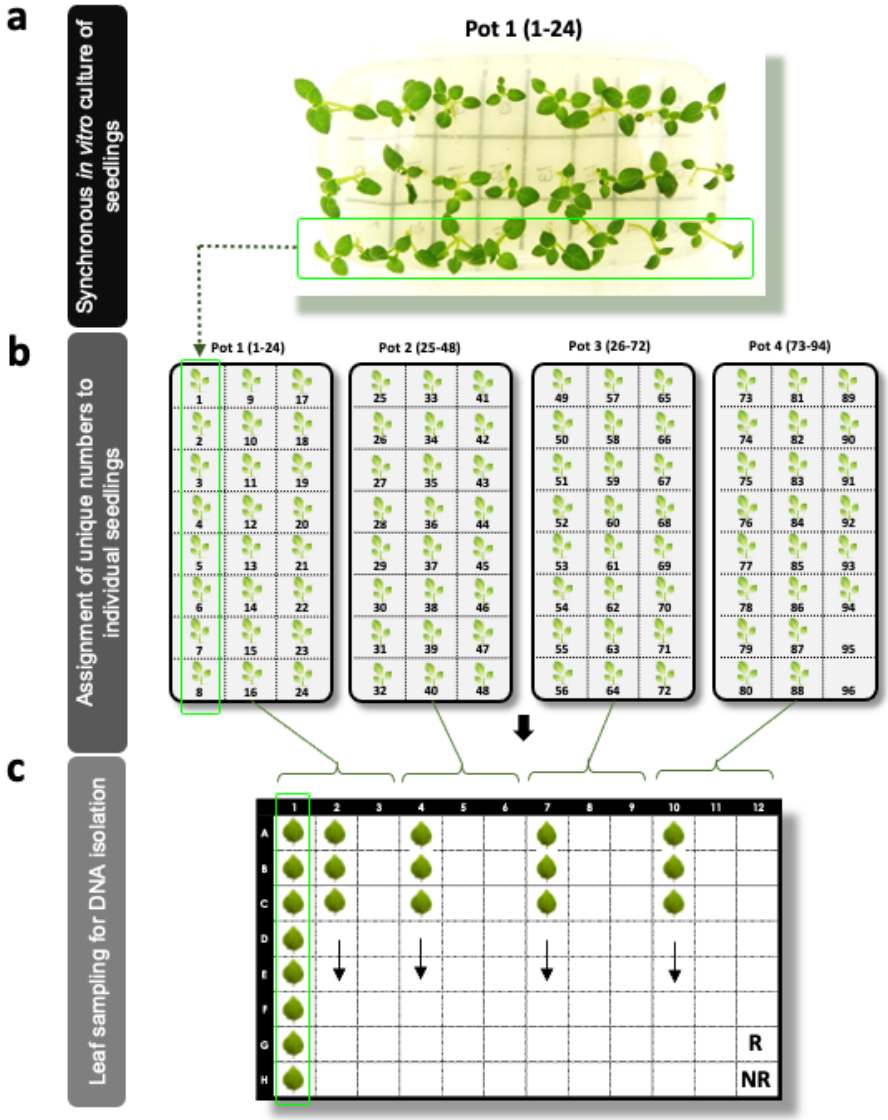

Figure 3. *In vitro* culture and sampling for the high-throughput recombinant screening. (a) Seedling are transferred to pots with MS20 medium and organized in groups of 24 plants to grow them synchronously. (b) Each plant is assigned a unique number to track them along the process. Every four pots will form a 96-well rack. (c) For each individual seedling, one leaf is collected for DNA isolation and transferred to a rack. The two last wells are filled with samples from the two parents (R and NR).

5. Add 250 µL of CTAB buffer to each sample and incubate at 65°C for 60 minutes (mix by inversion occasionally) and cool the samples down on ice for 15 minutes.
6. Add 250 µL of chloroform:isoamyl alcohol (24:1). Mix by inversion and centrifuge at 4000 rcf for 15 minutes. In the meantime, prepare a new rack with clean tubes and add 200 µL of isopropanol to each tube.
7. Transfer 200 µL of the aqueous phase to the new tubes containing isopropanol, mix by inversion and incubate at -20°C for 15 minutes.
8. Centrifuge for 15 minutes at 4000 rpm, remove the supernatant and wash the DNA pellets with 500 µL of 70% ethanol.
9. Remove the ethanol and dry the pellets (*see* **Note 14**).
10. Add 100 µL of MilliQ water. To evaluate the purity and quantity of the DNA, analyse some random samples using a spectrophotometer (*see* **Note 15**).
11. If needed, dilute the DNA to a final concentration around 20 ng/µL.

3.4.3. Genotyping

1. Analyse the entire rack with the two previously identified flanking markers (section 3.3) to identify the recombinant plants (Fig. 4).
2. Design more molecular markers between the flanking markers.
3. Analyse the recombinants (see section 3.4.4) and identify new flanking markers to narrow the mapping interval down.
4. If needed, return to section 3.4.1. This process should be iterated to fine-map the immune receptor, until the mapping interval is small enough for selecting candidate genes (*see* **Note 16**).

3.4.4. Phenotyping of recombinants plants

1. Transfer the recombinant genotypes to pots containing fresh MS medium.
2. Micro-propagate and transfer two plants per genotype to the greenhouse.
3. Phenotype the recombinant plants using the method of your choice (Fig. 5).
4. Combine the genotypic and phenotypic information to determine the position of the recombination in relation to the flanking markers and target locus (Fig. 6).

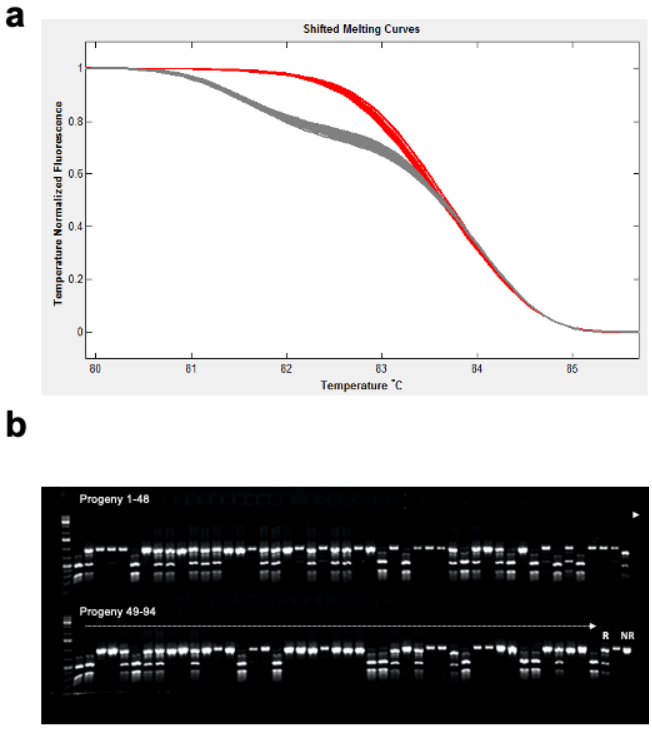

Figure 4. Genotyping of the mapping population (plants 1-94 and parents). (a) HRM marker showing two patterns of melting curves (red or grey). The two different patterns indicate two groups with genotypes corresponding to the R or NR parent. (b) Gel image of the same plants tested with a CAPS marker, showing two different band patterns: three bands for the R parent (and progeny) and one band for the NR parent (and progeny).

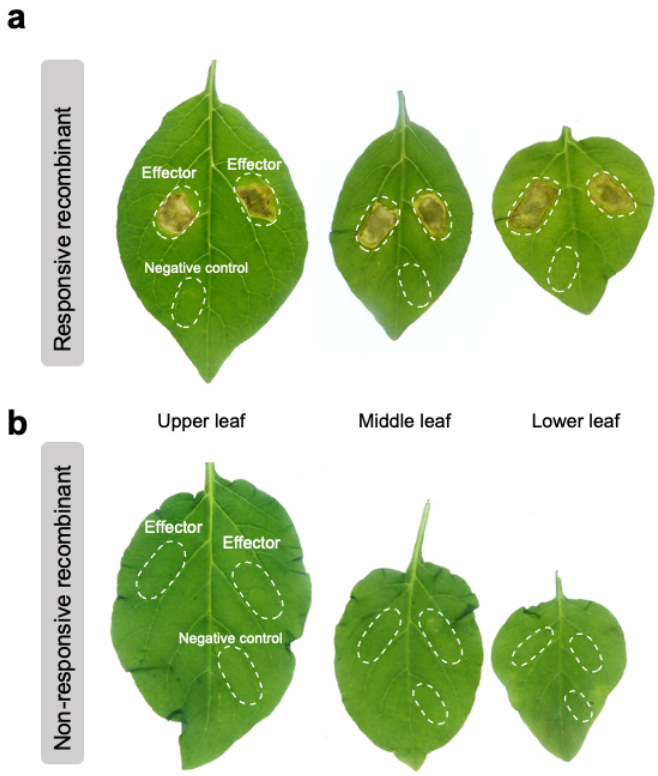

Figure 5. Phenotyping of recombinant plants for response to an effector. Three leaves from a recombinant are infiltrated with the effector in duplicate. A negative control is included. (a) Responsive recombinant that shows a clear hypersensitive response (HR) to the effector. (b) Non-responsive recombinant, unable to recognize the effector and no HR is observed.

4. Notes

1. The required restriction enzymes entirely depend on the sequence of the target. Commonly used enzymes are: *Eco*RI, *Bam*HI, *Hin*dIII, *Rsa*I, *Dra*I, among others.
2. To obtain the mapping population, sow around 100 seed from the F1 in the greenhouse and phenotype them for the response to the effector or pathogen. If the F1 segregation is compatible with a 1:1 ratio, it indicates that the R parent has the immune receptor and that it is in heterozygous state. If the F1 does not show segregation, a backcross population (BC1) is required, a R genotype from the progeny should be crossed with the NR parent and the segregation ratio should be determined. If the segregation is indeed 1:1 in the BC1, continue with this population.

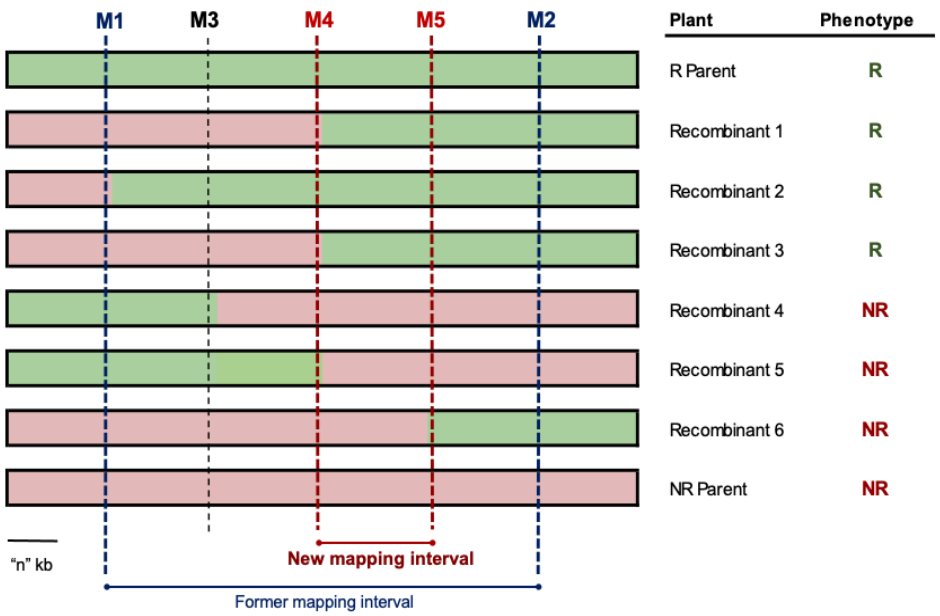

Figure 6. Fine-mapping. The markers M1 and M2 are used as flanking markers to identify recombination events and six recombinant plants (1-6) are identified. Then, new markers (M3, M4 and M5) are designed between the flanking markers and tested on the 6 recombinants and the parents. In parallel, the recombinants are phenotyped. Now, new flanking markers (M4 and M5) are identified and the mapping interval is narrowed down.

3. The size of the mapping interval obtained from the BSR-Seq depends on the number of individuals per bulk, the sequencing depth, and the density of polymorphisms of the mapping population. For each parameter, more is better [35]. In our hands the BSR-Seq worked well using between 15 and 34 individuals per bulk.
4. RNA purity is determined measuring the OD ratios 260/280 and 260/230, which should be above 2.0. The RNA integrity can be determined on an agarose gel, by evaluating the 28S and 18S rRNA bands.
5. For RNA isolation, it is possible to mix all the samples that form a bulk and then isolate the RNA from one sample. However, we consider it more appropriate to isolate the RNA from each sample, and then mix equal amounts of each to form the bulk RNA sample.
6. Generally, around 2 µg of RNA is required for sequencing. The depth of the sequencing will depend on the number of individuals used per bulk. For 30 individuals per bulk, we used around 40 million paired-end reads (150 bp) per sample, corresponding to 12 Gbp of raw sequencing data.

7. The number of required molecular markers varies between experiments. The aim is to obtain markers that cover the complete mapping interval.
8. Before analysing the entire population, test the markers in the parents and progeny with a known phenotype (use a subset of the plants included in the bulks). The selected markers are those that discriminate between R and NR plants. This test also gives information about the marker linkage phase.
9. For the HRM analysis, it is possible to genotype SNPs in bigger amplicons, however small amplicons allow for a better differentiation between variants. With bigger amplicons it is possible to detect additional mutations, which can result in more complex melting patterns that make it difficult to distinguish the variants [44].
10. Select the restriction enzyme that leads to clear differences in size between the cleaved and uncleaved PCR products.
11. After sterilizing the seeds of the mapping population, all the subsequent steps should be performed under sterile conditions.
12. Potato seeds are dormant directly after harvest, but will usually germinate rapidly after a period of cold-storage for 6 months. The use of gibberellin hastens the onset of germination and can obviate the need for storing the seeds before sowing [45]. The timing and rate of germination depends on the population. In our hands, the required time for germination after GA treatment varies between 2 weeks and a few months, and the germination percentage is between 30-90%.
13. Once the leaf sampling is done, keep the pots in a cold climate room (18 °C) until the recombinants are identified. In this way, the plants grow slowly, and it will be easier to keep them separated.
14. Dry the DNA pellet leaving the tubes open inside a fume hood, until residual ethanol has evaporated.
15. The DNA purity is determined by measuring the OD ratios 260/280 and 260/230, which should preferably (but not necessarily) be around 2.0.
16. The final mapping interval should be small enough to end up with a manageable number of candidate genes for the next cloning steps.

References

1. Stokstad, E., *The new potato.* Science, 2019. **363**(6427): p. 574-577.
2. Food and Agriculture Organization of the United Nations. *FAOSTAT Database*. 2017 November 5, 2019; Available from: http://www.fao.org/faostat/en/#data/QC.
3. Simko, I., et al., *Chapter 7 - Genetics of Resistance to Pests and Disease*, in *Potato Biology and Biotechnology*, D. Vreugdenhil, et al., Editors. 2007, Elsevier Science B.V.: Amsterdam. p. 117-155.
4. Kirk, W. and P. Wharton, *Chapter 11 - Fungal and Bacterial Disease Aspects in Potato Production*, in *The Potato: Botany, Production and Uses*, R. Navarre and M.J. Pavek, Editors. 2014, © CAB International: Washington, USA. p. 167-201.
5. Jo, K.R., et al., *Problematic Crops: 1. Potatoes*, in *Plant Pathogen Resistance Biotechnology*. p. 171-191.
6. Haverkort, A.J., et al., *Applied Biotechnology to Combat Late Blight in Potato Caused by Phytophthora Infestans.* Potato Research, 2009. **52**(3): p. 249-264.
7. Haverkort, A.J., et al., *Durable Late Blight Resistance in Potato Through Dynamic Varieties Obtained by Cisgenesis: Scientific and Societal Advances in the DuRPh Project.* Potato Research, 2016. **59**(1): p. 35-66.
8. Jones, J.D.G. and J.L. Dangl, *The plant immune system.* Nature, 2006. **444**(7117): p. 323-329.
9. Dodds, P.N. and J.P. Rathjen, *Plant immunity: towards an integrated view of plant-pathogen interactions.* Nat Rev Genet, 2010. **11**(8): p. 539-48.
10. Wang, Y., B.M. Tyler, and Y. Wang, *Defense and Counterdefense During Plant-Pathogenic Oomycete Infection.* Annual Review of Microbiology, 2019. **73**(1): p. 667-696.
11. Du, J. and V.G.A.A. Vleeshouwers, *New Strategies Towards Durable Late Blight Resistance in Potato*, in *The Potato Genome*, S. Kumar Chakrabarti, C. Xie, and J. Kumar Tiwari, Editors. 2017, Springer International Publishing: Cham. p. 161-169.
12. Vleeshouwers, V.G., et al., *Understanding and exploiting late blight resistance in the age of effectors.* Annu Rev Phytopathol, 2011. **49**: p. 507-31.
13. Du, J., et al., *Elicitin recognition confers enhanced resistance to Phytophthora infestans in potato.* Nat. Plants., 2015. **1**(4): p. 15034.
14. Zhu, S., et al., *Functional stacking of three resistance genes against Phytophthora infestans in potato.* Transgenic Research, 2012. **21**(1): p. 89-99.
15. Boschi, F., et al., *Enhanced Bacterial Wilt Resistance in Potato Through Expression of Arabidopsis EFR and Introgression of Quantitative Resistance from Solanum commersonii.* Frontiers in Plant Science, 2017. **8**(1642).
16. Kunwar, S., et al., *Transgenic Expression of EFR and Bs2 Genes for Field Management of Bacterial Wilt and Bacterial Spot of Tomato.* Phytopathology™, 2018. **108**(12): p. 1402-1411.
17. Wan, W.-L., et al., *Plant cell surface immune receptor complex signaling.* Current Opinion in Plant Biology, 2019. **50**: p. 18-28.
18. Ruiz de Galarreta, J.I., et al., *WildSolanum species as resistance sources against different pathogens of potato.* Potato Research, 1998. **41**(1): p. 57-68.
19. Vleeshouwers, V.G.A.A., Rietman, H., *In Planta Expression Systems*, in *Oomycete Genetics and Genomics*, S.K. K. Lamour, Editor. 2008. p. 455-475.
20. Du, J. and V.G.A.A. Vleeshouwers, *The Do's and Don'ts of Effectoromics*, in *Plant-Pathogen Interactions: Methods and Protocols*, P. Birch, J.T. Jones, and J.I.B. Bos, Editors. 2014, Humana Press: Totowa, NJ. p. 257-268.
21. Domazakis, E., et al., *Effectoromics-Based Identification of Cell Surface Receptors in Potato*, in *Plant Pattern Recognition Receptors: Methods and Protocols*, L. Shan and P. He, Editors. 2017, Springer New York: New York, NY. p. 337-353.

22. Ballvora, A., et al., *The R1 gene for potato resistance to late blight (Phytophthora infestans) belongs to the leucine zipper/NBS/LRR class of plant resistance genes.* The Plant Journal, 2002. **30**(3): p. 361-371.
23. Van Der Vossen, E., et al., *An ancient R gene from the wild potato species Solanum bulbocastanum confers broad-spectrum resistance to Phytophthora infestans in cultivated potato and tomato.* The Plant Journal, 2003. **36**(6): p. 867-882.
24. van der Vossen, E.A.G., et al., *The Rpi-blb2 gene from Solanum bulbocastanum is an Mi-1 gene homolog conferring broad-spectrum late blight resistance in potato.* The Plant Journal, 2005. **44**(2): p. 208-222.
25. Vleeshouwers, V.G.A.A., et al., *Effector Genomics Accelerates Discovery and Functional Profiling of Potato Disease Resistance and Phytophthora Infestans Avirulence Genes.* PLOS ONE, 2008. **3**(8): p. e2875.
26. Scheible, W.-R., O. Törjek, and T. Altmann, *From Markers to Cloned Genes: Map-Based Cloning*, in *Molecular Marker Systems in Plant Breeding and Crop Improvement*, H. Lörz and G. Wenzel, Editors. 2005, Springer Berlin Heidelberg: Berlin, Heidelberg. p. 55-86.
27. Hamilton, J.P. and C. Robin Buell, *Advances in plant genome sequencing.* The Plant Journal, 2012. **70**(1): p. 177-190.
28. Edwards, D. and J. Batley, *Plant genome sequencing: applications for crop improvement.* Plant Biotechnology Journal, 2010. **8**(1): p. 2-9.
29. Xu, X., et al., *Genome sequence and analysis of the tuber crop potato.* Nature, 2011. **475**(7355): p. 189-195.
30. Sharma, S.K., et al., *Construction of Reference Chromosome-Scale Pseudomolecules for Potato: Integrating the Potato Genome with Genetic and Physical Maps.* G3: Genes|Genomes|Genetics, 2013. **3**(11): p. 2031-2047.
31. Hardigan, M.A., et al., *Genome Reduction Uncovers a Large Dispensable Genome and Adaptive Role for Copy Number Variation in Asexually Propagated* Solanum tuberosum. The Plant Cell, 2016. **28**(2): p. 388-405.
32. Witek, K., et al., *Accelerated cloning of a potato late blight–resistance gene using RenSeq and SMRT sequencing.* Nature Biotechnology, 2016. **34**(6): p. 656-660.
33. Michelmore, R.W., I. Paran, and R.V. Kesseli, *Identification of markers linked to disease-resistance genes by bulked segregant analysis: a rapid method to detect markers in specific genomic regions by using segregating populations.* Proceedings of the National Academy of Sciences, 1991. **88**(21): p. 9828-9832.
34. Zou, C., P. Wang, and Y. Xu, *Bulked sample analysis in genetics, genomics and crop improvement.* Plant Biotechnology Journal, 2016. **14**(10): p. 1941-1955.
35. Liu, S., et al., *Gene mapping via bulked segregant RNA-Seq (BSR-Seq).* PLoS One, 2012. **7**(5): p. e36406.
36. Edae, E.A. and M.N. Rouse, *Bulked segregant analysis RNA-seq (BSR-Seq) validated a stem resistance locus in Aegilops umbellulata, a wild relative of wheat.* PLOS ONE, 2019. **14**(9): p. e0215492.
37. Dakouri, A., et al., *Analysis of genome-wide variants through bulked segregant RNA sequencing reveals a major gene for resistance to Plasmodiophora brassicae in Brassica oleracea.* Scientific Reports, 2018. **8**(1): p. 17657.
38. Ramirez-Gonzalez, R.H., et al., *RNA-Seq bulked segregant analysis enables the identification of high-resolution genetic markers for breeding in hexaploid wheat.* Plant Biotechnology Journal, 2015. **13**(5): p. 613-624.
39. Wang, Z., M. Gerstein, and M. Snyder, *RNA-Seq: a revolutionary tool for transcriptomics.* Nature Reviews Genetics, 2009. **10**(1): p. 57-63.
40. Lin, X., *Apoplastic effectors, MAMPs and surface immune receptors – the battlefront of the Phytophthora infestans – potato interaction.* PhD thesis Wageningen University, 2018.

41. Chen, S., et al., *fastp: an ultra-fast all-in-one FASTQ preprocessor.* Bioinformatics, 2018. **34**(17): p. i884-i890.
42. Dobin, A., et al., *STAR: ultrafast universal RNA-seq aligner.* Bioinformatics, 2012. **29**(1): p. 15-21.
43. Murashige, T. and F. Skoog, *A revised medium for rapid growth and bioassays with tobacco tissue cultures.* Physiologia Plantarum, 1962. **15**: p. 473-497.
44. Liew, M., et al., *Genotyping of Single-Nucleotide Polymorphisms by High-Resolution Melting of Small Amplicons.* Clinical Chemistry, 2004. **50**(7): p. 1156-1164.
45. Simmonds, N.W., *Experiments on the germination of potato seeds. I.* European Potato Journal, 1963. **6**(1): p. 45-60.

Chapter 3

Recognition specificity and fine mapping of the *Phytophthora* Pep-13/25 PAMP receptor in wild *Solanum*

Yerisf C. Torres Ascurra, Laura Dethier, Xiao Lin, Doret Wouters, Richard G. F. Visser, Thorsten Nürnberger and Vivianne G. A. A. Vleeshouwers

Parts of this chapter have been published in:

Lin X, Torres Ascurra YC, Fillianti H, Dethier L, de Rond L, Domazakis E, Aguilera-Galvez C, Kiros AY, Jacobsen E, Visser RGF, Nürnberger T and Vleeshouwers VGAA (2023) Recognition of Pep-13/25 MAMPs of Phytophthora localizes to an RLK locus in *Solanum microdontum*. *Front. Plant Sci.* 13:1037030. doi: 10.3389/fpls.2022.1037030

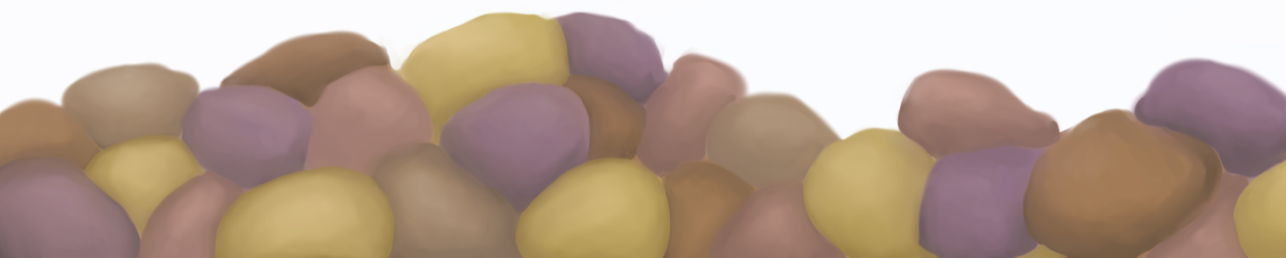

Abstract

Plants employ cell surface-localized pattern recognition receptors (PRRs) to recognize pathogen-associated molecular pattern (PAMPs) and mediate pattern-triggered immunity (PTI). PAMPs are typically considered conserved molecules or peptides, however recent studies have shown that they can occur as polymorphic patterns. Pep-13/25 is a PAMP derived from *Phytophthora* transglutaminases and reported to be conserved. In this study, we screened public databases and detected polymorphism of Pep-13/25 within *Phytophthora infestans* as well as across transglutaminases from diverse oomycete genera. In addition, we detected similar sequences to Pep-13/25 in some fungal species. We tested Pep-25-sensitive wild *Solanum* genotypes that are host species of *P. infestans* with four natural polymorphic versions of Pep-25 and we found a diverse profile of responses, which suggests the presence of diverse alleles of the Pep-25 receptor in these plants. Further, we genetically fine-mapped the Pep-25 receptor gene in *Solanum microdontum* subsp. *gigantophyllum* to a 0.081 cM region on the top of chromosome 3. Three BAC clones in this region were isolated and sequenced, and the putative Pep-25 receptor gene was localized to a complex receptor-like kinase (RLK) locus. This study is an important step toward the identification of the Pep-13/25 receptor, and the understanding of its dynamic interaction with this polymorphic PAMP.

Introduction

Plants employ cell surface and intracellular immune receptors to detect invasive microbes and activate immunity. The cell surface-localized pattern recognition receptors (PRRs) so far include receptor-like kinases (RLKs) or receptor-like proteins (RLPs), that recognize pathogen associated molecular patterns (PAMPs) and initiate pattern-triggered immunity (PTI) [1]. PTI confers protection to host non-adapted pathogens and partial immunity to host-adapted pathogens [2]. These adapted pathogens have evolved effectors to suppress PTI and manipulate the host system; in turn, plants deploy intracellular nucleotide-binding leucine-rich repeat receptors (NLRs) to recognize the effectors and initiate effector-triggered immunity (ETI), which provides a more robust immunity [3]. Historically, PTI and ETI were considered as two separated layers of plant immunity, yet they converge on downstream responses that include influx of Ca^{2+}, reactive oxygen species (ROS) production, mitogen-activated protein kinases (MAPK) cascades, induction of defense-related genes, and production of phytohormones [4]. Besides, recent studies showed that mutual potentiation of PTI and ETI are required for an effective immune response, PRRs are required for an effective ETI, which in turn enhances PTI responses by inducing the upregulation of its signalling components [5, 6].

PTI has always been considered ancient and stable, while ETI is considered very dynamic because of the continuous arms-race between *R* genes and effectors. The perception of flg22 (22 amino acids epitope contained by flagellin) is the best studied example of PTI. Many studies about flg22 indicate that pathogens modify their PAMPs to evade host recognition [7-9], which implies that PAMP diversification occurs as an effective pathogen virulence strategy [10]. In turn, some plants have developed polymorphic versions of FLS2 to detect this new version of flg22 [11, 12]. Besides, a recent study has reported a concerted expansion and/or contraction of NLRs and PRRs across plant species [13]. So, PTI is not as permanent as it was thought, instead, PAMPs and PRRs are under constant competition driven by their allelic diversification [10].

Phytophthora species are an important threat to agriculture and natural ecosystems since they cause some of the most destructive plant diseases in the world. *Phytophthora infestans*, infamous for causing the Irish potato famine, has remained a main threat for world agriculture. This oomycete pathogen causes late blight, the most devastating disease of potatoes that generates costs and losses close to € 9.4 billion each year [14]. Other *Phytophthora* species like *P. ramorum*, *P. sojae*, *P. capsici, P. cinnamomi* and *P. parasitica* are considered in the top 10 oomycete pathogens based on their economic and scientific relevance [15].

Plants sense several *Phytophthora* MAMPs using PRRs. For example, INF1, a major secreted elicitin from *P. infestans* is recognized by the LRR-RLP ELR isolated from *Solanum microdontum* [16, 17]. The conserved peptide nlp20 from NLPs present in many microbes, including *P. parasitica*, is recognized by RLP23 from *Arabidopsis thaliana* [18, 19]. The glycoside hydrolase 12 protein XEG1, produced by *P. sojae* is recognized by the LRR-RLP RXEG1 from *Nicotiana benthamiana* [20, 21]. Recently, it was shown that the ceramide Pi-Cer D from *P. infestans* activates defense responses in *Arabidopsis* and potato, Pi-Cer D is cleaved by the apoplastic ceramidase NCER2, and the resulting 9-methyl-branched sphingoid base is recognized by the lectin receptor-like kinase, RDA2 [22]. Despite the fact that several PRRs have been identified so far, many PAMPs remain orphans, like Pep-13, CBEL, PcF, SCR74, SCR96, OPEL, among others [23-28], from which the matching immune receptor has not been identified to date.

A cell wall-located 42 kDa glycoprotein (GP42) isolated from *P. sojae* culture filtrate, showed elicitor activity in cultured parsley cells and protoplasts [29]. The treatment of this glycoprotein with endo- and exopeptidases lead to the identification of a oligopeptide of 13 amino acids, Pep-13, as necessary and sufficient to trigger defense responses in parsley cells [23]. Pep-25 is a longer version of this peptide, that exhibited same elicitor activity as Pep-13 [23]. Pep-13, Pep-25, GP42 and *P. sojae* crude extract are able to trigger the same responses like influxes of H^+ and Ca^{2+}, effluxes of K^+ and Cl^-, oxidative burst, expression of defense-related genes and phytoalexin formation [23]. Besides, a high affinity binding site for Pep-13 was found in parsley microsomal membranes and protoplasts. By Alanine substitution scanning, two single amino acid residues, W-2 and P-5, (numbering according to position in Pep-13) were found important for both elicitor activity and binding, which indicated a link between the signal perception and the plant responses [23]. By chemical cross-linking, a 100 kDa protein from the parsley plasma membrane was identified as the putative receptor of Pep-13 or as a part of it [30, 31].

Later, GP42 was identified as a transglutaminase (TGase) present in *Phytophthora* species (including *P. infestans*), with Pep-13 as an exposed fragment within [32]. Other transglutaminases related to GP42 were found present in other Peronosporales (*Hyaloperonospora* and *Pythium* spp.) and marine *Vibrio* bacteria [33]. The Pep-13 sequence was found conserved among *Phytophthora* TGases, and mutational analysis revealed that the same amino acids from Pep-13 were important for both elicitor and enzyme activity, indicating the PAMP nature of this peptide [32]. Since Pep-13 was found present in *P. infestans*, it became important to study the interaction of Pep-13 with potato. Treatment of potato cells with Pep-13 resulted in ROS bursts and activation of defense-related genes, and Pep-13 infiltration of potato leaves produced accumulation of hydrogen peroxide, production of jasmonic and salicylic acids and hypersensitive response [34]. The Pep-13-triggered immune responses were

reported to be SERK3A/B-dependent in potato [35]. However, the Pep-13/25 receptor has remained elusive so far.

The analysis of the mating-induced gene M81 in *P. infestans* lead to the identification of a family of five genes with elicitor activities (M81, M81B, M81C, M81D and M81E) [36]. It was found that M81 lacked elicitor activity and was the most divergent compared to GP42. M81B was considered a pseudogene as no gene expression was detected, and the paralogous M81C, M81D and M81E showed conserved elicitor activity and were more similar to GP42 (63% to 71% of amino acid identity) [36]. The Pep-13 sequence from GP42 was found completely conserved in M81C, M81D and M81E, but differed by 3 amino acids in M81B and 6 amino acids in M81 [36].

In this study, we performed an *in silico* analysis of transglutaminases and their epitope Pep-13/25. We found putative transglutaminase sequences in several oomycete species (including Albugiales), and in three zoosporic fungal species. Besides, we found that Pep-13/25 shows polymorphism, even within the transglutaminase family of *P. infestans.* Wild Pep-25-sensitive *Solanum* genotypes were explored for their response to natural variants of Pep-25 and our findings suggest diversification of the Pep-13/25 receptor through evolution. Finally, the Pep-25 receptor was fine-mapped to a 0.081 cM LRR-RLK gene locus on the top of chromosome 3, which promises to lead to the identification of the Pep-13/25 receptor.

Results

Polymorphism of Pep-13/25 in *Phytophthora infestans*

Pep-13/25 are conserved plant immunogenic fragments from cell wall transglutaminases (TGases) present in several plant-pathogenic *Phytophthora* species [32]. BLAST searches of public databases using the TGase from *P. sojae* as query, retrieved a total of 285 sequences (excluding bacterial sequences). As expected, most of these sequences belonged to oomycetes, and specifically to the Peronosporales (*Phytopthhora* species with the highest number of predicted proteins, *Hyaloperonospora arabidopsidis*, *Nothophytophthora* sp., *Bremia lactuace* and *Peronospora effusa*), Albugiales (*Albugo candida* and *A. laibachi*) and Pythiales (*Globisporangium splendens* and *Pythium oligandrum*). Besides, we also found a few predicted TGases in fungal species like *Catenaria anguillulae*, *Rozella allomycis* and *Spizellomyces punctatus*, interestingly these species represent zoosporic fungi that belong to Cryptomycota or Chytridiomycota, phyla that are specially diverse in aquatic environments [37]. Representative Pep-13 and Pep-25 sequences from these TGases are shown in Fig 1a. These results indicated that Pep-13/25 presence is broadly distributed in oomycetes, and possibly in some fungal species. However, whether

these transglutaminases with polymorphic Pep-13 motifs retain elicitor and enzyme activity requires further experiments.

The transglutaminases from *Phytophthora infestans* were further explored. A total of 48 predicted protein sequences (from strains T30-4, 88069 and KR_2_A2) were retrieved from public databases, 8 incomplete and small sequences were excluded (Fig. S1). The sequences alignment and phylogenetic analysis show the formation of two main clades that separate the sequences related to M81C, M81D and M81E from the sequences more related to M81, and M81B (Fig. S2). Interestingly, the tree showed the formation of a sub clade (in pink) separated from M81C, D and E, which may represent a new transglutaminase gene not known previously. Based on the Pep-13/25 fragments of the 40 sequences analyzed, 15 unique Pep-13/25 sequences were selected (Fig 1b). The sequence alignment showed that the amino acids D-1 (first amino acid of Pep-25), V-8, W-9, Q-11, P-12 (first amino acids of Pep-13) are fully conserved within this transglutaminase family, while A-4, E-7, N-10, F-16 and V-18 are highly conserved, and higher polymorphism was observed in the rest of amino acids, including those inside Pep-13 (Fig 1b).

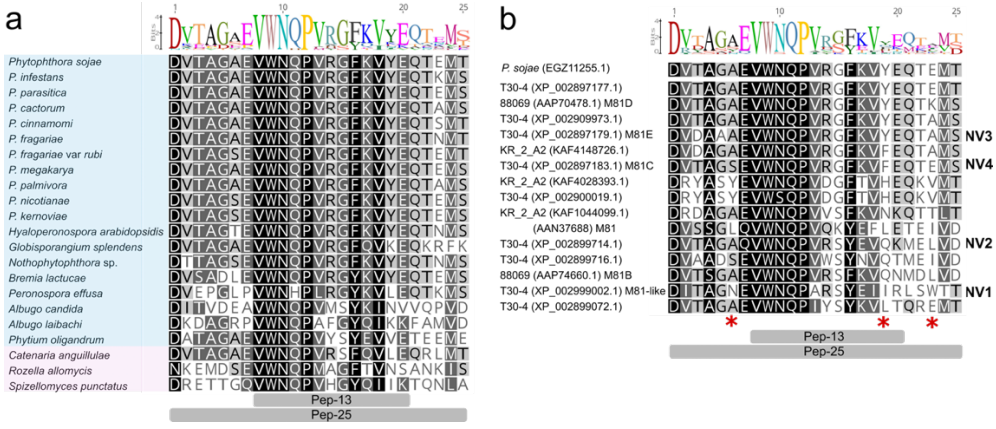

Figure 1. PAMP Pep-13/25 polymorphism in oomycetes and transglutaminase family from *P. infestans* a. Representative Pep-13 and Pep-25 sequences from transglutaminases sequences retrieved from public databases from oomycetes (light blue) and fungi (pink). **b.** Fifteen unique sequences for the epitope Pep-13/25 from transglutaminases sequences from *P. infestans* and the original Pep-25 reference from *P. sojae* [23]. For both cases, sequence logos representing conserved amino acids among the sequences are shown. Conserved amino acids are shaded in black, and semi-conserved residues are shaded in grey. Red asterisks indicate amino acid residues found under positive selection by PAML.

The expression level of 8 genes that encode for transglutaminases based on the Nimblegen microarray data from Haas et al. (2009) [38] was explored. It was found that the gene expression of all transglutaminases (except XP_002899072, from M81 /M81B cluster), is clearly induced early during infection (Fig. 2), which indicates an important function of these proteins during the interaction with the host plant. Besides, expression polymorphism between the 7 transglutaminases was noted, and by comparing specific transglutaminases among the 3 different strains as well (Fig. 2). These findings together suggest that diverse transglutaminases with different Pep-13/25 motifs function as enzymes in *P. infestans*. Based on the amino acid sequence alignment and gene expression profiles, we selected two natural variants with varying sequences on the Pep-13 region (NV1 and NV2), and two natural variants with conserved Pep-13 region but with varying sequences outside the Pep-13 region (NV3 and NV4) for further study (Fig. 1b).

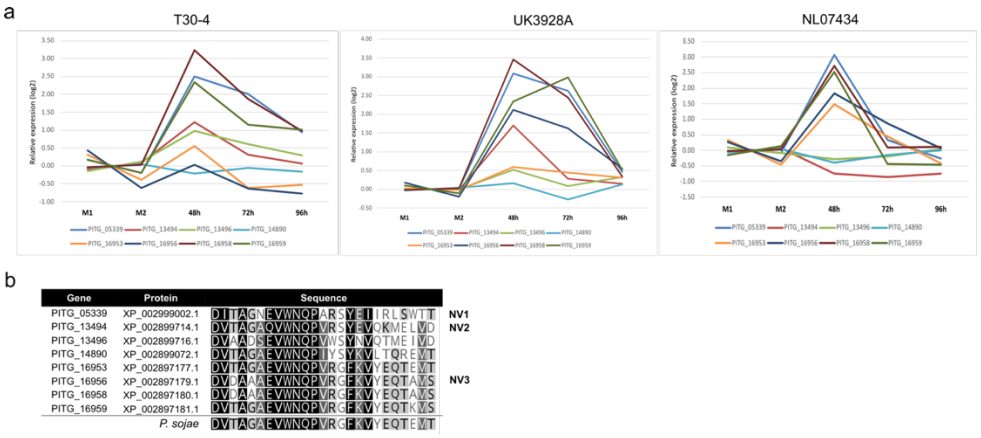

Figure 2. **Expression data of 8 transglutaminase genes from *P. infestans*. a.** Expression profile of transglutaminase genes family in *P. infestans* and infected potato. Gene expression is based on microarray data after Log2 normalization. The results were obtained from total RNA from mycelium grown on Rye medium (M1) or V8 medium (M2), and from Désirée infected leaves at 48h, 72h and 96h after inoculation with three *P. infestans* isolates T30-4, NL07434 and UK3928A. **b.** Protein encoded by the genes with expression data showed in a. Sequences of the Pep-13/25 motif are shown to visualize their diversity, and *P. sojae* is used as reference sequence. Conserved amino acids are shaded in black, and semi-conserved residues are shaded in grey.

Additionally, to study whether any positions in within Pep-25 may have been subject to diversifying selection, we used 17 nucleotide coding sequences of transglutaminases from *P. infestans* (isolates T30-4 and 88069) that were available in the NCBI, aligned the sequences and analyzed them using codeml from PAML [39]. Depending on the model used, different numbers of amino acids were found to be

under diversifying selection. The model M3 identified 45 amino acids under positive selection, these amino acids were distributed along the protein sequence, in the transglutaminase domain, but not in the signal peptide. Interestingly, three residues located to the Pep-13/25 motif (Fig. S3a). The model M8 detected 7 amino acids, and one of them was located in the Pep-25 motif (Fig. S3b). The selected natural variants showed polymorphism in the 3 amino acids found under positive selection by PAML (Fig 1b). These results suggest that diversifying selection has acted on some region within the transglutaminases from *P. infestans*, however, the Pep13/25 pattern is relatively conserved. Still, some significant diversifying selection was noted also within Pep13/25 and we decided to further explore the recognition of the natural variants of Pep-13/25.

Wild and cultivated potatoes show a diverse response to natural variants of Pep-25

In previous studies, we screened a collection of wild *Solanum* species and cultivated potatoes for HR induction upon infiltration with Pep-13 or its structural derivative Pep-25 [40]. We extended this screening and selected 29 responsive genotypes to test four natural variants from Pep-25 (NV1-4) (Table S1). We found that the screened genotypes show diverse response profiles, and four classes were distinguished (Fig. 3a). The class 1 includes genotypes from *S. demissum* and *S. bukasovii* species, that are sensitive to NV1 and NV4, but not to NV2 or NV3. Class 2 includes two genotypes from *S. tuberosum* Group Phureja and *S. microdontum* subsp. *gigantophyllum,* that are sensitive to all variants except NV2. Class 3 includes genotypes from *S. chacoense*, *S, berthaultii*, *S. hondelmanii*, *S. leptophyes*, *S. boliviense,* that are sensitive to NV3 and NV4, but not to NV1 or NV2. The major class 4 is represented by the plants sensitive to all the variants evaluated, and includes genotypes from *S. edinense*, *S. berthaultii*, *S. tuberosum* Group Phureja, *S. tuberosum* Group Andigenum, and two cultivars. Representative leaves of these genotypes are shown in Fig. 3b. The presence of 4 different recognition specificities, including quantitative variation within a class, suggests the existence of diverse alleles of Pep-25 receptor in *Solanum* species that might encode PRRs with different ligand specificities. Furthermore, compared to the other natural variants, NV2 was recognized by less genotypes, perhaps related to the lower expression level of its corresponding transglutaminase during infection, compared to the NV1- and NV3-containing transglutaminases. The prevention of PAMP production trough down regulation of gene expression is one pathogen strategy to avoid recognition [41], and may indicate a potential co-evolution of these PAMPs with their corresponding PRRs.

The observation of class 1 and 2 genotypes that recognize NV1 but not NV2, point to one amino acid inside Pep-13, E20 (numbering based on the amino acid positions in Pep-25), which change to K in NV2, may avoid recognition by these genotypes, but the change to R does not affect its recognition in the same genotypes. Interestingly, class 1 genotypes showing response to NV4, but not to NV3 indicate that amino acids

outside Pep-13 may be important for the elicitor activity in these *Solanum* plants. Our results indicated that the changes of the following amino acids T3D, G5A, E23A might avoid Pep-25 recognition by DMS364-1, DMS585-1 and BUK512-3. Interestingly, E23 was found under diversifying selection by PAML.

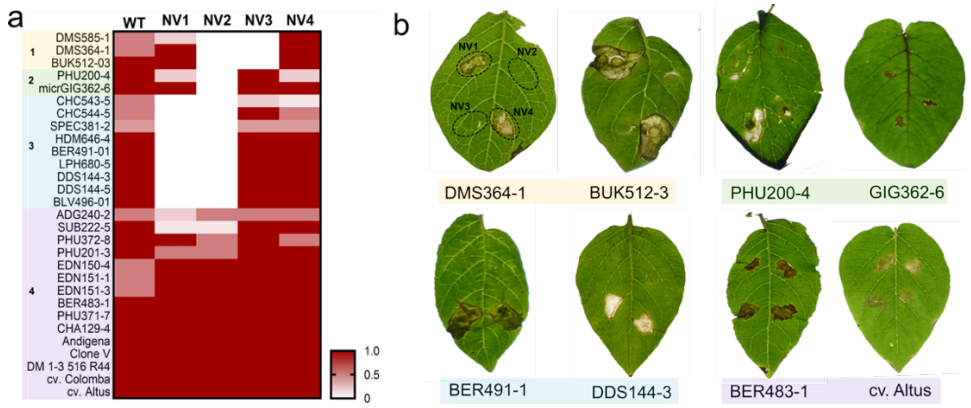

Figure 3. *Solanum* genotypes show a diverse response to Pep-25 and its natural variants a. Heat map of the responses of *Solanum* genotypes to the Pep-25 (WT and natural variants). HR induction was scored from 0 to 1 (0 indicates no symptoms, 1 indicates confluent cell death and intermediate values were also considered for chlorosis or increasing levels of patchy cell death). Four classes (1 to 4) are distinguished based on the sensitivity profile to the peptides. **b.** Examples of HR-induced by Pep-25 in some genotypes are shown.

GIG physical map and fine-mapping of the Pep-25 recognition

The genotype *S. microdontum* subsp. *gigantophylum* GIG3626-6 (GIG) showed to be sensitive to Pep-25, since a cell death response was produced upon Pep-25 infiltration (no cell-death was observed when Pep-13 was infiltrated) (Fig. 4a). GIG was crossed to *S. verrucosum* 3316-17 (Pep-25 non-sensitive), the F1 3341-15 was then crossed to MCD360-1 (Pep-25 non-sensitive), and the segregating F2 population (3521) (ratio 1:1) was used for a BSR-Seq analysis combined with a high-throughput recombinant screening approach [42]; this led to the mapping of Pep25-recognition to the top of the chromosome 3, fine mapping of the Pep-25 receptor within a 330 kb interval based on the DM 1-3 516 R44 genome v3.4, and sequencing of one BAC clone (isolated from a BAC library of GIG) [43]. In order to identify the candidate genes, we explored this BAC clone further. The gene annotation revealed the presence of 9 partial or complete LRR-RLK genes, but only two contained a signal peptide (Fig. S4a). Unfortunately, molecular markers designed across the BAC clone and tested on recombinant plants indicated that the mapping interval was not closed (Fig. S4b), which suggested that other candidate genes may be located outside this BAC clone.

To close the mapping interval, more molecular markers were designed (Table S2), 1783 additional plants from the population 3521, and the GIG BAC library were screened to find more recombinant plants, and increase the size of the physical map, respectively. The BAC library screening led to the identification of two new BAC clones (02 and 03) that overlapped BAC clones 01 on each side, and the assembly of the 3 clones led to the reconstruction of a 216 kb GIG physical (Fig. 4b). A new important recombinant plant was identified (3521-1489), and the genotyping of all recombinant plants narrowed the mapping interval, identifying HRM 1.429 and PCR S085 as flanking markers (Fig. 4c) The marker PCR S085 mapped to the BAC clone 03, in the position 210,116 kb of the GIG contig, however HRM 1.429 mapped outside the GIG contig, which indicated that the mapping interval includes the GIG contig plus an unsequenced GIG genomic sequence (Fig. 4c). The genetic distance of this interval was approximately 0.081 cM (3/3700).

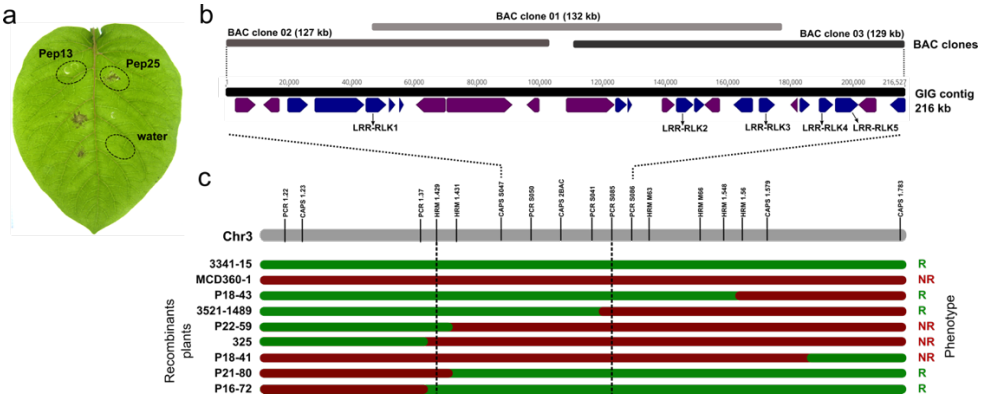

Figure 4. Fine mapping of the Pep-25 receptor. a. The Pep-25-sensitive genotype GIG362-6 (GIG) is shown. GIG leaves show no HR upon Pep-13 infiltration. **b.** The BAC screening led to the identification of 3 BAC clones (01, 02 and 03), which were assembled to generate the GIG contig of 216 kb. The gene annotation revelated the presence of 15 partial or full-length LRR-RLK (in blue), however only five of them contained signal peptide (LRR-RLK 1 to 5). **c.** The recombinants screening led to the identification of two new flanking markers, HRM 1.429 and PCR S085, but unfortunately one PCR S085 mapped inside the GIG contig. 3341-15 and MCD360-1 are the population parents. R: responsive, NR: non-responsive.

Candidate genes encode LRR-RLKs

The genes in the BAC contig were annotated, 15 leucine-rich repeat receptor-like kinase (LRR-RLK) genes located in this region (Fig. 4b), but only 5 were found to have signal peptide, and were considered as candidate genes of Pep-25 receptor (Fig.

S5a). These five LRR-RLK were cloned into overexpression vectors with 35S promoter and transformed into *Agrobacterium tumefaciens* strain AGL1, and then transiently expressed in *N. benthamiana* leaves followed by Pep-25 infiltration. However, none of the five tested candidate genes was responsible for Pep-25 recognition (Fig. S5b). Therefore, we speculate that the Pep-25 receptor likely locates in the un-sequenced region of the mapping interval.

Discussion

PAMPs are traditionally considered highly conserved, since they are indispensable for pathogen lifestyle [44]. However, many studies indicate that adapted pathogens can avoid PTI by allelic diversification of PAMPs. Sun et al. (2007) reported within-species variation of flagellin among *Xanthomonas campestris* pv. *campestris* strains to trigger responses in *Arabidopsis* [7]. Also, a flagellin region, different from flg22, flgII-28, was identified as PAMP and shown to be under diversifying selection within the *Pseudomonas syringae* pv. *tomato* strains [8]. *Agrobacterium tumefaciens* has evolved another modified flg22, flg22^{Atum}, that cannot be detected by FLS2, but can be recognized by FLS2^{XL} from *Vitis riparia*, a different form of FLS2 with broader ligand specificities [11]. Another polymorphic flg22, was identified in *Ralstonia solanacearum* (flg22^{Rso}) and has shown to evade perception by many plants, but was recognized by GmFLS2 from soybean [12]. These examples illustrate that a dynamic coevolution of PAMP and plant PRRs does exist.

Pep-13 was found conserved in cell wall transglutaminases from *Phytophthora* species, and required amino acids for enzyme activity were also shown important for the elicitor of the parent protein [32]. In this study we further explored transglutaminase sequences from available sequence databases. We found putative transglutaminases that were not reported previously in other oomycete species and three fungal species. Two of these fungi belong to the Chytridiomycota phylum, and *Rozella allomycis* (previously assigned to Chytridiomycotas) belongs to the Cryptomycota phylum that parasites chytrids [45]. Previously, since TGases were found also in marine *Vibrio* bacteria, it was hypothesized that oomycete transglutaminases were acquired from Vibrionales by horizontal gene transfer [33]. Curiously, here, we have found that fungi from Cryptomycotas and Chytridiomycotas, phyla that are highly diverse in aquatic environments, also have putative transglutaminases, and potentially could have been aquired by horizontal gene transfer from aqueous oomycetes as well. Furthermore, TGases from diverse genera showed distinct Pep13/25 sequences, which suggests that Pep-13/25 is a polymorphic PAMP with a broader distribution, beyond *Phytophthora*. To explore whether these natural variants exhibit similar enzyme and elicitor activity in their respective hosts, future work is needed.

Chemical inhibition and iRNA silencing of transglutaminases showed that they are important proteins for cell wall formation, stability and pathogenicity of *P. infestans* [46]. We retrieved 48 predicted transglutaminases sequences corresponding to three different strains of *P. infestans*, it was observed that the motif Pep-13/25 was highly polymorphic across the protein sequences analyzed (Fig. S2), and 15 unique Pep-13/25 motifs were identified. This indicates that even at species level, diversification of transglutaminases and particularly of Pep-13/25 is occurring, which is also supported by the finding that various amino acids are under positive selection.

Leaves of wild *Solanum* species, cultivated potato species and cultivars, showed HR upon infiltration of four natural variants of Pep-25, which indicated that they function as PAMPs and have elicitor activity. Additionally, based on the profile of HR of the sensitive genotypes treated with these variants, 4 classes of response were identified, which suggests that diverse alleles of the Pep-13/25 receptor with different ligand specificities occurs in *Solanum* species. Our results together suggest that allelic diversification is acting on the PAMP Pep-13/25, and at the same time, functional diversification might be occurring in the Pep-13/25 receptor to confers different ligand specificities, which suggests that a co-evolution between *Phytophthora* and *Solanum* hosts at the PAMP-PRR level. The cloning and characterization of the receptor could help to clarify and study further this dynamic interaction.

A *Solanum microdontum* subsp. *gigantophyllum* (GIG) is sensitive to Pep-25. In our attempt to clone the Pep-25 receptor, we identified a small interval (≈0.081 cM) in the top of the chromosome 3. We reconstructed the GIG physical map in that region and assembled 3 BAC clones to a contig of 216 kb, which showed to be rich in RLKs, since at least 15 full-length or partial RLK genes were annotated. Five of these contained signal peptides and were considered as candidate genes, but none of them gave cell death activity upon Pep-25 treatment. Unfortunately, we were unable to isolate more BAC clones to cover the whole mapping interval, but nonetheless, this work lay the groundwork for the cloning of the Pep-13/25 receptor from potato.

In summary, we showed that Pep-13/25 is a widely distributed PAMP in *Phytophthora,* other oomycetes and in some fungi. We found polymorphic amino acid residues within Pep-13/25 across oomycetes and fungi, and interestingly even within transglutaminases of *P. infestans.* The polymorphic Pep-13/25 epitopes relate to diverse recognition spectra from *Solanum* section *Petota* species. Finally, we fine-mapped the Pep-25 receptor to an RLK locus, which represents an important step towards the identification of a new receptor and of additional alleles with different ligands specificities, that may help to understand the dynamic interaction of PRRs and PAMPs.

Materials and Methods

Peptide synthesis

Pep25 (DVTAGAEVWNQPVRGFKYEQTEMTE) and the four natural variants NV1, NV2, NV3 and NV4 (DITAGNEVWNQPARSYEIIRLSWTT, DVTAGAQVWNQPVRSYEVQKMELVD, DVTAGSEVWNQPVRGFKVFEQTEMS and DVDAAAEVWNQPVRGFKVYEQTAMS, respectively) were synthesized by GenScript (USA). The peptides were dissolved in DMSO to a concentration of 1 mM, and in autoclaved tap water to a final concentration of 1 µM for infiltrations. The peptides were infiltrated into the abaxial side of plant leaves by a needleless syringe, and the cell death phenotype was scored 3 days after infiltration.

Plant materials

The genotypes were obtained from the wild *Solanum* collection of Plant Breeding, Wageningen University and Research [47] (Table S1), that is maintained *in vitro* on MS20 medium at 25 °C. Top shoots of plants were cut and clonally propagated and grown in climate chamber at 25 °C for 2 weeks. Plants were transferred to a climate-controlled greenhouse compartment at 22 °C/18 °C day/night temperature regime under long-day conditions and grown during 3-4 weeks. In all cases, three leaves per plant, and three plants per accession were used. To screen the segregating population, seeds were sterilized before germination. They were rinsed in 70% ethanol and soaked in a solution of 1.5% hypochlorite and Tween 20, then they were washed 3 times with autoclaved water to remove the hypochlorite. The seeds were sowed on MS20 medium supplemented with 1000 ppm GA3. After genotyping, the identified recombinants were moved to a climate-controlled greenhouse compartment and grown during 3-4 weeks for phenotyping.

In silico analysis

The protein sequences were obtained from Pfam (pfam.xfam.org). A total of 292 sequences belonging to the protein family PF16683 (Transglutaminase elicitor) were analyzed. Alignments were performed with MUSCLE [48] in Geneious Prime, the phylogenetic analysis was performed using W-IQ-Tree [49] and iTOL [50]. Protein annotations were performed using the plugin InterProScan from Geneious Prime (http://www.geneious.com). The diversifying selection analysis was performed with CODELM from the PAML software. Six models were tested (Null models M0, M1, M7 and alternative models M3, M2, M8) to identify the amino acids under positive selection.

BAC library screening

The BAC library of GIG362-6 was generated as described previously [51]. Primers were designed based on the BAC clone 01. The BAC library was genotyped for the markers 1-BAC500, 2-BAC500, 3-BAC500 and 5-BAC500 (Fig. S2a, Table S2) to identify BAC

clone 02 that overlap with BAC clone 01 on the left side; and with the markers BAC116, BAC129 and BAC130 (Fig. S2a, Table S2) to identify BAC clone 03 that overlap with BAC clone 01 on the right side.

Fine mapping

The seedlings were transferred to pots with MS20 medium and organized in groups of 24 plants to grow them synchronously, each plant was assigned a unique number to track them along the process, and every four pots will form a 96-well rack. The detailed protocols for DNA isolation, amplification of HRM and CAPS markers were described previously [42]. The recombinant genotypes were transferred to pots containing fresh MS medium, propagated, and transferred to the greenhouse for phenotyping by Pep-25 infiltration.

Candidate gene cloning and agroinfiltration

The coding region of the candidate genes was PCR-amplified from cDNA from GIG362-6 and firstly cloned into the Gateway entry vector pENTR, then shuffled into destination vector pK7WG2 with 35S promoter by LR reaction. The constructs were transformed into *Agrobacterium tumefaciens* strain AGL1 for transiently overexpression assay in plants. The agroinfiltration was performed in 4 –weeks-old *N. benthamiana* leaves, Pep-25 (2 µM) were infiltrated into the same leaves two days later, and the cell death responses were evaluated 3 to 5 days later.

Acknowledgements

This work was supported by Peruvian Council for science, technology and technological innovation (CONCYTEC) and FONDECYT contract 129-2017 (YCTA). We thank Isolde Bertram-Pereira for culturing *Solanum* plants, Henk Smid and Harm Wiegersma for their help in the greenhouse. We thank Dr. Helene Berges and Caroline Callot from the French Plant Genomic Resource Center (INRA-CNRGV) for their help to sequence the BAC clones.

References

1. Couto, D. and C. Zipfel, *Regulation of pattern recognition receptor signalling in plants.* Nature Reviews Immunology, 2016. **16**(9): p. 537-552.
2. Wang, Y., et al., *Evasion of plant immunity by microbial pathogens.* Nature Reviews Microbiology, 2022. **20**(8): p. 449-464.
3. Jones, J.D.G. and J.L. Dangl, *The plant immune system.* Nature, 2006. **444**(7117): p. 323-329.
4. Yuan, M., et al., *PTI-ETI crosstalk: an integrative view of plant immunity.* Current Opinion in Plant Biology, 2021. **62**: p. 102030.
5. Ngou, B.P.M., et al., *Mutual potentiation of plant immunity by cell-surface and intracellular receptors.* Nature, 2021. **592**(7852): p. 110-115.
6. Yuan, M., et al., *Pattern-recognition receptors are required for NLR-mediated plant immunity.* Nature, 2021. **592**(7852): p. 105-109.
7. Sun, W., et al., *Within-Species Flagellin Polymorphism in Xanthomonas campestris pv campestris and Its Impact on Elicitation of Arabidopsis FLAGELLIN SENSING2–Dependent Defenses.* The Plant Cell, 2006. **18**(3): p. 764-779.
8. Cai, R., et al., *The Plant Pathogen Pseudomonas syringae pv. tomato Is Genetically Monomorphic and under Strong Selection to Evade Tomato Immunity.* PLOS Pathogens, 2011. **7**(8): p. e1002130.
9. Clarke, C.R., et al., *Allelic variation in two distinct Pseudomonas syringae flagellin epitopes modulates the strength of plant immune responses but not bacterial motility.* New Phytologist, 2013. **200**(3): p. 847-860.
10. Vinatzer, B.A., C.L. Monteil, and C.R. Clarke, *Harnessing Population Genomics to Understand How Bacterial Pathogens Emerge, Adapt to Crop Hosts, and Disseminate.* Annual Review of Phytopathology, 2014. **52**(1): p. 19-43.
11. Fürst, U., et al., *Perception of Agrobacterium tumefaciens flagellin by FLS2XL confers resistance to crown gall disease.* Nature Plants, 2020. **6**(1): p. 22-27.
12. Wei, Y., et al., *An immune receptor complex evolved in soybean to perceive a polymorphic bacterial flagellin.* Nature Communications, 2020. **11**(1): p. 3763.
13. Ngou, B.P.M., et al., *Concerted expansion and contraction of immune receptor gene repertoires in plant genomes.* Nature Plants, 2022. **8**(10): p. 1146-1152.
14. Haverkort, A.J., et al., *Durable Late Blight Resistance in Potato Through Dynamic Varieties Obtained by Cisgenesis: Scientific and Societal Advances in the DuRPh Project.* Potato Research, 2016. **59**(1): p. 35-66.
15. Kamoun, S., et al., *The Top 10 oomycete pathogens in molecular plant pathology.* Molecular Plant Pathology, 2015. **16**(4): p. 413-434.
16. Kamoun, S., et al., *A Gene Encoding a Protein Elicitor of Phytophthora infestans Is Down-Regulated During Infection of Potato.* Molecular Plant-Microbe Interactions®, 1997. **10**(1): p. 13-20.
17. Du, J., et al., *Elicitin recognition confers enhanced resistance to Phytophthora infestans in potato.* Nature Plants, 2015. **1**(4): p. 15034.
18. Böhm, H., et al., *A Conserved Peptide Pattern from a Widespread Microbial Virulence Factor Triggers Pattern-Induced Immunity in Arabidopsis.* PLOS Pathogens, 2014. **10**(11): p. e1004491.
19. Albert, I., et al., *An RLP23–SOBIR1–BAK1 complex mediates NLP-triggered immunity.* Nature Plants, 2015. **1**(10): p. 15140.
20. Ma, Z., et al., *A Phytophthora sojae Glycoside Hydrolase 12 Protein Is a Major Virulence Factor during Soybean Infection and Is Recognized as a PAMP.* The Plant Cell, 2015. **27**(7): p. 2057-2072.

21. Wang, Y., et al., *Leucine-rich repeat receptor-like gene screen reveals that Nicotiana RXEG1 regulates glycoside hydrolase 12 MAMP detection.* Nature Communications, 2018. **9**(1): p. 594.
22. Kato, H., et al., *Pathogen-derived 9-methyl sphingoid base is perceived by a lectin receptor kinase in Arabidopsis.* bioRxiv, 2021: p. 2021.10.18.464766.
23. Nürnberger, T., et al., *High affinity binding of a fungal oligopeptide elicitor to parsley plasma membranes triggers multiple defense responses.* Cell, 1994. **78**(3): p. 449-460.
24. Mateos, F.V., M. Rickauer, and M.-T. Esquerré-Tugayé, *Cloning and Characterization of a cDNA Encoding an Elicitor of Phytophthora parasitica var. nicotianae That Shows Cellulose-Binding and Lectin-Like Activities.* Molecular Plant-Microbe Interactions®, 1997. **10**(9): p. 1045-1053.
25. Orsomando, G., et al., *Phytotoxic Protein PcF, Purification, Characterization, and cDNA Sequencing of a Novel Hydroxyproline-containing Factor Secreted by the Strawberry Pathogen Phytophthora cactorum *.* Journal of Biological Chemistry, 2001. **276**(24): p. 21578-21584.
26. Liu, Z., et al., *Patterns of Diversifying Selection in the Phytotoxin-like scr74 Gene Family of Phytophthora infestans.* Molecular Biology and Evolution, 2004. **22**(3): p. 659-672.
27. Chang, Y.-H., H.-Z. Yan, and R.-F. Liou, *A novel elicitor protein from Phytophthora parasitica induces plant basal immunity and systemic acquired resistance.* Molecular Plant Pathology, 2015. **16**(2): p. 123-136.
28. Chen, X.-R., et al., *SCR96, a small cysteine-rich secretory protein of Phytophthora cactorum, can trigger cell death in the Solanaceae and is important for pathogenicity and oxidative stress tolerance.* Molecular Plant Pathology, 2016. **17**(4): p. 577-587.
29. Parker, J.E., et al., *An extracellular glycoprotein from Phytophthora megasperma f. sp. glycinea elicits phytoalexin synthesis in cultured parsley cells and protoplasts.* Mol. Plant-Microbe Interact, 1991. **4**: p. 19-27.
30. Nürnberger, T., et al., *Covalent cross-linking of the Phytophthora megasperma oligopeptide elicitor to its receptor in parsley membranes.* Proceedings of the National Academy of Sciences of the United States of America, 1995. **92**(6): p. 2338-2342.
31. Nennstiel, D., D. Scheel, and T. Nürnberger, *Characterization and partial purification of an oligopeptide elicitor receptor from parsley (Petroselinum crispum).* FEBS Letters, 1998. **431**(3): p. 405-410.
32. Brunner, F., et al., *Pep-13, a plant defense-inducing pathogen-associated pattern from Phytophthora transglutaminases.* The EMBO Journal, 2002. **21**(24): p. 6681-6688.
33. Reiss, K., et al., *Structural and Phylogenetic Analyses of the GP42 Transglutaminase from Phytophthora sojae Reveal an Evolutionary Relationship between Oomycetes and Marine Vibrio Bacteria*.* Journal of Biological Chemistry, 2011. **286**(49): p. 42585-42593.
34. Halim, V.A., et al., *The oligopeptide elicitor Pep-13 induces salicylic acid-dependent and -independent defense reactions in potato.* Physiological and Molecular Plant Pathology, 2004. **64**(6): p. 311-318.
35. Nietzschmann, L., et al., *Early Pep-13-induced immune responses are SERK3A/B-dependent in potato.* Scientific Reports, 2019. **9**(1): p. 18380.
36. Fabritius, A.-L. and H.S. Judelson, *A Mating-Induced Protein of Phytophthora infestans Is a Member of a Family of Elicitors with Divergent Structures and Stage-Specific Patterns of Expression.* Molecular Plant-Microbe Interactions®, 2003. **16**(10): p. 926-935.
37. Medina, E.M. and N.E. Buchler, *Chytrid fungi.* Current Biology, 2020. **30**(10): p. R516-R520.
38. Haas, B.J., et al., *Genome sequence and analysis of the Irish potato famine pathogen Phytophthora infestans.* Nature, 2009. **461**(7262): p. 393-398.
39. Yang, Z., *PAML 4: Phylogenetic Analysis by Maximum Likelihood.* Molecular Biology and Evolution, 2007. **24**(8): p. 1586-1591.

40. Lin, X., et al., *Recognition of Pep-13/25 MAMPs of Phytophthora localizes to an RLK locus in Solanum microdontum.* Frontiers in Plant Science, 2023. **13**.
41. Buscaill, P. and R.A.L. van der Hoorn, *Defeated by the nines: nine extracellular strategies to avoid microbe-associated molecular patterns recognition in plants.* The Plant Cell, 2021. **33**(7): p. 2116-2130.
42. Torres Ascurra, Y., et al., *Identification of Solanum Immune Receptors by Bulked Segregant RNA-Seq and High-Throughput Recombinant Screening*, in *Solanum tuberosum: Methods and Protocols*, D. Dobnik, et al., Editors. 2021, Springer US: New York, NY. p. 315-330.
43. Lin, X., *Apoplastic effectors, MAMPs and surface immune receptors*, in *the battlefront of the Phytophthora infestans - potato interaction*. 2018, Wageningen University: Wageningen.
44. Nürnberger, T. and B. Kemmerling, *Pathogen-Associated Molecular Patterns (PAMP) and PAMP-Triggered Immunity*, in *Annual Plant Reviews online*. p. 16-47.
45. Money, N.P., *Chapter 1 - Fungal Diversity*, in *The Fungi (Third Edition)*, S.C. Watkinson, L. Boddy, and N.P. Money, Editors. 2016, Academic Press: Boston. p. 1-36.
46. Brus-Szkalej, M., et al., *A family of cell wall transglutaminases is essential for appressorium development and pathogenicity in <em>Phytophthora infestans</em&gt.* bioRxiv, 2021: p. 2021.11.23.469665.
47. Vleeshouwers, V.G.A.A., et al., *SolRgene: an online database to explore disease resistance genes in tuber-bearing Solanumspecies.* BMC Plant Biology, 2011. **11**(1): p. 116.
48. Edgar, R.C., *MUSCLE: a multiple sequence alignment method with reduced time and space complexity.* BMC Bioinformatics, 2004. **5**(1): p. 113.
49. Trifinopoulos, J., et al., *W-IQ-TREE: a fast online phylogenetic tool for maximum likelihood analysis.* Nucleic Acids Research, 2016. **44**(W1): p. W232-W235.
50. Letunic, I. and P. Bork, *Interactive Tree Of Life (iTOL) v4: recent updates and new developments.* Nucleic Acids Research, 2019. **47**(W1): p. W256-W259.
51. Lin, X., et al., *Divergent Evolution of PcF/SCR74 Effectors in Oomycetes Is Associated with Distinct Recognition Patterns in Solanaceous Plants.* mBio, 2020. **11**(3): p. e00947-20.

Supplementary data

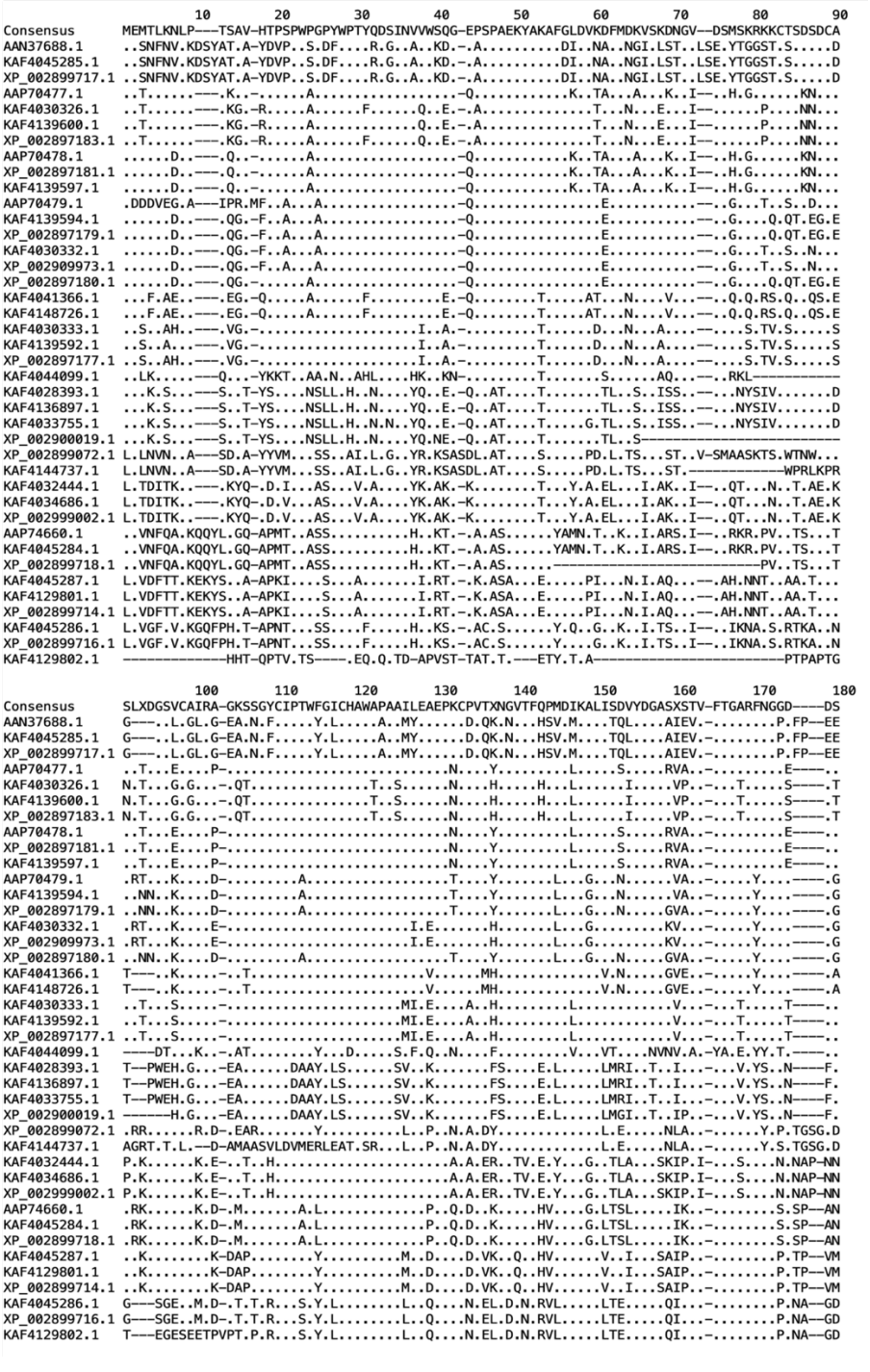

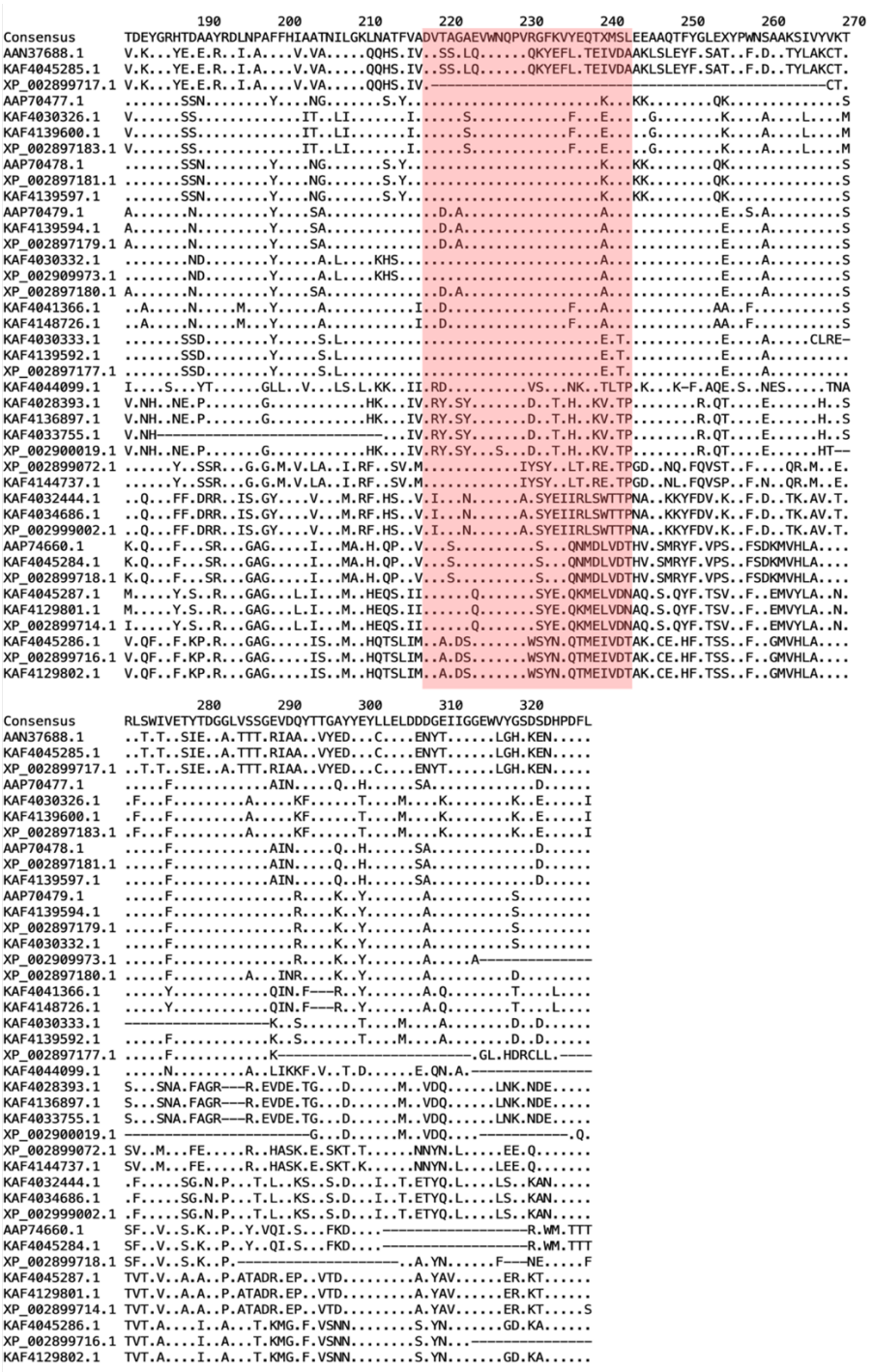

Supplementary figure 1. Alignment of 40 transglutaminase protein sequences from *P. infestans*. Pep-13/25 sequences are shaded in red.

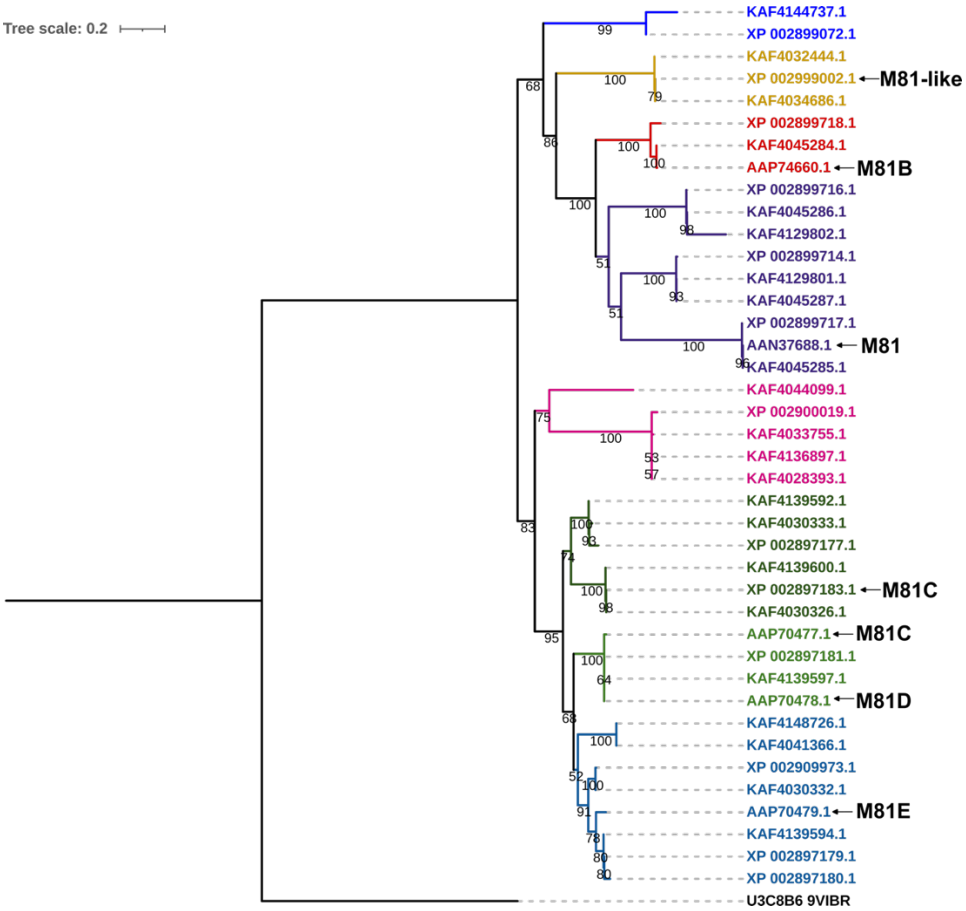

Supplementary figure 2. Phylogenetic tree of transglutaminase protein sequences retrieved from the NCBI.

a

Model	lnL	Estimates of parameters	Positively selected sites
M0 (one-ratio)	-10942.152011	ω=0. 30927	Not allowed
M1 (nearly neutral)	-10327.559836	p_0=0.89408	Not allowed
M2 (positive selection)	-10287.048322	p_0=0.83045, p_1=0.08478, p_2=0.08477, ω_2=0.34103	251 H, **332 R**
M3 (discrete)	-10264.395987	p_0=0.78432, p_1=0.18374, p_2=0.03194, ω_0=0.00856, ω_1=0.37444, ω_2=1.34259	**184 M**, 188 D, **192 Q**, 195 H, 198 S, **215 V**, 218 Q, 236T, 244 K, 245 K, **251 H, 253 G**, 255 K, **256 K, *258 T*, 261 N,** 264 A, 265 S, 271 E, **302 A**, 310 Y, **326 S, 332 R, 334 A, 348 S, 349 T,** 358 N, **381 S**, 391 A, 404 Y, **408 K,** 412 K, 417 T, **422 Q**, **423 K,** 428 S, 448 T, 451 G, **454 S, 457 A**, 459 N, 460 Q, 465 Q, 468 H, 478 E
M7 (beta)	-10287.224382	p=0.07105, q=0.50791	Not allowed
M8 (beta&ω)	-10263.137162	p_0=0.97689, p=0.12818, q=1.28918, ω_1=1.47490	192 Q, 251 H, 258 T, **332 R**, 408 K, 457 A, 460 Q

b

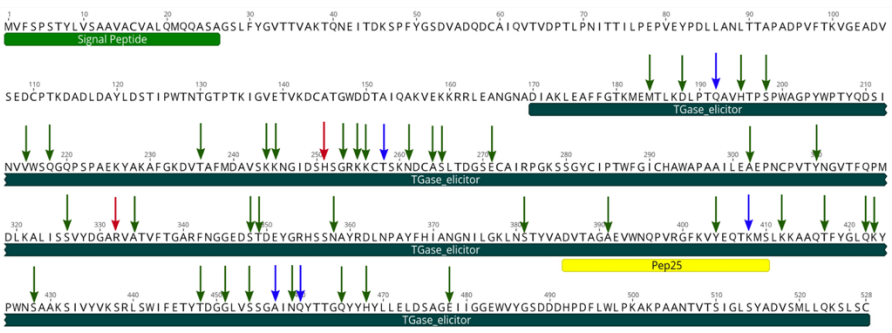

Supplementary figure 3. **Diversifying selection analysis. a.** Model used to identify amino acids under positive selection. **b.** Protein sequence of the transglutaminase from *P. sojae* with signal peptide, transglutaminase domain, and Pep-25 is shown. The amino acids found under positive selection by the three models (M2, M3, M8) are indicated with red arrows, by two models (M3, M8) are indicated with blue arrows, and by only one model (M3) are indicated with green arrows.

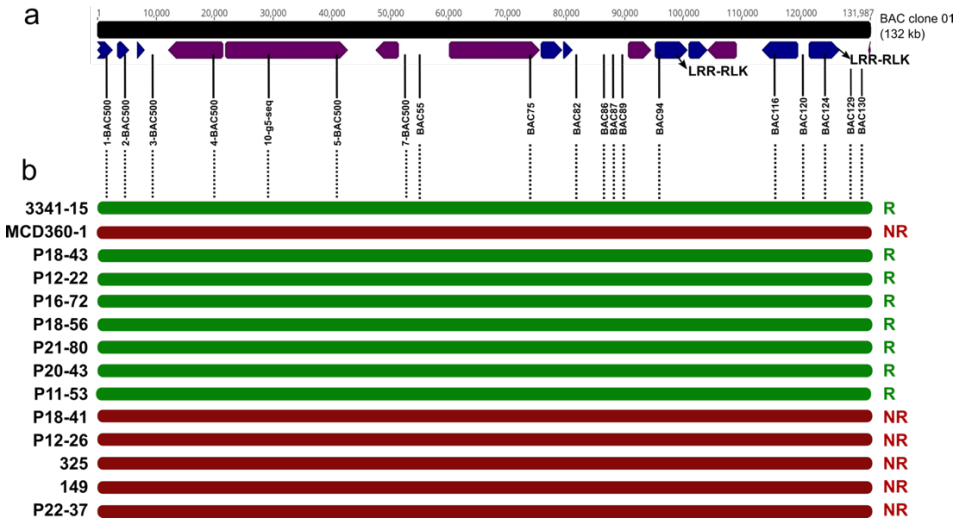

Supplementary figure 4. **GIG BAC clone and screening of recombinants. a.** BAC clone 01 from GIG of 132kb. Annotation showed the presence 9 partial or full-length LRR-RLKs (in blue), only two genes contained signal peptide (are indicated with arrows as LRR-RLK). **b.** The analysis of markers designed inside the BAC on the recombinant plants identified, showed that they all co-segregate, which indicated that the mapping interval is not closed.

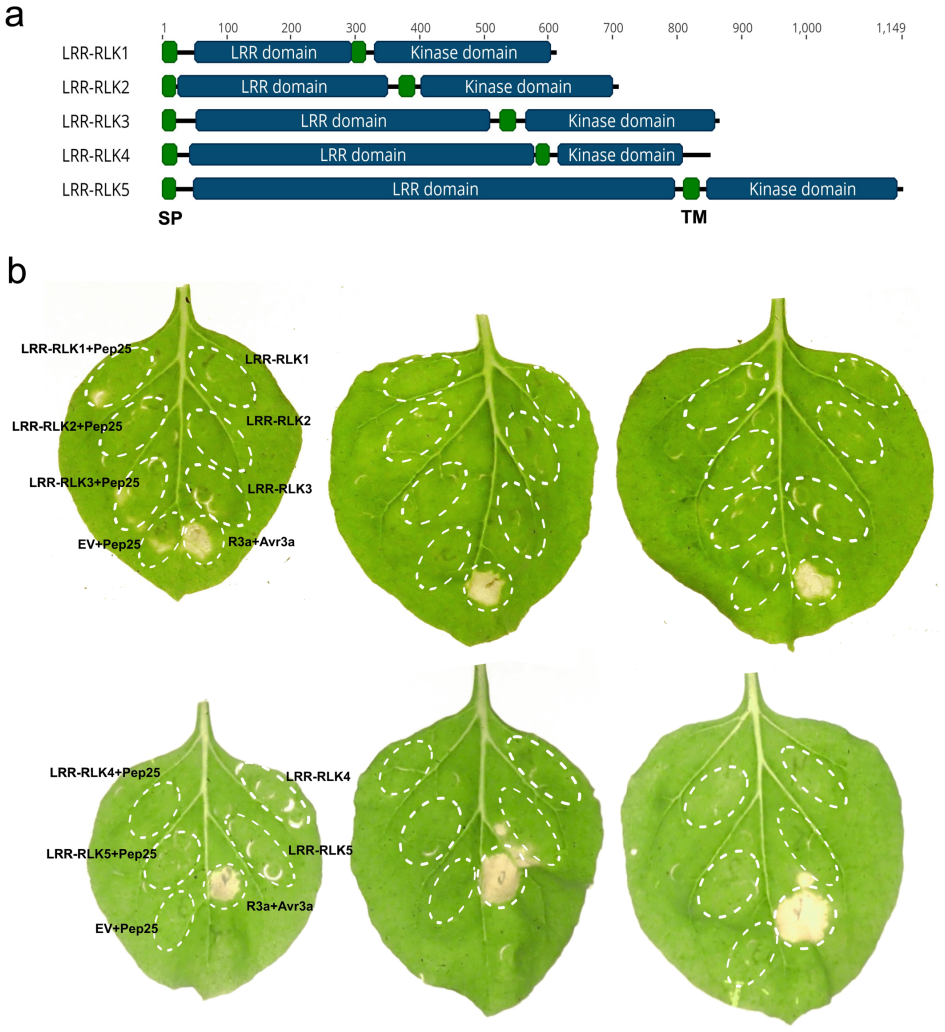

Supplementary figure 5. Protein annotation of candidate genes and functional analysis. a. Predicted domain structure of the five candidate genes. They all showed the presence of signal peptide (SP), a non-cytoplasmic domain that contain the LRRs, a transmembrane domain (TM) and a cytoplasmic domain that contains the kinase domain. **b.** The five candidate genes (LRR-RLK1, LRR-RLK2, LRR-RLK3, LRR-RLK4 and LRR-RLK5) were transiently expressed in *N. benthamiana* leaves through agroinfiltration, OD600 = 1.0. Pep-25 peptide (2 µM) was infiltrated in the same leaf 2 days after the agroinfiltration. The photos were taken 3 days after the peptide infiltration. Co-expression of *R3a* and *AVR3a* were used as a positive control, empty vector and Pep-25 were used as negative controls.

Supplementary table 1. List of *Solanum* genotypes. The genotypes, species and abbreviations are shown in different columns.

Genotype	Species	Species abbreviation
585-1	*S. demissum*	DMS
364-1	*S. demissum*	DMS
512-03	*S. bukasovii*	BUK
200-4	*S. tuberosum* Group Phureja	PHU
362-6	*S. microdontum* subsp. *gigantophyllum*	micrGIG
543-5	*S. chacoense*	CHC
544-5	*S. chacoense*	CHC
381-2	*S. species*	SPEC
646-4	*S. hondelmannii*	HDM
491-01	*S. berthaultii*	BER
680-5	*S. leptophyes*	LPH
144-3	*S. doddsii*	DDS
144-5	*S. doddsii*	DDS
496-01	*boliviense*	BLV
240-2	*S. tuberosum* Group Andigenum	ADG
222-5	*S. tuberosum* Group Andigenum	SUB
372-8	*S. tuberosum* Group Phureja	PHU
201-3	*S. tuberosum* Group Phureja	PHU
150-4	*S. edinense*	EDN
151-1	*S. edinense*	EDN
151-3	*S. edinense*	EDN
483-1	*S. berthaultii*	BER
371-7	*S. tuberosum* Group Phureja	PHU
128-1	*S. tuberosum* Group Chaucha	CHA
Andigena	*S. tuberosum* Group Andigenum	
Clone V	*Solanum tuberosum*	
DM 1-3 516 R44	*Solanum tuberosum*	
cv. Colomba	*Solanum tuberosum*	
cv. Altus	*Solanum tuberosum*	

Supplementary table 2. Sequence of the primers used to amplify the molecular markers used in this study. Type of markers and annealing temperature are given.

Primer	Marker type	Restriction enzyme	Sequence	Ta (° C)
PCR1.22-F	PCR-based	NA	TGCTGAAGAAAAGGACATGT	59
PCR1.22-R			TAATTCTCAACTTCACCGGT	
CAPS1.23-F	CAPS	EcoRI	GGTCGAGTCCCTGATTTT	57
CAPS1.23-R			TGAAGCGCGAGTAATTT	
PCR1.37-F	PCR-based	NA	ATGGACAACACATTCAGGTT	60
PCR1.37-R			GTTATGCCTAGTTCAGCCAT	
HRM1.429-F	HRM	NA	AAGGTGAGGAGTCTTGGGAGG	64
HRM1.429-R			CTTCAGCGTGTGTCTTTGCC	
HRM1.431-F	HRM	NA	TCCTCATCCAGCAAGACGTT	64
HRM1.431-R			GACATCAGGCAGAGACTAAGCA	
CAPS S047-F	CAPS	BclI	CAAGAGGAGGATAAGTACGC	60
CAPS S047-R			AAGGGTAGGCTTAACGTATT	
PCR S050-F	PCR-based	NA	CAACTTCCAAAGGGCATAAC	60
PCR S050-R			ACTTCTGCAACTTCGACTAC	
CAPS 2BAC-F	CAPS	RsaI	GCCTCTTTGGTACGGTTCAATAA	60
CAPS 2BAC-R			GAGTAGATAGGACCCTGCACATA	
PCR S041-F	PCR-based	NA	GTGAAAGACAGTGTTGAGAC	60
PCR S041-R			ACAAGCAAGAGACTTCATCA	
PCR S085-F	PCR-based	NA	ATGGCGGAAGTTATGTTCTT	60
PCR S085-R			ATCCAGCTTAATTTGTCCGT	
PCR S086-F	PCR-based	NA	GGGATTTCACTGGGTATGTT	60
PCR S086-R			AACTTTTACTGCGACTGAGT	
HRM M63-F	HRM	NA	GTGAAACATAGCACTGCTAGA	54
HRM M63-R			CACTAGGATGATGGTCTTTGA	
HRM M66-F	HRM	NA	GTGAATCCCACTAATAGCAACA	58
HRM M66-R			CTTTTCCAGGTATGGGAATCT	
HRM1.548-F	HRM	NA	AGAATGTCAACTCTTCATGCATACG	64
HRM1.548-R			CACTGGATATGTAGTTGATGGACG	
HRM1.56-F	HRM	NA	AAAGGGTCCATATTTAACACCTCAC	62
HRM1.56-R			TTTTATGGGGTTGGGGATTATCTTC	
CAPS1.579-F	CAPS	Bme1390I	CGTAACATCCTCACCCCAAG	60
CAPS1.579-R			AACGCCCAGAAAGAAATCGA	
CAPS1.783-F	CAPS	HindIII	GGTTTGGAAGAGAGTGGCAA	58
CAPS1.783-R			CTGTTCTGGACCCAAGGTTC	

Supplementary table 2. (continued)

Primer	Marker type	Restriction enzyme	Sequence	Ta (° C)
1-BAC500-F	PCR-based	NA	GGAAGCTTCCAAATCCAAAGTTG	60
1-BAC500-R			GATGGTGCTGAGAAAAAATCCA	
3-BAC500-F	PCR-based	NA	TTGGGGATTCTATGATACACGTC	60
3-BAC500-R			TGCAAGAGCACATGTTACACATG	
4-BAC500-F	PCR-based	NA	ATAGGGGTCCATTAGATCATTTCG	60
4-BAC500-R			GGCATAGTTGAGTCTTTTCCCTT	
10-g5-seq-F	PCR-based	NA	GGATGATATCGACAACCACTACA	60
10-g5-seq-R			TGAATCCTGATAGGCTATTCGTG	
5-BAC500-F	PCR-based	NA	TAATTTTTGGTGGGTTGTGCAC	60
5-BAC500-R			CATCATGGAAAGATGGGATATGTG	
7-BAC500-F	PCR-based	NA	TAATTCTCAAACTCTCGGACCTG	60
7-BAC500-R			CTGGAGACGTGATGGTTAATTTC	
BAC55-F	PCR-based	NA	AGTAGTGGGTTATAGATGGA	60
BAC55-R			CCTCTTACTCCATACTTACC	
BAC75-F	PCR-based	NA	TAGGACTAGTTCGTTGCTA	60
BAC75-R			CAACCTTTCAGAACAGTC	
BAC82-F	PCR-based	NA	GCAACAACACAATACACTAC	60
BAC82-R			TACATAGAGACAACACCGTA	
BAC86-F	PCR-based	NA	GTCTTAACAGAGGACAACAG	60
BAC86-R			TGGGGAGAAAGTACTACTAC	
BAC87-F	PCR-based	NA	CCTACCTTTCTCATCTATGT	60
BAC87-R			GTCTCTCTGTAAATGTCCAG	
BAC89-F	PCR-based	NA	GGTAAGCTCTCACTAAGTTT	60
BAC89-R			ATAGTTTCTGATACCTCGAC	
BAC94-F	PCR-based	NA	CTTCATGCTTGTTAGGTAG	60
BAC94-R			GGAGGAGAAGAAATATGAG	
BAC116-F	PCR-based	NA	GACAGTGTTCCCTTGTATAC	60
BAC116-R			CTTATGAGGAATTAGAGGAC	
BAC120-F	PCR-based	NA	GCAGATTAAGAACACAGAAG	60
BAC120-R			ACATCACGAGTCATCTAGTT	
BAC124-F	PCR-based	NA	GGAGATCTTCAACATATCAC	60
BAC124-R			TATGTCACAGCCTTTATATG	
BAC129-F	PCR-based	NA	AACAACAACACGTCTACC	60
BAC129-R			AAAGGTTAGGTGTGTCTTAG	
BAC130-F	PCR-based	NA	TCAATTAGCTCTTCTCTCTT	60
BAC130-R			CAGATAAAGAAGGAGATAGG	

Chapter 4

Functional diversification of a wild potato immune receptor at its center of origin

Yerisf C. Torres Ascurra, Lisha Zhang, AmirAli Toghani, Chenlei Hua, Nandeesh Jalahalli Rangegowda, Andres Posbeyikian, Hsuan Pai, Xiao Lin, Pieter J. Wolters, Doret Wouters, Reinhoud de Blok, Niels Steigenga, Maxence J.M. Paillart, Richard G. F. Visser, Sophien Kamoun, Thorsten Nürnberger and Vivianne G. A. A. Vleeshouwers

This chapter was published as:
Torres Ascurra, Y. C., Zhang, L., Toghani, A., Hua, C., Rangegowda, N. J., Posbeyikian, A., ... & Vleeshouwers, V. G. (2023). Functional diversification of a wild potato immune receptor at its center of origin. Science, 381(6660), 891-897.

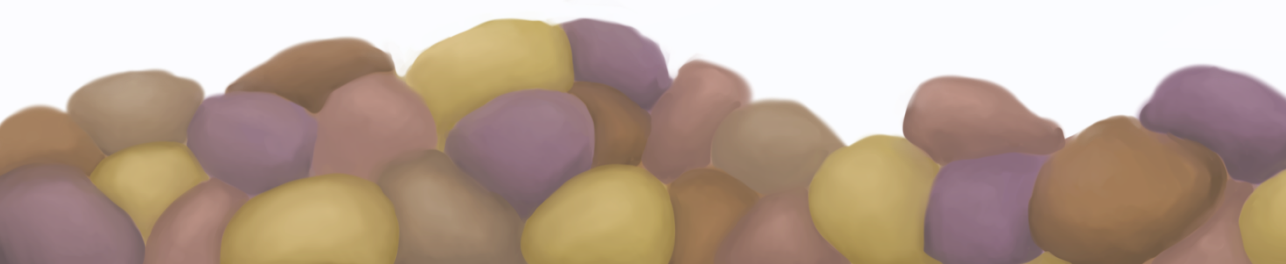

Abstract

Plant cell surface pattern recognition receptors (PRRs) and intracellular immune receptors cooperate to provide immunity to microbial infection. Both receptor families have coevolved at an accelerated rate, but the evolution and diversification of PRRs is poorly understood. We have isolated potato surface receptor Pep-13 receptor unit (PERU) that senses Pep-13, a conserved immunogenic peptide pattern from plant pathogenic *Phytophthora* species. PERU, a leucine-rich repeat receptor kinase, is a bona fide PRR that binds Pep-13 and enhances immunity to *Phytophthora infestans* infection. Diversification in ligand binding specificities of PERU can be traced to sympatric wild tuber-bearing *Solanum* populations in the Central Andes. Our study reveals the evolution of cell surface immune receptor alleles in wild potato populations that recognize ligand variants not recognized by others.

Plant cell surface pattern recognition receptors (PRRs) and intracellular immune receptors cooperate to provide robust resistance to microbial infection (*1-3*). The synergistic activation of plant immunity by spatially separated plant immune receptors suggests their co-evolution. A strong correlation in the number of genes encoding surface and intracellular immune receptors observed across the plant lineage supports the concept of mutual potentiation of immune responses initiated in different plant cell compartments (*4, 5*).

It is assumed that pathogen pressure in ecological niches drives plant immune receptor evolution (*5, 6*), but evidence for diversification of plant PRR sequences and functions among natural plant populations is lacking. We hypothesized that a PRR might recognize Pep-13, a conserved microbial immunogenic 13-amino-acid fragment from a cell wall glycoprotein (GP42) with transglutaminase (TG) activity (*7-9*). TGs are produced by several plant-pathogenic oomycete *Phytophthora* species, including *P. infestans*, the causal agent of potato late blight disease and the Great Irish Famine (*10-12*). Pep-13 triggers a hypersensitive response and other immunity-associated responses in diverse plant species, including the solanaceous host plant, potato (*10*).

Potato *PERU* senses oomycete-derived pattern Pep-13

We screened a collection of wild *Solanum* species and cultivated potato genotypes for cell death induction when infiltrated with Pep-13 or its structural derivative, Pep-25 (*7, 13*). To identify the Pep-13-receptor by a map-based cloning approach, we crossed genotype *Solanum tuberosum* Group Phureja DM 1-3 516 R44 (DM) and genotype *S. tuberosum* RH89-039-16 (RH) (Fig. 1A). DM is a Pep-13/Pep-25 sensitive genotype, which was previously used to establish the potato reference genome (*14*). RH is a Pep-13/Pep-25-insensitive genotype. We back-crossed the F1 generation 3240-4 to the RH parent, and used the resulting F2 population (3648) for genetic mapping (*15*). Pattern sensitivity segregated in a 1:1 ratio, suggesting that a single, dominant gene encodes the corresponding receptor (fig. S1A). Pep-13/Pep-25 sensitivity was previously mapped to the top of chromosome 3 (*13*), and subsequent marker-assisted fine-mapping yielded a 55.2 kb fragment containing 7 open-reading frames, three of which encode leucine-rich repeat receptor kinases (LRR-RKs a-c) (fig. S1B). LRR-RKs consist of an extracellular LRR domain, a transmembrane-spanning domain and an intracellular serine/threonine protein kinase domain, which is absent in LRR receptor proteins (LRR-RPs). LRR ectodomain-containing receptors are the predominant type of plant PRRs known to date and have evolved to recognize primarily proteinaceous microbial patterns or phytocytokines (*16-18*).

To determine which LRR-RK candidate gene sequence confers Pep-13 sensitivity, we performed transient expression assays in the solanaceous model plant, *Nicotiana*

benthamiana. *Agrobacterium* infection-mediated expression of LRR-RK b, but not of LRR-RK a or c-encoding cDNA sequences resulted in plant cell death after treatment with either Pep-13 or GP42 (Fig. 1B). We thus designated LRR-RK b Pep-13 receptor unit (PERU). PERU is a canonical plant LRR-RK that hosts an ectodomain composed of 27 LRRs linked by a transmembrane domain to an intracellular serine-threonine protein kinase domain (fig. S2). Stable expression of *PERU* cDNA in Pep-13-insensitive potato cultivar Atlantic resulted in Pep-13-inducible cell death, production of reactive oxygen species (ROS) and accumulation of the plant stress hormone, ethylene (Fig. 1C-E, fig. S3). These responses were not observed in wild-type Atlantic or in control lines transformed with empty vector only. Inactivation of the *PERU* locus in Pep-13-sensitive DM by CRISPR-Cas9 mutagenesis provided direct proof for a causal role of PERU in Pep-13 pattern recognition. To abolish *PERU* gene expression, genotype DM was stably transformed with CRISPR-Cas9 and 4 sgRNA, CRISPR lines were genotyped, and deletion and frameshift mutations were found, resulting in loss of Pep-13-induced cell death, ROS burst and ethylene production (Fig. 1F-H). In sum, these results document a role for potato PERU in Pep-13 pattern recognition.

A PERU- SERK3 complex mediates Pep-13/Pep-25-induced defenses and plant cell death

LRR-type PRRs recognize their cognate ligands by binding to their LRR ectodomains (*19*). We investigated ligand-receptor binding in vitro and in planta. To test for physical interaction of PERU and Pep-25 in vitro, we incubated recombinant hexa-histidine (His_6)-tagged PERU LRR ectodomain protein ($PERU^{LRR}$-His_6) with biotinylated Pep-25 (Pep-25-bio) before treatment with the homo-bifunctional cross-linker ethylene glycol bis (succinimidyl succinate) (EGS) to stabilize the ligand-receptor complex (*8*). Pep-25-bio is as active as Pep-25 (fig. S4). Following $PERU^{LRR}$-His_6 immunoprecipitation, bound Pep-25-bio was visualized by streptavidine/anti-streptavidine antisera (fig. S5). A large molar excess of free Pep-13 competitively abolished ligand-receptor complex formation, which suggests direct and specific ligand binding by $PERU^{LRR}$. The affinity constant of the ligand/receptor interaction (K_D=88.9 nM) is close to ligand concentrations required for immune activation in *p35S::PERU-expressing* Pep-13-insensitive *Solanum hjertingii* or in Pep-13-sensitive potato DM (EC_{50}=9.8 nM or 44 nM respectively), indicating that the PERU ectodomain is sufficient for ligand binding (fig. S5). To analyze the Pep-25-bio/PERU interaction in planta, we treated leaves of *N. benthamiana* plants expressing Green Fluorescent Protein (GFP)-tagged PERU (*p35S::PERU-GFP)* with ligand prior to EGS treatment. Precipitation of PERU-GFP protein and subsequent detection of bound ligand corroborated ligand-receptor binding observed in vitro (Fig. 2A). Again, excess of Pep-13 abolished ligand binding. We did not observe an inhibitory effect when a biologically inactive Pep-13 mutant peptide, Pep-13W231A (tryptophan residue 231 mutated to alanine, amino acid numbering corresponds to full-length GP42 sequence (*10*)), was used as competitor (Fig. 2A).

Notably, a W231A mutant of GP42 did not only abolish its plant defense-eliciting activity, but also reduced its TG activity by 98.5% (*10*). Altogether, these data demonstrate specific binding of Pep-13 to its high-affinity binding site, PERU.

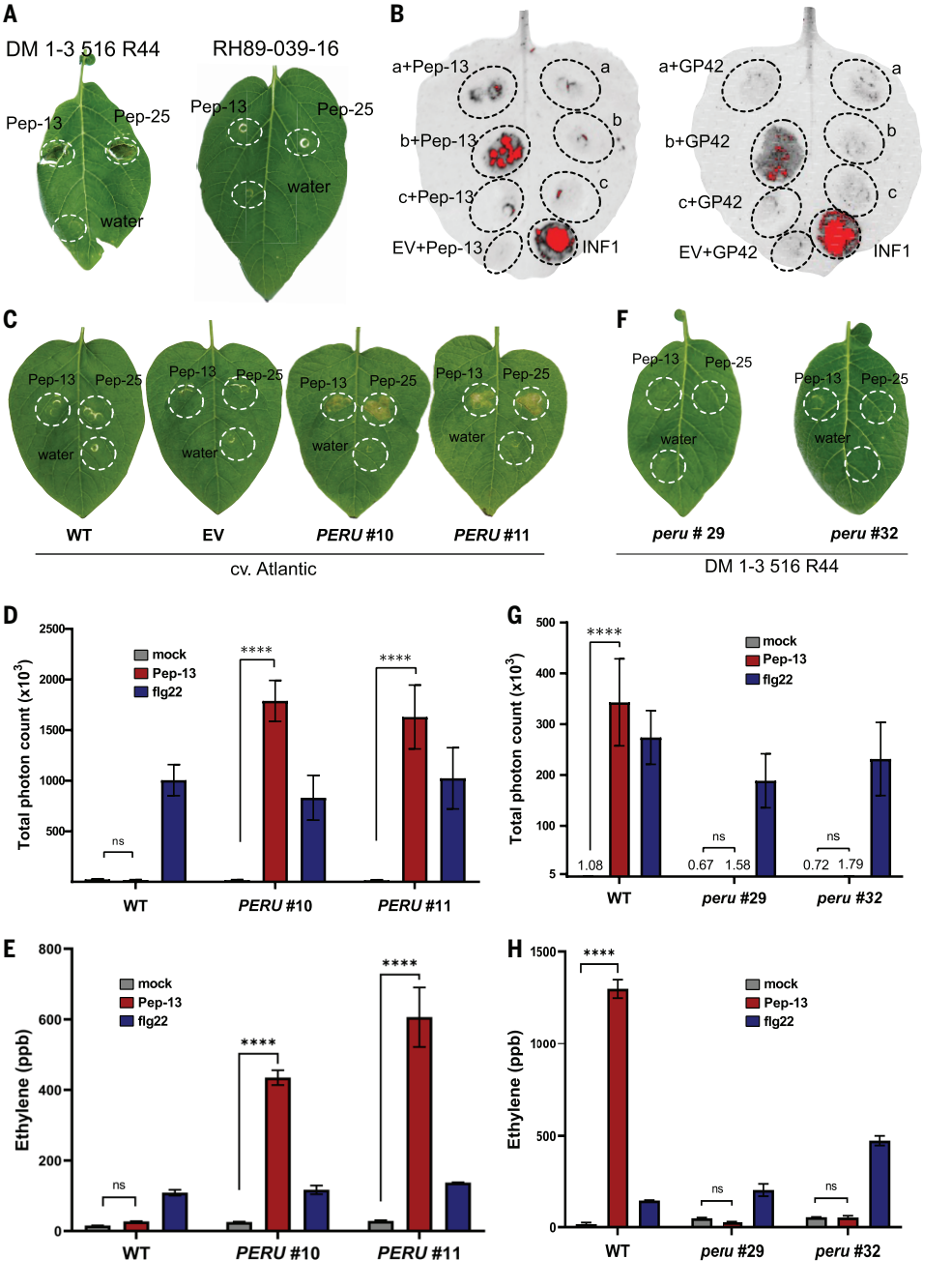

Figure 1. PERU confers response to Pep-13. (A) The genotype DM 1-3 516 R44 (DM) shows cell death response upon infiltration of Pep-13 and Pep-25, while the genotype RH89-039-16 (RH) does not. **(B)** Representative *N. benthamiana* leaves co-agroinfiltrated with the candidate genes "a", "b" or "c", and Pep-13 or the full-length glycoprotein GP42, show that candidate "b" confers cell death to Pep-13 (left leaf) and GP42 (right leaf), whereas candidates "a" and "c" do not. Cell death was visualized by red light imaging system at 3 days post infiltration (*20*). **(C)** Potato cultivar Atlantic (WT) is non-sensitive to Pep-13/25, transgenic Atlantic expressing *PERU* (*PERU*#10 and *PERU*#11) show cell death after Pep-13/25 infiltration, cv. Atlantic transformed with empty vector (EV) is included as negative control. **(D)** Total ROS production, and **(E)** Ethylene accumulation after treatment with 1μM Pep-13, flg22 or water as control in potato cv. Atlantic WT, EV, *PERU* #10 and #11. **(F)** CRISPR lines *peru* #29 and #32 are insensitive to Pep-13/25. **(G)** Total ROS production, and **(H)** Ethylene accumulation after treatment with 1μM Pep-13, flg22 or water as control, in DM (WT) and lines *peru* #29 and *peru* #32. Data were analyzed using one-way ANOVA with Tukey's test, (**** p-value ≤ 0.0001). All experiments were performed three times with similar results, and representative experiments are shown.

The LRR-RK BAK1/SERK3 (BRASSINOSTEROID INSENSITIVE 1-ASSOCIATED KINASE1/SOMATIC EMBRYOGENESIS RECEPTOR KINASE 3) forms ligand-induced receptor/co-receptor complexes with plant LRR-RK-type PRRs (*17, 18, 21*). We found Pep-13 pattern-induced complex formation of PERU and SERK3A after transient co-expression of *p35S::PERU^{DM}-GFP* and *p35S::SERK3A^{DM}-Myc* in *N. benthamiana* plants (Fig. 2B). Virus-induced gene silencing of *SERK3* (*TRV::NbSERK3*) in *N. benthamiana* resulted in a massive reduction in Pep-13-induced hypersensitive cell death and ROS production in *TRV::NbSERK3* plants (Fig. 2C, fig. S6), suggesting that PERU recruits SERK3 in a pattern-dependent manner. Silencing of SOBIR1 (SUPPRESSOR OF BAK1-INTERACTING KINASE1) (*TRV::NbSOBIR1/-like*), which is exclusively required for the function of LRR-RP-type PRRs, did not affect Pep-13-induced cell death formation. In contrast, *Phytophthora infestans* elicitin INF1-induced cell death mediated by activation of LRR-RP-type ELR (ELICITIN RESPONSE) (*22*), is reduced in both TRV::Nb*SERK3* and TRV::Nb*SOBIR1/-like* plants (Fig. 2C).

In solanaceous *N. benthamiana*, activation of plant immunity and cell death by LRR-RP-type PRRs requires lipase-like ENHANCED DISEASE SUSCEPTIBILITY 1 (EDS1) (*23*) and helper NUCLEOTIDE-BINDING LRR (hNLR) REQUIRED FOR HYPERSENSITIVE RESPONSE-ASSOCIATED CELL DEATH 2, 3 and 4 (NRC2, NRC3, NRC4) (*24, 25*). Since LRR-RK-type PRRs have not previously been implicated in activating plant cell death in any plant system, we tested whether these proteins are required for PERU signalling. *N. benthamiana* plants transiently expressing *p35S::PERU^{DM}* developed cell death symptoms upon infiltration of Pep-13 or GP42 (Fig. 1B), and produced ethylene upon treatment with Pep-25 (fig. S4). Transient expression of *p35S::PERU^{DM}-GFP* in *N. benthamiana* mutants lacking EDS1 and related PHYTOALEXIN-DEFICIENT 4 (PAD4) (*26, 27*) or hNLRs NRC2/3/4 (*24*) had no reducing effect on elicitor-induced cell death and ethylene production (fig S7). Altogether, we find substantial differences in the molecular mechanisms controlling plant immune responses upon activation of different classes of LRR-type PRRs in this plant.

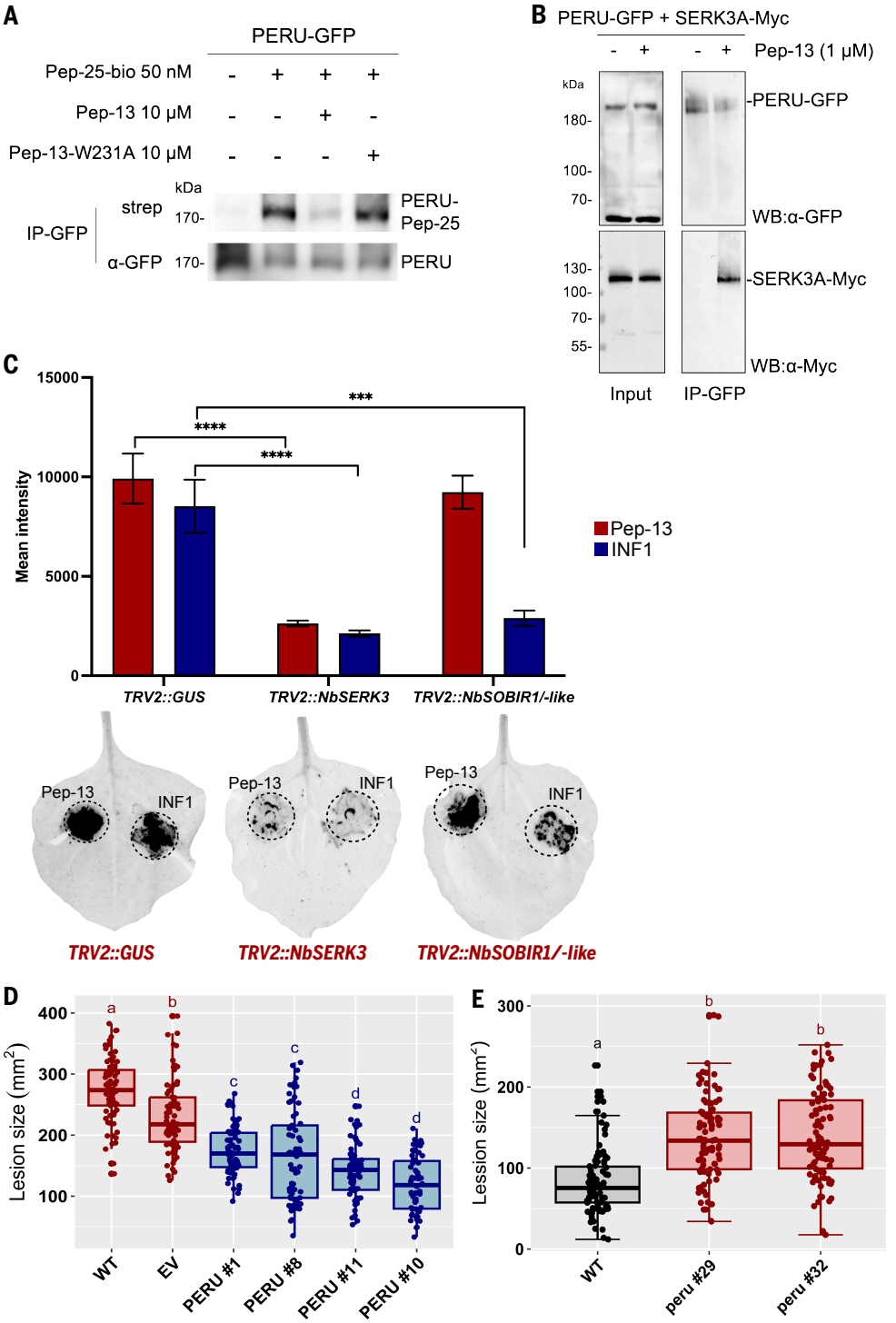
A
PERU-GFP
Pep-25-bio 50 nM - + + +
Pep-13 10 µM - - + -
Pep-13-W231A 10 µM - - - +
kDa
IP-GFP
strep
170-
PERU-Pep-25
α-GFP
170-
PERU
B
PERU-GFP + SERK3A-Myc
- + - + Pep-13 (1 µM)
kDa
180-
100-
70-
-PERU-GFP
WB:α-GFP
130-
100-
70-
55-
-SERK3A-Myc
WB:α-Myc
Input
IP-GFP
C
Mean intensity
15000
10000
5000
0
***
****
****
Pep-13
INF1
TRV2::GUS
TRV2::NbSERK3
TRV2::NbSOBIR1/-like
Pep-13
INF1
Pep-13
INF1
Pep-13
INF1
TRV2::GUS
TRV2::NbSERK3
TRV2::NbSOBIR1/-like
D
Lesion size (mm2)
400
300
200
100
a
b
c
c
d
d
WT
EV
PERU #1
PERU #8
PERU #11
PERU #10
E
Lesion size (mm2)
300
200
100
0
a
b
b
WT
peru #29
peru #32

Figure 2. PERU recognizes Pep-13, is dependent on SERK3 and confers enhanced resistance to *Phytophthora infestans*. (A) Binding of biotinylated Pep-25 to PERU. PERU-GFP transiently expressed in *N. benthamiana* served as receptor, Pep-25-bio peptide as ligand, and unlabeled Pep-13 and Pep-13W231A peptides as competitors. Streptavidin-AP (strep) was used to detect ligand binding to receptor. **(B)** PERU-GFP and SERK3A^{DM}-Myc were transiently expressed in *N. benthamiana* and treated with Pep-13 or water as control. Proteins were subjected to coimmunoprecipitation with GFP trap beads and immunoblotting with tag-specific antibodies. This experiment was performed in duplicate with similar results. **(C)** Cell death induced by Pep-13 peptide and INF1 protein (as control) in TRV2::*NbSERK3 N. benthamiana* leaves was significantly reduced compared with TRV2::*GUS*. Pep-13–induced cell death was not reduced in leaves treated with TRV2::*NbSOBIR1-like*. Representative leaves are shown at the bottom. Data were analyzed using one-way ANOVA with Tukey's test, (****P-value ≤ 0.0001, ***P-value < 0.001, **P-value < 0.01). **(D)** Leaves of cv. Atlantic WT, and transgenic EV (negative control), *PERU* #1, #8, #10, and #11 intact plants were spot-inoculated with *P. infestans* strain Dinteloord, and lesion sizes measured at 4 dpi. All transgenic lines expressing PERU showed smaller lesions than WT or EV. (E) DM (WT) and CRISPR lines peru #29 and #32 were spot-inoculated with *P. infestans* strain Dinteloord. Lesion sizes were measured at 4 dpi. Larger lesions were observed in the CRISPR lines *peru* #29 and #32. Data were analyzed using one-way ANOVA with Tukey's test (P-value ≤ 0.05), different letters indicate significant differences. All experiments were performed 3 times with similar results and representative results are shown.

PERU confers enhanced resistance to *P. infestans*

Potato varieties used in agricultural production are often susceptible to major plant pathogens, including species of the genus *Phytophthora (28)*. Genetic engineering provides one way of increasing plant resistance in crop plants. Ectopic expression of plant PRRs is known to confer novel microbial pattern recognition specificities and enhanced pathogen resistance to crop plants (*16, 22, 29, 30*). For infection assays with the virulent *P. infestans* isolate, Dinteloord, we obtained four potato cultivar Atlantic lines stably expressing *p35S::PERU*, and two DM lines stably transformed with CRISPR-Cas9 and 4 sgRNA to disable *PERU* gene expression. By scoring disease lesions four days post infection we found that *PERU*-transgenic lines were significantly less damaged when compared to wild-type plants or to lines transformed with vector only (Fig. 2D). Likewise, CRISPR-Cas9-generated *peru* mutant lines were significantly more susceptible to infection when compared to wild-type DM (Fig. 2E). Hence, PERU confers quantitative resistance against the pervasive potato late blight pathogen.

Diversification of PERU ligand specificities in wild potato populations

Pep-13/25-induced plant defenses have been studied in parsley and potato cell suspensions, as well as in leaves of a cultivated potato clone, Désirée (*7, 10*). Alanine scanning mutagenesis of Pep-13 sequences revealed that mutant Pep-13W231A abolished elicitor activity, mutation of proline 234 (Pep-13P234A) reduced it, and replacement of the remaining amino acid residues (including tyrosine 241, Pep-

13Y241A) did not significantly affect activities of the mutant peptides (*7, 8, 10*). We found the same pattern of ligand responses in the Pep-25-sensitive genotype DM, which was used for PERU identification (Fig. 1 and 3A, data S1). To determine the frequency of biologically active *PERU* alleles in *Solanum* sect. *Petota (31)*, we analyzed 476 genotypes corresponding to 98 species (97 wild, and 1 cultivated potato species) for cell death triggered by Pep-25 and its described mutant variants (data S1). 350 (74 %) of these genotypes did not develop cell death in response to Pep-25, indicating that most wild *Solanum* genotypes in this collection lack an active *PERU* allele (data S1). Pep-25 and its mutants were tested for cell death induction on all 126 Pep-25-sensitive genotypes (Fig. 3A). Overall, we observed at least five different recognition specificities, including substantial qualitative and quantitative variations in their abilities to respond to Pep-25 and its mutants. Wild potato genotypes grouped in class 1 include DM and exhibit the same ligand response patterns as described for cultivated potato cultivar Désirée previously (*7, 8, 10*) (Fig. 3A). These accounted for 25% of all Pep-25-sensitive genotypes (Fig. 3A). Other genotypes showed responsiveness to Pep-13W231A, but failed to respond to Pep-13P234A (class 2), others failed to respond to both Pep-13P234A and Pep-13W241A (class 3), and some genotypes failed to respond to all mutant peptides of Pep13 (class 4). Some *Solanum* genotypes, such as *Solanum leptophyes* (LPH) 680-5, exhibit sensitivities to all Pep-25 variants tested and were categorized as class 5 genotypes (Fig. 3A). Altogether, our findings reveal that wild *Solanum* species bear diverse *PERU* alleles that differ from $PERU^{DM}$ and, thus encode PRRs with distinct ligand specificities.

We assessed plant defense and cell death-inducing activities of Pep-25 wild-type and mutant peptides in potato genotypes expressing $PERU^{DM}$ (class 1 genotype) or $PERU^{LPH}$ (class 5 genotype) (Fig. 3B) in greater detail. We found that $PERU^{LPH}$-expressing plants recognized all Pep-25 variants, whereas $PERU^{DM}$ did not mount cell death in response to Pep-25W231A. To corroborate these findings and to rule out that potato genotype-specific properties account for altered PERU ligand binding specificities, we transiently expressed $PERU^{DM}$ or $PERU^{LPH}$-encoding sequences in Pep-13-insensitive *S. hjertingii*. Again, infiltration of Pep-25 wild-type and mutant peptides yielded the same response pattern as observed before (Fig. 3B), with all Pep-25 mutants inducing cell death in $PERU^{LPH}$ plants only (Fig. 3C). Thus, differences in ligand specificities of PERU proteins from $PERU^{DM}$ or $PERU^{LPH}$-expressing plants are features of the receptor proteins themselves rather than of co-receptors or other auxiliary factors.

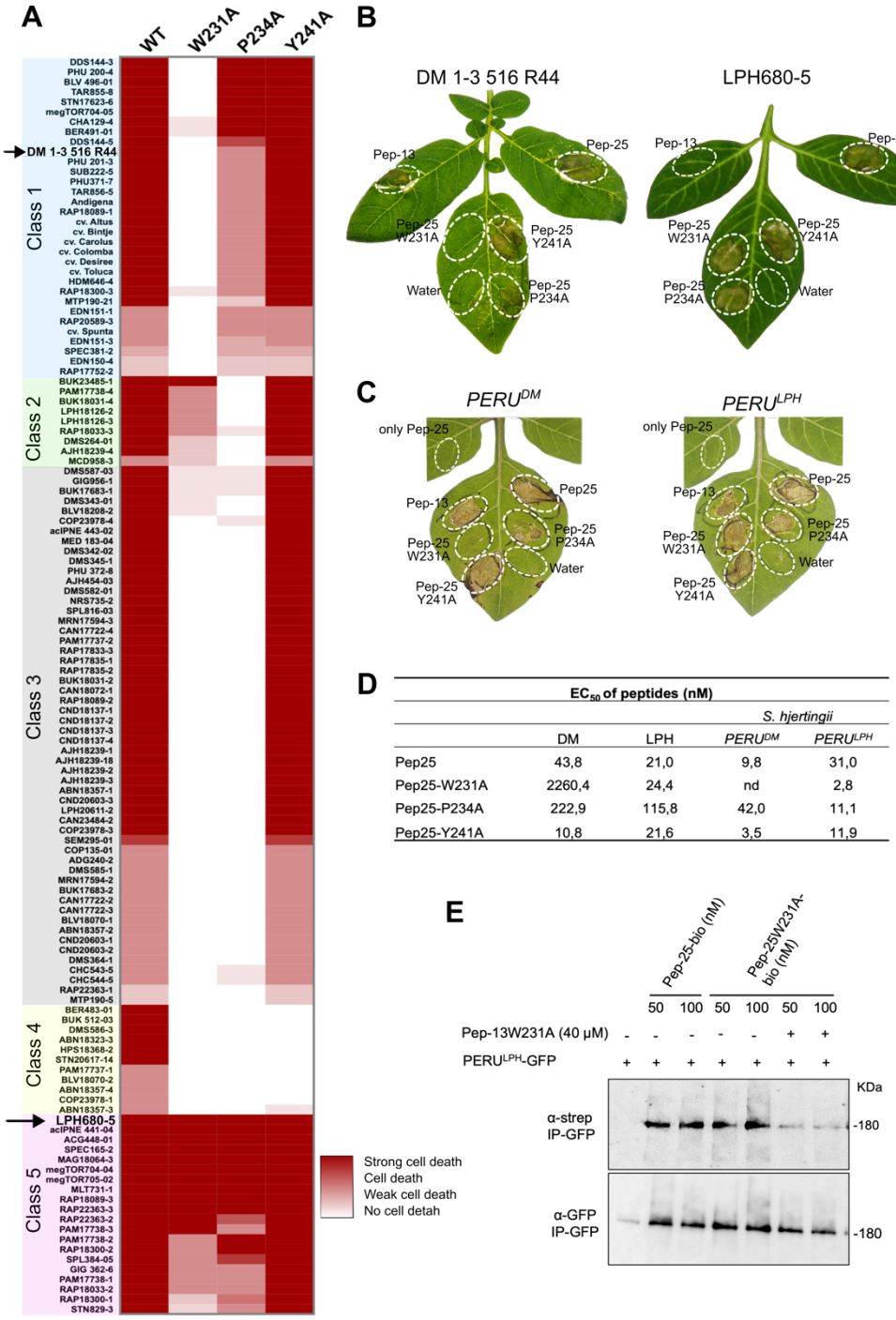

EC_{50} of peptides (nM)				
			S. hjertingii	
	DM	LPH	*PERU^DM*	*PERU^LPH*
Pep25	43,8	21,0	9,8	31,0
Pep25-W231A	2260,4	24,4	nd	2,8
Pep25-P234A	222,9	115,8	42,0	11,1
Pep25-Y241A	10,8	21,6	3,5	11,9

Figure 3. Functional diversification of PERU in *Solanum* section *Petota*. (A) Heat map of cell death responses of *Solanum* accessions to Pep-25 (WT) and Pep-25W231A, Pep-25P234A, Pep-25Y241A mutants reveals five different classes (1-5) of recognition specificities. DM 1-3 516 R44 (class 1) and LPH680-5 (class 5) are marked with arrows. **(B)** Cell death induction by Pep-13, Pep-25, and mutants in DM and LPH plants. In DM, Pep-25W231 induces no cell death, and Pep-25P234A induces weaker cell death; while in LPH, Pep-25W231A and Pep-25-P234A-induced cell death is similar to that caused by Pep-25. **(C)** *PERU^{DM}* or *PERU^{LPH}* were transiently expressed in Pep-13-insensitive *S. hjertingii* by agroinfiltration. Infiltration of Pep-13/25 and Pep-25 mutant peptides yielded the same response pattern as observed in DM and LPH plants. **(D)** EC_{50} values were determined by quantification of elicitor-induced production of ethylene in *DM* or LPH plants, and in *S. hjertingii* plants transiently transformed with either *PERU^{DM}* or *PERU^{LPH}*; nd, not determined. **(E)** Receptor/ligand binding assays show that PERU^{LPH} specifically bound both Pep-25-bio and Pep-25W231A-bio as ligands, and Pep-13W231A efficiently competes for ligand binding to PERU^{LPH}. All experiments were performed 3 times with similar results, and representative experiments are shown.

We further analyzed biological activities of Pep-25 and its mutants by quantifying elicitor-induced production of the stress hormone ethylene in *PERU^{DM}* or *PERU^{LPH}* potato plants and in *S. hjertingii* plants transiently transformed with either *PERU* allele (Fig. 3D, E). Determination of elicitor concentrations required to induce half-maximal ethylene production (EC_{50}) corroborated qualitative data from cell death assays (Fig. 3B, C). Pep-25W231A proved as active as Pep-25 only when tested on *PERU^{LPH}*-expressing plants. We found substantially reduced or no activity of this peptide in plants expressing *PERU^{DM}* (Fig. 3D, E). In agreement with that, *PERU^{LPH}* plants bound both Pep-25-bio and Pep-25W231A-bio in receptor-ligand binding assays (Fig. 3E). Likewise, Pep-13W231A efficiently blocked ligand binding to PERU^{LPH} (Fig. 3E), but not to PERU^{DM} (Fig. 2A). Altogether, our data obtained from ligand binding assays and from plant defense activation studies confirm that *PERU^{DM}* and *PERU^{LPH}* encode related LRR-RK immune receptors that have diversified in ligand specificities. Our findings further suggest that functional diversification has occurred within this immune receptor family during evolution, resulting in PERU alleles that recognize Pep-13 variants not recognized by others.

Evolutionary history of PERU

To obtain information about the origin of *PERU* alleles, we studied their geographic distribution and genetic variation (Fig. 4). We developed a computational pipeline to extract PERU sequences from 6,630,292 predicted proteins from 124 Solanaceae genome assemblies and for comparison extracted sequences of FLS2 (FLAGELLIN-SENSING 2), a conserved LRR-RK that detects bacterial flagellin (fig. S8; data S2) (*3*). Both PERU and FLS2 clustered in well-supported clades within the LRR-RK subgroup XII indicating a monophyletic origin within the Solanaceae (fig. S9) (*5*). All plant LRR-RK-type PRRs currently known fall into this clade, including *Arabidopsis* FLS2 and EF-TU

RECEPTOR (EFR), or rice Xa21 (*16, 32*). This pipeline yielded 114 PERU clade sequences from 17 species and 180 FLS2 clade sequences from 33 species with the PERU clade sequences exhibiting markedly more diversity than FLS2 clade (fig. S9, data S3, S4, S5). The same primers employed to isolate *PERU* (DM) facilitated the isolation of 26 responsive homologs and 25 non-responsive homologs (data S6). The amplified and genome extracted sequence datasets were then combined for phylogenomic analyses, which revealed that the PERU sequences encoding Pep-13-responsive PERU alleles fall into one clade whereas the non-responsive homologs are scattered throughout the tree (Fig. 4A, fig. S10A-B). The PERU^{LPH} sequences are embedded within a tighter PERU^{DM} clade indicating that evolution of a new ligand specificity and, hence, functional diversification has occurred within the PERU receptor family of *Solanum* (Fig. 4A, fig. S10A). Our phylogenomics analyses of *PERU* sequences further suggest that potato PERU^{DM} and the PEP-13 receptor in parsley are distinct proteins, although they share similar ligand specificities (Fig. 3) (*7, 10*).

Metazoan and plant immune receptors have been targeted by positive, diversifying selection, which accelerates the divergence between homologous proteins (*33, 34*). To identify amino acids under diversifying selection in the proteins encoded by *PERU* alleles, we applied maximum likelihood models of codon substitution using the program codeml from PAML (*35, 36*). We found a total of 11 residues (S118, E172, L194, Q198, R245, E339, E391, L392, A416, Q489, R590) to be under positive selection according to the three models tested (table S1). We further used AlphaFold2 to predict the tertiary structure of the PERU^{DM} ectodomain (fig. S11). All residues, but one (S118) found to be under positive selection are located on the concave side of the LRR structure, consistent with observations made for binding of the bacterial flagellin epitope flg22 to the *Arabidopsis* LRR-RK FLS2 (*37*). As observed for other immune receptors, diversifying selection may have driven functional diversification of PERU receptors in wild potato populations. We further observed that Pep-25-insensitive genotypes were found across the American continent ranging from the United States to Chile and Argentina (Fig. 4B). In contrast, Pep-25 sensitivity clustered among species that belong to species of the section Tuberosa or Piurana which thrive predominantly in the Andean region of Bolivia and Peru (Fig. 4C), suggesting that the PERU receptor family arose in this region. Wild potatoes carrying *PERU^{LPH}* alleles also cluster in this region, suggesting that functional diversification of *PERU* alleles in wild potato populations has occurred at its center of origin. *PERU* alleles from multiple potato cultivars used today for crop production all cluster with *PERU^{DM}* (Fig. 4A, fig. S10A), suggesting that PERU has been maintained during domestication (*13*).

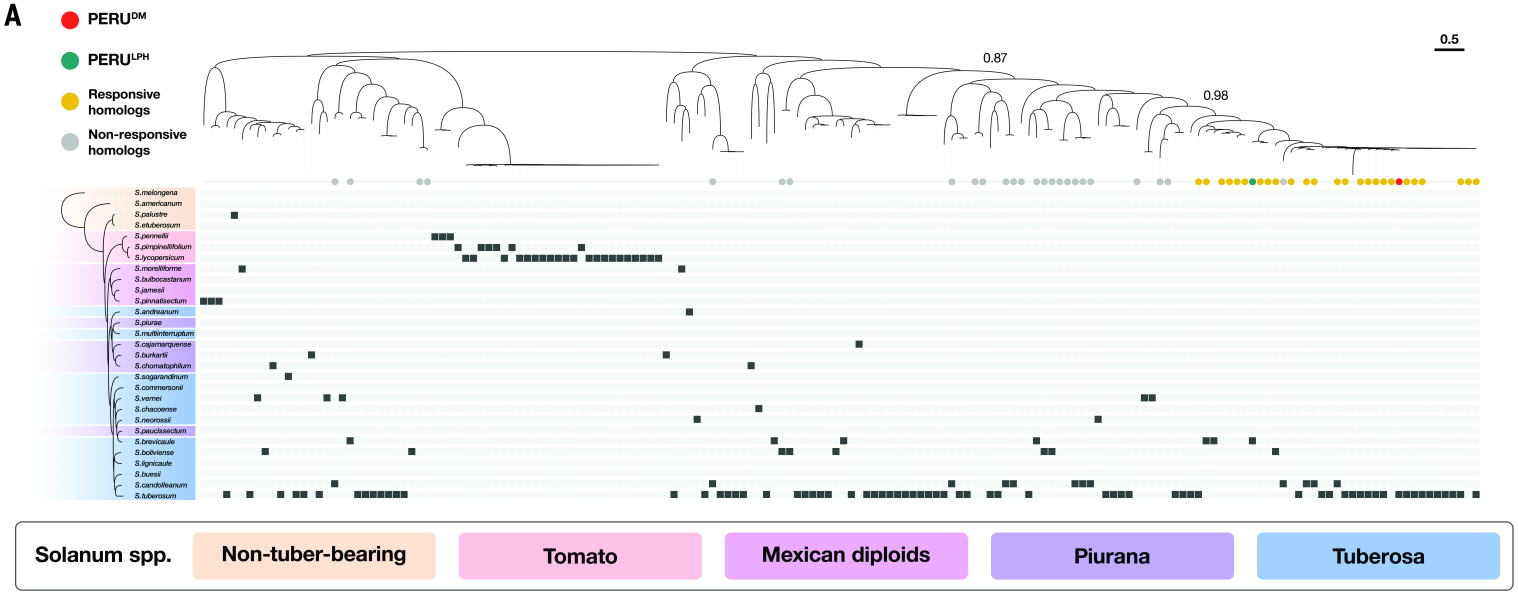

Figure 4. Phylogenetics and geographic distribution of PERU. (A) Heatmap representation of presence/absence of PERU homologs across *Solanum* species. The PERU^{DM}, PERU^{LPH}, and the Pep-13 responsive homologs grouped together in a single clade, while the non-responsive homologs were distributed throughout the phylogenetic tree. Bootstrap values are shown for the clade containing all tested homologs (0.87) and the clade containing the responsive PERU^{DM} homologs (0.98). The *Solanum* phylogeny was adapted from (*38*). **(B)** Kernel density distribution map of 266 genotypes insensitive to Pep-25 that are distributed from the Southern USA to Northern Chile; and **(C)** Kernel density distribution map of 98 sensitive genotypes that cluster in Peru and Bolivia. Red shades indicate high density, yellow shades indicate lower density, the blue dots represent individual geo-coordinates of accessions, and bar plots represent the number of genotypes along different latitudes of the continent. Available geographic coordinates of 364 genotypes (Data S1) were used to elaborate the maps.

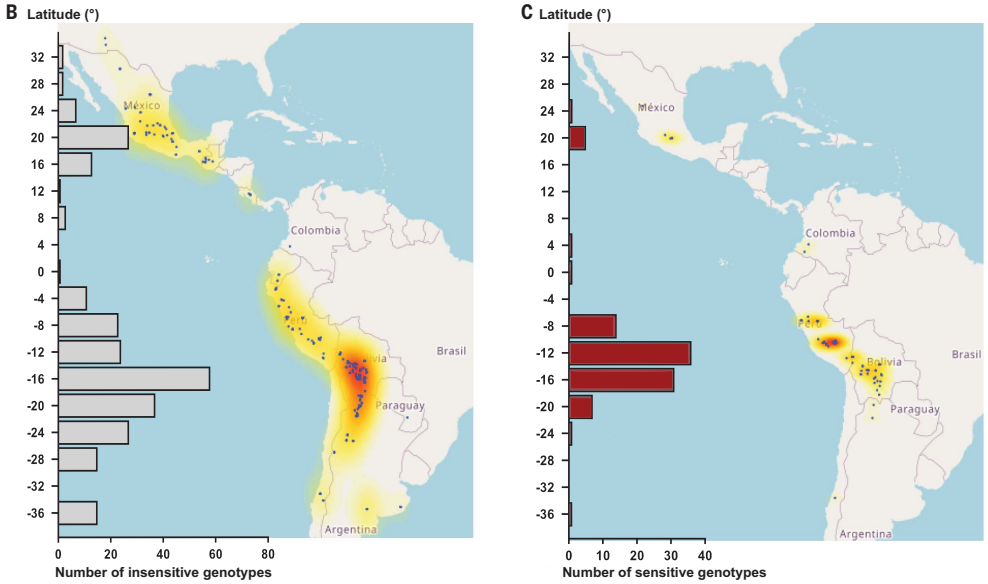

Figure 4 (continued).

Discussion

In this study, we characterize potato PERU as a bona fide plant PRR conferring *P. infestans* recognition. PERU binds Pep-13/25 patterns that are conserved among species of the genus *Phytophthora*, hetero-dimerizes with BAK1 in a ligand-dependent manner, mediates activation of plant immunity, and increases resistance to a devastating potato disease.

Different ligand response specificities observed among wild *Solanum* accessions indicate that functional diversification within this PRR family has occurred at the site of origin of the predominant allele, PERU^{DM}. The explicit use of wild potato populations instead of plant materials that have undergone substantial genetic rearrangements during crop breeding implies that natural forces have been major drivers of immune receptor diversification. The Pep-13 pattern is widespread and highly conserved among plant-associated oomycetes (*10*), a trait that has likely facilitated the evolution of plant PRRs that recognize it. Although residue W231 is invariant in known sequences of *Phytophthora* TGs, polymorphisms affecting the elicitor activity of wild-type Pep-13 might occur, since pathogen pressure in defined ecological niches is assumed to shape immune receptor reservoirs in metazoans and plants (*5*). It is thus conceivable that functional diversification of PERU was driven by escape mutations

within *Phytophthora* Pep-13 patterns that enable Pep-13-producing pathogen strains to elude recognition by the predominant allele, PERU^{DM}. Microbial evasion strategies to avoid plant immune activation encompass alterations within immunogenic patterns, thus disabling their recognition by plant PRRs (*39, 40*). In turn, individual plant species have evolved to perceive polymorphic patterns or, alternatively, structurally unrelated immunogenic molecules (*41-45*). Likewise, phylogenetically distinct PRRs have evolved in different plant species to recognize structurally unrelated epitopes within individual microbial patterns (*46, 47*).

We report here the identification of a potato cell surface PRR from the Central Andes and its natural origin in wild potatoes. Our analysis highlights PRR diversification in sympatric, natural potato populations.

Acknowledgments: We acknowledge our colleagues Ton Bisseling, Judith Fliegmann, Evert Jacobsen, Thomas Lahaye, Rosa Lozano-Durán, Jane E. Parker, Detlef Weigel and Sebastian Wolf for critical reading. We thank Dirkjan Huigen for assistance with crossing and greenhouse work organization; Harm Wiegersma and Henk Smid for excellent plant care; Jiorgos Kourelis and Yu Sugihara for assistance with the phylogenomics, Joe Win for advices with PAML analysis; Sergio Landeo for help with ROS assays; Jan Schaart, William de Martinez and Daniel Monino Lopez for help with CRISPR/Cas constructs cloning; Isolde Bertram Pereira for culturing *Solanum* plants; Matthieu Joosten for VIGS constructs; Geert Kessel for providing *P. infestans* isolates; Aviv Andriani for help with disease tests; Johannes Stuttmann for providing *N. benthamiana eds1*, *pad4* and *eds1 pad4* lines, and Tatiana Marti Ferrando for help with molecular work. We recognize the 'Apoplastic interactions' session of the 17th IS-MPMI meeting in Portland 2016 that led to initiating the search for the Pep-13 receptor. We dedicate this work to Dierk Scheel who started the study on Pep-13 and who sadly passed away recently.

Funding: This work was supported by the following:
Peruvian Council for science, technology and technological innovation (CONCYTEC) FONDECYT contract 129-2017 (Y.C.T.A.).
Deutsche Forschungsgemeinschaft grant CRC1101-D10 (T.N.), Nu70/17-1 (T.N.).
The Gatsby Charitable Foundation
BBSRC, UK, BBS/E/J/000PR9795
BBSRC, UK, BBS/E/J/000PR9796
BBSRC, UK, BBS/E/J/000PR9798.

Data and materials availability: Sequences of cloned homologs were deposited in the National Center for Biotechnology Information database, www.ncbi.nlm.nih.gov (accession nos. OQ999431 to OQ999482). All other data, sequences, datasets, and scripts for the phylogenomic analyses are available in the manuscript, the supplementary material or deposited at Zenodo (48). Most of the wild Solanum accessions were in possession of WUR Plant Breeding before Nagoya rules applied, part of the material was obtained later from the Center of Genetic Resources, The Netherlands for which we refer to Access and Benefit-Sharing (https://www.absfocalpoint.nl/ en/absfocalpoint.htm) at their website (https://cgngenis.wur.nl).

References

1. B. P. M. Ngou, H.-K. Ahn, P. Ding, J. D. G. Jones, Mutual potentiation of plant immunity by cell-surface and intracellular receptors. *Nature* **592**, 110-115 (2021).
2. M. Yuan *et al.*, Pattern-recognition receptors are required for NLR-mediated plant immunity. *Nature* **592**, 105-109 (2021).
3. J. Rhodes, C. Zipfel, Jonathan D. G. Jones, Bruno P. M. Ngou, Concerted actions of PRR- and NLR-mediated immunity. *Essays in Biochemistry*, (2022).
4. R. N. Pruitt *et al.*, The EDS1–PAD4–ADR1 node mediates *Arabidopsis* pattern-triggered immunity. *Nature* **598**, 495-499 (2021).
5. B. P. M. Ngou, R. Heal, M. Wyler, M. W. Schmid, J. D. G. Jones, Concerted expansion and contraction of immune receptor gene repertoires in plant genomes. *Nature Plants* **8**, 1146-1152 (2022).
6. C. Aguilera-Galvez *et al.*, Two different *R* gene loci co-evolved with *Avr2* of *Phytophthora infestans* and confer distinct resistance specificities in potato. *Studies in Mycology* **89**, 105-115 (2018).
7. T. Nürnberger *et al.*, High affinity binding of a fungal oligopeptide elicitor to parsley plasma membranes triggers multiple defense responses. *Cell* **78**, 449-460 (1994).
8. T. Nürnberger, D. Nennstiel, K. Hahlbrock, D. Scheel, Covalent cross-linking of the *Phytophthora megasperma* oligopeptide elicitor to its receptor in parsley membranes. *Proceedings of the National Academy of Sciences U.S.A.* **92**, 2338-2342 (1995).
9. V. G. A. A. Vleeshouwers *et al.*, Understanding and exploiting late blight resistance in the age of effectors. *Annual Review of Phytopathology* **49**, 507-531 (2011).
10. F. Brunner *et al.*, Pep-13, a plant defense-inducing pathogen-associated pattern from *Phytophthora* transglutaminases. *The EMBO Journal* **21**, 6681-6688 (2002).
11. B. J. Haas *et al.*, Genome sequence and analysis of the Irish potato famine pathogen *Phytophthora infestans*. *Nature* **461**, 393-398 (2009).
12. W. E. Fry *et al.*, Five reasons to consider *Phytophthora infestans* a reemerging pathogen. *Phytopathology* **105**, 966-981 (2015).
13. X. Lin *et al.*, Recognition of Pep-13/25 MAMPs of Phytophthora localizes to an RLK locus in *Solanum microdontum*. *Frontiers in Plant Science* **13**, (2023).
14. G. M. Pham *et al.*, Construction of a chromosome-scale long-read reference genome assembly for potato. *GigaScience* **9**, (2020).
15. V. G. A. A. Vleeshouwers *et al.*, SolRgene: an online database to explore disease resistance genes in tuber-bearing *Solanum* species. *BMC Plant Biology* **11**, (2011).
16. F. Boutrot, C. Zipfel, Function, discovery, and exploitation of plant pattern recognition receptors for broad-spectrum disease resistance. *Annual Review of Phytopathology* **55**, 257-286 (2017).
17. W.-L. Wan, K. Fröhlich, R. N. Pruitt, T. Nürnberger, L. Zhang, Plant cell surface immune receptor complex signaling. *Current Opinion in Plant Biology* **50**, 18-28 (2019).
18. A. M. Escocard de Azevedo Manhães, F. A. Ortiz-Morea, P. He, L. Shan, Plant plasma membrane-resident receptors: Surveillance for infections and coordination for growth and development. *Journal of Integrative Plant Biology* **63**, 79-101 (2021).
19. D. Couto, C. Zipfel, Regulation of pattern recognition receptor signalling in plants. *Nature Reviews Immunology* **16**, 537-552 (2016).
20. S. Landeo Villanueva, M. C. Malvestiti, W. van Ieperen, M. H. A. J. Joosten, J. A. L. van Kan, Red light imaging for programmed cell death visualization and quantification in plant–pathogen interactions. *Molecular Plant Pathology* **22**, 361-372 (2021).
21. T. A. DeFalco, C. Zipfel, Molecular mechanisms of early plant pattern-triggered immune signaling. *Molecular Cell* **81**, 3449-3467 (2021).
22. J. Du *et al.*, Elicitin recognition confers enhanced resistance to *Phytophthora infestans* in potato. *Nature Plants* **1**, 15034 (2015).

23. S. H. E. J. Gabriëls *et al.*, An NB-LRR protein required for HR signalling mediated by both extra- and intracellular resistance proteins. *The Plant Journal* **50**, 14-28 (2007).
24. C.-H. Wu, K. Belhaj, T. O. Bozkurt, M. S. Birk, S. Kamoun, Helper NLR proteins NRC2a/b and NRC3 but not NRC1 are required for Pto-mediated cell death and resistance in *Nicotiana benthamiana*. *New Phytologist* **209**, 1344-1352 (2016).
25. J. Kourelis *et al.*, The helper NLR immune protein NRC3 mediates the hypersensitive cell death caused by the cell-surface receptor Cf-4. *PLOS Genetics* **18**, e1010414 (2022).
26. J. Ordon *et al.*, Generation of chromosomal deletions in dicotyledonous plants employing a user-friendly genome editing toolkit. *The Plant Journal* **89**, 155-168 (2017).
27. J. Gantner, J. Ordon, C. Kretschmer, R. Guerois, J. Stuttmann, An EDS1-SAG101 Complex is essential for TNL-mediated immunity in *Nicotiana benthamiana*. *The Plant Cell* **31**, 2456-2474 (2019).
28. V. G. A. A. Vleeshouwers *et al.*, A Laboratory assay for *Phytophthora infestans* resistance in various *Solanum* species reflects the field situation. *European Journal of Plant Pathology* **105**, 241-250 (1999).
29. S. Lacombe *et al.*, Interfamily transfer of a plant pattern-recognition receptor confers broad-spectrum bacterial resistance. *Nature Biotechnology* **28**, 365-369 (2010).
30. I. Albert *et al.*, An RLP23–SOBIR1–BAK1 complex mediates NLP-triggered immunity. *Nature Plants* **1**, 15140 (2015).
31. D. M. Spooner, M. Ghislain, R. Simon, S. H. Jansky, T. Gavrilenko, Systematics, diversity, genetics, and evolution of wild and cultivated potatoes. *The Botanical Review* **80**, 283-383 (2014).
32. B. P. M. Ngou, P. Ding, J. D. G. Jones, Thirty years of resistance: Zig-zag through the plant immune system. *The Plant Cell* **34**, 1447-1478 (2022).
33. L. Quintana-Murci, A. G. Clark, Population genetic tools for dissecting innate immunity in humans. *Nature Reviews Immunology* **13**, 280-293 (2013).
34. P. S. Kahlon, R. Stam, Polymorphisms in plants to restrict losses to pathogens: From gene family expansions to complex network evolution. *Current Opinion in Plant Biology* **62**, 102040 (2021).
35. Z. Yang, PAML 4: Phylogenetic analysis by maximum likelihood. *Molecular Biology and Evolution* **24**, 1586-1591 (2007).
36. Z. Liu *et al.*, Patterns of diversifying selection in the phytotoxin-like scr74 gene family of *Phytophthora infestans*. *Molecular Biology and Evolution* **22**, 659-672 (2004).
37. Y. Sun *et al.*, Structural basis for flg22-induced activation of the *Arabidopsis* FLS2-BAK1 immune complex. *Science* **342**, 624-628 (2013).
38. D. Tang *et al.*, Genome evolution and diversity of wild and cultivated potatoes. *Nature* **606**, 535-541 (2022).
39. P. Buscaill, R. A. L. van der Hoorn, Defeated by the nines: nine extracellular strategies to avoid microbe-associated molecular patterns recognition in plants. *The Plant Cell* **33**, 2116-2130 (2021).
40. Y. Wang, R. N. Pruitt, T. Nürnberger, Y. Wang, Evasion of plant immunity by microbial pathogens. *Nature Reviews Microbiology* **20**, 449-464 (2022).
41. N. R. Colaianni *et al.*, A complex immune response to flagellin epitope variation in commensal communities. *Cell Host & Microbe* **29**, 635-649.e639 (2021).
42. U. Fürst *et al.*, Perception of *Agrobacterium tumefaciens* flagellin by FLS2XL confers resistance to crown gall disease. *Nature Plants* **6**, 22-27 (2020).
43. K. Parys *et al.*, Signatures of antagonistic pleiotropy in a bacterial flagellin epitope. *Cell Host & Microbe* **29**, 620-634.e629 (2021).
44. S. Snoeck *et al.*, Evolutionary gain and loss of a plant pattern-recognition receptor for HAMP recognition. *eLife* **11**, e81050 (2022).
45. Y. Wei *et al.*, An immune receptor complex evolved in soybean to perceive a polymorphic bacterial flagellin. *Nature Communications* **11**, 3763 (2020).

46. T. Murakami *et al.*, Distribution of flagellin CD2-1, flg22, and flgII-28 recognition systems in plant species and regulation of plant immune responses through these recognition systems. *Bioscience, Biotechnology, and Biochemistry* **86**, 490-501 (2022).
47. L. Zhang *et al.*, Distinct immune sensor systems for fungal endopolygalacturonases in closely related Brassicaceae. *Nature Plants* **7**, 1254-1263 (2021).
48. A. Thogani, Git Repository: Phylogenetics of PERU and FLS2 LRR-RK immune receptors in the Solanaceae plant family, version 1, Zenodo 2023; https://doi.org/10.5281/zenodo.8079625.
49. T. Murashige, F. Skoog, A revised medium for rapid growth and bio assays with tobacco tissue cultures. *Physiologia Plantarum* **15**, 473-497 (1962).
50. E. Domazakis *et al.*, The ELR-SOBIR1 complex functions as a two-component receptor-like kinase to mount defense against *Phytophthora infestans*. *Molecular Plant-Microbe Interactions* **31**, 795-802 (2018).
51. J. Du, Rietman, H., Vleeshouwers, V. G. A. A., Luo, W. T. , Agroinfiltration and PVX agroinfection in potato and *Nicotiana benthamiana*. *Journal of Visualized Experiments* **83**, (2014).
52. Y. Torres Ascurra, X. Lin, P. J. Wolters, V. G. A. A. Vleeshouwers, in *Solanum tuberosum: Methods and Protocols,* D. Dobnik, K. Gruden, Ž. Ramšak, A. Coll, Eds. (Springer US, New York, NY, 2021), pp. 315-330.
53. R. G. F. Visser, in *Plant Tissue Culture Manual: Supplement 7,* K. Lindsey, Ed. (Springer Netherlands, Dordrecht, 1997), pp. 301-309.
54. C. Engler *et al.*, A Golden Gate modular cloning toolbox for plants. *ACS Synthetic Biology* **3**, 839-843 (2014).
55. D. Monino-Lopez *et al.*, Allelic variants of the NLR protein Rpi-chc1 differentially recognize members of the *Phytophthora infestans* PexRD12/31 effector superfamily through the leucine-rich repeat domain. *The Plant Journal* **107**, 182-197 (2021).
56. M. A. Pombo *et al.*, Transcriptome-based identification and validation of reference genes for plant-bacteria interaction studies using *Nicotiana benthamiana*. *Scientific Reports* **9**, 1632 (2019).
57. C. E. Caten, J. L. Jinks, Spontaneous variability of single isolates of *Phytophthora infestans*. I. Cultural variation. *Canadian Journal of Botany* **46**, 329-348 (1968).
58. S. R. Eddy, Accelerated profile HMM searches. *PLOS Computational Biology* **7**, e1002195 (2011).
59. K. Katoh, D. M. Standley, MAFFT multiple sequence alignment software version 7: Improvements in performance and usability. *Molecular Biology and Evolution* **30**, 772-780 (2013).
60. M. N. Price, P. S. Dehal, A. P. Arkin, FastTree 2 – Approximately maximum-likelihood trees for large alignments. *PLOS ONE* **5**, e9490 (2010).
61. F. Teufel *et al.*, SignalP 6.0 predicts all five types of signal peptides using protein language models. *Nature Biotechnology* **40**, 1023-1025 (2022).
62. I. Letunic, P. Bork, Interactive Tree Of Life (iTOL) v5: an online tool for phylogenetic tree display and annotation. *Nucleic Acids Research* **49**, W293-W296 (2021).
63. K. Tamura, G. Stecher, S. Kumar, MEGA11: Molecular evolutionary genetics analysis version 11. *Molecular Biology and Evolution* **38**, 3022-3027 (2021).
64. Z. Yang, W. S. W. Wong, R. Nielsen, Bayes Empirical Bayes inference of amino acid sites under positive selection. *Molecular Biology and Evolution* **22**, 1107-1118 (2005).
65. M. Mirdita *et al.*, ColabFold: making protein folding accessible to all. *Nature Methods* **19**, 679-682 (2022).
66. J. Jumper *et al.*, Highly accurate protein structure prediction with AlphaFold. *Nature* **596**, 583-589 (2021).

Supplementary information

Materials and Methods

Plant material

Potato plants were maintained and clonally propagated in vitro on MS medium (*49*) supplemented with 20% sucrose at 25 °C. For experiments, 2 weeks old plantlets were transferred to sterilized soil and grown in regulated greenhouse compartments at 18-22 °C, 16h/8h day/night regime and 70% relative humidity. *Nicotiana benthamiana* plants were generated from seeds and grown under the same greenhouse conditions.

Peptides and protein

Peptides were synthesized by Genscript USA Inc, prepared as 1 mM stock solutions in (DMSO), and diluted in MilliQ water or sterile tap water before use. INF1 was produced as described previously (*50*).

Peptide infiltrations

Peptides were infiltrated at 1 μM concentrations into the abaxial side of leaves of at least 3 plants per genotype (three leaves per plant were used), using needleless syringes. The cell death intensity was scored 3-4 days after infiltration as previously described (*51*). A scale from 0 to 1 was used, based on the cell death percentage of the infiltrated area. 0 indicates no symptoms, 1 indicates confluent cell death and intermediate values were also considered for chlorosis or increasing levels of patchy cell death. Average scores ≤ 0.2 were considered as non-responsive and excluded from further analysis. The classification of potato genotypes into classes 1-5 is based on their ability to develop cell death after treatment with Pep-25 and the mutant peptides Pep-25W231A, Pep-25P234A and P-25Y241A.

Genetic mapping of *PERU*

An F1 population (named 3240) was generated by crossing the double monoploid *Solanum tuberosum* group Phureja DM 1-3 516 R44 as female parent with the diploid *Solanum tuberosum* RH89-039-16 as male parent. To generate a segregating population, one individual from F1 (3240-4) was backcrossed with RH89-039-16. To confirm the previous mapping of the receptor a small set of the population (30 individuals) and the parents were genotyped with 20 molecular markers.

For the fine-mapping a high-throughput recombinant screening was followed (*52*). Briefly, seeds were sown in vitro, the emerging seedlings were transferred to new pots containing MS20 medium. DNA of the individual seedlings was isolated and genotyped with two flanking markers. The recombinant plants were transferred to the greenhouse and phenotyped for Pep-13-induced cell death. This process was iterated until a small mapping interval was obtained. Molecular markers like HRM

(High resolution melting), CAPS (Cleaved amplified polymorphic sequence) and PCR-absence/presence were developed based on DM genome sequence *(14)*. In the first round of fine-mapping 12 markers spanning 1.3 Mb of the top of chromosome 3 were used and 1,918 plants were genotyped, and in the second round of fine-mapping, additional 15 markers were developed to genotype 289 plants. The primers used to genotype the plants are listed in table S2.

Cloning of candidate genes and homologs

Leaves from DM and Pep-25-responding wild *Solanum* spp. were infiltrated with 1 μM Pep-25 and harvested after 5 hours. RNA was isolated using the RNeasy Plant Mini Kit (Qiagen) and converted to cDNA using the Maxima H minus reverse transcriptase kit (Thermo Scientific). Specific primers (table S2) were designed and sequences encoding candidate Pep-13 receptors were cloned into pENTR™/D-TOPO® vector and then transferred to the destination vector pK7WG2, under 35S promoter.

Transient expression of Pep-13 receptor candidate-encoding genes in *N. benthamiana*.

Cells of *Agrobacterium tumefaciens* strain AGL1 were transformed with Pep-13 receptor candidate-encoding gene constructs and agroinfiltration assays were performed as described *(21)*. Leaf infiltration with Pep-13 with GP42 were performed 2 days upon infections with *A. tumefaciens*. Three days after the peptide infiltration, the leaves were scanned in a ChemiDoc MP imaging system, model Universal Hood III (Bio-Rad), and cell death images were acquired with filters capturing the light emitted in the red visible spectrum (filter 605/50) *(46)*.

Stable transformation of potato cultivar Atlantic

Stable transformation of potato cultivar Atlantic with a *35S::PERU* construct in plasmid pK7WG2 was carried out using routine potato transformation protocols (*53*). Fourteen independent transgenic lines were tested for the presence of *PERU*-encoding sequences using gene-specific primers. All but one line tested positive and responded to Pep-13. Lines *PERU*#10 and *PERU*#11 were selected for further experiments.

Ethylene production

Leaves of 4-week old potato plants were cut in round pieces (6.0 mm diameter) and floated in MilliQ water overnight. Four leaf pieces were incubated in sealed 10 ml vials containing 0.6 mL 20mM MES buffer, pH5.7 and the indicated elicitor. Ethylene accumulation was measured after 4 hours of incubation by gas chromatographic analysis (TraceGC1300 (InterScience, Breda, NL) coupled with a flame ionization detector (FID, Temperature = 260°C, cycle time = 3 min, columns: Agilent J&W GS-GasPro 10m 0.32 mm ID coupled with Agilent J&W GS-GasPro 20m 0.32 mm ID to assure backflush, injection volume: 250 μL)) of 3.5 mL of the air drawn from the closed vial with a syringe. At least three measurements were performed for each treatment.

ROS production

Leaves of 4-week-old potato plants were cut in round pieces (6.0 mm diameter), placed in 96 well white plate containing 50 µL of MilliQ water, and incubated overnight. Water was removed and replaced with 50 µL of fresh MilliQ water. After that, 50 µL of a solution containing 10 µg horseradish peroxidase, 50 µM luminol L-012, and elicitor was added. Luminescence was determined using a CLARIOstar plate reader (BMG LABTECH) over a period of 3 hours.

Generation of *PERU* knockout DM plants

Golden Gate cloning was used to generate the constructs as described previously (*54, 55*). Four sgRNAs that target the LRR domain were designed using CRISPOR (http://crispor.tefor.net/), and synthesized as sense and antisense primers (Biolegio BV, The Netherlands). The four sgRNAs were fused to U6-26 promoter and terminator from *Arabidopsis thaliana*, and cloned into the level 1 acceptors pICH47761, pICH47772, pICH47781, and pICH4491 respectively. Then, they were assembled into the Level 2 acceptor pICSL4723 together with NPTII, Cas9 and turbo RFP. Stable transformation of DM 1-3 516 R44 was performed using routine potato transformation protocols (*53*). Gene-specific primers (CC-238-fw & CC-1440-rv and CC-4225-fw & CC-5129-rv) were used to amplify and sequence *PERU* fragments of the transformants. CC-238-fw & CC-1440-rv product showed the occurrence of 2 deletions (15 and 72 bp) and 1 big deletion (418 bp) in the CRISPR lines *peru* #29 and #32 respectively. Pep-13 infiltrations and ROS assays were performed to confirm the phenotype. The primers used for cloning the gRNAs and for genotyping the transformants are listed in table S2.

Virus-induced gene silencing assays

Cotyledons of 2 week-old tobacco seedlings were infiltrated with 1:1 mixtures of pTRV1 and pTRV2::*NbSERK3,* pTRV2::*NbSOBIR1/-like*, pTRV2::*PDS*, or pTRV2::*GUS*, at a final OD_{600} of 1.0. TRV:PDS and TRV:GUS were used as controls. After two weeks, Pep-13 or INF1 protein were infiltrated, and the leaves were scanned in a ChemiDoc MP imaging system (Universal Hood III, Bio-Rad) and cell death images were acquired with filters capturing the light emitted in the red visible spectrum (filter 605/50) *(46)*.

Quantitative reverse-transcription PCR

Leaf discs were sampled and stored at -80 °C. RNA isolation was performed using RNeasy Plant Mini Kit (Qiagen) and following the manufacturer instructions. The iScript™ cDNA Synthesis Kit (Bio-rad) and iScript Reverse transcription supermix (Bio-rad) were used for cDNA synthesis and RT-qPCR. *NbUbe35* and *NbNQO* were used as reference genes (*56*).

Phytophthora infestans infection assay

Disease tests were performed on whole plants as previously described *(27)*. The *P. infestans* isolate Dinteloord was grown at 18 °C in the dark on rye agar medium (*57*) supplemented with 20g/L sucrose. To obtain zoospores, the mycelium was flooded with cold water (4 °C), the suspension was transferred to a new tube and incubated at 4 °C for 2 hours. The number of zoospores was counted and adjusted to $5x10^4$ zoospores/mL for inoculation. Intact, four weeks-old potato plants were spot-inoculated with zoospore suspensions. Lesion diameters were measured at 3, 4 and 5 dpi.

In vivo cross-linking and immunoprecipitation assays

A. tumefaciens (strain GV3101) harboring the corresponding constructs were grown in LB medium with appropriate antibiotics at 28 °C overnight, harvested and resuspended in 10 mM $MgCl_2$, 10 mM MES pH 5.7, 200 µM acetosyringone to desired OD_{600}. The cultures carrying appropriate constructs were mixed to final OD_{600} = 0.1 $construct^{-1}$, incubated at room temperature for 1-2 hours, and infiltrated into 5-6-week-old *N. benthamiana* plants. Leaves were harvested 48 hours after infiltration of bacteria for the following assays.

For in vivo cross-linking, leaves of *N. benthamiana* expressing PERU-GFP were infiltrated with Pep-25-bio or Pep-25W231A-bio with or without unlabeled Pep-13 or Pep-13W231A peptides as competitor. For cross-linking of peptides to the receptor, 2 mM ethylene glycol bis (succinimidyl succinate) (EGS) was co-infiltrated into the leaves. After 20 minutes, the leaves were harvested and frozen in liquid nitrogen. For immunoprecipitations, membrane proteins of infiltrated *N. benthamiana* leaves were extracted using extraction buffer (150 mM NaCl, 50 mM Tris·HCl pH 8.0, 1% NP-40, protease inhibitor cocktail (RoChe)), adjusted to a final concentration of 1 mg ml^{-1} and immuno-adsorbed by means of their GFP-tags on GFP-Trap agarose beads (ChromoTek). Immunoblots were developed either directly with Streptavidin-alkaline phosphatase conjugate (Roche), with anti-GFP antibodies (Torrey Pines Biolabs) or anti-myc antibodies (Sigma-Aldrich), followed by staining with secondary antibodies coupled to alkaline phosphatase and CDP-Star (Roche) as substrates.

Protein expression and purification in insect cells

The sequence encoding ectodomain of $PERU^{24-779}$ with an N-terminal gp67 secretion signal peptide was amplified by nested PCR and cloned into pOET1C transfer vector (*Apa*I-*Sac*II sites) with C-terminal 6xHis-fusion (Oxford Expression Technologies). The resulting plasmids were transfected into Sf9 cells by using flashBAC GOLD kit (Oxford Expression Technologies). High Five cells (Invitrogen) were infected with 3% (vol/vol) virus at a density of $1x10^6$ cells ml^{-1} and incubated at 27 °C for 48 hours. The secreted proteins were purified from the supernatant by a HisTrap excel column (GE Healthcare). Bound proteins were eluted in a buffer containing 50 mM Tris·HCl pH 8.0, 200 mM NaCl, 500 mM imidazole and further purified by size-exclusion

chromatography (Superdex 200 Increase 10/300, GE Healthcare) in a buffer containing 20 mM NaAc pH 5.0, 200 mM NaCl.

In vitro ligand binding assays

The purified His_6-tagged PERU LRR ectodomain protein ($PERU^{LRR}$-His_6) was mixed with 2 mM EGS and Pep-25-bio, with or without unlabeled Pep-13 peptide in binding buffer (20 mM NaAc pH 5.0, 200 mM NaCl). After incubation at room temperature for 30 minutes, streptavidin agarose resin (Thermo Scientific) was added and further incubated on a rotor at 4 °C for 1 hour. The resin was washed with binding buffer for 3 times. $PERU^{LRR}$-His_6 bound Pep-25-bio peptides were detected by immunoblots as described above. The band intensities of streptavidin were measured using ImageJ.

Phylogenomic analyses

A database of 6,630,292 protein sequences was assembled from 124 Solanaceae genomes (data S4). Receptor kinases (RKs) were then extracted from the compiled protein dataset using hmmsearch (HMMER v3.3.2) [--max], utilizing the PF00069 Pfam HMM profile, with only sequences bearing a single protein kinase (PK) domain retained (*58*). These RK sequences were then subjected to a search for leucine-rich repeat (LRR) domains using the Pfam PF00560, PF13855, PF08263, and PF13516 HMM profiles, with sequences identified by any of these profiles considered to possess an LRR domain. The PK domain sequences were then extracted using the domain boundaries within the domain table output from hmmsearch for alignment and phylogenetic analysis. A phylogenetic tree was constructed using MAFFT v7.520 [--anysymbol] and FastTree v2.1.11 [default options], involving 42,697 sequences from the previous step and 33 reference sequences, including $PERU^{DM}$. LRR-RK subgroups were annotated based on their representatives (data S7, S8) (*59, 60*).

LRR-RK Subgroup XII, which contained FLS2 and $PERU^{DM}$, was extracted and the PK domains were realigned to generate a new phylogenetic tree (data S9). Major branches close to $PERU^{DM}$ and FLS2 were identified and extracted. While FLS2 clade was easy to identify, $PERU^{DM}$ clade required multiple iterations of zooming, filtering, and realignment to improve resolution and identify the best branch defining the $PERU^{DM}$ clade. Sequences with potential truncated PK domains were excluded using Geneious prime software (https://www.geneious.com/), based on the length distribution graph.

$PERU^{DM}$ and FLS2 clades were then subjected to additional refining steps: the N-terminally truncated sequences without the LRRNT cap (PF08263) were removed, as were sequences with additional domains to PK and LRR. Sequences with incorrect gene models were trimmed, specifically those with incorrect start codons (N-terminal extension). PERU sequences were checked to determine whether the first intron was miscalled in the alignment. Lastly, sequences without a signal peptide, as determined by SignalP 6.0, were filtered out (*61*). Next, potentially truncated FLS2 sequences were

removed by setting a length threshold of 1150 amino acids and over based on FLS2 clade sequence length distribution (data S5, S10). Finally, the full-length sequences of refined PERU^{DM} and FLS2 clades were used to make the final phylogenetic trees in the same way as described before. The phylogenetic trees were visualized by iTOL and annotated manually (62). The species tree was adapted from *(47)*. All datasets, scripts and instructions for these analyses are available in the GitHub repository on Zenodo *(48)*.

Positive selection analysis

36 full-length nucleotide sequences were used, that form the PERU clade (Fig. 4A), to generate a codon alignment using MUSCLE from MEGA software package (63). To identify which PERU amino acids have been affected by diversifying selection, we used maximum likelihood models of codon substitution. Analyses were performed with the program CODEML from the PAML package *(34)*. The six models recommended were tested (Null models M0, M1, M7 and alternative models M3, M2, M8, respectively) Statistical significance was tested by comparing the null models with their respective alternative models. Twice the difference in log likelihood ratio between a null model and an alternative model was compared with a chi-squared (χ^2) distribution. The degrees of freedom were determined by the difference in the numbers of parameters estimated from the pair of models. The likelihood ratios of the two models test whether an alternative model fits the data better than the null model. Positively selected sites were identified using the Bayes Empirical Bayes analysis implemented in CODEML (64).

Structural analysis using AlphaFold2 and LRR prediction

The ectodomain of PERU^{DM} (PERU^{DM}-ECD) which comprises residues 39-768 was modelled using AlphaFold2 (AF2) through ColabFold v1.5.2 (65, 66), following guidelines on the document (https://colab.research.google.com/github/sokrypton/ColabFold/blob/main/batch/AlphaFold2_batch.ipynb). Twelve iterative recycles and an AMBER relaxation step were incorporated in the modelling. From the 5 independent models generated by AF2, we selected the highest-ranking model based on the average per-residue confidence metric, pLDDT. The number of LRRs were checked manually and confirmed by AF2.

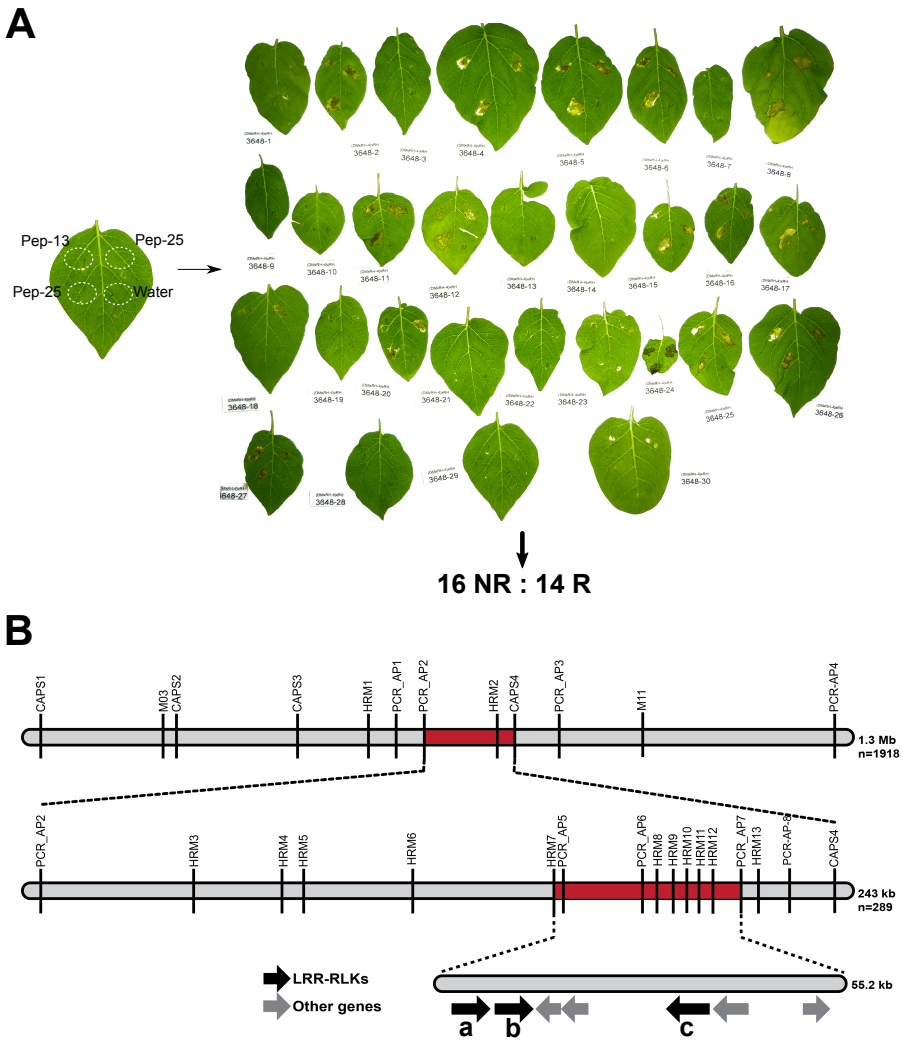

Fig. S1. Map-based cloning of *PERU* from DM 1-3 516 R44. (A) The F2 segregating population 3648 was phenotyped for a cell death response (R, responsive; NR, non-responsive) to Pep-13/25 and segregated in a 1:1 ratio. **(B)** Two flanking markers PCR_AP2 and CAPS4 were identified after the high throughput screening of 1918 individuals from the mapping population, narrowing the mapping interval to 243 kb. To further fine-map the region, 15 molecular markers were developed and 289 additional individuals were genotyped to find new recombination events. As a result, a final mapping interval of 55.2 kb was obtained, which contains 7 genes, 3 of which ("a", "b" and "c") encode LRR-RKs. Other genes (grey arrows, from left to right) include sequences encoding SOS3-interacting protein, seed dormancy control domain containing protein, neutral/alkaline non-lysosomal ceramidase and homeodomain-like superfamily protein.

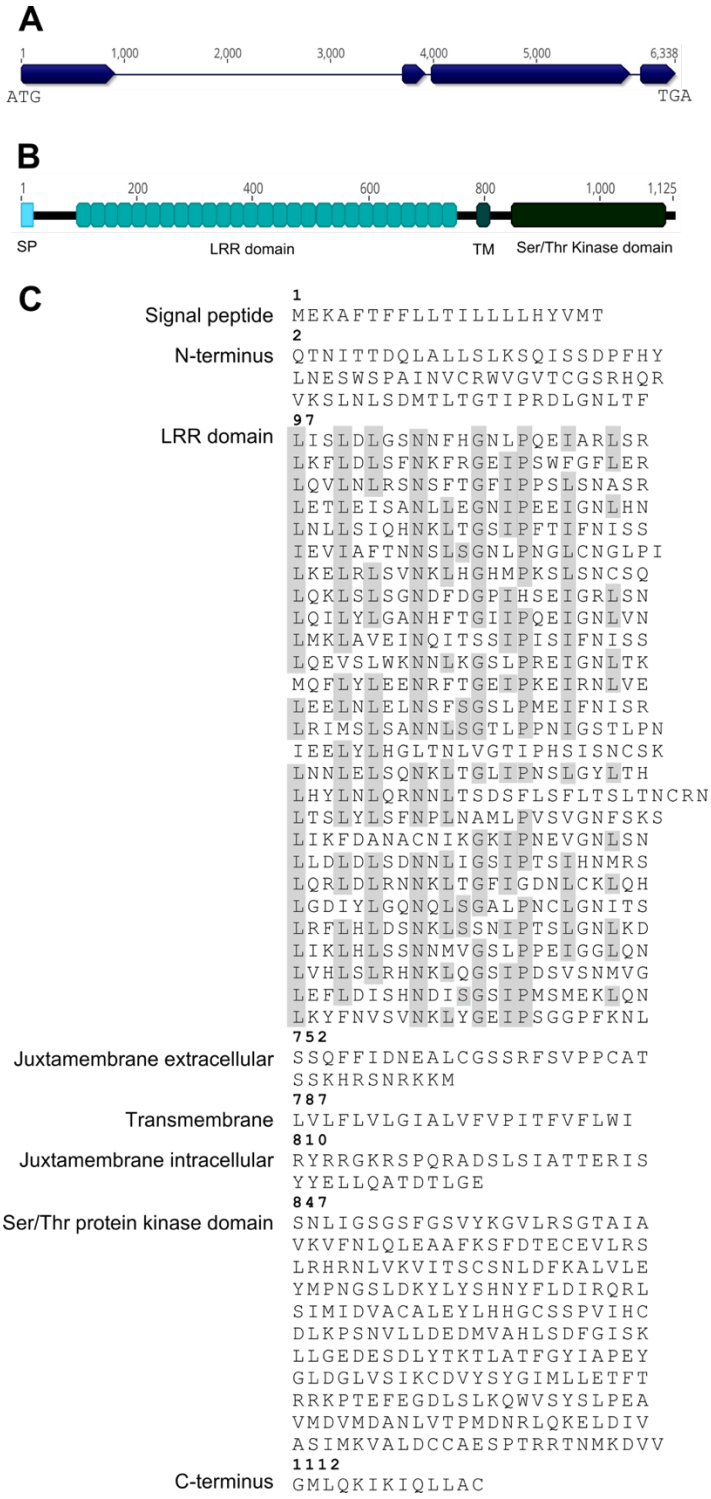

Fig. S2. Schematic representation of *PERU* and its encoded LRR-RK. (A) Intron/exon structure of the *PERU* gene. **(B)** Schematic representation of the PERU protein consisting of 1,125 amino acid residues. **(C)** Primary structure of the PERU protein, containing a signal peptide for secretion; an extracellular LRR domain that consists of 27 repeats of the consensus sequence LXXLXLXXNXGXIPXXJGNLXX (highlighted in grey), and is flanked by two cysteine pairs (highlighted in dark grey); a single transmembrane domain; an intracellular juxta-membrane domain that contains the putative endocytosis motif YXXØ; and a Ser/Thr kinase domain.

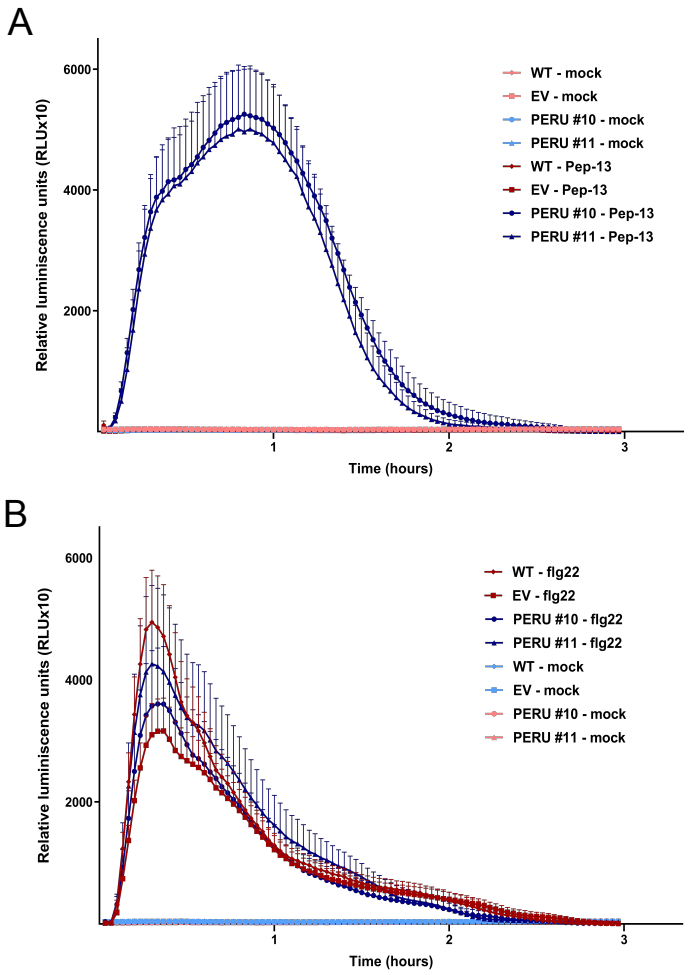

Fig. S3. ROS production in potato. Cultivar Atlantic (WT), Atlantic transformants stably expressing empty vector (EV) or *p35S::PERU* (lines #10 and #11) were treated with water (mock), or 1 μM Pep-13 **(A)** or with water, or 1 μM flg22 **(B)**. Mean values ± standard error of eight replicates are shown. Assays were performed in triplicate with similar results.

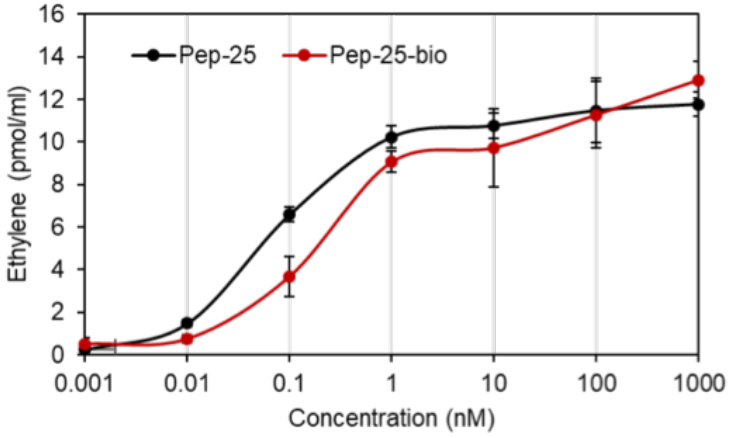

Fig. S4. Ethylene-inducing activity of biotinylated Pep-25 peptide in *N. benthamiana*. Ethylene accumulation in *N. benthamiana* leaves transiently expressing *p35S::PERU-GFP* was measured 4 hours after treatment with Pep-25 or biotinylated Pep-25 (Pep-25-bio). Bars represent means ± standard deviation of two or three replicates. Assays were performed in triplicate with similar results.

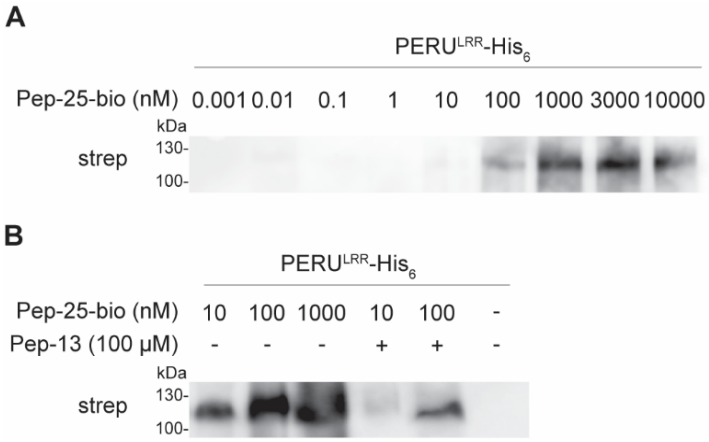

Fig. S5. In vitro binding of PERU^{LRR}-His$_6$ to Pep-25-bio. (A) Recombinant His$_6$-tagged PERU LRR ectodomain protein (PERU^{LRR}-His$_6$, 10 nM) was incubated with increasing concentrations of biotinylated Pep-25 (Pep-25-bio) as ligand. Ligand-receptor complexes were precipitated with streptavidin agarose and visualized on protein blots using Streptavidin-Alkaline Phosphatase (strep). Band intensities of strep were measured by ImageJ. The average of the affinity constants determined from five independent experiments is K_D=88.9 nM. **(B)**, Ligand binding competition experiments were conducted as in (A) using 100 mM Pep-13 as competitor. This experiment was repeated four times.

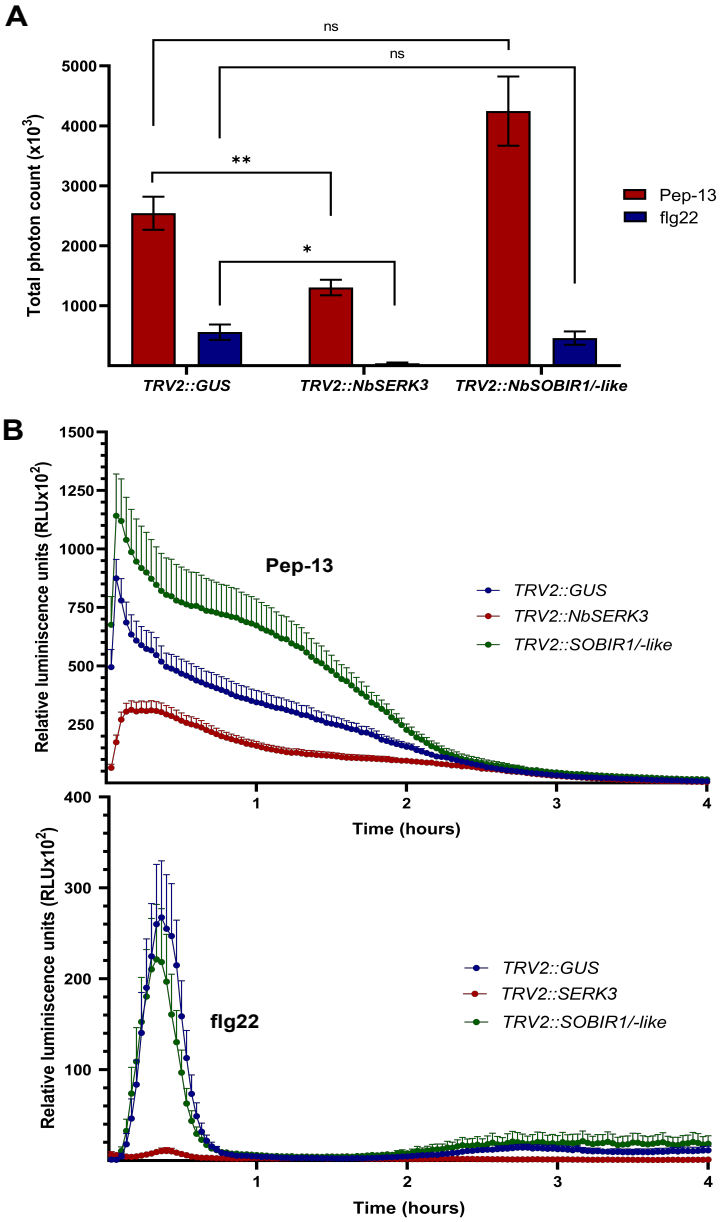

Fig. S6. Silencing of *NbSERK3* reduces the ROS burst induced by Pep-13. (A) Total photon count and **(B)** kinetics of ROS burst induced by 1 μM Pep-13 or 1 μM flg22 (as positive control) in *N. benthamiana* leaves expressing constructs *NbTRV2::NbSERK3*, *NbTRV2::NbSOBIR1/-like* or *TRV2::GUS* as control for virus-induced gene silencing. Data from (A) were analyzed using Welch ANOVA and Dunnett's T3 multiple comparison test, (*p-value 0.05, **p-value<0.01, ns non-significant). Mean values ± standard error of eight replicates are shown. Assays were performed in triplicate with similar results and representative results are shown.

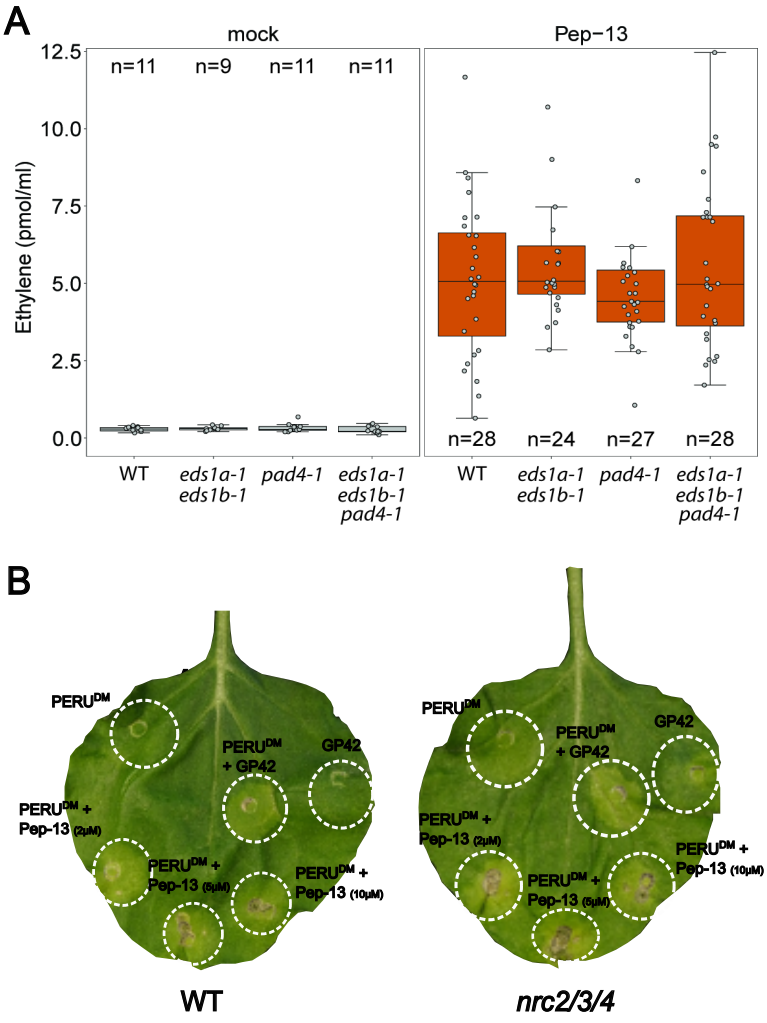

Fig S7. Pep-13-induced defenses are not impaired in *N. benthamiana* mutant genotypes transiently expressing *PERU^{DM}*. (A) Ethylene accumulation 3 hours after treatment with water (mock) or 1 μM Pep-13 in *N. benthamiana* wild-type (WT) and CRISPR mutants (eds1, pad4, and eds1/pad4) leaves transiently transformed with *PERU^{DM}-GFP*. Data points (grey dots) from three independent experiments are shown (n with exact numbers are indicated in the box plots) and plotted as box plots (center line: median, bounds of box: the first and third quartiles, whiskers: 1.5x the interquartile range, error bar: minima and maxima). **(B)** Representative WT and nrc2/3/4 mutants *N. benthamiana* leaves co-agroinfiltrated with *PERU^{DM}*, and Pep-13 (at 3 different concentrations) or the full-length glycoprotein *GP42*. Cell death was visualized at 3 days post infiltration.

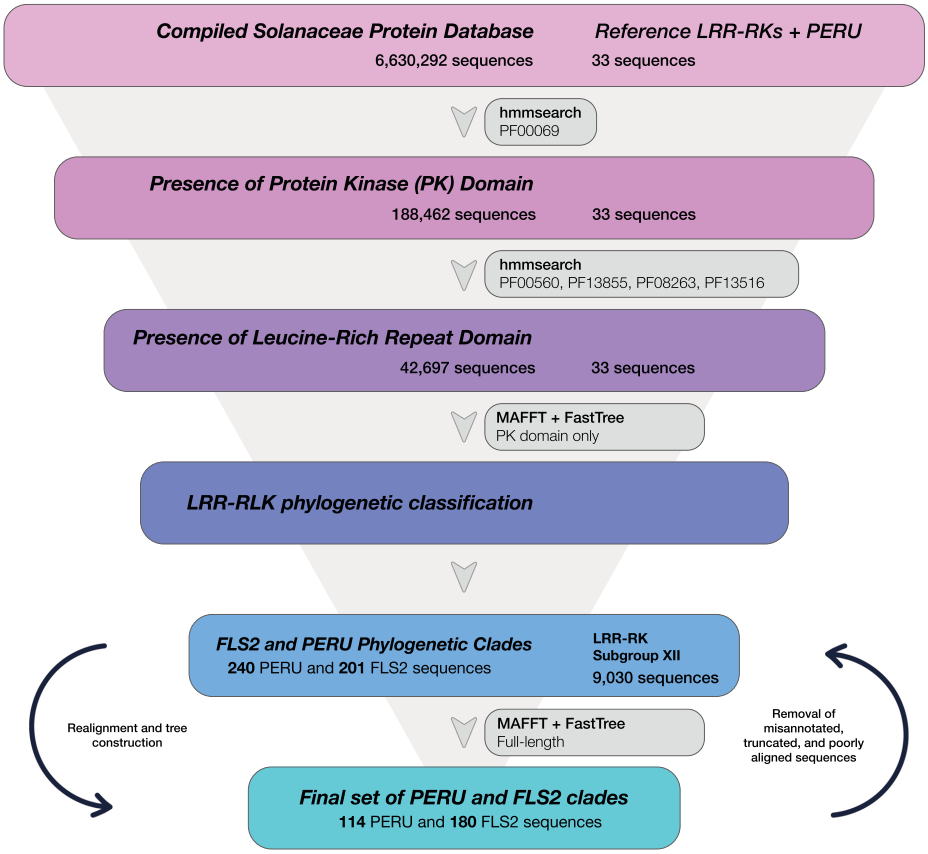

Fig S8. Bioinformatics pipeline to extract PERU and FLS2 clades. From a database containing 6,630,292 predicted sequences from 124 Solanaceae genomes, 42,697 LRR-RK proteins were obtained (table S4). These proteins were categorized based on known LRR-RK subgroups. FLS2 and PERU sequences from subgroup XII were then extracted and iteratively refined. Phylogenetic analyses were ultimately conducted using a final selection of 114 PERU and 180 FLS2 sequences.

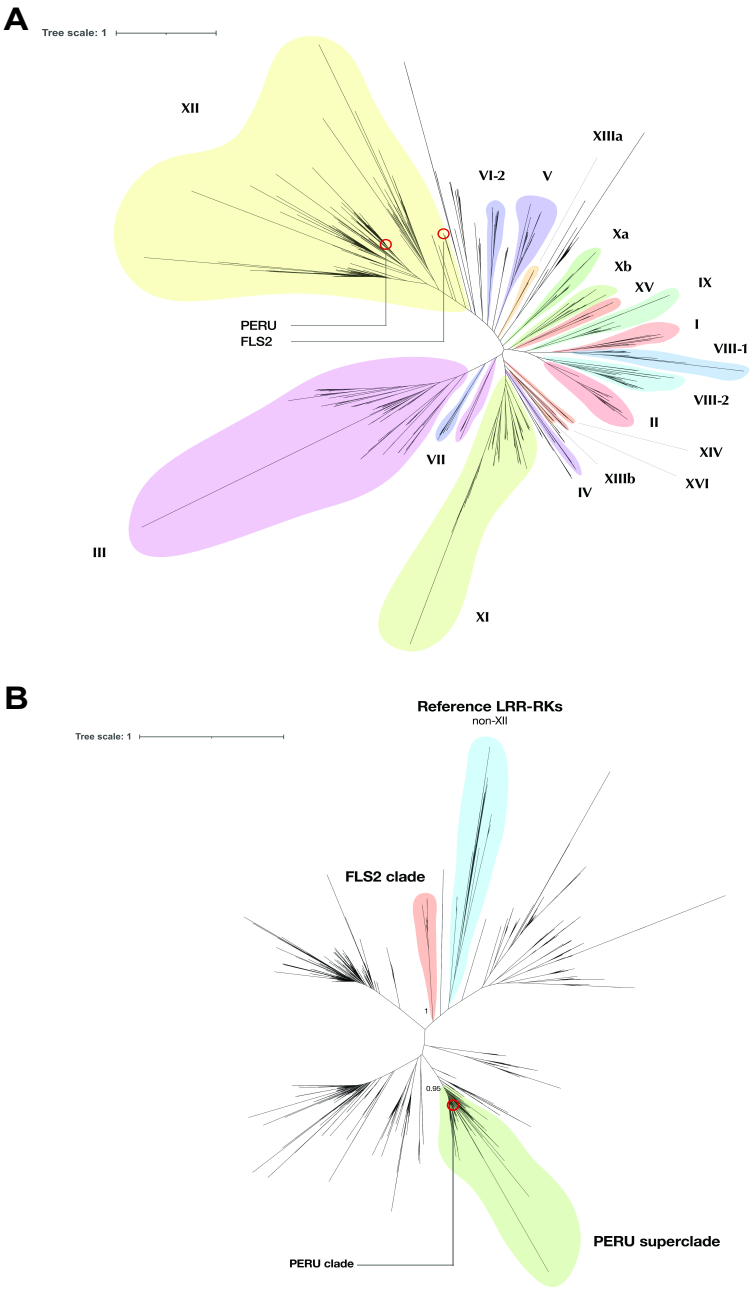

Fig S9. PERU and FLS2 formed distinct, well-supported clades within the LRR-RK subgroup XII. A. A phylogenetic tree showing the LRR-RK classification for 42,697 LRR-RK proteins. Both PERU and FLS2 are located within the XII subgroup and have monophyletic origin. **B.** LRR-RK subgroup XII phylogenetic tree showing PERU and FLS2 are located in distinct and well-supported phylogenetic clades. The numerical values presented correspond to the bootstrap values for major branches for the clades that contain PERU and FLS2.

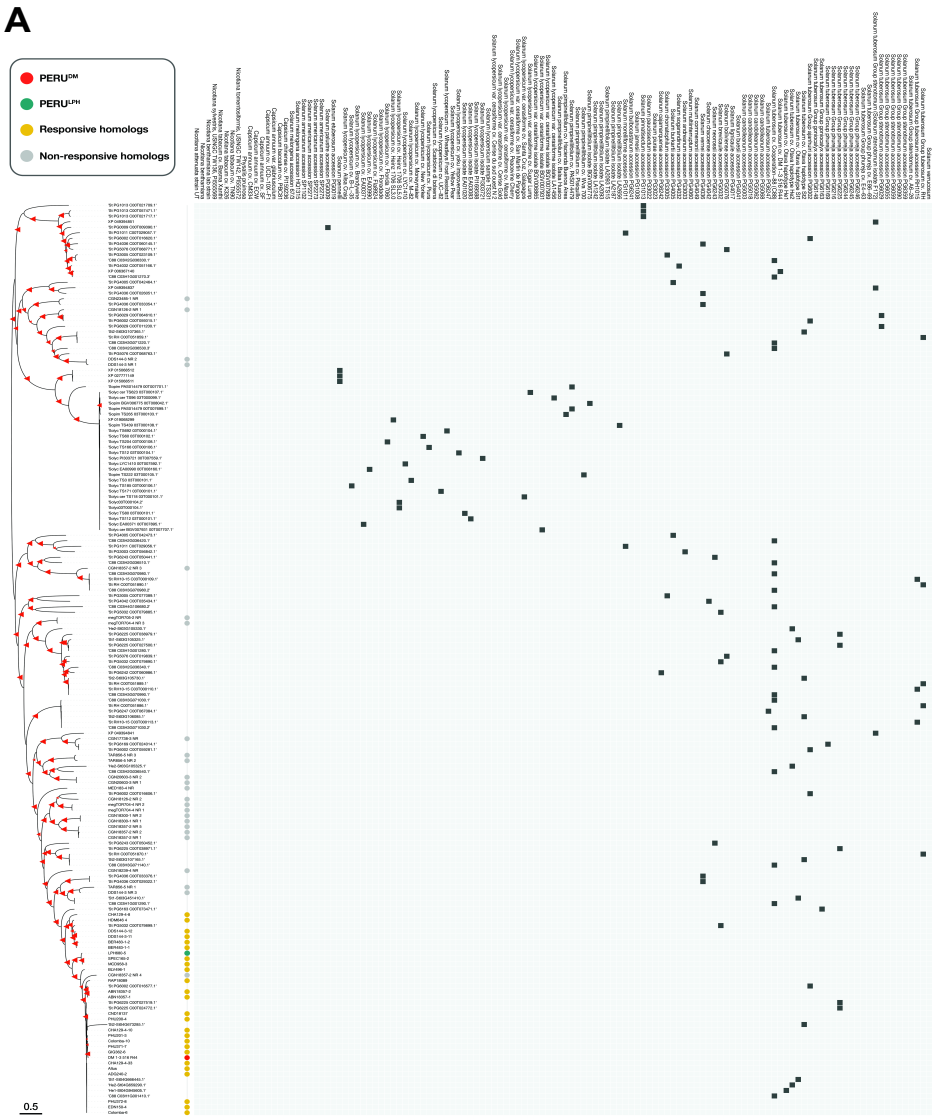

Fig S10. Heatmap representation of presence/absence of PERU phylogenetic clade across *Solanum* species. A. The PERU^{DM}, PERU^{LPH}, and the Pep-13 responsive homologs clustered together in a single clade, while the non-responsive homologs were scattered throughout the phylogenetic tree. **B.** FLS2 clade demonstrated uniformity in distribution and little variation across the Solanum genus, with most species possessing at least one copy. The bootstrap values for all branches are illustrated with triangles.

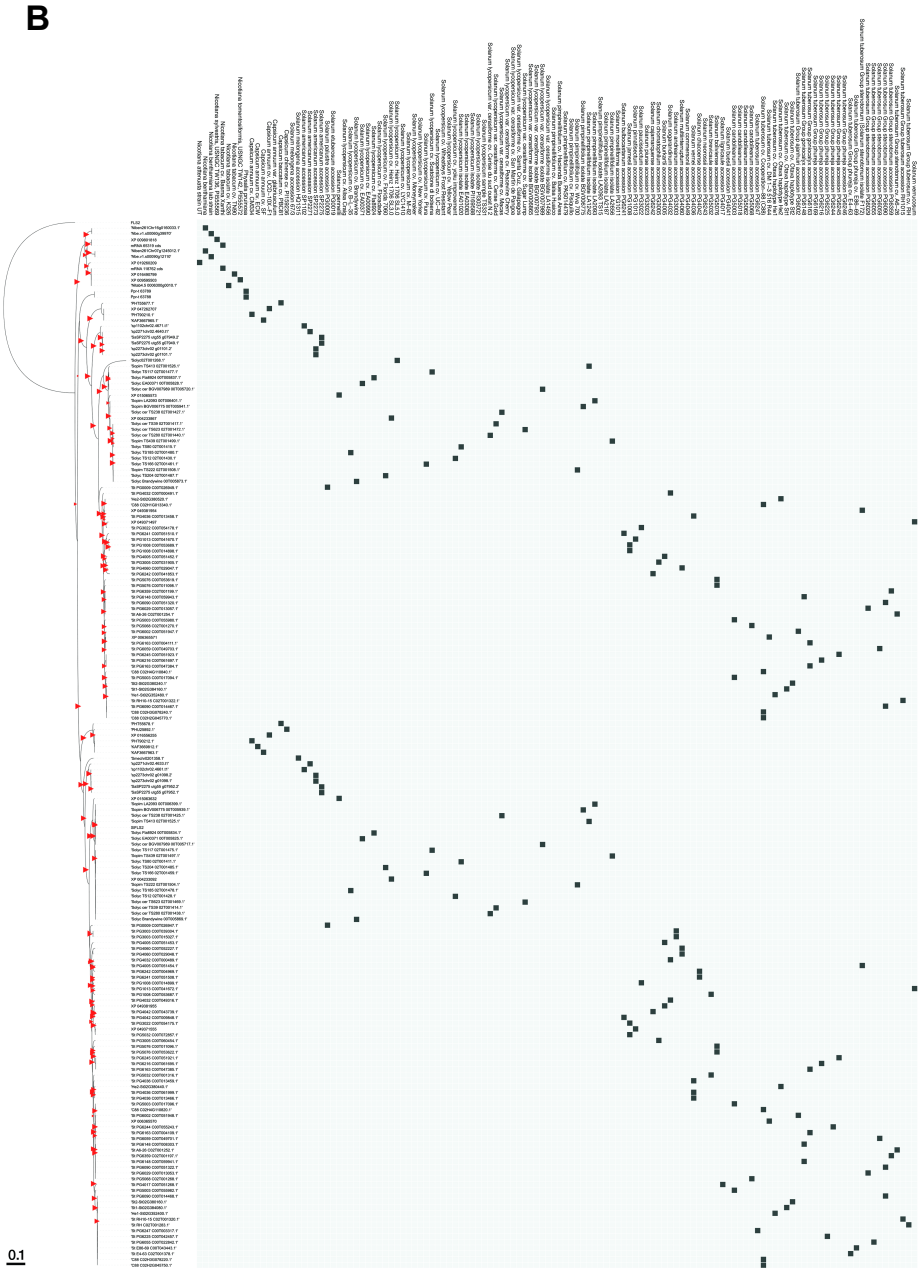

Fig S10. (Continued)

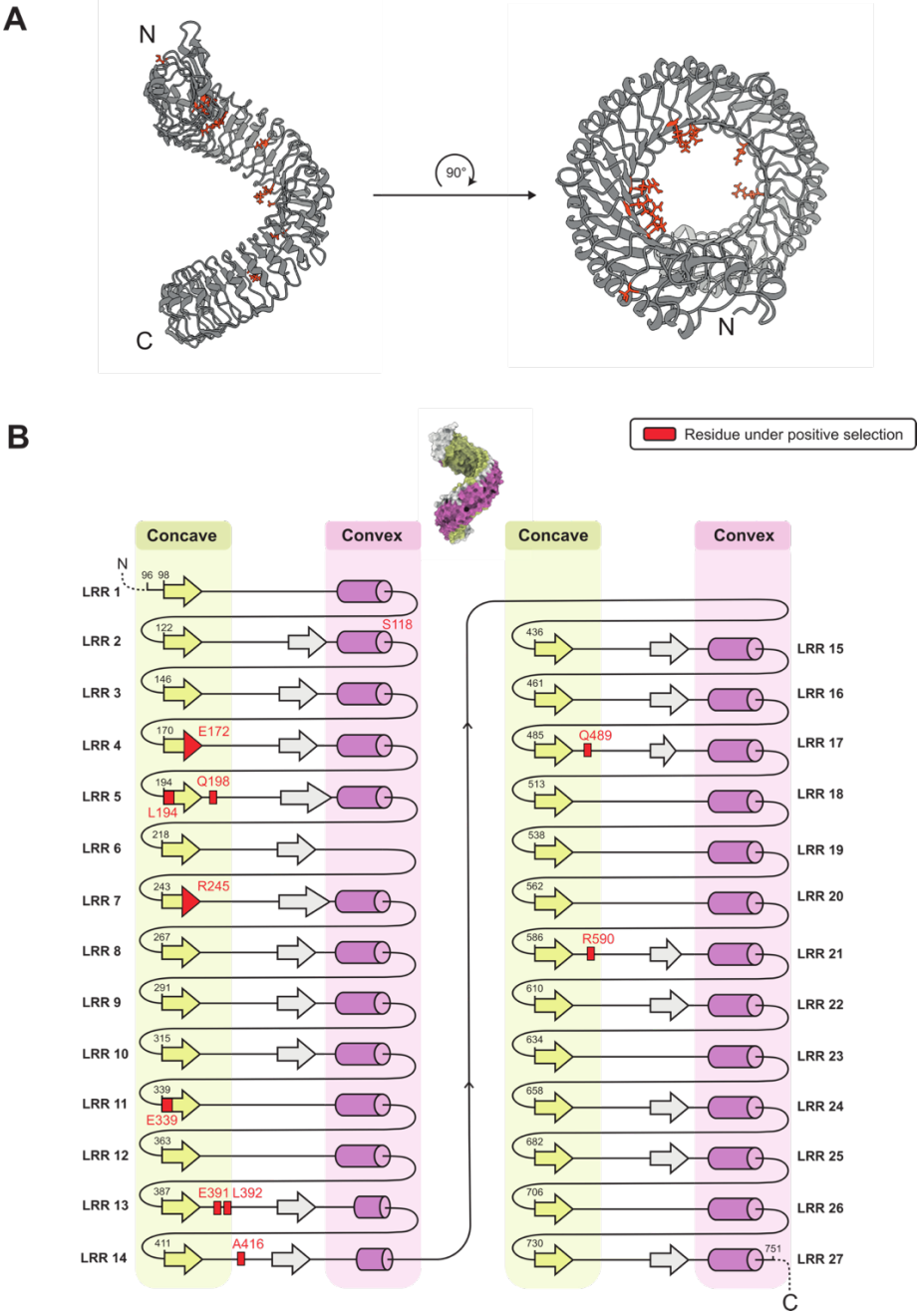

Fig S11. AlphaFold2 model of PERU^{DM}-ectodomain with residues found under positive selection. **A.** AlphaFold2 model for the ectodomain of PERU^{DM}, which closely resembles the experimentally validated structure of FLS2. The 11 residues found to be under positive selection after performing PAML analysis are marked in red. **B.** Schematic representation of the LRR domain of PERU^{DM} (residues 96-751) including secondary structures and the residues highlighted in (A)

Table S1. Diversifying selection analysis using PAML. CODELM from the PAML software was used, six models were tested (Null models M0, M1, M7 and alternative models M2, M3, M8).

Model of selection	lnL[a]	Estimates of parameters	Positively selected sites[b]	Model comparison	2ΔL[c]	d.f[d]	p-value
M0 (one-ratio)	-7990.55	ω=0.547	Not allowed				
M1 (nearly neutral)	-7864.81	p_0=0.702	Not allowed				
M2 (positive selection)	-7805.74	p_0=0.676, p_1=0.280, p_2=0.044, ω_2=6.959	**118 S**, 172 E, 194 L, **198 Q**, **245 R**, **339 E**, **391 E**, **392 L**, **416 A**, **489 Q**, **590 R**	M1 vs. M2	118.14	2	0.0
M3 (discrete)	-7799,84	p_0=0.760, p_1=0.225, p_2=0.015, ω_0=0.008 ω_1=2.032 ω_2=12.91	**4 A**, 5 F, 6 T, **7 F**, 12 I, **16 L**, 22 Q, 26 T, 31 A, 46 Y, **48 N**, 52 S, **54 A**, **56 N**, **59 R**, 63 V, 65 C, 66 G, 67 S, **68 R**, **71 R**, **79 D**, **81 T**, 85 T, 90 L, 99 L, 102 G, **103 S**, 115 A, **116 R**, **118 S**, 119 R, **124 D**, **127 F**, **129 K**, 130 F, 131 R, **142 E**, **143 R**, **145 Q**, **146 V**, **150 R**, **151 S**,**157 F**, **172 E**, 180 G, **193 N**, **194 L**, **196 S**, **197 I**, **198 Q**, **199 H** , **201 K**, **215 S**, 217 E, 218 V, 223 N, **225 S**, 241 L, 243 E, **245 R**, **248 V**, **252 H**, **257 K**, **267 K**, **272 G**, 291 I, **296 A**, **315 K**, **317 A**, **325 S**, **339 E**, **344 K**, 348 K, 382 L, 387 E, 388 L, **389 N**, **390 L**, **391 E**, **392 L**, **411 I**, **412 M**, **413 S**, **416 A**, **472 L**, **479 Y**, **484 H**, **485 Y**, **489 Q**, **510 N**, **512 T**, **513 S**, 515 Y, **534 K**, **562 D**, **564 D**, 566 S, 579 H, **581 M**, 587 L, **588 D**, **590 R**, 591 N, 607 H, **621 A**, **629 I**, **634 F**, **635 L**, **636 H**, , **658 K**, **660 H**, **676 G**, 681 V, 693 S,697 S, 698 V, 702 V, 703 G, 705 E, 706 F, **713 D**, 714 I, **717 S**, **722 M**, 727 N, 738 L, 745 G, 749 K, **758 D**, 764 G, **765 S**, 774 A, 778 K, **785 K**, **788 V**, 791 L, 792 V, **803 T**, **805 V**,**820 R**, 825 S, 827 A, 844 L, 845 G, **862 V**, **864 R**, 893 R, 901 V, 926 D, 927 K, 961 S, 1000 Y, **1059 L**, 1066 V, **1078 R**, 1079 L, 1087 A, **1098 A**, 1102 T, **1118 K**, 1123 A	M0 vs. M3	381.42	4	0.0
M7 (beta)	-7872.88	p=0.006, q=0.009	Not allowed				
M8 (beta&ω)	-7808.25	p_0=0.937, p=0.025, q=0.066, ω_1=5.70	**118 S**, 142 E, 172 E, 194 L, **198 Q**, **245 R**, **339 E**, **391 E**, **392 L**, 416 A, **489 Q**, 590 R	M7 vs. M8	129.26	2	0.0

[a]lnL = log likelihood value.

[b]Amino acid sites inferred to be under diversifying selection with a probability >95% are shown, >99% are shown in bold, sites predicted by the three models are underlined.

[c]Likelihood ratio test: 2ΔL= 2(lnL alternative hypothesis - lnL null hypothesis

Table S2. Sequence of primers used in this study.

Primer name	Sequence
PCR_AP1-fw	ATGACCAAATATCCGCCTTT
PCR_AP1-rv	CCAAGGTACATTTGCCAAAG
PCR_AP2-fw	CACCCCTTACCACTTTTCTT
PCR_AP2-rv	ATAAAGCATTGGGTCGAACT
PCR_AP3-fw	GTGTTATTTGAGTTGCAGG
PCR_AP3-rv	AGAAGTGGTGGCATTTGG
PCR_AP4-fw	AGGAGGGGAAAAGATATCGA
PCR_AP4-rv	CAAGGACGGGAACTTTCTTA
PCR_AP5-fw	ATGTCACTAGCCTAGAATTT
PCR_AP5-rv	GTGCTTTATCTAACAACGTA
PCR_AP6-fw	GGATCTTCTTGAAGGCATTG
PCR_AP6-rv	TTTTGGATGATCTGGCACG
PCR_AP7-fw	TATACAACTGACCCCTACTT
PCR_AP7-rv	TCCCCACAACTAGTACTATT
PCR_AP8-fw	AGCCTTGGAGCAACGGTAAA
PCR_AP8-rv	GGCTCGTTTGGTGTGAGAGA
HRM-1-fw	AATTTGTGTTTTGGGCTTCC
HRM-1-rv	AACGCTAGAGGAAGAATGTT
HRM-2-fw	GACCACAAACAGTAGACAGT
HRM-2-rv	AAACTCCGTTCCAAGTCAAA
HRM-3-fw	GTGAAACATAGCACTGCTAGA
HRM-3-rv	CACTAGGATGATGGTCTTTGA
HRM-4-fw	ACTCAGTCGTCAGTAAAAGT
HRM-4-rv	CATGATGGGTACAATGTAT
HRM-5-fw	ATACGATATGTATGCATCCT
HRM-5-rv	CCAAACTTTTAGTAGTAACG
HRM-6-fw	GAGTTCCAATATACCAACAG
HRM-6-rv	CATATATGTCACAGCCTTTA
HRM-7-fw	CATAAAGCTGTAATATGTGC
HRM-7-rv	AGTTCCATCAAGTAGCTATC
HRM-8-fw	CAAGAGACTTACAACATGTG
HRM-8-rv	GTATTCTGATCCAAATGG
HRM-9-fw	AGCTTATCTGTTTTTCTAGC
HRM-9-rv	CTCTACTCTGTATGGTCCAC

Table S2. (Continued)

Primer name	Sequence
HRM-10-fw	GACCACAAACAGTAGACAGT
HRM-10-rv	AAACTCCGTTCCAAGTCAAA
HRM-11-fw	ACACTTCACCATTACACTTC
HRM-11-rv	CACAGAAACTATACAGAAGACA
HRM-12-fw	CTAAGCTTATCAATTACGAG
HRM-12-rv	ACGTGGTAAAACTGATAA
HRM-13-fw	AATTCTAGCTCCGCCACTGG
HRM-13-rv	GGTTACGGAGAAGGGTTGCA
CAPS1-fw	GCTTGTCTCTGTGTTATTGC
CAPS1-rv	ACTAGGAGAAGCAGTAGGAG
CAPS2-fw	TGCTTTAGTTTGATCGGTGA
CAPS2-rv	TGGAGAGAGAGTTCAGTAGG
CAPS3-fw	CTTAGTCTCTGCCTGATGTC
CAPS3-rv	AAAGGCTGCGATACTGATAG
CAPS4-fw	GCTATCCTACAAAGACCGTC
CAPS4-rv	GCAAATAAACTCTCAAAGGGA
a-start-fw	CACCATGGAGAAGGCCTTGAGAT
a-stop-rv	CTAATTACTTTGAGCCGAGGT
b-start-fw	CACCATGGAGAAAGCCTTCACAT
b-stop-rv	TCAGCATGCAAGAAGTTG
b-start-fw2	CACCCACATGTTACTAGCGATATC
b-start-fw3	CACCACATGTTACTAGCGATATCA
c-start-fw	CACCATGATGGAGAAAACAGAGG
c-stop-rv	CTGGATCACGCTGCCTCG
sgRNA-1-fw	ATTGAGAAATAGCACGCTTGTCT
sgRNA-2-fw	ATTGGTGCCTGTAAGAGTCATGT
sgRNA-3-fw	ATTGAGTGAAACTTCTTGCAATG
sgRNA-4-fw	ATTGAATTTGATGAAGTTAGCCG
sgRNA-1-rv	AAACAGACAAGCGTGCTATTTCT
sgRNA-2-rv	AAACACATGACTCTTACAGGCAC
sgRNA-3-rv	AAACCATTGCAAGAAGTTTCACT
sgRNA-4-rv	AAACCGGCTAACTTCATCAAATT
CC-238-fw	TGCAGCGTCTCTTCCTCGAT
CC-1440-rv	GATGACCACACACGTGTCCT
CC-4225-fw	TTGATGAAGTTAGCCGTGGAGA
CC-5129-rv	TTTCTCAAGTCCAGGCGCTG

The following datasets are available at Zenodo (48)

Data S1. Pep-25 and the three peptide mutants were tested for HR induction on 477 genotypes. HR was scored from 0 to 1, and only genotypes with HR value higher than. 0.2 were considered for further analysis. [a] Unique ID for Centre for Genetic Resources, the Netherlands (CGN) (https://cgngenis.wur.nl/), and SolR gene database (https://www.plantbreeding.wur.nl/SolRgenes/). [b] Species name (Spooner et al. 2014). [c] Cladistic relationships are based on plastid or nuclear investigations (Spooner et al. 2014).

Data S2. Genome metadata used in the phylogenomic analysis.

Data S3. Per species statistics of LRR-RK distribution.

Data S4. Per genome statistics of LRR-RK distribution.

Data S5. PERU clade sequence and metadata.

Data S6. List of responsive and non-responsive homologs sequence and metadata.

Data S7. Reference LRR-RK sequence and metadata.

Data S8. LRR-RK sequence and metadata.

Data S9. LRR-RK Subgroup XII sequence and metadata.

Data S10. FLS2 clade sequence and metadata.

Chapter 5

Stacking of PRRs in potato to achieve enhanced resistance against *Phytophthora infestans*

Yerisf C. Torres Ascurra, Doret Wouters, Richard G. F. Visser, Thorsten Nürnberger and Vivianne G. A. A. Vleeshouwers

This manuscript was published as:

Torres Ascurra, Y. C., Wouters, D., Visser, R., Nuernberger, T. & Vleeshouwers, V. (2023). Stacking of PRRs in potato to achieve enhanced resistance against *Phytophthora infestans*. bioRxiv, 2023-9.

Abstract

Plants employ pattern recognition receptors (PRRs) to sense pathogen-associated molecular patterns (PAMPs) or apoplastic effectors at the plant cell surface, as well as nucleotide-binding domain leucine-rich-repeat-containing receptors (NLRs) to sense effectors inside the plant cell. Breeding for potato resistance to *P. infestans* has focused on the use of NLRs, however, these genes are typically quickly overcome since the matching avirulence genes evolve exceptionally quickly. Here, we stacked two PRRs, *PERU* and *RLP23,* that recognize the rather conserved *Phytophthora* PAMPs Pep-13/25 and nlp20, respectively, in the potato cultivar Atlantic, and evaluated their effect on *P. infestans* resistance. We found that PERU and RLP23 cooperate for the early immune responses like the accumulation of reactive oxygen species (ROS) and production of ethylene by recognizing their corresponding PAMPs. Furthermore, we show that potato plants overexpressing these two PRRs are slightly less affected by *P. infestans* compared to the single transformants. Together, our data suggest that pyramiding of surface receptors can provide additional enhanced resistance against pathogens, however, more effective or synergistic combinations that may include intracellular NLR receptors should be explored.

Potato (*Solanum tuberosum* L.) is one of the most important food crops worldwide with a production of more than 359 million tons in 2020 [1]. However, potato is severely affected by the late blight disease with yield losses estimated at 15-20% globally [2]. *Phytophthora infestans*, the causal agent of late blight, is a very destructive oomycete that can dismantle a complete potato field within days [3]. *P. infestans* has remained the most important threat for potato production, mainly because of its elevated virulence and distinctive genome architecture that underpins its evolutionary potential and ability to rapidly adapt to resistant plants [4, 5].

Breeding for resistance against *P. infestans* in potato has been focused on the use of intracellular nucleotide-binding domain leucine-rich-repeat-containing receptors (NLRs) encoded by resistance (*R*) genes. NLRs activate immune responses upon recognition of effector proteins secreted by pathogens, leading to effector-triggered immunity (ETI) [6]. Almost 50 *R* genes have been identified from wild tuber-bearing relatives of potato [7]; however, most, if not all, *R* genes have been overcome by *P. infestans* because of the rapid evolution of the matching avirulence (Avr) effectors, by diverse mechanisms such as mutation, gene loss, suppression and gene silencing that leads to loss of recognition [4]. Some recently identified genes including *RB/Rpi-blb1*, *Rpi-vnt1*, *Rpi-Smira2/R8*, *Rpi-blb2* confer broad-spectrum resistance to most of the tested *P. infestans* strains, according to long term field assays [8, 9]. Also *Rpi-amr1* from *Solanum americanum* was found to confer resistance to all 19 tested *P. infestans* isolates in transgenic potato [10]. However, the durability of these newer *Rpi* genes remains to be evaluated after prolonged deployment at larger acreages.

Despite the quick evolution of virulent races, stacking of *R* genes is considered an effective strategy to obtain a more durable resistance against *P. infestans* in potato. Three resistance genes to *P. infestans* (*Rpi*), *Rpi-sto1*, *Rpi-vnt1.1* and *Rpi-blb3* from the potato wild relatives *S. stoloniferum*, *S. venturii* and *S. bulbocastanum,* respectively, were placed into a single binary vector PBINPLUS and transformed to the cultivar Désirée, which led to a broad resistance spectrum, with no silencing effects observed under laboratory conditions [11]. These transgenic plants (and plants with single *R* gene) were evaluated in field trials in The Netherlands and Belgium for two years. Only the plants with the stacked genes remained healthy until the end of the season, while plants with single *R* genes showed disease symptoms [12]. In another study, the *NLR* genes *Rpi-blb1*, *Rpi-blb2* from *S. bulbocastanum* and *Rpi-vnt1.1* from *S. venturii* were cloned in one transcriptional unit and transformed into the cultivars Désirée and Victoria. The transgenic events showed complete resistance to *P. infestans* in field trials in Uganda during three consecutive seasons [13]. Still, the durability of the resistance obtained by gene stacking should be carefully evaluated over years, especially if virulence to the individual *R* genes occurs in the local pathogen populations. For example, old potato cultivars such as 'Pentland Dell' (R1R2R3) and

'Escort' (R1R2R3R10) nowadays succumb to late blight since virulent races have evolved [14]. In bread wheat, introduction of a transgene cassette of five resistance gene initially led to resistance to aggressive and highly virulent *Puccinia graminis* f. sp. *tritici* (*Pgt*) isolates, however a new *Pgt* isolate that can overcome several genes from this cassette has already emerged [15]. A similar scenario can be predicted for the *R* gene destroyer, *P. infestans* [3], and its favorite host, potato; it is only dependent on the passage of time.

Unlike ETI, the pattern-triggered immunity (PTI) has not been extensively explored in potato yet. PTI employs the pattern recognition receptors (PRR) to detect pathogen-associated molecular patterns (PAMPs) and trigger immunity [6]. PRRs can be receptor-like kinases (RLKs) or receptor-like proteins (RLPs), depending on the presence or absence of the kinase domain, respectively [16]. PRR-mediated immunity is thought to be more durable, since PAMPs are conserved structures or patterns essential for microbial viability or lifestyle, and shared by distinct groups of microorganisms [17, 18]. PAMPs are less likely to change and PRR are therefore considered to confer a more stable and broad-spectrum resistance compared to NLR [19, 20]. Resistance activity based on PRR can even be obtained beyond host plant families. The transfer of the PRR EFR from *Arabidopsis thaliana* to *Nicotiana benthamiana* and *Solanum lycopersicum,* based on the recognition of the conserved elf18 peptide, led to increased resistance to diverse plant pathogenic bacteria including *Pseudomonas*, *Agrobacterium*, *Xanthomonas* and *Ralstonia* [21]. Recently, we have cloned and characterized a new PRR, called *PERU* (Pep-13 receptor unit) from the *Solanum tuberosum* Group Phureja DM 1-3 516 R44, which is a receptor-like kinase that binds the PAMP Pep-13. Pep-13 is an oligopeptide of 13 amino acids, identified within a cell wall-associated transglutaminase (TGase), that showed to be necessary and sufficient to trigger defense responses in parsley and is conserved among different *Phytophthora* species [22, 23]. In potato, Pep-13 triggers oxidative burst and hypersensitive-like cell death, induces the accumulation of salicylic acid, jasmonic acid and the expression of defense-related genes [24, 25]. PERU interacts physically with Pep-13 and forms a complex with BAK1 upon Pep-13 treatment to trigger defense responses; furthermore, the overexpression and knock-out of *PERU* results in an enhanced resistance and increased susceptibility respectively, which indicates that PERU contributes to the resistance in potato against *P. infestans* [26].

The PRR RLP23 from *Arabidopsis thaliana* recognizes nlp20, a conserved peptide of 20 amino acids in Necrosis and Ethylene-inducing Peptide 1 (NEP1)-like proteins (NLPs) produced by bacteria, fungi, and oomycetes [27, 28]. This peptide is sufficient to trigger immune responses in Arabidopsis and other *Brassicaceae* species [28, 29], and

it was shown that ectopic expression of RLP23 in potato enhances immunity to *Phytophthora infestans* [29].

Whereas NLRs typically provide complete, or high levels of resistance to *P. infestans,* PERU and RLP provide lower levels of quantitative resistance [4, 26, 29]. We hypothesize that the combination of various PRRs may generate a more adequate level of resistance. In this study we stacked the newly found receptor PERU and RLP23, and investigated if the presence of two PRRs strengthens the immune responses in potato upon PAMP treatment, and generates a more robust resistance to *P. infestans*.

Potato cultivar Atlantic plants were transformed with pK7WG2::*PERU* and the lines *PERU*#10 and *PERU*#11 were obtained and characterized in a previous study [26]. In addition, cv. Atlantic explants were transformed with pB7WG2::*RLP23*, and transformants were obtained. Potato plants were maintained and clonally propagated *in vitro* on MS medium supplemented with 20% sucrose at 25 °C. Seven transformants were evaluated by PCR using different primer combinations (Table S1), and six events turned out to be positive for the transgene. For phenotyping, leaves of 4-week-old plants were treated with nlp20 and the ROS production was measured. Five lines tested positive, namely *RLP23* #1, #2, #4, #5, and #7 (fig. S1a). Double transformants were generated by co-transformation of cv. Atlantic explants with pK7WG2::*PERU* and pB7WG2::*RLP23.* A total of nine double transformants were obtained and subjected to PCR analysis to verify the presence of both genes. The PCR results confirmed the presence of PERU and RLP23 in all nine lines. Subsequently, six lines were randomly selected for phenotyping. ROS production upon nlp20 (fig. S1b) or Pep-13 (fig. S1c) treatment was measured in these six PCR-positive lines, and 5 of them tested positive for both genes, namely PERU/RLP23 #1, #4, #10, #27, #29 (fig. S1b, c).

To avoid the use of saturating doses, we determined EC_{50} by quantifying the ethylene accumulation using increasing concentrations of the peptides nlp20 and Pep-13. We found that Pep-13 triggers ethylene production in potato plants at nanomolar concentration (EC_{50}=2.40 nM) (Fig. 1A), while nlp20 triggers responses at micromolar concentration (EC_{50}=1.76 µM) (Fig. 1B). Indeed, the double transformants treated with both peptides showed no increase in ROS production (fig S2a), nor ethylene accumulation (fig. S2b), compared with the responses upon Pep-13 treatment alone, which indicated a saturation of the system. Therefore, based on the EC_{50} results, we decided to use 10 nM Pep-13 and 1µM nlp20 for the following experiments.

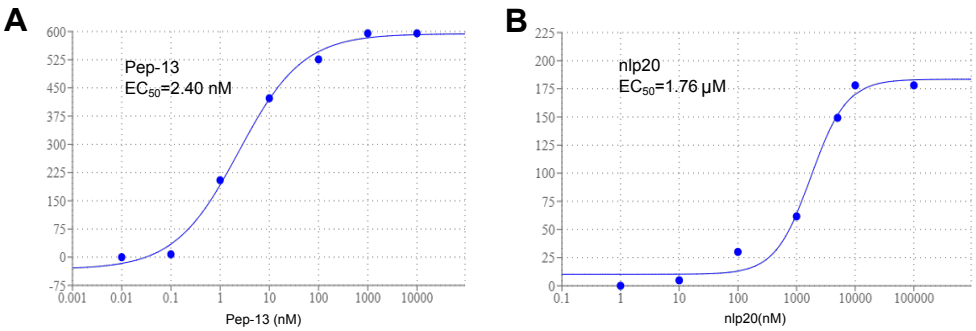

Figure 1. **EC_{50} determination of Pep-13 and nlp20 in cv. Atlantic potato plants**. Seven different concentrations of Pep-13 (**A**) and nlp20 (**B**) were used to measure the ethylene accumulation in leaves of 4-week-old plants. The plants were much more sensitive to Pep-13 compared to nlp20. The curves and EC_{50} values were obtained in AAT Bioquest.

To test if the presence of two stacked PRRs in potato has an additive effect on the PTI responses to the corresponding molecular patterns, we treated the double transformants with 10 nM Pep-13 and 1 µM nlp20 separately and together, and measured ROS production and ethylene biosynthesis [31]. We observed that in all 4 lines tested, the ROS burst upon Pep-13 treatment is stronger than upon nlp20 treatment, even when Pep-13 is used at nanomolar concentrations (Fig. 2A). This shows that potato cultivar Atlantic is much more sensitive to Pep-13 than nlp20, perhaps because *PERU* can operate in its native background potato, unlike RLP23 that is from Arabidopsis. The treatment of lines expressing *PERU* and *RLP23,* with Pep-13 and nlp20 together, showed a trend of additive effect of PRR stacking on ROS production, which however was not statistically significant (Fig. 2A). We observed this trend in PERU/RLP23 #10, #27, #29, but not in PERU/RLP23 #1. In terms of ethylene accumulation, we found an additive effect upon treatment of combined Pep-13 and nlp20 (Fig. 2B), which was statistically significant for PERU/RLP23 #1, but not significant for PERU/RLP23 #10, #27, #29.

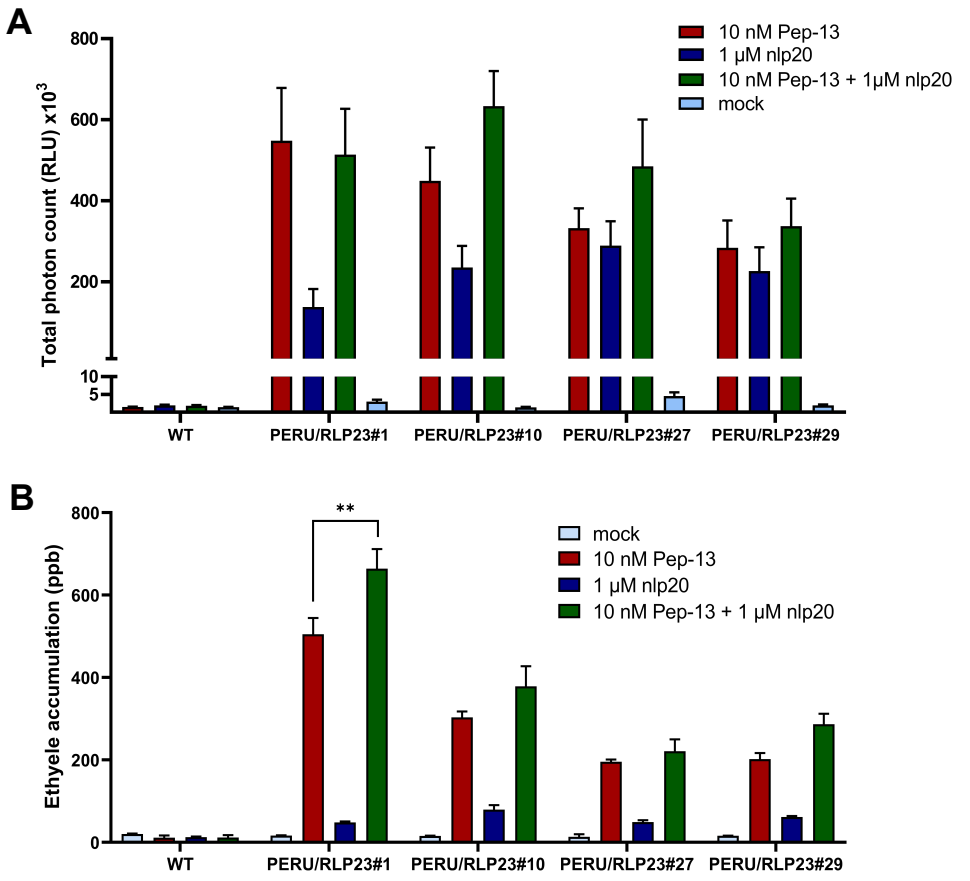

Figure 2. **Early immune responses in PERU/RLP23 double transformants treated with Pep-13, nlp20, and Pep-13+nlp20**. Leaf discs from four PERU/RLP23 double transformants were selected and treated with 10 nM Pep-13, 1 µM nlp20 and 10 nM Pep-13 + 1 µM nlp20 at the same time. **A.** ROS burst was measured, and the total photon count is shown. An additive effect was observed in the PERU/RLP23 transformants #10, #27 and #29. **B.** The ethylene production was measured, and a significantly higher production was found in PERU/RLP23 #1 in presence of 10 nM Pep-13 and 1µM nlp20 compared to the treatment with single peptides. One-way ANOVA was performed to analyze significant differences between treatments (**$P \leq 0.01$).

Furthermore, we noticed that the treatment of the double transformants with both peptides produced a change in the shape of the ROS burst curve, it showed two phases instead of one, that resembles the junction of curves produced by Pep-13 and nlp20 individually (Fig. 3). To verify that the additive effect is result of the specific recognition of the peptides by their respective receptor, we used the single transformants as controls and treated them with 10 nM Pep-13 and 1 µM nlp20,

separately and together. In general, we found that the treatment of single transformants with both peptides, produces no accumulative effect on ROS burst (fig. S3), as expected. Only for PERU #11, we found a minor, not significant increase in ROS when the leaf discs were treated with Pep-13 and nlp20, possibly attributable to variations in the sampled leaves. Besides, the single transformants treated with both Pep-13 and nlp20, showed a normal ROS curve, with only one phase and no changes in shape were observed (fig. S4). Altogether, these results indicate that the stacking of PERU and RLP23 have a small additive but not synergistic effect on the early immune responses like ROS burst and ethylene accumulation.

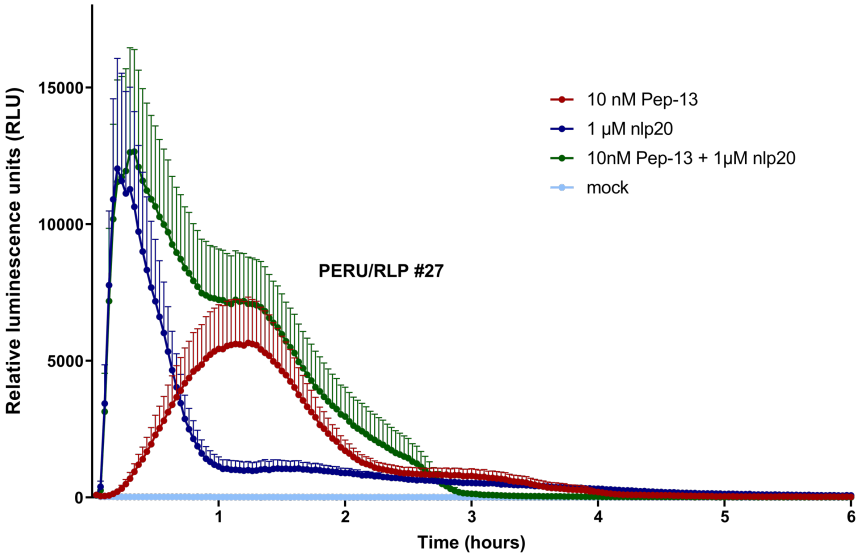

Figure 3. Biphasic ROS curves in PERU/RLP23 double transformant plants. ROS production in transformant PERU/RLP23 #27 treated with Pep-13, nlp20, Pep-13+nlp20, and water (mock). A biphasic curve is produced upon treatment with both Pep-13+nlp20 peptides.

Transformation of individual PRRs has been successfully applied to generate more resistant crops to diseases, although a rather modest level of quantitative resistance is achieved against late blight in potato [21, 29, 32]. We investigated if the stacking of the PRRs *PERU* and *RLP23* in potato can provide a stronger resistance to *P. infestans*. An infection assay was performed as previously described [33], using the WT potato cultivar Atlantic, two single transformant lines per gene (PERU #10, #11, RLP #1, #4), and two double transformant lines (PERU/RLP23 #27, #29). Five plants per genotype, and three compound leaves per plant were spot-inoculated with the highly aggressive *P. infestans* isolate Dinteloord under controlled conditions, and the lesion sizes were measured at 3, 4 and 5 dpi. We observed that *PERU* and *RLP23* contribute

to the resistance against *P. infestans*, in line with previously reported findings [26, 29]. The lines overexpressing one PRR or both PRRs are less susceptible to *P. infestans* compared to the WT line, and they showed significant smaller lesion sizes at the three time-points of evaluation (3, 4 and 5 dpi) ($P<0.05$) (Fig. 4A). The double transformants showed smaller lesions compared to the single transformants at 3dpi, which may indicate that the stacking of the PRRs has a small additive effect on the resistance against *P. infestans* (Fig. 4A). Representative leaves displaying this effect are shown in Fig 4B. At 3 dpi, PERU/RLP23 #29 showed significant smaller lesions, and PERU/RLP23 #27 also showed significant smaller lesions than the single transformants, except for RLP23 #4. At 4dpi, PERU/RLP23 #29 still showed significant differences when compared to the single transformants except for to RLP23 #4, while PERU/RLP23 #27 showed significant smaller lesions compared to PERU #11 and RLP #1. Finally, at 5dpi PERU/RLP23 #29 showed significant smaller lesions compared to PERU #11 and RLP23 #1 only, and PERU/RLP23 #27 showed significant smaller lesions compared to PERU #10,11 and RLP #1. These results suggest a potential role of PRRs stacking to increase resistance to *Phytophthora infestans*.

In this study, we hypothesized that the stacking of PRRs could provide more robust resistance to potato against *P. infestans*, an approach that has not been reported so far. We observed that PERU and RLP23 cooperate during early PTI responses like ROS burst and ethylene accumulation upon oomycete patterns treatment (Pep-13 and nlp20), to ultimately slightly enhance the resistance to *P. infestans* infection. Increasing the number of replicates is likely to strengthen the statistical support for our findings.

Additive effects of other PAMPs, elf18 and flg22, on the extracellular alkalinization, were reported previously for Arabidopsis cells, when the peptides were used at non-saturating doses (0.03 nM or 0.06 nM), but not at saturating doses (100 nM or 200 nM) [34]. Additive effect of 1 nM flg22 and 10 nM elf18 on the plasma membrane depolarization was reported as well [35]. In another study, the combined use of different PAMPs showed that certain combinations have additive effect or synergistic effect, while other combinations mutually suppress [36]. The combination of flg22 + elf18, flg22 + LOS (lipo-oligosaccharides from *Xanthomonas campestris* pv. *campestris*), flg22 + core oligosaccharides (also from *X. campestris* pv. *campestris*), and LOS + core oligosaccharides showed a significant increase of calcium ion influx compared to the individual PAMPs, and remarkably flg22 + LOS combination seemed to be synergistic [36]. However, combination of flg22 and oligogalacturonan (OGA) showed a reduced calcium ion influx and ROS burst, compared to the response to flg22 alone. Therefore, for an effective use of PRRs, different combinations of their corresponding PAMPs should be evaluated, to determine if they have an additive, synergistic or antagonistic effect.

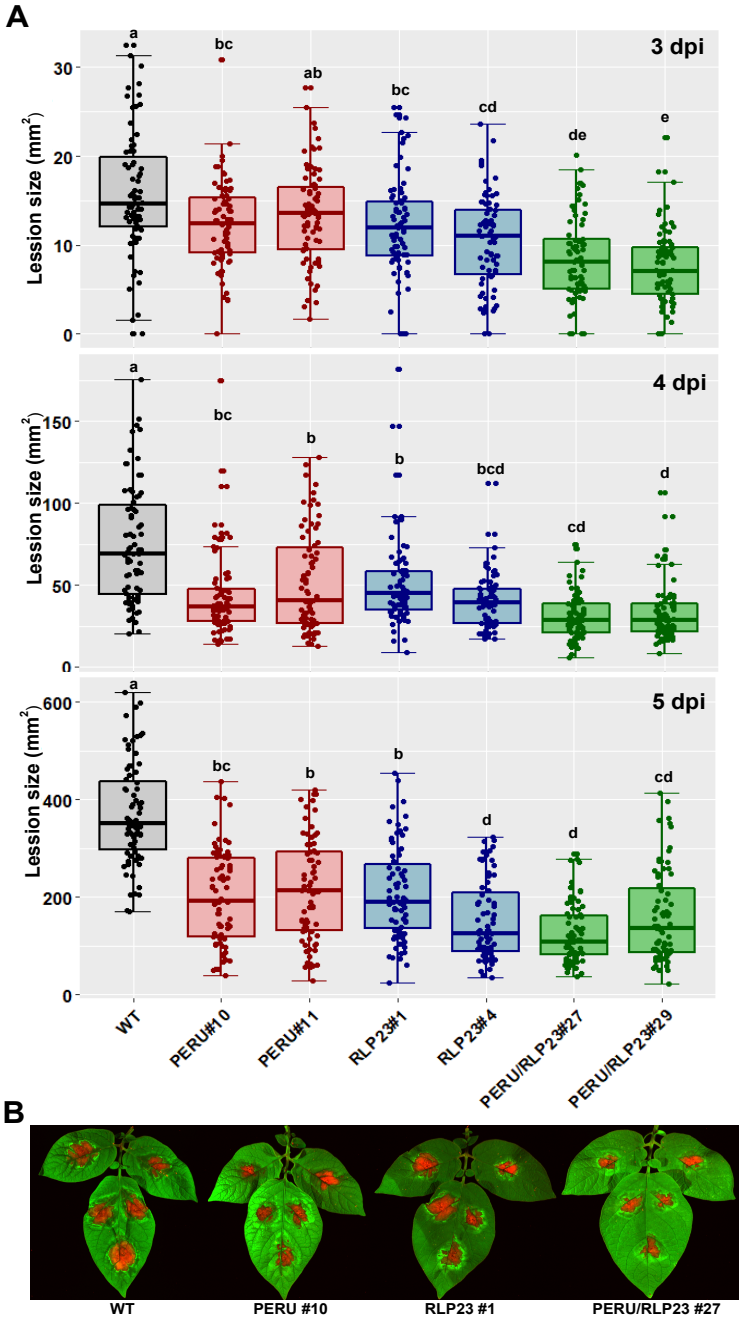

Figure 4. **Stacked PRRs have a positive effect on *Phytophthora infestans* resistance**. **A.** Leaves of intact potato plants were spot-inoculated with the oomycete *P. infestans*, strain Dinteloord, and lesion sizes (mm²) were determined at 3, 4 and 5 dpi **B.** Representative leaves at 4 dpi are shown for Atlantic control (WT), Atlantic-PERU #10, Atlantic-RLP23 #1 and Atlantic PERU/RLP23 #27.

Various stacking strategies involving PRRs can be deployed in crops to increase resistance against pathogens. For example, in potato, a PRR and a QTL have been stacked; *EFR* from *A. thaliana* were transferred into a commercial potato line, in which quantitative resistance has been introgressed from *S. commersoni*, showing that *EFR* expression and quantitative resistance have a significant additive effect on the resistance to bacterial wilt caused by *Ralstonia solanacearum* [37]. Secondly, the stacking of PRRs and NLRs, transgenic tomato lines were generated using *Bs2*, an NLR from *Capsicum annuum* for resistance to *Xanthomonas* spp.*,* and *EFR*. As a result, the expression of both genes significantly reduced bacterial incidence and increased the yield [38]. Remarkably, recent studies have shown that PRRs are required by NLR-mediated immunity, NLR-signaling components are required by PRR-mediated immunity, and that these two layers of immunity potentiate mutually [39-42]. Besides this functional relationship, an evolutionary correlation of the number of PRRs and NLRs across plants was revealed [43], which likely implies that PRRs and NLRs are interdependent and that operate synergistically to provide strong immune responses against pathogens. These findings suggests that the transfer of PRRs combined with NLRs is a promising strategy to combat diseases.

Other known PRRs involved in oomycetes recognition could be useful in future experiments, like ELICITIN RECEPTOR (ELR) (from the wild potato species *Solanum microdontum*) or RESPONSE TO ELICITIN (REL) (from *Nicotiana benthamiana*) that mediate the recognition of various elicitins from *Phytophthora* species [32, 44], like RXEG (from *Nicotiana benthamiana*) that recognizes XEG1 of *P. sojae* [45], or RDA2 (from *A. thaliana*) that recognizes 9-methyl sphingoid base from *P. infestans* [46]. Furthermore, several well-known MAMPs and apoplastic effectors from *Phytophthora* remain orphan and their corresponding PRRs are yet unknown, such as CBEL, PcF, SCR74, SCR91, among others [47, 48]. Despite the need of further research, our results are promising and suggest that PRR stacking could be a valuable tool in the battle against *Phytophthora infestans* and other plant pathogens.

Acknowledgements

This work was supported by the Peruvian Council for science, technology and technological innovation (CONCYTEC) and FONDECYT contract 129-2017 (YCTA). We thank Dirk Jan Huigen for assistance in the greenhouse, Harm Wiegersma and Henk Smid for excellent plant care, Geert Kessel for providing *P. infestans* isolate Dinteloord, and Aviv Andriani for providing advice on disease tests.

References

1. FAO. *FAOSTAT Statistical Database*. 2022 17-03-2022]; Available from: https://www.fao.org/faostat/en/#data/QCL.
2. Haverkort, A.J., et al., *Applied Biotechnology to Combat Late Blight in Potato Caused by Phytophthora Infestans.* Potato Research, 2009. 52(3): p. 249-264.
3. Fry, W., *Phytophthora infestans: the plant (and R gene) destroyer.* Molecular Plant Pathology, 2008. 9(3): p. 385-402.
4. Vleeshouwers, V.G.A.A., et al., *Understanding and Exploiting Late Blight Resistance in the Age of Effectors.* Annual Review of Phytopathology, 2011. 49(1): p. 507-531.
5. Haas, B.J., et al., *Genome sequence and analysis of the Irish potato famine pathogen Phytophthora infestans.* Nature, 2009. 461(7262): p. 393-398.
6. Jones, J.D.G. and J.L. Dangl, *The plant immune system.* Nature, 2006. 444(7117): p. 323-329.
7. Paluchowska, P., J. Śliwka, and Z. Yin, *Late blight resistance genes in potato breeding.* Planta, 2022. 255(6): p. 127.
8. Vossen, J.H., et al., *The Solanum demissum R8 late blight resistance gene is an Sw-5 homologue that has been deployed worldwide in late blight resistant varieties.* Theoretical and Applied Genetics, 2016. 129(9): p. 1785-1796.
9. Dong, S.-m. and S.-q. Zhou, *Potato late blight caused by Phytophthora infestans: From molecular interactions to integrated management strategies.* Journal of Integrative Agriculture, 2022. 21(12): p. 3456-3466.
10. Witek, K., et al., *A complex resistance locus in Solanum americanum recognizes a conserved Phytophthora effector.* Nature Plants, 2021. 7(2): p. 198-208.
11. Zhu, S., et al., *Functional stacking of three resistance genes against Phytophthora infestans in potato.* Transgenic Research, 2012. 21(1): p. 89-99.
12. Haesaert, G., et al., *Transformation of the potato variety Desiree with single or multiple resistance genes increases resistance to late blight under field conditions.* Crop Protection, 2015. 77: p. 163-175.
13. Ghislain, M., et al., *Stacking three late blight resistance genes from wild species directly into African highland potato varieties confers complete field resistance to local blight races.* Plant Biotechnology Journal, 2019. 17(6): p. 1119-1129.
14. Rietman, H., et al., *Qualitative and Quantitative Late Blight Resistance in the Potato Cultivar Sarpo Mira Is Determined by the Perception of Five Distinct RXLR Effectors.* Molecular Plant-Microbe Interactions®, 2012. 25(7): p. 910-919.
15. Luo, M., et al., *A five-transgene cassette confers broad-spectrum resistance to a fungal rust pathogen in wheat.* Nature Biotechnology, 2021. 39(5): p. 561-566.
16. Couto, D. and C. Zipfel, *Regulation of pattern recognition receptor signalling in plants.* Nature Reviews Immunology, 2016. 16(9): p. 537-552.
17. Nürnberger, T. and B. Kemmerling, *Chapter 1 PAMP-Triggered Basal Immunity in Plants*, in *Advances in Botanical Research*. 2009, Academic Press. p. 1-38.
18. Thomma, B.P.H.J., T. Nürnberger, and M.H.A.J. Joosten, *Of PAMPs and Effectors: The Blurred PTI-ETI Dichotomy.* The Plant Cell, 2011. 23(1): p. 4-15.
19. Du, J. and V.G.A.A. Vleeshouwers, *New Strategies Towards Durable Late Blight Resistance in Potato*, in *The Potato Genome*, S. Kumar Chakrabarti, C. Xie, and J. Kumar Tiwari, Editors. 2017, Springer International Publishing: Cham. p. 161-169.
20. Wan, W.-L., et al., *Plant cell surface immune receptor complex signaling.* Current Opinion in Plant Biology, 2019. 50: p. 18-28.
21. Lacombe, S., et al., *Interfamily transfer of a plant pattern-recognition receptor confers broad-spectrum bacterial resistance.* Nature Biotechnology, 2010. 28(4): p. 365-369.

22. Nürnberger, T., et al., *High affinity binding of a fungal oligopeptide elicitor to parsley plasma membranes triggers multiple defense responses.* Cell, 1994. 78(3): p. 449-460.
23. Brunner, F., et al., *Pep-13, a plant defense-inducing pathogen-associated pattern from Phytophthora transglutaminases.* The EMBO Journal, 2002. 21(24): p. 6681-6688.
24. Halim, V.A., et al., *The oligopeptide elicitor Pep-13 induces salicylic acid-dependent and -independent defense reactions in potato.* Physiological and Molecular Plant Pathology, 2004. 64(6): p. 311-318.
25. Halim, V.A., et al., *PAMP-induced defense responses in potato require both salicylic acid and jasmonic acid.* The Plant Journal, 2009. 57(2): p. 230-242.
26. Torres Ascurra, Y.C., et al., *Functional diversification of a wild potato immune receptor at its center of origin.* Science, 2023. 381(6660): p. 891-897.
27. Gijzen, M. and T. Nürnberger, *Nep1-like proteins from plant pathogens: Recruitment and diversification of the NPP1 domain across taxa.* Phytochemistry, 2006. 67(16): p. 1800-1807.
28. Böhm, H., et al., *A Conserved Peptide Pattern from a Widespread Microbial Virulence Factor Triggers Pattern-Induced Immunity in Arabidopsis.* PLOS Pathogens, 2014. 10(11): p. e1004491.
29. Albert, I., et al., *An RLP23–SOBIR1–BAK1 complex mediates NLP-triggered immunity.* Nature Plants, 2015. 1(10): p. 15140.
30. Torres Ascurra, Y.C., et al., *Functional diversification of a wild potato PRR immune receptor at its center of origin.* Manuscript submitted for publication, 2023.
31. Boller, T. and G. Felix, *A Renaissance of Elicitors: Perception of Microbe-Associated Molecular Patterns and Danger Signals by Pattern-Recognition Receptors.* Annual Review of Plant Biology, 2009. 60(1): p. 379-406.
32. Du, J., et al., *Elicitin recognition confers enhanced resistance to Phytophthora infestans in potato.* Nature Plants, 2015. 1(4): p. 15034.
33. Vleeshouwers, V.G.A.A., et al., *A Laboratory Assay for Phytophthora infestans Resistance in Various Solanum Species Reflects the Field Situation.* European Journal of Plant Pathology, 1999. 105(3): p. 241-250.
34. Zipfel, C., et al., *Perception of the Bacterial PAMP EF-Tu by the Receptor EFR Restricts Agrobacterium-Mediated Transformation.* Cell, 2006. 125(4): p. 749-760.
35. Jeworutzki, E., et al., *Early signaling through the Arabidopsis pattern recognition receptors FLS2 and EFR involves Ca2+-associated opening of plasma membrane anion channels.* The Plant Journal, 2010. 62(3): p. 367-378.
36. ASLAM, S.N., et al., *Microbe-associated molecular pattern (MAMP) signatures, synergy, size and charge: influences on perception or mobility and host defence responses.* Molecular Plant Pathology, 2009. 10(3): p. 375-387.
37. Boschi, F., et al., *Enhanced bacterial wilt resistance in potato through expression of arabidopsis efr and introgression of quantitative resistance from solanum commersonii.* Frontiers in Plant Science, 2017. 8.
38. Kunwar, S., et al., *Transgenic Expression of EFR and Bs2 Genes for Field Management of Bacterial Wilt and Bacterial Spot of Tomato.* Phytopathology®, 2018. 108(12): p. 1402-1411.
39. Ngou, B.P.M., et al., *Mutual potentiation of plant immunity by cell-surface and intracellular receptors.* Nature, 2021. 592(7852): p. 110-115.
40. Yuan, M., et al., *Pattern-recognition receptors are required for NLR-mediated plant immunity.* Nature, 2021. 592(7852): p. 105-109.
41. Pruitt, R.N., et al., *The EDS1–PAD4–ADR1 node mediates Arabidopsis pattern-triggered immunity.* Nature, 2021. 598(7881): p. 495-499.
42. Tian, H., et al., *Activation of TIR signalling boosts pattern-triggered immunity.* Nature, 2021. 598(7881): p. 500-503.
43. Ngou, B.P.M., et al., *Concerted expansion and contraction of immune receptor gene repertoires in plant genomes.* Nature Plants, 2022. 8(10): p. 1146-1152.

44. Chen, Z., et al., *Convergent evolution of immune receptors underpins distinct elicitin recognition in closely related Solanaceous plants.* The Plant Cell, 2023.
45. Wang, Y., et al., *Leucine-rich repeat receptor-like gene screen reveals that Nicotiana RXEG1 regulates glycoside hydrolase 12 MAMP detection.* Nature Communications, 2018. 9(1): p. 594.
46. Kato, H., et al., *Pathogen-derived 9-methyl sphingoid base is perceived by a lectin receptor kinase in Arabidopsis.* bioRxiv, 2021: p. 2021.10.18.464766.
47. Lin, X., et al., *Divergent Evolution of PcF/SCR74 Effectors in Oomycetes Is Associated with Distinct Recognition Patterns in Solanaceous Plants.* mBio, 2020. 11(3): p. e00947-20.
48. Gaulin, E., et al., *Cellulose Binding Domains of a Phytophthora Cell Wall Protein Are Novel Pathogen-Associated Molecular Patterns.* The Plant Cell, 2006. 18(7): p. 1766-1777.
49. Visser, R.G.F., *Regeneration and transformation of potato by Agrobacterium tumefaciens*, in *Plant Tissue Culture Manual: Supplement 7*, K. Lindsey, Editor. 1997, Springer Netherlands: Dordrecht. p. 301-309.

Supplementary information

Materials and Methods

Plant materials. Potato plants were maintained and clonally propagated in vitro on MS medium supplemented with 20% sucrose at 25 °C. For experiments, 2 weeks old plantlets were transferred to sterilized soil and grown in regulated greenhouse compartments at 18-22 °C, 16h/8h day/night regime and 70% relative humidity.

Peptides and protein. Peptides were synthesized by Genscript USA Inc, prepared as 1mM stock solutions in (DMSO), and diluted in MilliQ water or sterile tap water before use. We used nlp20 from *Phytophthora parasitica* (AIMYSWYFPKDSPVTGLGHR) and Pep-13 from *P. sojae* (VWNQPVRGFKVYE).

Constructs and stable transformation. *PERU* was cloned in pK7WG2 under the 35S promotor, and *RLP23* was cloned in pB7WG2 [29]. Stable transformation of potato cultivar Atlantic was carried out using routine potato transformation protocols [49]. To generate the single transformants, potato internodes were co-cultivated with *Agrobacterium tumefaciens* AGL1 contained the specific construct. The explants were transferred to a regeneration medium with 100 mg/L kanamycin or 2mg/L phosphinothricin (PPT, glufosinate ammonium) as selection agent. To obtain the double transgenic lines, potato internodes were co-transformed with the two *A. tumefaciens* cultures, and the explants were transferred to a regeneration medium with 100 mg/L kanamycin and 2mg/L PPT. The regenerants were genotyped using specific primers targeting *virG*, selection marker, *35S*, *PERU* and *RLP23*. Subsequently, the plants were phenotyped by ROS to test the response conferred by *PERU* or *RLP23*.

Measurement of ethylene accumulation. Leaves of 4-week old potato plants were cut in round pieces (6.0 mm diameter) and floated in MilliQ water overnight. Four leaf pieces were incubated in sealed 10 ml vials containing 0.6 mL 20 mM MES buffer, pH5.6 and the indicated elicitor. Ethylene accumulation was measured after 4 hours of incubation by gas chromatographic analysis (TraceGC1300 (InterScience, Breda, NL) coupled with a flame ionization detector) of 3.5 mL of the air drawn from the closed vial with a syringe. At least, three replicates were measured for each treatment.

Measurement of ROS production. Leaves of 4-week-old potato plants were cut in round pieces (6.0 mm diameter), placed in 96 well white plate containing 50 µL of MilliQ water, and incubated overnight. Water was removed and replaced with 50 µL of new MilliQ water. After that, 50 µL of a solution containing 10 µg horseradish peroxidase, 50 µM luminol L-012, and the desired elicitor. Luminescence was

measured using a CLARIOstar plate reader (BMG LABTECH) over a period of at least 3 hours.

***Phytophthora infestans* infection assay.** Disease tests were performed as previously described [32]. In brief, *P. infestans* isolate Dinteloord from our in-house collection was grown on rye agar medium supplemented with 20 g/L sucrose at 18 °C in the dark. To obtain zoospores, the mycelium was flooded with cold water (4 °C), the suspension was transferred to a new tube and incubated at 4 °C for approximately 2 hours. The number of zoospores was counted and adjusted to $5x10^4$ zoospores/mL for inoculation. Intact, four-weeks-old plants of potato cv. Atlantic WT along with two single transformants expressing *PERU*, two single transformants expressing *RLP23,* two double transformants expressing *PERU* and *RLP23* were spot-inoculated with zoospore suspensions. Five plants per genotype, and third to fifth fully developed leaves (counted from the top) were used. Three leaflets per compound leaf were inoculated (three spots per main leaflet, and one spot per other small leaflets) by pipetting 10 µl droplets on the abaxial side. Lesion diameters were measured at 3, 4 and 5 dpi. The experiment was performed twice.

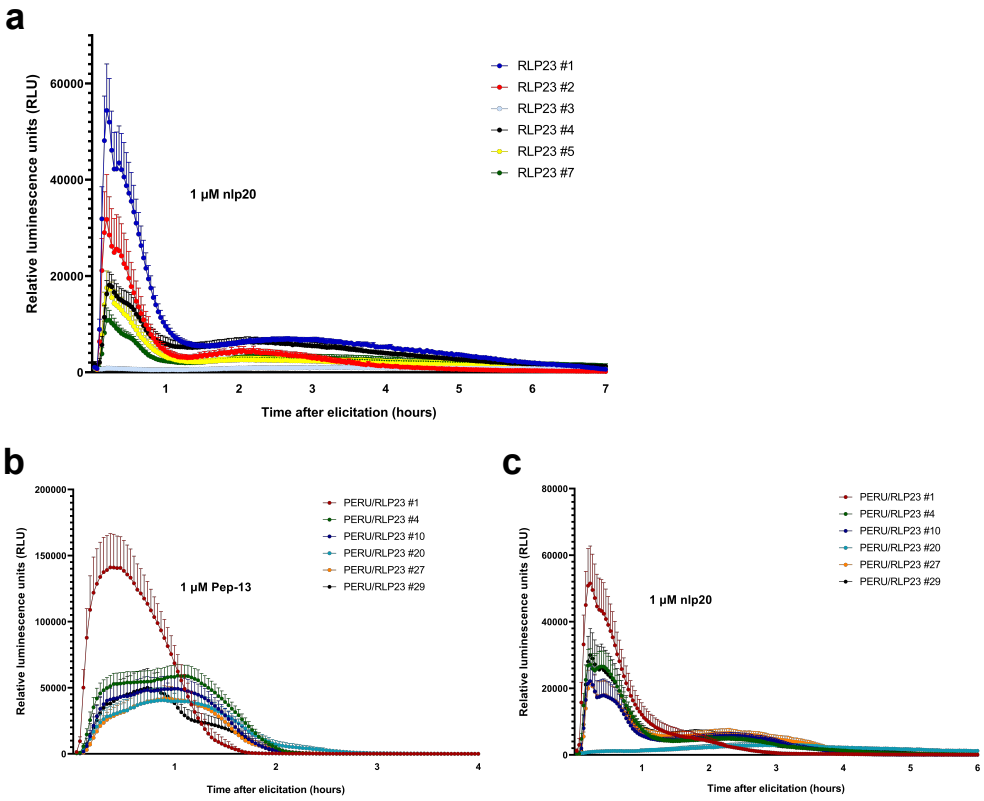

Supplementary figure 1. **Stacking of *PERU* and *RLP23* in potato**. **a.** ROS production for single transformants of potato cultivar Atlantic treated with nlp20. Six transgenic lines were treated with 1 µM nlp20, the line RLP23 #3 was genotyped negative by PCR and included here as a control. Five transgenic lines positives for RLP23 presence were identified: RLP23 #1, #2, #4, #5, #7. **b.** ROS production in double transformants of potato cultivar Atlantic treated with Pep-13. Six transgenic lines were treated with 1 µM Pep-13, and all resulted positive. **c.** ROS production for double transformants of potato cultivar Atlantic treated with nlp20. Lines were treated with 1 µM nlp20, all lines except PERU/RLP23 #20 resulted positive.

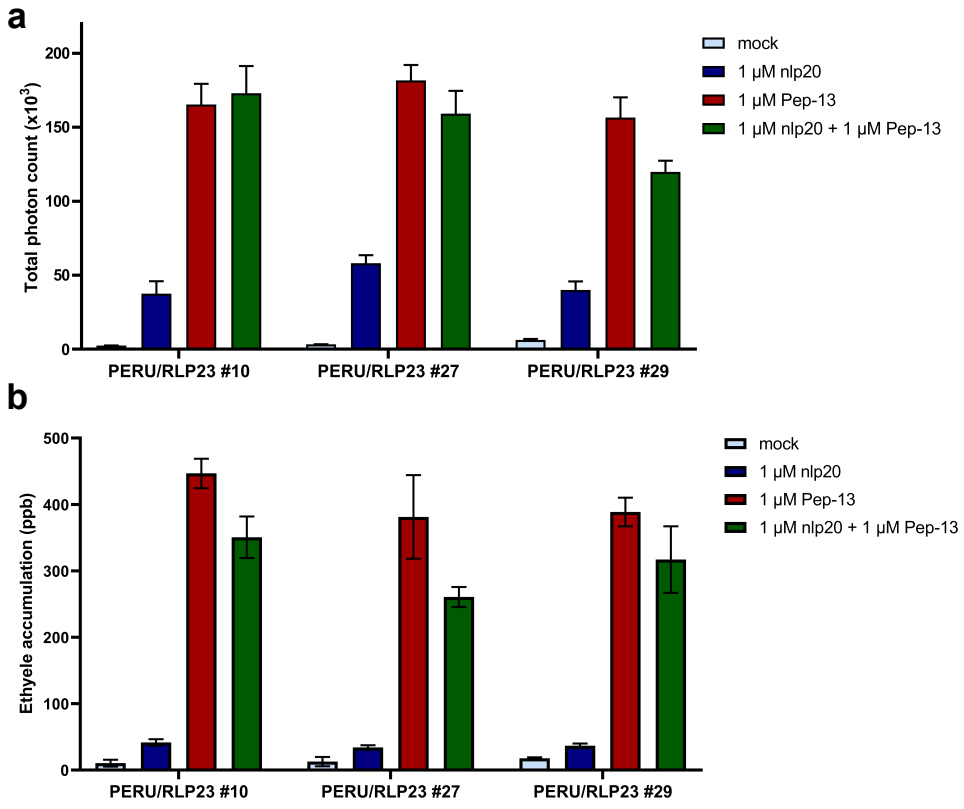

Supplementary figure 2. **Early immune responses to saturating doses of PAMPs in PERU/RLP23 double transformants**. **a.** ROS production and **b.** ethylene accumulation in the double transformants PERU/RLP23 #10, #27 and #29 treated with saturating concentration of patterns (1 µM Pep-13, 1 µM nlp20, and a combination of 1 µM Pep-13 and 1 µM nlp20).

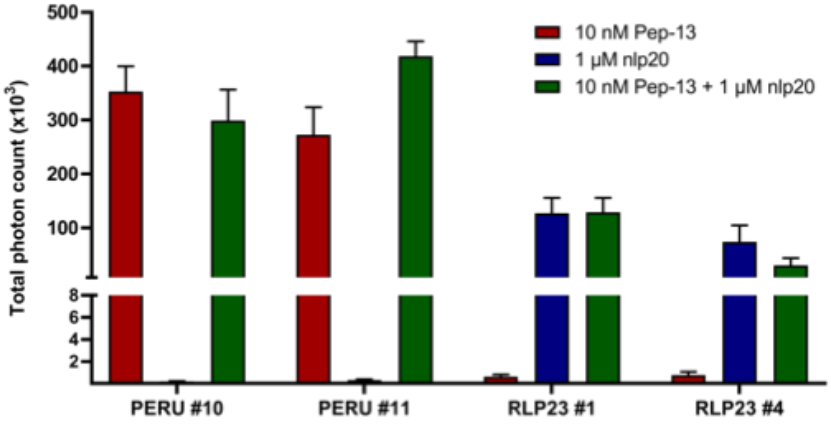

Supplementary figure 3. **ROS production in the single transformants.** Total photon count in PERU #10, PERU #11, RLP23 #1 and RLP23 #4 plants treated with 10 nM Pep13, 1 µM nlp20, or a combination of 10 nM Pep-13 and 1 µM nlp20.

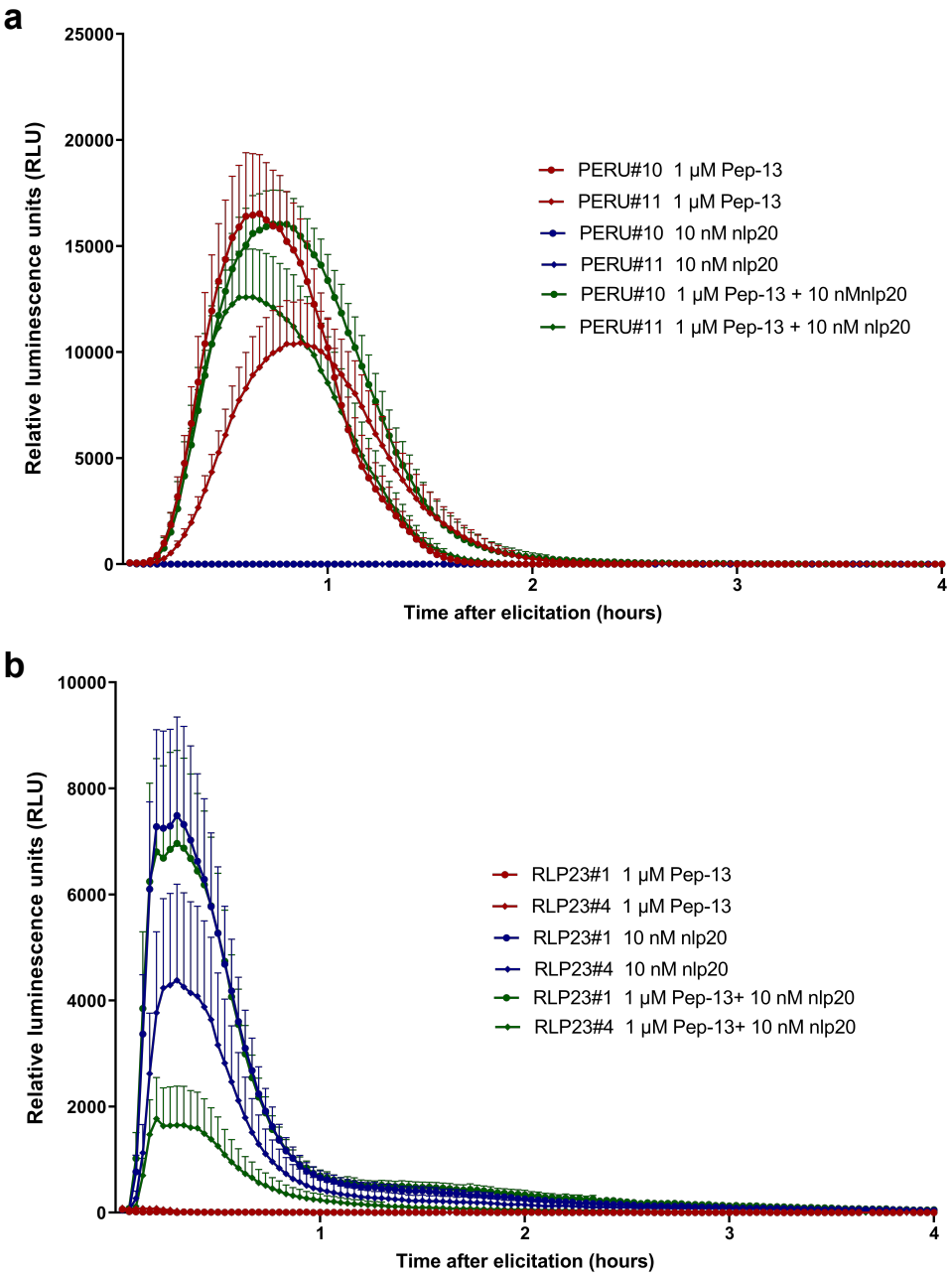

Supplementary figure 4. Curves of ROS burst in the single transformants. a. PERU #10, PERU #11, and **b.** RLP23 #1, RLP23 #4 plants were treated with 10 nM Pep-13, 1 µM nlp20, or a combination of 10 nM Pep-13 and 1 µM nlp20. The measurement of ROS production was conducted over a period of 4 hours.

Supplementary table 1. Sequence of primers used in this study.

Primer name	Sequence 5' ® 3'	Target
pK7-F	CTATTCTAGTCGACCTGCAG	pK7WG2 vector
pK7-R	GAGACTGGTGATTTTTGCGG	pK7WG2 vector
35S-F	TGCTGACCCACAGATGGTTA	CaMV 35S promotor
35S-R	CGGCGAGTTCTGTTAGATCC	CaMV 35S promotor
NPTII-F	GCGTTCAAAAGTCGCCTAAG	nptII (kanamycin resistance)
NPTII-R	AGTGACAACGTCGAGCACAG	nptII (kanamycin resistance)
virG-F1	GCCGACAGCACCCAGTTCAC	virG virulence gene
virG-R1	CCTGCCGTAAGTTTCACCTCACC	virG virulence gene
bar-F	GAGACGTACACGGTCGACTC	Bar gene
bar-R	ACGTTGAAGGAGCCACTGAG	Bar gene
RLP23-F	CATCCCGTTGACCCTGGAAA	RLP23 gene
RLP23-R	AAGAGGCACCATCACAGAGC	RLP23 gene
PERU-F	GGCTCTGTCTACAAAGGCGT	PERU gene
attR-R	CCGCGGGATATCACCACTTT	PERU gene

Supplementary table 2. Constructs used in this study.

Construct	Binary vector	*A. tumefasciens* strains	Reference
PERU	pK7WG2	AGL1	Torres Ascurra et al. 2023
RLP23	pB7WG2	AGL1	Alberts et al. 2015

Chapter 6

General discussion

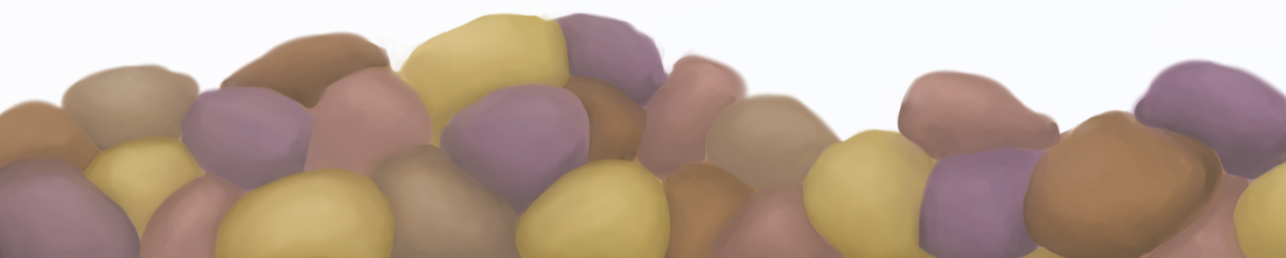

As generally known, potato is susceptible to many pathogens (including fungi, bacteria, viruses, oomycetes and nematodes) that can affect all parts of the plant, leading to compromised quality and diminished yields [1]. Among these, the oomycete *Phytophthora infestans* is the major threat for potato worldwide, causing annual losses of € 9.4 billion [2, 3]. Potato breeding for resistance to *P. infestans* has focused mainly on the use of *Resistance to P. infestans* (*Rpi*) genes, which encode intracellular nucleotide-binding leucine-rich repeat receptors (NLRs) that specifically recognize pathogen effectors and trigger immunity. While *Rpi* genes have shown to confer a robust resistance, their effectiveness has been compromised due to the high evolutionary potential of the pathogen, that results in evasion of recognition [4]. Therefore, it is crucial to explore alternative sources of resistance or even immunity.

Another class of receptors, the pattern recognition receptors (PRRs), that are located at the plant cell surface, typically recognize more conserved pathogen-associated molecular patterns (PAMPs) to initiate the immune response. Notably, unlike NLRs, the PRRs have not been extensively studied nor exploited for potato breeding, emphasizing the need to explore the potential of PRR-mediated immunity in enhancing resistance not only in potato but also in other crops. In this thesis, our primary objective was to clone the elusive receptor of the orphan PAMP, known as Pep-13, which has remained mysterious for almost three decades, and subsequently conduct a comprehensive characterization of this new receptor.

The challenge of cloning immune receptors in potato

To study and exploit a gene in a plant breeding program, it must be identified first. Traditionally, the isolation of new potato *Rpi* genes has followed the map-based cloning strategy, which involves the generation of mapping populations, development of a high number of molecular markers, screening of thousands of recombinant plants and generation of a physical map for the region of interest [5]. Employing this approach, our research group previously cloned various NLRs [6] and the first potato PRR, Elicitin response (ELR) from *Solanum microdontum* MDC360-1 [7]. Despite its effectiveness, the whole process requires several years.

However, recent advancements of new sequencing technologies resulting in a high quality reference potato genome [8], and other potato genomes available to date, are greatly accelerating gene cloning [9, 10]. The combination of bulked segregant analysis (BSA) and RNA-Seq has resulted in an efficient mapping strategy, the so-called bulked segregant RNA-Seq (BSR-Seq) [11]. This strategy not only provides the genetic position for a gene of interest, but it produces a high number of single nucleotide polymorphisms (SNPs) that can be used as molecular markers for further

fine-mapping, and gene expression data that can help to prioritize the candidate genes. BSR-Seq was first applied in maize, to map and clone the *glossy3* (*gl3*) gene [11], and afterwards, it has been applied to other crops. In wheat, it allowed the mapping of a major disease resistance gene, *Yr15*, to a 0.77 cM interval, and the development of molecular markers for breeding programs [12]. In Chinese cabbage, BSR-Seq was applied to map the gene responsible for male sterility, and the region of interest was mapped to a 1.7 Mb region [13].

In potato, the BSR-Seq approach was effectively applied to map the gene responsible for the recognition of the PAMP Pep-13/25 to the top of the chromosome 3 of *Solanum microdontum* subsp. *gigantophyllum* GIG362-6 [14]. The further fine-mapping of the region was facilitated by a high throughput recombinant screening that combines the genotyping of seedlings grown under *in vitro* conditions, and the phenotyping of only the recombinant plants (**Chapters 2 and 3**). However, the lack of a high-quality genome of the wild potato GIG362-6 that carried the Pep-13/25 receptor, impeded the narrowing down of the mapping interval and the final identification of the receptor from this genotype.

Besides BSR-Seq, other approaches have emerged to accelerate gene cloning. The *R* gene enrichment and sequencing (RenSeq) method reduces the genome complexity, enables the capture and sequencing of NB-LRR genes, and was used in potato to increase the number of identified NB-LRRs, from 438 to 755 [15]. The combination of RenSeq and single-molecule real-time (SMRT) sequencing (SMRT RenSeq) allowed the cloning of *Rpi-amr3i*, resistance gene against *P. infestans* from *Solanum americanum*; showing its potential for rapid cloning of *R* genes [16]. RenSeq was also combined with EMS mutagenesis and association genetics to develop MutRenSeq and AgRenSeq respectively. MutRenSeq approach is independent of fine mapping, and led to the rapid cloning of the resistance genes *Sr22* and *Sr45* from hexaploid bread wheat against the stem rust *Puccinia graminis* f.sp. *tritici* [17]; and AgRenSeq used natural genomic variation of a panel of 174 *Aegilops tauschii* lines to clone the stem rust resistance genes *Sr33*, *Sr45* (previously identified by MutRenSeq), *Sr46* and *SrTA1662* [18]. Lastly, the RLP/RLK enrichment sequencing (RLP/KSeq), and adaption of RenSeq to identify PRRs, successfully fine-mapped the SCR74 receptor to a 43-kb interval, in a wild potato [19]. These examples demonstrate the versatility and broad applications of the enrichment sequencing technology. However, it should be noted that this biased approach relies on known gene sequences to develop bait libraries, which may fail to detect atypical immune receptors and other types of resistance that do not rely on receptors [20].

Two functionally linked immunity layers

Plant immunity is traditionally viewed as a two-layers system [21]. The cell surface-located PRRs recognize PAMPs and provide basal immunity to non-adapted pathogens, known as pattern-triggered immunity (PTI) [21]. However, adapted pathogens are able to evade PTI by means of secreted effectors, and in turn plants have evolved intracellular NLRs to recognize the effectors and activate a more robust immunity, the so-called effector-triggered immunity (ETI) [21]. Remarkably, two complementary studies have shown that PRRs are required by NLR-mediated immunity, NLR-signaling components are required by PRR-mediated immunity [22, 23], depicting plant immunity as a unified system, composed of functional interdependent branches that mutually potentiate to provide robust resistance against pathogens [24]. These findings might indicate that combining PRRs and NLRs is a promising strategy for enhancing disease resistance in plants. Furthermore, while the qualitative distinction between PTI/ETI, PRR/NLR, and PAMP/EFFECTOR does aid in conceptualizing plant immunity, these terms should be refined. PTI and ETI appear to function as a unit or exist as a blurred dichotomy, with no clear differences that can be strictly assigned to each [25].

The non-steady pair PAMP-PRR

PAMPs were originally defined as highly conserved molecules within a class of microbes that have an essential function for the organism and therefore difficult to change or mutate [26-28]. PAMPs are recognized by two types of PRRs, receptor-like kinases (RLKs) or receptor-like proteins (RLPs) that lack a kinase domain [29]. It has been shown that some PAMPs evolve undetectable epitopes to avoid host recognition and in turn plant PRRs have diversified to sense these non-steady patterns [30, 31].

The PAMP flg22, a conserved epitope from bacterial flagellin, is detected in *Arabidopsis* by the receptor-like kinase FLAGELLIN SENSING 2 (FLS2) [32, 33]. However, some bacterial species like *Agrobacterium*, *Rhizobium* and *Xanthomonas* have flagellins with divergent flg22 sequences and as a consequence they cannot be recognized as PAMP [34]. For instance, the flg22 epitope of *Agrobacterium tumefaciens* is highly different from standard flg22, and consequently, $flg22^{Atum}$ evades recognition by FLS2 of Arabidopsis. Remarkably, the $flg22^{Atum}$ epitope is sensed in the wild grape species *Vitis riparia* by FLS2XL, which provides sensitivity to typical flg22 as well [35]. Additionally, it has been reported that plant species have evolved to detect other peptides within the bacterial flagellin. For instance, a population genomics analysis of a large collection of *Pseudomonas syringae* pv. tomato revealed a second flagellin epitope, flgII-28 [36], which triggers immune

responses in several Solanaceae, including tomato, potato and pepper [37]. A map-based cloning strategy using natural variation in tomato identified the gene encoding an RLK named FLAGELLIN-SENSING 3 (FLS3) as the receptor of flgII-28 [38]. Lastly, a third epitope in the C-terminal region of flagellin, termed CD2-1, from *Acidovorax avenae* is recognized by an unknown receptor in rice [39]. These studies together show the capacity of adapted pathogens to overcome PTI through PAMP diversification, and how hosts evolve novel immunoreceptors to detect them.

The Pep-13 receptor

The PAMP Pep-13, first identified within the glycoprotein GP42 of *Phytophthora sojae* [40], was considered a highly conserved PAMP only encountered in oomycetes [41]. In **Chapter 3**, we screened public databases and interestingly detected polymorphism in the PAMP Pep-13/25 within transglutaminases from *P. infestans* as well as across other oomycetes and fungi species. To study the plant side, Pep-25-sensitive wild *Solanum* genotypes were tested with natural polymorphic versions of Pep-25 and a diverse profile of responses was found, which indicates that these genotypes harbor yet unknown Pep-25 receptors with different ligand specificity. These results indicate on the one hand, that Pep-13/25 is more polymorphic and is present in other kingdoms, such as fungi. On the other hand, they suggest that the Pep-13/25 receptor has also diversified in *Solanum* genotypes. However, it is important to note that these results are preliminary and only provide a glimpse of the overall scenario. To ascertain the actual extent of diversification in Pep-13, a more extensive and meticulous search should be conducted. Similarly, additional representative genotypes from the *Solanum* section *Petota* should be tested. Furthermore, it is worth exploring the immunogenic characteristics of other regions within *Phytophthora* GP42-related proteins, as these aspects remain unexplored.

In **Chapter 4,** we aimed to identify and study the Pep-13 receptor. Fortunately, the doubled monoploid and *de novo* sequenced potato *S. tuberosum* Group Phureja DM 1-3 516 R44 (DM) showed responsive to Pep-13, indicating the presence of the Pep-13 receptor. Consequently, we opted to switch the mapping population, design a high number of new molecular markers to cover the region, and utilize the recently developed long-read chromosome-scale genome assembly (v6.1) of DM [8]. This updated genome assembly revealed the sequence of the previous unannotated fragments in the region, filling in the gaps. Through these steps, we successfully narrowed the mapping interval to 55.2 kb, and identified three candidate LRR-RLKs. Transient expression assays of the candidate genes pinpointed the specific receptor of Pep-13, designated as the ***Pe****p-13* ***R****eceptor* ***U****nit* (*PERU*). Stable expression of PERU in Pep-13-insensitive potato cultivar Atlantic and inactivation of the *PERU* locus in Pep-

13-sensitive DM by CRISPR-Cas9 mutagenesis corroborated the role of PERU for the recognition of Pep-13.

The PERU protein contains a signal peptide for secretion, an extracellular LRR domain, that consists of 27 repeats, and an intracellular Ser/Thr kinase domain. The *in vitro* ligand binding assays indicated that the PERU ectodomain is sufficient for ligand binding. The use of Pep-13 and a biologically inactive Pep-13 mutant peptide, Pep-13W231A [41], as competitor, *in planta* assays, demonstrated the specific binding of Pep-13 to its high-affinity receptor, PERU. Besides, we demonstrated that PERU and SERKA form a complex upon Pep-13 binding, and as expected SOBIR1 is not required by this complex (Fig 1A). The sites on PERU required for interaction with its ligand Pep-13 or to SERK3A remain to be identified.

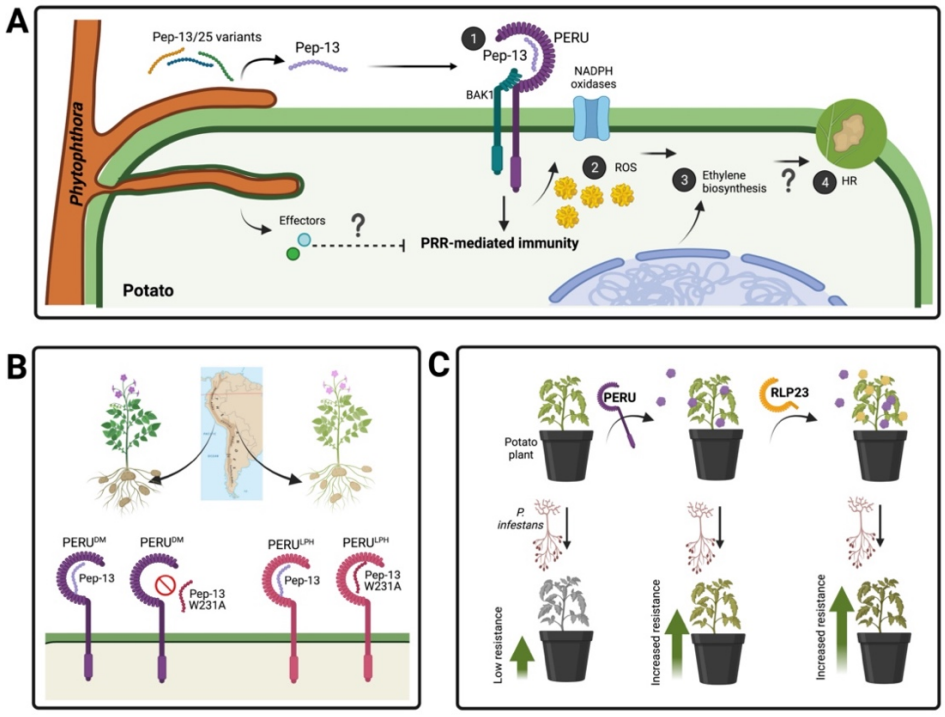

Figure 1. Overview of the findings of this thesis. A. (1) Pep-13 is recognized by the potato LRR-RLK. PERU. The PERU-BAK1 receptor complex formation upon Pep-13 binding activates the signaling cascade resulting in PRR-based immunity. (2) PTI responses includes ROS burst, (3) ethylene accumulation and (4) hypersensitive cell death. B. *Solanum leptophyes* (LPH) 680-5, showed sensitivity to all Pep-25 variants tested, including the inactive Pep-13W231A. DM in contrast showed insensitive to Pep-13W231A. The geographical information of the genotypes indicates that the functional diversification of this related PRRs has occurred in the Andes region. C. PERU transfer to a Pep-13-insensitive potato cultivar increased its resistance against *P. infestans*. The

stacking of PERU and RLP23 improved early immune responses, and slightly enhances the resistance against *P. infestans*. This figure was created with Biorender.

Functional diversification of PRRs

Previous studies in parsley and in leaves of the potato cultivar Désirée, revealed that mutant Pep-13W231A abolished elicitor activity, mutation of proline 234 (Pep-13P234A) reduced it, and replacement of the remaining amino acid residues (including tyrosine 241, Pep-13Y241A) did not significantly affect activities of the mutant peptides [40, 41]. In **Chapter 4**, we found the same pattern of ligand responses in the Pep-25-sensitive genotype DM, which was used for PERU identification. To explore the pattern of ligand responses in the *Solanum* tuber-bearing species, 476 genotypes corresponding to 98 species (97 wild, and 1 cultivated potato species) were tested for cell death triggered by Pep-25 and its three described mutant variants [41]. Most genotypes showed no response to the tested peptide, indicating a lack of responsive *PERU* alleles. These non-responsive genotypes belong to species classified in nuclear clades 1 and 3 [42]. On the other hand, the 126 Pep-25-sensitive genotypes mainly correspond to species classified in the nuclear clade 4 or "complex", with the exception of *S. acroglossum* which belongs to clade 3 [42]. Interestingly, at least five different recognition specificities were detected within the Pep-25-sensitive genotypes, indicating that *Solanum* tuber-bearing species bear diverse PERU alleles encoding PRRs with distinct ligand specificities (**Chapter 4**).

Remarkably, some genotypes, such as *Solanum leptophyes* (LPH) 680-5, showed sensitivity to all Pep-25 variants tested. So, the defense responses (i.e., cell death upon peptide infiltrations and ethylene accumulation) were explored further in DM and LPH plants, confirming that effectively LPH harbors different sensitivity compared to DM. To exclude background effects on the ligand specificity, we cloned the LPH allele (*PERU*^{LPH}). The transient expression of *PERU*^{DM} and *PERU*^{LPH} in an amenable genotype for agroinfiltration, *Solanum hjertingii* HJT349-3, corroborated the previous findings. Additionally, the receptor-ligand binding assays showed that PERU^{LPH} binds both Pep-25-bio and Pep-25W231A-bio, and likewise, an excess of Pep-13W231A efficiently blocks ligand binding to PERU^{LPH}. These results clearly demonstrated that these two related PERU receptors have diversified in ligand specificities within closely related species (**Fig. 1B).**

While the residue W231 is found conserved in known *Phytophthora* transglutaminase sequences (**Chapter 3**), the possibility of a mutation occurring at this residue cannot be ruled out. Consequently, we can presume that functional diversification of PERU was driven by escape mutations within *Phytophthora* Pep-13 patterns that enable Pep-13-producing pathogen strains to elude recognition by the predominant allele, PERU^{DM}, and some *Solanum* species have evolved diverse alleles, like *PERU*^{LPH}, to

recognize evasive patterns. However, to clearly understand the co-evolution of the *Solanum* PERU and *Phytophthora* Pep-13, a screening of *Solanum* tuber-bearing species for sensitivity to natural variants of Pep-13 (**Chapter 3**) should be further expanded. High-throughput genome sequencing or LRR-RLKs-enriched sequencing of responsive genotypes, and non-responsive genotypes, and the subsequent bioinformatic analysis would facilitate the isolation of more *PERU* alleles, crucial information for a deeper understanding of the PERU evolutionary history.

To disclose the evolutionary history of PERU, in **Chapter 4**, we performed a phylogenomic analysis. A computational pipeline allowed the extraction of PERU sequences from a huge number of proteins predicted from 124 Solanaceae genome assemblies. FLS2 sequences were also obtained for comparison purposes. The phylogenomic analysis identified 114 PERU homologs from 17 species, clustered the PERU and FLS2 clades in the LRR-RK subgroup XII, and indicated a monophyletic origin of PERU within the Solanaceae. Additionally, we observed that the PERU receptor sequences are clearly much more diverse than the FLS2 receptor sequences. Subsequently, the obtained PERU sequences were combined with responsive and 25 non-responsive cloned homologs sequences, and subjected to phylogenetic analysis. Interestingly, the responsive PERU alleles fall into one clade whereas the non-responsive alleles are dispersed along the tree.

The phylogenomic results corroborated the findings of our previously mentioned big screening. For instance, sequences from and more related to the 'responsive' clade originate mainly from species of the Tuberosa series but also from the Piurana series, which have now been assigned to clades 3 and 4, respectively, but not from Mexican diploids, non-tuber bearing *Solanum* nor tomato species. These findings are consistent with the results obtained from the screening, in which we found no recognition in the *S. bulbocastanum* , *S. cardiophyllum, S. lesteri, S. michoacanum, S. morelliforme, S. pinnatisectum, S. polyadenium, S. tarnii* or *S. ehrenbergii* species, and with previous findings in our research group, in which tomato, eggplant, pepper and *Nicotiana* accessions were tested and none of them showed sensitivity to Pep-13/Pep-25 [14]. These results together indicate that the PERU receptor family has emerged in the *Solanum* tuber-bearing species. Furthermore, the only genotype identified as Pep-13/25 sensitive, but outside the clade 4, belongs to *S. acroglossum* from the Piurana series. Unfortunately, we were not able to clone the homolog from *S. acroglossum*, but we presume that this genotype may contain the ancestral PERU receptor.

The geographical origin information of genotypes employed in our big screening [43], traced the origin of the PERU receptor to the central Andes of Peru and Bolivia. Wild genotypes that exhibit sensitivity to all tested peptides, such as LPH or from *S. acaule*, *S. acroglossum*, *S. megistacrolobum* species are native to Peru and Bolivia, suggesting that the functional diversification of PERU has occurred at its place of origin.

The phylogenetic analysis also showed that the PERU^{LPH} sequences are clustered in a very well supported clade close to the PERU^{DM} clade, which indicate that the new ligand specificity has emerged within the PERU receptor family of *Solanum*. To understand what is behind the functional diversification, we used the program codeml from PAML [44], to identify residues under positive selection. Remarkably, from the 11 residues found under positive selection, prediction of the PERU^{DM} ectodomain based on AlphaFold2 revealed that 10 residues are located on the inner surface of the LRR domain, the region expected to bind Pep-13. This observation is consistent with the solved crystal structure of the FLS2LRR-flg22-BAK1LRR complex, where flg22 binds to the concave surface of FLS2LRR [45]. This indicates that positive selection is driving the functional diversification of the PERU receptor family.

Evolution of PRRs has shown to be dynamic and maybe comparable to evolution of NLRs. In accordance with the functional interdependence of PRRs and NLRs, recently it was found an evolutionary correlation between the numbers of these two receptor types. Proteomes from 350 publicly available genomes were studied and a strong positive linear correlation was found for % NB-ARC - % LRR-RLPs, and % NB-ARC - % LRR-RLKs involved in recognition (subgroup XII), indicating that PRRs involved in pathogen recognition and NLRs gene families expand or contract together [46]. The study of the level of polymorphism of LRR-RP-, LRR-RLK- and NLR- encoding genes in 80 Arabidopsis accessions showed that LRR-RP and NLR genes exhibit similar sequence diversity, whereas LRR-RK genes showed lower variation [47]. However, other species might have experienced divergent outcomes based on the specific pathogen pressures they encounter, so generalization should be avoided, since each receptor has a particular history. The NLR ZAR1 exemplified this point. NLRs are recognized by their rapid evolution even at the intraspecific level [48], however ZAR1 is conserved in a wide range of angiosperm species, which origin was traced to the Jurassic era [49]. We believe that PERU represent a unique kind of LRR-RLK, with a highly dynamic evolutionary trajectory. The new insights from PERU and ZAR1 suggest that the simple and straightforward distinction of conserved vs dynamic evolutionary features of PRRs vs NLRs should be nuanced.

In **Chapter 4**, we have observed that PERU sequences, in contrast to more conserved FLS2 sequences that are present across angiosperms, show high amino acid sequence polymorphism and are restricted to few related species. Distinctively, we have demonstrated the evolution of new ligand specificities for PERU in closely related species that share geographical habitats and are subjected presumably to same pathogen pressures, pointing to a dynamic evolution of this peculiar receptor, driven likely by natural forces. Alternatively, FLS2XL able to recognize the evasive epitope flg22^{Atum} was found in *Vitis vinifera* [35], distant species to *Arabidopsis thaliana*.

In other cases, plant species can evolve different PRRs to recognize distinct epitopes within a single microbial pattern. FLS3 from tomato recognizes flagellin epitope flgII-28 that is distinct from flg22 [38]. The *A. thaliana* receptor-like protein 42 (RLP42) recognizes a conserved 9-amino-acid fragment pg9 within fungal endopolygalacturonases (PGs), and still unknow receptors from *A. arenosa* and *Brassica rapa* recognize the structurally distinct fragments pg20 and pg36, respectively, within PGs [50]. Convergent evolution was found for elicitins recognition as well. The sensor ELR, isolated from *Solanum microdontum* [7], and the phylogenetically divergent *N. benthamiana* RESPONSE TO ELICITIN (REL) are able to recognize the elicitin INF1 [51]. The receptor-like protein RLP30 binds a small cysteine-rich protein (SCP) that occurs in many fungi and oomycetes, which is also recognized by the unrelated *Nicotiana benthamiana* RLP RE02, and other Brassicaceae [52]. These studies illustrate the complex and dynamic evolution of plant PRRs to face the evasive polymorphic pathogen patterns.

Despite the same ligand specificities of PERU and the still unknown Pep-13 receptor from parsley, our phylogenomic analysis suggests these two receptors are phylogenetically divergent. Hence, it can be assumed that convergent evolution of Pep-13 recognition by tuber bearing *Solanum* species and parsley have occurred. In potato, we have found that the recognition of Pep-13 by PERU induces a hypersensitive cell death, something unusual for RLKs, and that has not been reported in parsley leaves. There is limited knowledge about PRRs and the hypersensitive cell death trigger by some of them. Recently, it was found that the RLP Cf-4-triggered cell death upon recognition of Avr4 requires of the *N. benthamiana* NRC3 [53]. However, we found that the PERU-triggered hypersensitive cell death is not affected in mutants of EDS1/PAD4 nor NRC2/3/4. So, the mechanisms behind the RLK-triggered hypersensitive cell death need further investigation.

PRRs for breeding resistance

PRRs can be used to confer new sensitivity to previously unrecognized PAMPs and enhance resistance. The interfamily transfer of *A. thaliana* EFR increases resistance to *Ralstonia solanacearum* in tomato [54]. The ectopic expression of Arabidopsis *RLP23* in potato enhances resistance to the oomycete *P. infestans* and to the fungus *Sclerotinia sclerotiorum* [55]. Transgenic *Citrus sinensis* expressing *NbFLS2* showed enhanced disease resistance to *Xanthomonas citri* [56]. The interespecies transfer of *S. microdontum* ELR to *S. tuberosum* exhibited a significant contribution to the resistance against *P. infestans* [7].

The expression of *PERU* improves resistance against *P. infestans,* while its knock-out renders potato more susceptible to this pathogen (Fig. 1C) (**Chapter 4**). However, we

observed that most potato cultivars showed Pep-13-responsive, indicating that these cultivars harbor *PERU* or other *PERU* allele, which suggests that PERU has been maintained during domestication [14]. Despite that, these cultivars are susceptible to *P. infestans*, indicating that this pathogen has adapted to overcome the PERU-based immunity. We have found two effectors that are able to suppress the Pep-13-mediated hypersensitive cell death (data not shown), and their roles need to be studied further. The identification or engineering and subsequent deployment of PRR alleles with different ligand specificities (found in wild species) are expected to confer a better level of resistance.

We also explored the combined effect of PERU and RLP23 transfer against *P. infestans* (Fig. 1C) (**Chapter 5**). We found that PERU and RLP23 cooperate during early PTI responses like ROS burst and ethylene accumulation upon oomycete patterns treatment (Pep-13 and nlp20), responses that ultimate slightly enhance the resistance to *P. infestans* infection. Although the results showed an improvement in resistance, to optimize the utilization of PRRs, different combinations of their corresponding PAMPs should be evaluated first, to determine if they confer an additive, synergistic or antagonistic effect, as it was reported previously in Arabidopsis [57]. Alternatively, the recently demonstrated interdependency of PRRs and NLRs [22, 23, 47] suggests that the stacking of these two kinds of receptors may offer a logical approach to achieving robust resistance to pathogens.

Many aspects about the deployment of PERU for breeding resistance remain unexplored. For instance, the contribution of PERU to resistance in soybean, pepper or strawberry against other *Phytophthora* species like *P. sojae*, *P. capsici*, or *P. cactorum*, respectively. Similarly, the level of resistance that PERU might confer against non-*Phytophthora* pathogens that also harbor the epitope Pep-13, for instance *Hyaloperonospora arabidopsidis, Bremia lactucae, Peronospora effuse, Albugo species or Phytium* species. In those cases, a more adequate level of resistance conferred by PERU can be anticipated, since those pathogens might have not evolved the specific effectors to suppress PERU-mediated immunity, or to target and manipulate proteins in other plants different to *Solanum* tuber-bearing species.

Non-host resistance can be considered as the result of pathogen effectors unable to suppress PTI [58]. Some studies indicate that effectors may be aligned to some hosts and not to others [59]. For instance, the *P. infestans* apoplastic effector EPIC1 that effectively targets *Solanum* RCR3 protease, does not inhibit protease activity of MRP2, the RCR3 homolog in the nonhost plant *Mirabilis jalapa*; and reciprocally, PmEPIC1 from *P. mirabilis*, pathogen of *M. jalapa*, effectively targets MRP2, but not RCR3 from potato [60]. Another study found that RxLR effectors from *P. infestans* do not enhance susceptibility in the nonhost Arabidopsis, or do not interact with their ortholog targets in Arabidopsis [61]. A new study has shown that pepper owns multiple NLRs

recognizing *P. infestans* effectors, for instance CaRpi-blb2a, a homolog of Rpi-blb2, that is not suppressed by the *P. infestans* effector PITG_15278 [62]. The study postulates that these NLRs contribute to non-host resistance of pepper against *P. infestans* [62]. Altogether, these studies demonstrate that pathogen effectors need to evolve hand in hand with their targets to appropriately suppress them.

Recently, the engineering of the helper NLR protein NRC2 led to evasion of suppression by the potato cyst *Globodera rostochiensis* effector, SPRYSEC15 (SS15), and to ultimately resurrection of NLR sensors like Rx, Pto and GPa2 [63]. A similar engineering approach can be applied to restore PRR-mediate immunity, already suppressed by effectors from adapted pathogens. The *P. infestans* effector AVR3a interacts with and stabilizes host U-box E3 ligase CMPG1, that is required for hypersensitive cell death mediated by INF1 [64], while the PiSFI3 effector interacts with StUBK, a positive regulator of specific PTI pathways in both potato and *Nicotiana benthamiana* to suppress early immune transcriptional responses [65]. The *P. infestans* effector PITG20303 targets and stabilizes StMKK1, a potato MAPK cascade protein, suppressing PTI [66]. These are just few examples of candidate targets for engineering and restoration of effective PTI.

The understanding of the plant-pathogen interface is essential to confer disease resistance to crops. Recently, a groundbreaking artificial intelligence (AI)-based structure prediction tool called AlphaFold-multimer has demonstrated remarkable success in predicting interactions between proteins from pathogens and their host plants [67, 68]. For instance, AlphaFold-multimer has been employed to predict novel sequence motifs binding to the ATG8 autophagy protein family, with a 90% accuracy in determining AIM/LIR motifs [69]. This tool was also effectively employed to screen 11,274 protein pairs, leading to the identification of 15 small secreted proteins (SSPs) from plant pathogens that are predicted to obstruct chitinases and proteases, including four experimentally validated novel pathogen-derived inhibitors that target a tomato-secreted immune protease P69B [70]. Likely, AI-guided approaches will accelerate the identification of new plant-pathogen interactions, and the engineering of receptors and pathogen targets, to ultimately achieve a more durable and broader resistance.

Concluding remarks

In this thesis, my work was mainly focused on the identification and characterization of the elusive Pep-13 receptor. The PAMP Pep-13 was found more polymorphic and widespread than previously thought. The fine-mapping and complementation assays revealed that an LRR-RLK conferred recognition of Pep-13 and was named PERU. We demonstrate that PERU binds to Pep-13 in a specific manner, after which a complex

with SERK3A is formed. PERU confers quantitative resistance against *P. infestans*, and its stacking with RLP23 improves the resistance against this pathogen. Interestingly, we demonstrated that functional diversification of the PERU receptor family has occurred at its place of origin, reflecting a high evolutionary dynamic. Despite these findings, many aspects remain to be studied. For instance, the PERU ligand binding sites, the responsible residues or LRRs for the different ligand specificities, co-evolution of potato PERU and *Phytophthora* Pep-13, contribution of PERU to resistance to other pathogens. The full understanding of the interaction of PERU-Pep-13 will facilitate its engineering and deployment, to ultimately obtain more and more durable resistant crops.

List of references

1. Simko, I., et al., *Chapter 7 - Genetics of Resistance to Pests and Disease*, in *Potato Biology and Biotechnology*, D. Vreugdenhil, et al., Editors. 2007, Elsevier Science B.V.: Amsterdam. p. 117-155.
2. Haverkort, A.J., et al., *Societal Costs of Late Blight in Potato and Prospects of Durable Resistance Through Cisgenic Modification.* Potato Research, 2008. **51**(1): p. 47-57.
3. Haverkort, A.J., et al., *Durable Late Blight Resistance in Potato Through Dynamic Varieties Obtained by Cisgenesis: Scientific and Societal Advances in the DuRPh Project.* Potato Research, 2016. **59**(1): p. 35-66.
4. Vleeshouwers, V.G.A.A., et al., *Understanding and Exploiting Late Blight Resistance in the Age of Effectors.* Annual Review of Phytopathology, 2011. **49**(1): p. 507-531.
5. Scheible, W.R., O. Törjek, and T. Altmann, *From Markers to Cloned Genes: Map-Based Cloning*, in *Molecular Marker Systems in Plant Breeding and Crop Improvement*, H. Lörz and G. Wenzel, Editors. 2005, Springer Berlin Heidelberg: Berlin, Heidelberg. p. 55-86.
6. Paluchowska, P., J. Śliwka, and Z. Yin, *Late blight resistance genes in potato breeding.* Planta, 2022. **255**(6): p. 127.
7. Du, J., et al., *Elicitin recognition confers enhanced resistance to Phytophthora infestans in potato.* Nature Plants, 2015. **1**(4): p. 15034.
8. Pham, G.M., et al., *Construction of a chromosome-scale long-read reference genome assembly for potato.* GigaScience, 2020. **9**(9).
9. van Lieshout, N., et al., *Solyntus, the New Highly Contiguous Reference Genome for Potato (Solanum tuberosum).* G3 Genes | Genomes | Genetics, 2020. **10**(10): p. 3489-3495.
10. Hoopes, G., et al., *Phased, chromosome-scale genome assemblies of tetraploid potato reveal a complex genome, transcriptome, and predicted proteome landscape underpinning genetic diversity.* Molecular Plant, 2022. **15**(3): p. 520-536.
11. Liu, S., et al., *Gene Mapping via Bulked Segregant RNA-Seq (BSR-Seq).* PLOS ONE, 2012. **7**(5): p. e36406.
12. Ramirez-Gonzalez, R.H., et al., *RNA-Seq bulked segregant analysis enables the identification of high-resolution genetic markers for breeding in hexaploid wheat.* Plant Biotechnology Journal, 2015. **13**(5): p. 613-624.
13. Tan, C., et al., *Mapping of the male sterile mutant gene ftms in Brassica rapa L. ssp. pekinensis via BSR-Seq combined with whole-genome resequencing.* Theoretical and Applied Genetics, 2019. **132**(2): p. 355-370.
14. Lin, X., et al., *Recognition of Pep-13/25 MAMPs of Phytophthora localizes to an RLK locus in Solanum microdontum.* Frontiers in Plant Science, 2023. **13**.
15. Jupe, F., et al., *Resistance gene enrichment sequencing (RenSeq) enables reannotation of the NB-LRR gene family from sequenced plant genomes and rapid mapping of resistance loci in segregating populations.* The Plant Journal, 2013. **76**(3): p. 530-544.
16. Witek, K., et al., *Accelerated cloning of a potato late blight–resistance gene using RenSeq and SMRT sequencing.* Nature Biotechnology, 2016. **34**(6): p. 656-660.
17. Steuernagel, B., et al., *Rapid cloning of disease-resistance genes in plants using mutagenesis and sequence capture.* Nature Biotechnology, 2016. **34**(6): p. 652-655.
18. Arora, S., et al., *Resistance gene cloning from a wild crop relative by sequence capture and association genetics.* Nature Biotechnology, 2019. **37**(2): p. 139-143.
19. Lin, X., et al., *RLP/K enrichment sequencing; a novel method to identify receptor-like protein (RLP) and receptor-like kinase (RLK) genes.* New Phytologist, 2020. **227**(4): p. 1264-1276.

20. Wolters, P.J., et al., *Tetraose steroidal glycoalkaloids from potato can provide complete protection against fungi and insects*. 2023, eLife Sciences Publications, Ltd.
21. Jones, J.D.G. and J.L. Dangl, *The plant immune system.* Nature, 2006. **444**(7117): p. 323-329.
22. Ngou, B.P.M., et al., *Mutual potentiation of plant immunity by cell-surface and intracellular receptors.* Nature, 2021. **592**(7852): p. 110-115.
23. Yuan, M., et al., *Pattern-recognition receptors are required for NLR-mediated plant immunity.* Nature, 2021. **592**(7852): p. 105-109.
24. Lu, Y. and K. Tsuda, *Intimate Association of PRR- and NLR-Mediated Signaling in Plant Immunity.* Molecular Plant-Microbe Interactions®, 2021. **34**(1): p. 3-14.
25. Thomma, B.P.H.J., T. Nürnberger, and M.H.A.J. Joosten, *Of PAMPs and Effectors: The Blurred PTI-ETI Dichotomy.* The Plant Cell, 2011. **23**(1): p. 4-15.
26. Boller, T. and G. Felix, *A Renaissance of Elicitors: Perception of Microbe-Associated Molecular Patterns and Danger Signals by Pattern-Recognition Receptors.* Annual Review of Plant Biology, 2009. **60**(1): p. 379-406.
27. Boutrot, F. and C. Zipfel, *Function, Discovery, and Exploitation of Plant Pattern Recognition Receptors for Broad-Spectrum Disease Resistance.* Annual Review of Phytopathology, 2017. **55**(1): p. 257-286.
28. Nürnberger, T., et al., *Innate immunity in plants and animals: striking similarities and obvious differences.* Immunological Reviews, 2004. **198**(1): p. 249-266.
29. Couto, D. and C. Zipfel, *Regulation of pattern recognition receptor signalling in plants.* Nature Reviews Immunology, 2016. **16**(9): p. 537-552.
30. Ingle, R.A., M. Carstens, and K.J. Denby, *PAMP recognition and the plant–pathogen arms race.* BioEssays, 2006. **28**(9): p. 880-889.
31. McCann, H.C., et al., *Identification of innate immunity elicitors using molecular signatures of natural selection.* Proceedings of the National Academy of Sciences, 2012. **109**(11): p. 4215-4220.
32. Gómez-Gómez, L. and T. Boller, *FLS2: An LRR Receptor–like Kinase Involved in the Perception of the Bacterial Elicitor Flagellin in Arabidopsis.* Molecular Cell, 2000. **5**(6): p. 1003-1011.
33. Chinchilla, D., et al., *The Arabidopsis Receptor Kinase FLS2 Binds flg22 and Determines the Specificity of Flagellin Perception.* The Plant Cell, 2005. **18**(2): p. 465-476.
34. Felix, G., et al., *Plants have a sensitive perception system for the most conserved domain of bacterial flagellin.* The Plant Journal, 1999. **18**(3): p. 265-276.
35. Fürst, U., et al., *Perception of Agrobacterium tumefaciens flagellin by FLS2XL confers resistance to crown gall disease.* Nature Plants, 2020. **6**(1): p. 22-27.
36. Cai, R., et al., *The Plant Pathogen Pseudomonas syringae pv. tomato Is Genetically Monomorphic and under Strong Selection to Evade Tomato Immunity.* PLOS Pathogens, 2011. **7**(8): p. e1002130.
37. Clarke, C.R., et al., *Allelic variation in two distinct Pseudomonas syringae flagellin epitopes modulates the strength of plant immune responses but not bacterial motility.* New Phytologist, 2013. **200**(3): p. 847-860.
38. Hind, S.R., et al., *Tomato receptor FLAGELLIN-SENSING 3 binds flgII-28 and activates the plant immune system.* Nature Plants, 2016. **2**(9): p. 16128.
39. Katsuragi, Y., et al., *CD2-1, the C-Terminal Region of Flagellin, Modulates the Induction of Immune Responses in Rice.* Molecular Plant-Microbe Interactions®, 2015. **28**(6): p. 648-658.
40. Nürnberger, T., et al., *High affinity binding of a fungal oligopeptide elicitor to parsley plasma membranes triggers multiple defense responses.* Cell, 1994. **78**(3): p. 449-460.
41. Brunner, F., et al., *Pep-13, a plant defense-inducing pathogen-associated pattern from Phytophthora transglutaminases.* The EMBO Journal, 2002. **21**(24): p. 6681-6688.

42. Spooner, D.M., et al., *Systematics, Diversity, Genetics, and Evolution of Wild and Cultivated Potatoes.* The Botanical Review, 2014. **80**(4): p. 283-383.
43. Vleeshouwers, V.G.A.A., et al., *SolRgene: an online database to explore disease resistance genes in tuber-bearing Solanumspecies.* BMC Plant Biology, 2011. **11**(1): p. 116.
44. Yang, Z., *PAML 4: Phylogenetic Analysis by Maximum Likelihood.* Molecular Biology and Evolution, 2007. **24**(8): p. 1586-1591.
45. Sun, Y., et al., *Structural Basis for flg22-Induced Activation of the Arabidopsis FLS2-BAK1 Immune Complex.* Science, 2013. **342**(6158): p. 624-628.
46. Man Ngou, B.P., et al., *Concerted expansion and contraction of immune receptor gene repertoires in plant genomes.* bioRxiv, 2022: p. 2022.01.01.474684.
47. Pruitt, R.N., et al., *The EDS1–PAD4–ADR1 node mediates Arabidopsis pattern-triggered immunity.* Nature, 2021. **598**(7881): p. 495-3,499A-499O.
48. Lee, R.R.Q. and E. Chae, *Variation Patterns of NLR Clusters in Arabidopsis thaliana Genomes.* Plant Communications, 2020. **1**(4): p. 100089.
49. Adachi, H., et al., *Jurassic NLR: Conserved and dynamic evolutionary features of the atypically ancient immune receptor ZAR1.* The Plant Cell, 2023.
50. Zhang, L., et al., *Distinct immune sensor systems for fungal endopolygalacturonases in closely related Brassicaceae.* Nature Plants, 2021. **7**(9): p. 1254-1263.
51. Chen, Z., et al., *Convergent evolution of immune receptors underpins distinct elicitin recognition in closely related Solanaceous plants.* The Plant Cell, 2023. **35**(4): p. 1186-1201.
52. Yang, Y., et al., *Convergent evolution of plant pattern recognition receptors sensing cysteine-rich patterns from three microbial kingdoms.* Nature Communications, 2023. **14**(1): p. 3621.
53. Kourelis, J., et al., *The helper NLR immune protein NRC3 mediates the hypersensitive cell death caused by the cell-surface receptor Cf-4.* PLOS Genetics, 2022. **18**(9): p. e1010414.
54. Lacombe, S., et al., *Interfamily transfer of a plant pattern-recognition receptor confers broad-spectrum bacterial resistance.* Nature Biotechnology, 2010. **28**(4): p. 365-369.
55. Albert, I., et al., *An RLP23–SOBIR1–BAK1 complex mediates NLP-triggered immunity.* Nature Plants, 2015. **1**(10): p. 15140.
56. Hao, G., et al., *Reduced Susceptibility to Xanthomonas citri in Transgenic Citrus Expressing the FLS2 Receptor From Nicotiana benthamiana.* Molecular Plant-Microbe Interactions®, 2016. **29**(2): p. 132-142.
57. ASLAM, S.N., et al., *Microbe-associated molecular pattern (MAMP) signatures, synergy, size and charge: influences on perception or mobility and host defence responses.* Molecular Plant Pathology, 2009. **10**(3): p. 375-387.
58. Uma, B., T. Swaroopa Rani, and A.R. Podile, *Warriors at the gate that never sleep: Non-host resistance in plants.* Journal of Plant Physiology, 2011. **168**(18): p. 2141-2152.
59. McLellan, H., P.C. Boevink, and P.R.J. Birch, *How to convert host plants into nonhosts.* Trends in Plant Science, 2023. **28**(8): p. 876-879.
60. Dong, S., et al., *Effector Specialization in a Lineage of the Irish Potato Famine Pathogen.* Science, 2014. **343**(6170): p. 552-555.
61. McLellan, H., et al., *Exploiting breakdown in nonhost effector–target interactions to boost host disease resistance.* Proceedings of the National Academy of Sciences, 2022. **119**(35): p. e2114064119.
62. Oh, S., et al., *Nucleotide-binding leucine-rich repeat network underlies nonhost resistance of pepper against the Irish potato famine pathogen Phytophthora infestans.* Plant Biotechnology Journal, 2023. **21**(7): p. 1361-1372.
63. Contreras, M.P., et al., *Resurrection of plant disease resistance proteins via helper NLR bioengineering.* Science Advances, 2023. **9**(18): p. eadg3861.

64. Bos, J.I.B., et al., Phytophthora infestans *effector AVR3a is essential for virulence and manipulates plant immunity by stabilizing host E3 ligase CMPG1.* Proceedings of the National Academy of Sciences, 2010. **107**(21): p. 9909-9914.
65. He, Q., et al., *Phytophthora infestans effector SFI3 targets potato UBK to suppress early immune transcriptional responses.* New Phytologist, 2019. **222**(1): p. 438-454.
66. Du, Y., et al., *Phytophthora infestans RXLR effector PITG20303 targets a potato MKK1 protein to suppress plant immunity.* New Phytologist, 2021. **229**(1): p. 501-515.
67. Evans, R., et al., *Protein complex prediction with AlphaFold-Multimer.* bioRxiv, 2021: p. 2021.10.04.463034.
68. Jumper, J., et al., *Highly accurate protein structure prediction with AlphaFold.* Nature, 2021. **596**(7873): p. 583-589.
69. Ibrahim, T., et al., *AlphaFold2-multimer guided high-accuracy prediction of typical and atypical ATG8-binding motifs.* PLOS Biology, 2023. **21**(2): p. e3001962.
70. Homma, F., J. Huang, and R.A.L.v.d. Hoorn, *Alphafold-multimer predicts cross-kingdom interactions at the plant-pathogen interface.* bioRxiv, 2023: p. 2023.04.03.535425.

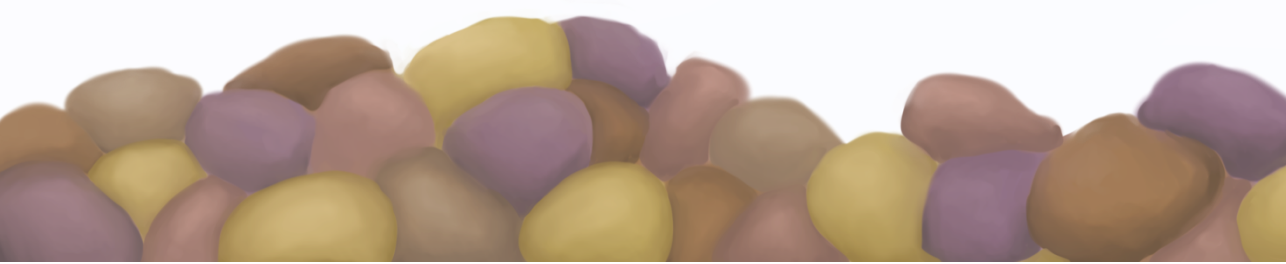

Summary

Potato (*Solanum tuberosum* L.) is the most important non-cereal food crop, serving as a dietary staple for 1.3 billion people worldwide. Potato is susceptible to a wide variety of pests and pathogens such as insects, nematodes, viruses, bacteria, fungi and oomycetes. Late blight, caused by the oomycete *Phytophthora infestans*, is the most destructive disease of potatoes. It contributed to the Irish Potato Famine in the mid-19th century, and it remains the major threat for potato production to date.

Breeding for resistance to *P. infestans* in potato has historically centered on the use of dominant resistance genes (*Rpi* genes*)*. However, most of them have shown to be not durable. Another line of defense in potato against *P. infestans,* that is less explored, takes place at the cell surface. This immune response is based on the recognition of pathogen-associated molecular patterns (PAMPs) by pattern recognition receptors (PRRs). In case of potato, only a single PRR was previously identified, the receptor like protein ELR, which recognizes INF1 from *P. infestans* and enhances resistance against this pathogen.

Nearly 30 years ago, a peptide motif, Pep-13, was identified within a glycoprotein (GP42) from *Phytophthora sojae*. Pep-13 was found to be sufficient to elicit immune responses in parsley cells. Subsequent studies revealed that GP42 is present in other *Phytophthora* species and that the Pep-13 sequence is highly conserved among them. Mutational analysis found that the amino acid residues that are required for the elicitor activity of Pep-13 are also necessary for the transglutaminase activity, indicating that Pep-13 exhibits characteristics of PAMPs. While it was found that Pep-13 shows activity in potato cells and leaves, the receptor of Pep-13 was not identified. This thesis aimed to unveil and characterize the Pep-13 receptor in potatoes.

In **Chapter 2**, a detailed protocol to identify new PRRs is described. This method consists, first, of the use of Bulked segregant RNA-Seq (BSR-Seq) to circumvent the conventional genetic mapping that involves the development of a high number of molecular markers. The bioinformatic analysis of the sequencing results leads to the delineation of a mapping interval. Furthermore, this analysis generates single nucleotide polymorphism (SNP) markers, which will prove useful for the fine-mapping process. The subsequent high-throughput recombinant screening of *in vitro* plants, along with the phenotyping of only the recombinant plants, optimizes the fine-mapping process in terms of time, space and labor.

In **Chapter 3**, the previously described protocol was implemented to determine the location of the potato receptor of Pep-13/25 (Pep-25 is a slightly longer version of Pep-

13). BSR-Seq of responsive and non-responsive bulks allowed the mapping of the Pep-25 receptor to the top of chromosome 3 of the genotype GIG362-6 from the wild species *Solanum microdontum* subsp. *gigantophyllum*. The further fine-mapping, BAC library screening and BAC sequencing culminated in the reconstruction of the GIG362-6 physical map, and determination of a reduced mapping interval, which unfortunately was not completely covered by the BAC sequences. The candidate genes in the mapping interval tested negative in complementation assays of agroinfiltration, suggesting that the Pep-13/25 receptor is most probably located within the unsequenced segment of the mapping interval. Additionally, Pep-13/25 polymorphism among transglutaminase protein sequences of *Phytophthora,* oomycetes and other filamentous pathogens was explored. This examination yielded four Pep-13/25 variants, which are tested in wild *Solanum* tuber-bearing species, revealing different recognition specificities.

The absence of a high-quality genome sequence of GIG362-6 hampered the identification of the Pep-25 receptor. So, in **Chapter 4,** we decided to exploit the reference potato genome genotype DM1-3 516 R44, which is Pep-13/25 responsive, and has a high-quality genome sequence. A new mapping population was generated, and the receptor was fine-mapped to another genomic region with candidate genes, all encoding leucine-reach repeat receptor like kinases (LRR-RLKs). The complementation assays revealed us the identity of the gene responsible for the recognition of Pep-13, which was named *PERU* (**Pe**p-13 **R**eceptor **U**nit). A multidisciplinary approach was taken to characterize this new PRR. Using ligand binding assays, we demonstrate that PERU interacts specifically with Pep-13 and that it forms a complex with BAK1 in a ligand dependent manner. Unlike SOBIR1 (which is not required for RLK-mediated immunity), BAK1 is shown to be required for the Pep-13-triggered responses. Disease assays using transgenic lines overexpressing *PERU* or knock-out plants for *PERU* indicate that PERU enhances immunity against *P. infestans*.

In **Chapter 4**, we delved further into the presence and distribution of Pep-13/25 recognition in the *Solanum* tuber-bearing species. Examination of 477 genotypes reveals that, unlike DM1-3 516 R44, which is unable to recognize the inactive variant Pep25-W231A, 10 genotypes show a strong hypersensitive response (HR) for Pep-25 and all its variants. For example, *Solanum leptophyes* LPH680-5, whose receptor, $PERU^{LPH}$, was cloned and studied in more detail, showcases that two receptors have diversified in function, resulting in different ligand specificities. Geographical data of the genotypes employed for the screening indicated that Pep-25-sensitive genotypes are mainly located in Peru and Bolivia, while insensitive genotypes are distributed throughout the entire American continent, ranging from the United States till Chile and Argentina. Genotypes harboring $PERU^{DM}$ alleles or $PERU^{LPH}$ alleles predominantly occur in Peru and Bolivia. Together, these findings point to the Andes of Peru and

Bolivia as the place of origin of this receptor family and of the functional diversification.

In **Chapter 4,** a phylogenomic analysis allowed the mining of 114 PERU-like sequences and FLS2 sequences for comparison, showing that the PERU sequences are highly diverse when compared to FLS2. The PAML analysis of the responsive PERU sequences reveals 11 amino acid residues under positive selection, and interestingly, a prediction with AlphaFold located 10 of the 11 residues on the concave part of the LRR domain, which fits with the expected site for Pep-13 binding. The phylogenetic tree of the PERU sequences suggests that the PERU receptor family has originated within the *Solanum* tuber-bearing species. Altogether, our results unveil a distinctive receptor that, unlike other RLKs, exhibits remarkable diversity. This receptor is restricted to species within the *Solanum* section *Petota* and showcases diversification even among closely related species.

In **Chapter 5**, we attempted to enhance the potato immune response to *P. infestans* by combining the RLK PERU with the RLP RLP23, both of which have individually been demonstrated to increase the resistance to *P. infestans*. We observed that transgenic potato plants from the cultivar Atlantic exhibit different sensitivity to Pep-13 and nlp20, as demonstrated by EC50 determination. Additionally, stacking these two PRRs showed an additive effect on potato immune responses, such as ROS and ethylene accumulation, as well as a modest additive effect on protection against *P. infestans*.

In **Chapter 6**, the findings of this thesis are presented and discussed in a broader perspective. Summing up, my thesis work has advanced the understanding of the first line of defense against *P. infestans* in potatoes and can contribute to achieve a more durable resistance to late blight.

Samenvatting

Aardappel (*Solanum tuberosum* L.) is het belangrijkste voedselgewas dat niet tot de granen behoort, en dient als hoofdvoedsel voor 1,3 miljard mensen wereldwijd. Aardappelplanten zijn vatbaar voor een breed scala aan ziekten en plagen, die veroorzaakt worden door insecten, nematoden, virussen, bacteriën, schimmels en oömyceten. *Phytophthora infestans* is een oömyceet die de beruchte aardappelziekte 'Phytophthora' veroorzaakt, de meest destructieve ziekte van aardappels. Phytophthora leidde tot de Ierse hongersnood halverwege de 19e eeuw en vormt tot op heden een grote bedreiging voor de aardappelproductie.

Veredeling voor Phytophthora-resistentie is tot nu toe gefocust geweest op het inkruisen van dominante resistentiegenen (Rpi-genen). Echter, de meeste van deze genen geven geen duurzame resistentie. Een andere afweerreactie die minder onderzocht is, vindt plaats als receptoren aan het oppervlak van de plantencel (PRRs) pathogeen-geassocieerde moleculaire patronen (PAMPs) herkennen. In het geval van aardappels is slechts één enkele PRR eerder geïdentificeerd, namelijk ELR, een 'receptor-like protein' dat INF1 van *P. infestans* herkent en de resistentie tegen Phytophthora versterkt.

Bijna 30 jaar geleden werd een peptide van 13 aminozuren (Pep-13) geïdentificeerd in een glycoproteïne (GP42) van *Phytophthora sojae*. Pep-13 bleek voldoende te zijn om afweerreacties op te wekken in peterseliecellen. Vervolgonderzoek toonde aan dat GP42 aanwezig is aan in andere *Phytophthora*-soorten, én dat de Pep-13-sequentie zeer geconserveerd is tussen deze soorten. Mutatieanalyse liet zien dat de aminozuurresiduen die nodig zijn voor de elicitor-activiteit van Pep-13 ook noodzakelijk zijn voor de transglutaminase-activiteit, wat aangeeft dat Pep-13 kenmerken vertoont van een PAMP. Een reactie op Pep-13 werd ook gevonden in aardappel, maar de receptor van Pep-13 bleek onbekend. Het doel van dit proefschrift is het identificeren en karakteriseren van de Pep-13-receptor in aardappel.

In **Hoofdstuk 2** wordt een gedetailleerd protocol beschreven om nieuwe PRRs te identificeren. Deze methode omvat het gebruik van Bulked Segregant RNA-Seq (BSR-Seq) om de conventionele genetische mapping te omzeilen, waarbij de ontwikkeling van een groot aantal moleculaire merkers nodig zou zijn. De bio-informatica-analyse van de sequenties leidt tot de afbakening van een mapping-interval. Bovendien genereert deze analyse enkele nucleotide-polymorfisme (SNP) merkers, die nuttig zijn voor het fine-mapping proces. De daaropvolgende grootschalige recombinanten screening van *in vitro* planten, samen met de fenotypering van de recombinanten, optimaliseert het fine-mapping proces wat betreft tijd, ruimte en arbeid.

In **Hoofdstuk 3** wordt het eerder beschreven protocol geïmplementeerd om de locatie van de aardappelreceptor van Pep-13/25 te bepalen. (Pep-25 is een iets langere versie van Pep-13.) BSR-Seq van Pep-13/25-herkennende en niet-herkennende bulks maakte het mogelijk om de receptor van Pep-25 te lokaliseren aan de top van chromosoom 3, in de wilde aardappel *Solanum microdontum* subsp. *gigantophyllum* GIG362-6. De verdere fine-mapping, BAC-screening en -sequencing resulteerden in de reconstructie van de fysieke kaart van GIG362-6, en een verkleind mapping-interval. Dit werd helaas niet volledig gedekt door de BAC-sequenties. De kandidaatgenen in het mapping-interval testten allemaal negatief in complementatie-assays van agro-infiltratie, wat suggereerde dat de Pep-13/25-receptor zich waarschijnlijk niet binnen dit segment van het mapping-interval bevindt. Daarnaast werd het polymorfisme van Pep-13/25 onderzocht bij transglutaminase-eiwitsequenties van *Phytophthora* soorten, andere oömyceten, en schimmels. Dit leverde vier natuurlijke varianten van Pep-13/25 op, die verschillende specificiteit van herkenning lieten zien na infiltratie in bladeren van wilde knoldragende *Solanum*-soorten.

De afwezigheid van een hoogwaardige genoomsequentie van GIG362-6 bemoeilijkte de identificatie van de Pep-25-receptor. Daarom besloten we in **Hoofdstuk 4** gebruik te maken van het referentiegenoom van DM1-3 516 R44 (DM), een plant die ook Pep-13/25 herkent. We genereerden een nieuwe mappingpopulatie en de receptor werd gelokaliseerd in een ander genomisch gebied met kandidaatgenen, die allemaal coderen voor LRR receptor-like kinasen (LRR-RLKs). Complementatie-assays onthulden de identiteit van het gen verantwoordelijk voor de herkenning van Pep-13, dat *PERU* (**Pe**p-13 **R**eceptor **U**nit) werd genoemd. De nieuwe PRR te werd gekarakteriseerd met een multidisciplinaire aanpak. Met behulp van ligand-bindingsassays toonden we aan dat PERU specifiek bindt met Pep-13 en dat het een (ligand-afhankelijk) complex vormt met BAK1. In tegenstelling tot SOBIR1 (dat niet nodig is voor door RLK-gebaseerde immuniteit), blijkt BAK1 nodig te zijn voor de door Pep-13 geïnduceerde responsen. Ziekteproeven met transgene aardappelplanten waarin *PERU* tot expressie gebracht is, en met *PERU* knock-out planten, gaven aan dat PERU de resistentie tegen *P. infestans* verhoogt.

In **Hoofdstuk 4** zijn we dieper ingegaan op de aanwezigheid en verspreiding van de Pep-13/25-herkenning in de knoldragende *Solanum* soorten. We infiltreerden 477 genotypen met mutanten van Pep-25. In tegenstelling tot DM, die niet in staat is om de inactieve variant Pep25-W231A te herkennen, vonden we 10 wilde genotypen die een sterke overgevoeligheidsreactie (HR) vertonen op Pep-25 en alle geteste varianten. Bijvoorbeeld, *Solanum leptophyes* LPH680-5, waarvan we vervolgens ook de receptor, $PERU^{LPH}$, kloneerden. We toonden aan dan $PERU^{DM}$ en $PERU^{LPH}$ een

verschillende specificiteit hebben. Geografische gegevens van de genotypen uit de screen gaven aan dat Pep25-gevoelige genotypen voornamelijk voorkomen in Peru en Bolivia, terwijl ongevoelige genotypen zijn verspreid over het hele Amerikaanse continent, variërend van de Verenigde Staten tot Chili en Argentinië. Genotypen met $PERU^{DM}$-allelen of $PERU^{LPH}$-allelen komen vooral voor in Peru en Bolivia. Deze bevindingen wijzen samen naar de Andes in Peru en Bolivia als de oorsprong van de PERU-familie en de functionele diversificatie van deze receptoren.

Een fylogenomische analyse in **Hoofdstuk 4** leidde tot 114 PERU-achtige sequenties. Door deze te vergelijken met FLS2-sequenties vonden we dat de PERU-sequenties zeer divers zijn in vergelijking met FLS2. Een PAML-analyse van de responsieve PERU-sequenties onthulde 11 aminozuurresiduen onder positieve selectie. Interessant genoeg toonde een voorspelling met AlphaFold aan dat 10 van de 11 residuen zich bevinden in het concave deel van het LRR-domein, wat overeenkomt met de verwachte bindingsplaats voor Pep-13. De fylogenetische boom van de PERU-sequenties suggereert dat de PERU-receptorfamilie is ontstaan binnen de knoldragende *Solanum*-soorten die voorkomen in de Andes. Samengevat onthullen onze resultaten dat PERU een opmerkelijke diversiteit vertoont, in tegenstelling tot andere RLKs. Het voorkomen van PERU is beperkt tot knoldragende *Solanum*-soorten en toont diversificatie zelfs tussen nauw verwante soorten.

In **Hoofdstuk 5** hebben we geprobeerd de Phytophthora-resistentie van aardappel te verhogen door PERU te combineren met RLP23, waarvan voor beide afzonderlijk is aangetoond de resistentie tegen *P. infestans* te verhogen. We vonden dat transgene aardappelplanten van het ras Atlantic verschillende gevoeligheid vertonen voor Pep-13 en nlp20, zoals aangetoond door EC50-bepalingen. Het stapelen van deze twee PRRs liet een additief effect zien op afweerreactiereacties, zoals ROS- en ethyleenaccumulatie, evenals een bescheiden verdere verhoging resistentie tegen *P. infestans*.

In **Hoofdstuk 6** worden de bevindingen van dit proefschrift besproken in een breder perspectief. Samengevat heeft mijn proefschrift bijgedragen aan een beter begrip van de eerste verdedigingslinie tegen *P. infestans* in aardappels en kan het bijdragen aan het bereiken van een duurzamere resistentie tegen Phytophthora.

Resumen

La papa (*Solanum tuberosum* L.) es el cultivo alimenticio no cereal más importante del mundo. Aproximadamente 1.3 mil millones de personas consumen papa regularmente. La papa es susceptible a una amplia variedad de plagas y patógenos, tales como insectos, nemátodos, virus, bacterias, hongos y oomicetos. El tizón tardío, causado por el oomiceto *Phytophthora infestans*, es la enfermedad más destructiva de la papa. Este patógeno fue el causante la hambruna irlandesa a mediados del siglo XIX y representa la principal amenaza para la producción de papa hasta la fecha.

El mejoramiento genético de la papa para obtener resistencia a *P. infestans* se ha centrado históricamente en el uso de genes de resistencia dominantes (genes *Rpi*). Sin embargo, se ha demostrado que la mayoría no son duraderos. Otra línea de defensa de la papa contra *P. infestans*, menos estudiada, ocurre en la superficie celular. Esta respuesta inmune se basa en el reconocimiento de patrones moleculares asociados a patógenos (PAMP) por receptores de reconocimiento de patrones (PRR). En el caso de la papa, solo se había identificado un PRR, el receptor ELR, que reconoce INF1 de *P. infestans* y incrementa la resistencia de papa a este patógeno.

Hace casi 30 años se identificó el péptido Pep-13, dentro de una glicoproteína (GP42) de *Phytophthora sojae*. Se encontró que Pep-13 es suficiente para desencadenar respuestas inmunes en células de perejil. Estudios posteriores revelaron que la proteina GP42 está presente en otras especies de *Phytophthora* y que la secuencia de Pep-13 es altamente conservada entre ellas. Un análisis mutacional encontró que los aminoácidos necesarios para la actividad elicitora de Pep-13 también son necesarios para la actividad enzimática de GP42, indicando que Pep-13 exhibe características de PAMP. Si bien se descubrió que Pep-13 muestra actividad en las células y hojas de la papa, su receptor no fue identificao. El objetivo de esta tesis es identificar y caracterizar el receptor de Pep-13 en papas.

El **Capítulo 2** describe un protocolo detallado para identificar nuevos PRRs. Este método consiste, en primer lugar, en el uso de Bulked segregant RNA-Seq (BSR-Seq) para prescindir del mapeo genético convencional que implica el desarrollo de un elevado número de marcadores moleculares. El análisis bioinformático de los resultados del secuenciamiento conduce a la delimitación de un intervalo de mapeo. Además, este análisis genera marcadores single nucleotide polymorphism (SNP), que resultarán útiles para el proceso de mapeo fino. Posteriormente, el cribado de alto redimiento de plantas *in vitro* para identificar las plantas

recombinantes, junto con el fenotipado de únicamente de las plantas recombinantes, optimiza el proceso de mapeo fino en términos de tiempo, espacio y trabajo.

En el **Capítulo 3**, se implementó el protocolo descrito anteriormente para determinar la ubicación del receptor de Pep-13/25 en papa (Pep-25 es una versión ligeramente más larga de Pep-13). El análisis BSR-Seq de los bulks sensibles y no sensibles permitió mapear el receptor de Pep-25 en la parte superior del cromosoma 3 del genotipo GIG362-6 de la especie silvestre *Solanum microdontum* subsp. gigantophyllum. El mapeo fino posterior, la exploración de la librería de BACs y la secuenciación de BACs culminaron en la reconstrucción del mapa físico GIG362-6 y la reducción del intervalo de mapeo, que desafortunadamente no fue cubierto completamente por las secuencias de los BACs. Los genes candidatos en el intervalo de mapeo resultaron negativos en los ensayos de complementación de agroinfiltración, lo que sugiere que el receptor Pep-13/25 probablemente esté ubicado dentro del segmento no secuenciado del intervalo de mapeo. Además, se exploró el polimorfismo de Pep-13/25 en secuencias de transglutaminasas de *Phytophthora*, oomicetos y otros patógenos filamentosos. Con este análisis se encontraron cuatro variantes de Pep-13/25, que fueron evaluadas en parientes silvestres de papa, revelando diferentes especificidades de reconocimiento.

La ausencia de una secuencia del genoma de alta calidad de GIG362-6 dificultó la identificación del receptor Pep-25 en la capítulo anterior. En el **Capítulo 4**, decidimos explotar el genotipo del genoma de la papa de referencia, DM1-3 516 R44, que responde a Pep-13/25 y tiene una secuencia genómica de alta calidad. Se generó una nueva población de mapeo y el receptor fue mapeado en otra región genómica. Se econtraron tres genes candidatos que codifican para quinasas tipo receptor con repeticiones ricas en leucina (LRR-RLKs). Los ensayos de complementación revelaron la identidad del gen responsable del reconocimiento de Pep-13, el cual fue denominado PERU (del inglés **Pe**p-13 **R**eceptor **U**nit). Se siguió un enfoque multidisciplinario para caracterizar este nuevo PRR. Utilizando ensayos de unión de ligando, demostramos que PERU interactúa específicamente con Pep-13 y que forma un complejo con BAK1 de manera dependiente de Pep-13. A diferencia de SOBIR1 (que no es necesaria para la inmunidad mediada por RLKs), demostramos que BAK1 es necesaria para las respuestas desencadenadas por Pep-13. Los ensayos de enfermedad empleando líneas transgénicas que sobreexpresan *PERU* o plantas knock-out para *PERU* indican que PERU contribuye a la inmunidad contra *P. infestans*.

En el **Capítulo 4**, profundizamos más en la presencia y distribución del reconocimiento de Pep-13/25 en las especies tuberosas del género *Solanum*. El análisis de 477 genotipos reveló que, a diferencia del DM1-3 516 R44, que no

reconoce la variante inactiva Pep-25-W231A, 10 genotipos muestran una fuerte respuesta de hipersensibilidad (HR) a Pep-25 y todas sus variantes. Por ejemplo, *Solanum leptophyes* LPH680-5, cuyo receptor, PERU^{LPH}, fue clonado y estudiado con más detalle, demuestra que dos receptores han diversificado su función, dando como resultado diferentes especificidades de reconocimiento de ligando. Los datos geográficos de los genotipos empleados en el análisis indicaron que los genotipos capaces de reconocer Pep-25 se encuentran principalmente en Perú y Bolivia, mientras que los genotipos insensibles a Pep-25 y sus variants se distribuyen por todo el continente americano, desde Estados Unidos hasta Chile y Argentina. Los genotipos que albergan alelos *PERU^{DM}* o alelos *PERU^{LPH}* se encuentran predominantemente en Perú y Bolivia. En conjunto, estos hallazgos señalan a los Andes de Perú y Bolivia como el lugar de origen de esta familia de receptores y de su diversificación funcional.

En el **Capítulo 4**, un análisis filogenómico permitió extraer 114 secuencias similares a PERU y secuencias FLS2, mostrando que las secuencias de PERU son muy diversas en comparación con FLS2. El análisis PAML de las secuencias sensibles de PERU revela 11 residuos de aminoácidos se encuentran bajo selección positiva y, curiosamente, una predicción con AlphaFold localizó 10 de los 11 residuos en la parte cóncava del dominio LRR, lugar esperado de unión a Pep-13. El árbol filogenético de las secuencias de PERU sugiere que la familia de receptores PERU se ha originado dentro de las especies tuberosas del género *Solanum*. En conjunto, nuestros resultados revelan que PERU es un receptor particular que, a diferencia de otros RLKs, exhibe una diversidad notable. Este receptor está restringido a especies dentro de *Solanum* section *Petota* y muestra diversificación incluso entre especies estrechamente relacionadas.

En el **Capítulo 5** intentamos mejorar la respuesta inmune de la papa a *P. infestans* combinando el RLK PERU y el RLP RLP23, los cuales han demostrado individualmente aumentar la resistencia a *P. infestans*. Observamos que las plantas de papa transgénicas del cultivar Atlantic exhiben diferente sensibilidad a Pep-13 y nlp20, como lo demuestra la determinación de EC50. Además, el stacking de estos dos PRRs mostró un efecto aditivo sobre las respuestas inmunes de papa, como la producción de ROS y etileno, así como un modesto efecto aditivo sobre la protección contra *P. infestans*.

En el **Capítulo 6**, los hallazgos de esta tesis se presentan y discuten desde una perspectiva más amplia. En resumen, mi trabajo de tesis representq un aporte en la comprensión de la primera línea de defensa en papa contra *P. infestans* y puede contribuir para lograr una resistencia más duradera al tizón tardío.

Acknowledgements

I would like to express my sincere appreciation to all the great people who have supported, contributed and made possible the completion of this thesis.

First and foremost, I want to express my deepest gratitude to my dear supervisor, **Vivianne!**, I can't find the right words to describe the immense appreciation I feel. I used to say to my friends in Radix, 'I am really lucky to have Vivianne as my supervisor,' and this sentiment remains absolutely true. From the moment I arrived in The Netherlands, I could sense your support and constant presence. You have not only believed in me but, more importantly, you have understood me. Your guidance and support have not only empowered me to carry out experiments but have also nurtured my ability to work independently as a researcher. I am genuinely thankful for your confidence and for all the opportunities you've provided for my growth. I consider you my mentor, I've learned so much from you, not only academically but also on a personal level. I'll miss our weekly meetings, whether they were in person or online. Despite my fears and doubts, you've always had a way of making me feel at peace, safe, and comforted. I've felt comfortable discussing my thoughts and concerns with you, and that means the world to me.

Richard, I want to express my sincere gratitude for the opportunity to pursue a PhD in the Plant Breeding Department, and for being my promoter. I appreciate your support and confidence. I also value the time you dedicated to reviewing my chapters and providing invaluable feedback. Thank you.

I would like to extend my gratitude to Vivianne's team: Doret, Jaap, Aviv, Tatiana, Luigi, Jasmine and Guillermo. **Doret**, thanks for your invaluable assistance in the labs and greenhouse. You were always generous in sharing advice, protocols, kits, primers, plasmids, cultures, and more. I will remember the pretty birthday's decorations. **Jaap**, we often turned to you whenever we have question, doubts, ideas, or help, and you never hesitated to help and share your expertise. **Aviv**, my favorite PhD buddy, thanks for always being there for me, both personally and academically. Having your help in the lab and greenhouse, and in the office whenever we've just felt like talking, have been invaluable. Big thanks for accepting being my paranymph. I already miss you. **Tatiana**, thanks for the always funny chats in Spanish, for the memorable mountain biking experience, and for your support. **Luigi**, it was great meeting you, I really admire your calmness and kindness, wish you all the best. **Jasmine,** I met you during your master's thesis, and it's wonderful to see that you'll be continuing as a PhD student. **Guillermo**, I haven't had the chance to meet you in person, but I've heard nothing but good things about you, success!

The completion of my PhD journey wouldn't have been possible without the fantastic teamwork of my collaborators. **Thorsten Nürnberger**, you initiated the Pep-13 story and generously collaborated with us to discover the Pep-13 receptor. I deeply appreciate our productive meetings, where you consistently aimed to elevate our research and provided invaluable feedback. I'm truly grateful for the opportunity to visit your lab in Tübingen, as I've always wanted to delve deeper into biochemistry and become more familiar with these techniques. Meeting you in person during my visit to Providence was an absolute pleasure. **Sophien Kamoun**, I am thankful for your substantial contribution to our paper, as well as for the constructive meetings, emails, advice, and insights into the PAML analysis. It was an honor to collaborate with you. I would also like to extend my gratitude to **Lisha** and **Chenlei** from Tübingen. Your kindness during my visit was greatly appreciated, and I'm thankful for your willingness to share your biochemistry knowledge and expertise. Thanks to **AmirAli** and **Andy** from the Sainsbury Lab for their extraordinary work in the phylogenomic analysis and Alphafold prediction, respectively, which significantly enriched our PERU story. Our paper in Science became a reality thanks to the combined efforts of these exceptional people.

Thanks to the master students that worked with me, **Laura Dethier**, **Niels Steigenga**, **Almudena Pelaez** and **Nandi Jalahalli**. Your contributions to this thesis have been invaluable, and I appreciate the hard work each of you put into it. Your dedication and effort have played a crucial role for the completion of this thesis. Thank you all for your outstanding contributions.

I'd also like to express my gratitude to the lab managers, **Linda** and **Danny**. Your kindness and support are really appreciated. I truly value the pleasant atmosphere in Lab E1.162, which always made me feel comfortable. Special gratitude to **Dirkjan**, for your kindness, and nice chats. I really appreciate all your support in performing crosses, harvesting seeds, and growing plants in corridor 12. Without your assistance, I couldn't have conducted all the experiments I did. Thank you!
Big thanks to **Gert**, you are a smart guy, I used to ask a lot of questions to you, and you were always willing to share. Thanks for your help in the molecular and the phyto labs. I'd also like to extend my thanks to **Marjan**, **Bernadette** and **Isolde** for their support and assistance, as well as for providing a well-organized workspace for tissue culture work.

To my dear friends, your support during the tough times is precious to me. I'm truly grateful for your friendship. **Dong**, Dondon, thanks for agreeing to be my paranymph. Your frankness and straightforwardness, which were initially unfamiliar to me, have been eye-opening, and I've learned to value those qualities. I will miss the incredible dinners, particularly those unforgettable hotpots. Your company and our shared sporting moments, whether it was basketball, volleyball, ping pong, tennis, squash, or

running... we've truly done it all, and those memories will stay with me. **Elizabeth**, Eli, thanks for all the moments we shared. I admire your strength and patience. I will miss our sportive moments too, the dinners, the dessert times, the nice chats, and our secondhand shopping adventures. **Lorena**, Lore, from my first days in Wageningen, you were generous, showing me around, and introducing me to people. Thanks for always keeping in touch, wish you all the best. **Sri**, Atik, I must say you are not just a kind and good person, you are always open and accepting of everybody, without judgment. Thanks for being my friend, for nice dinners, for the walks, and open conversations. **Han,** you started as Dong's friend in the beginning, and I'm truly grateful that you became my friend too. I admire your always upbeat mood and warm-hearted nature. Thanks for the many enjoyable dinners we've shared, our memorable sporting moments and the trips. It was a pleasure meeting you. **Carolina**, Caro, I may have had the misfortune of meeting you towards the end of your PhD journey, but the time we had was more than enough to realize what a truly great person you are. I want to express my heartfelt thanks for being there at the beginning of my PhD and for generously sharing your expertise with me. I've learned a lot.

Most importantly, I want to express my deepest gratitude to my family. To my mother **Zoraya**, my sisters **Yozi** and **Nela**, despite being thousands of kilometers apart, I always knew that with one call, I could hear your voices and see your faces. Thank you for being my unwavering support and for always believing in me. To my father, **Carlos**, your consistent communication and interest in my research and life in The Netherlands have meant a lot to me. To my niece and nephew, **Anel** and **Terry**, thanks for bringing immense happiness into my life. You truly are the best. Anel, mi reina, a special thank you for the cover; I absolutely love it. **Pancho**, your immense love for your family is admirable. You're an excellent father. Last but not least, to my babies 🐾, Floky, Mauri, and Pepa, you three are the best friends and companions anyone could ever wish for.

¡¡ Gracias !!

About the author

Yerisf Carla Torres Ascurra was born on the 10th of June 1988 in Junin, Peru. She grew up in the quiet and small town of Jauja, nestled in the mountains of Peru. In 2005, she relocated to Lima to pursue a 5-year BSc in Biology, Genetics, and Biotechnology at the National University of San Marcos (UNMSM). In 2014, she completed a MSc in Molecular Biology at the same university, and in 2017, she was awarded a scholarship for doctoral studies abroad. Consequently, in 2018, she moved to the Netherlands to commence her PhD at the Laboratory of Plant Breeding at Wageningen University and Research.

Potato field in Jauja, Junin.

List of publications

- **Torres Ascurra YC**, Wouters D, Visser RGF, Nürnberger T & Vleeshouwers VGAA. Stacking of PRRs in potato to achieve enhanced resistance against *Phytophthora infestans*. bioRxiv 2023.09.07.556738; doi: https://doi.org/10.1101/2023.09.07.556738.

- **Torres Ascurra YC**, Zhang L, Toghani A, Hua C, Rangegowda NJ, Posbeyikian A, Pai H, Lin X, Wolters PJ, Wouters D, de Blok R, Steigenga N, Paillart MJM, Visser RGF, Kamoun S, Nürnberger T, Vleeshouwers VGAA. Functional diversification of a wild potato immune receptor at its center of origin. *Science* **381**, 891-897 (2023). DOI: 10.1126/science.adg5261.

- **Torres Ascurra YC**, Lin X, Wolters PJ, Vleeshouwers VGAA. Identification of *Solanum* Immune Receptors by Bulked Segregant RNA-Seq and High-Throughput Recombinant Screening. *Solanum tuberosum: Methods and Protocols,* 2021; 2354:315-330. DOI: 10.1007/978-1-0716-1609-3_15.

- Lin X, **Torres Ascurra YC**, Fillianti H, Dethier L, de Rond L, Domazakis E, Aguilera-Galvez C, Kiros AY, Jacobsen E, Visser RGF, Nürnberger T, Vleeshouwers VGAA. Recognition of Pep-13/25 MAMPs of *Phytophthora* localizes to an RLK locus in *Solanum microdontum*. *Frontiers in Plant Science,* 13:1037030 (2023). DOI: 10.3389/fpls.2022.1037030.

- Saraiva, M., Ściślak, M. E., **Torres Ascurra Y**., Ferrando, T. M., Zic, N., Henard, C., van West P., Trusch F, & Vleeshouwers, V. G. The molecular dialog between oomycete effectors and their plant and animal hosts. *Fungal Biology Reviews* 43 (2022). DOI: 10.1016/j.fbr.2022.10.002.

- Ponce OP, **Torres Y**, Prashar A, Buell R, Lozano R, Orjeda G, Compton L. Transcriptome profiling shows a rapid variety-specific response in two Andigenum potato varieties under drought stress. *Frontiers in Plant Science*, 13:1003907 (2022). DOI: 10.3389/fpls.2022.1003907.

- Sharma SK, Bolser D, de Boer J, Sønderkær M, Amoros W, Carboni MF, D'Ambrosio JM, de la Cruz G, Di Genova A, Douches DS, Eguiluz M, Guo X, Guzman F, Hackett CA, Hamilton JP, Li G, Li Y, Lozano R, Maass A, Marshall D, Martinez D, McLean K, Mejía N, Milne L, Munive S, Nagy I, Ponce O, Ramirez M, Simon R, Thomson SJ, **Torres Y**, Waugh R, Zhang Z, Huang S, Visser RG, Bachem CW, Sagredo B, Feingold SE, Orjeda G, Veilleux RE, Bonierbale M, Jacobs JM, Milbourne D, Martin DM, Bryan GJ. Construction of reference chromosome-scale pseudomolecules for potato: integrating the potato genome with genetic and physical maps. *G3: Genes, Genomes, Genetics*, 3 (11), 2031-2047 (2013). DOI: 10.1534/g3.113.007153

- **Torres Ascurra, Y**., Lozano R.; Merino C.; Orjeda G. Identificación de genes relacionados a sequía en papas nativas empleando RNA-Seq. Rev. peru biol. [online]. 2013, vol.20, n.3. pp.211-214. ISSN 1727-9933

The research described in this thesis was financially supported by the Peruvian Council for science, technology, and technological innovation (CONCYTEC) FONDECYT contract 129-2017 (to YCTA).

Financial support from Wageningen University for printing this thesis is gratefully acknowledged.

Cover design by **Anel Yozara Lopez Torres**